



Norwegian University of
Science and Technology

Design and Construction of an Autonomous, Miniature Drilling Rig

Contribution to the DrillboticsTM Competition

2017

Runa Linn Egeland

Astrid Lescoeur

Martin Aagaard Olsen

Mayuran Vasantharajan

Petroleum Geoscience and Engineering

Submission date: June 2017

Supervisor: Sigve Hovda, IGP

Co-supervisor: Alexey Pavlov, IGP

Norwegian University of Science and Technology
Department of Geoscience and Petroleum

Abstract

The Society of Petroleum Engineers' (SPE) sub-committee DSATS (Drilling System Automation Technical Section) [14] has, the last two years, organized a student competition in an effort to accelerate the uptake of automation in the drilling industry. The competition is called Drillbotics™[10] and this is a report of the Norwegian University of Science and Technology's (NTNU) contribution.

The main objective of the competition was to design a fully automated drilling rig that could autonomously drill a vertical well as quickly as possible while maintaining rig and drill string integrity. The winning team was selected based on a set of criteria such as performance, quality of wellbore and data handling [13]. The purpose of this report is to present the team's solution to the problem, describe the rig's main design features and present the main results from the test day. It will also seek to highlight issues related to drilling automation.

The proposed rig design was developed based on new ideas and innovative solutions, as well as current industry practices and guidelines provided by DSATS. Through research and analysis, an evaluation of the most likely drilling related problems and dysfunctions was made and this provided the basis for dimensioning the drilling machine and for designing the control system.

One of the main issues addressed was ensuring that sufficient weight on bit (WOB) could be applied without causing pipe failure. A nozzle was added in the pipe to increase the pipe's internal pressure and thereby also the geometrical stiffness of the pipe. Unfortunately, due to delays and insufficient testing, the internal pressure was not increased as much as originally planned during the on-site test. However, another design feature was implemented to reduce the risk of failure which consisted of adding a roller bearing on the drill deck to increase the buckling limit of the pipe.

Another challenge was to mitigate vibrations in the drill string. This was achieved by adding points of stabilization at the level of the drill deck and at the surface of the rock. This successfully damped the amplitude of the vibrations and stabilized the string while drilling. Through testing, resonance frequencies were detected which made it possible to plan the operating window of the rig above or below the resonance frequencies.

Another important design feature was how the machine optimized the control parameters to increase the speed of drilling. Both the rotational speed of the string and the weight applied to the drill string could be monitored and adjusted while drilling. The optimization function aimed to keep a constant drill string torque set point by adjusting the WOB. This method enabled relatively smooth transitions between different rock formations and reactions to dysfunctions related to stuck pipe and torsional vibrations.

The performance of the rig design and control algorithms was observed and measured by DSATS members during the on-site test at the university 8th June 2017. The drilling rig was able to autonomously drill a vertical well through the rock sample provided by DSATS. The machine continuously sought to optimize the operation by adjusting the control variables and reacted to problems that occurred during the operation.

Trondheim, 2012-06-13

Martin Olsen, Runa Linn Egeland, Mayuran Vasantharajan and Astrid Lescoeur

Sammendrag

Society of Petroleum Engineers' (SPE) underavdeling DSATS (Drilling System Automation Technical Section) [14] har de siste to årene holdt en internasjonal studentkonkurranse, kalt Drillbotics™[10], for å øke interessen for automasjon i boreindustrien. Denne masteroppgaven presenterer NTNU's bidrag.

Målet med konkurransen er å designe og bygge en autonom borerigg som kan bore en vertikal brønn så raskt som mulig, samtidig som den bevarer riggens og borestrengens integritet. Vinnerlaget vil bli kåret basert på en rekke kriterier som utførelse, brønnkvalitet og behandling og visualisering av data [13]. Formålet med rapporten er å legge frem lagets løsning på problemet, beskrive riggens design og egenskaper, og presentere hovedresultatene fra testfasen og konkurransedagen.

Riggens design ble utviklet basert på nye ideer og innovative løsninger, metoder brukt i industrien og retningslinjer gitt av DSATS. Gjennom studier og analyse har de mest sannsynlige borerelaterte problemene blitt evaluert og dette har lagt grunnlaget for dimensionering av boremaskinen og kontrollsystemets arkitektur.

En av utfordringene som ble adressert var å sørge for at nok vekt kunne bli lagt på borestrengen uten å forårsake skade på utstyret. Løsningen som blir lagt frem i denne rapporten er å legge til en dyse nederst i rret for å øke rørets indre trykk og dermed øke dets geometriske stivhet. På grunn av forsinkelser og lite testing ble ikke trykket like mye som planlagt.

En annen utfordring var å mitigere vibrasjoner i borestrengen. Dette ble gjort ved å legge til innspenninger på boredekket og ved overflaten av steinen. I tillegg ble systemets naturlige frekvenser estimert for å kunne kartlegge resonansintervaller. Dette bidro til å redusere amplituden av vibrasjonene, stabilisere borestrengen under operasjonen og bestemme operasjonsvinduet.

En annen viktig funksjonalitet er hvordan maskinen optimaliserer kontrollparametrene for å øke borehastigheten. Både rotasjonshastigheten til borestrengen og vekten som blir lagt på strengen kan overvåkes og justeres under boreoperasjonen. Optimaliseringsfunksjonen prøver å holde et konstant dreiemoment på borestrengen ved å justere hastigheten til heisemotoren. Denne metoden

gjorde det mulig å opnå gjevne overganger mellom ulike formasjoner og respondere til problemer som låst borestreng og torsjonelle vibrasjoner.

Denne masteroppgaven har resultert i konstruksjonen av en autonom borerigg som kan bore en vertikal brønn gjennom ukjente formasjoner. Maskinen søker kontinuerlig etter å optimalisere operasjonen ved å justere kontrollvariabler og respondere til problemer som oppstår under operasjonen. Funksjonaliteten til riggen ble testet foran medlemmer av DSATS 8.juni 2017 i anledning Drillbotics™konkurransen.

Trondheim, 2012-06-13

Martin Aagaard Olsen, Runa Linn Egeland, Mayuran Vasantharajan and Astrid Lescoeur

å

Acknowledgments

We would like to thank Sigve Hovda and Alexey Pavlov for supervision, guidance and sharing their knowledge and insight. They provided us with continuous support, gave us feedback and evaluated our work.

Noralf Vedvik provided us with valuable help with designing and constructing the rig and the necessary equipment.

Steffen Wærnes Moen helped with the electronic design and instrumentation of the rig. He ensured that the control system could be set up and that all necessary communication was enabled.

Tor Berge Gjersvik was of great help when conducting the vibration analysis and his extensive experience from the industry also provided us with ideas and solutions for the drilling related issues.

We would also like to thank John-Morten Godhavn for taking the initiative to make a team from NTNU join the competition, as well as for help with the automation and control system design.

We would like to express our gratitude to Statoil for financial support, and the Department of Petroleum Engineering and Applied Geophysics for giving us the opportunity to work on this project. This project has given us the opportunity to gain hands-on experience with machinery, sensors, data handling, and control requirements, as well as developing experience working in multi-disciplinary teams which will be directly applicable to the future career in the industry.

Finally, we would like to thank ABB for sponsoring us with the PLC and providing us with the motor and the controller for the hoisting system, and Lyng Drilling for providing us with the custom made 1.125", 6-cutter PDC bit.

Team Bio

As part of their specialization project and their master thesis at NTNU, four students formed a team to compete in the Drillbotics™ competition. All four students, Runa Linn Egeland, Astrid Lescoeur, Martin Olsen and Mayuran Vasantharajan, are final year MSc students in Petroleum Engineering. The students are specializing in drilling engineering and building an automated drilling rig was the focus of their master thesis.

Alexey Pavlov holds an MSc in Applied Mathematics (1998, Russia) and a PhD in Mechanical Engineering (2004, The Netherlands) with specialization, in both cases, in automatic control and optimization systems. He has held research positions at Ford Motor Co. (2000, USA), Eindhoven University of Technology (2004-2005, The Netherlands), NTNU (2005-2009, Norway) and Statoil (2009-2016, Norway). In the latter position he developed a number of novel automation and optimization technologies for drilling and production systems. Since 2017 he has been working as a professor in Petroleum Cybernetics at the Department of Geoscience and Petroleum, NTNU, focusing on digital and automation solutions for the Oil and Gas industry.

Sigve Hovda got his master thesis in mathematics in 1999 from the Norwegian University of Life Sciences. He received a PhD in medical ultrasound on the heart in 2007 from the Department of Computer Science at the Norwegian University of Science and Technology. Between 2008 and 2014 he worked in Verdande Technology. The main product of the company was a software for real-time surveillance of the drilling process. He was the Principal Research Engineer and was leading the group that created a software for automatic detection of unwanted events during drilling. From 2015, he has held a position as an Associate Professor in drilling at the Department of Geoscience and Petroleum at the Norwegian University of Science and Technology. His main research focus is on drill string dynamics and automatic pattern recognition of real-time drilling data.

Noralf Vedvik received his bachelor degree in automation engineering in 2013, and masters degree in subsea engineering in 2015 from the Norwegian University of Science and Technology. From 2015 he has held a position as a senior engineer at the Department of Geoscience and Petroleum at the Norwegian University of Science and Technology. His main task is to assist research projects

with technical and mechanical solutions.

Steffen W. Moen received his bachelor degree in electronics engineering in 2011 from the Sør-Trøndelag University College, and a master degree in electronic design and instrumentation in 2013 from the Mid Sweden University. From 2013 he has been a consultant for GlucoSet AS where he assists in developing a fiber optic blood glucose sensor. From 2015 he has held a position as a Senior Engineer at the Department of Geoscience and Petroleum at the Norwegian University of Science and Technology. His main task is to assist research projects and students with electronics and instrumentation.

John-Morten Godhavn graduated with an MSc in 1992 and a PhD in 1997, both from the Department of Engineering Cybernetics at NTNU. He holds a position as a principal researcher at Statoil's Research Center in Trondheim, Norway, working on drilling automation research projects. He also holds a position as an adjunct Professor at the Institute for Petroleum Technology, NTNU.

Tor Berge Gjersvik graduated with an MSc in 1977 and a PhD in 1982 from the Department of Petroleum Engineering and Applied Geophysics. He currently holds a position as an adjunct Professor in Petroleum Subsea Technology.



Figure 1: From upper left to lower right: Astrid Lescoeur, Martin Aagaard Olsen, Mayuran Vasantharajan, Runa Linn Egeland, Alexey Pavlov, John-Morten Godhavn, Noralf Verner, Sigve Hovda, Stian W. Moen and Tor Berge Gjersvik

Table of Contents

Abstract	i
Sammendrag	iii
Acknowledgment	vi
Team Bio	vii
List of Abbreviations	xxvii
1 Introduction and Overview	1
1.1 Rig structure	2
1.2 Weight on Bit	3
1.3 Vibrations	4
1.4 Control System	4
2 Safety	7
2.1 Safety Hazards during Construction	8
2.1.1 Rig Construction	8
2.1.2 Electrical Practices	8
2.2 Safety Hazards during Testing Phase	8
2.3 Storage and Maintenance	9
2.4 Safety During Transportation	9
2.5 Safety Hazards During Operation	10
2.5.1 Unloading and Handling of Rock Sample	10

TABLE OF CONTENTS

2.5.2	Electrical System	11
2.5.3	Safety Factors and Dimensioning	12
2.5.4	Hoisting System	12
2.5.5	Circulation System	13
2.5.6	Control System	13
2.5.7	Emergency Shutdown of System	14
2.5.8	Safety Measures Related to Drill Pipe Pressure	15
2.6	Project Risk	16
3	Hardware	19
3.1	As-Built Rig Design	20
3.1.1	Rig Structure	20
3.1.2	Mobility of Rig	23
3.1.3	Hoisting System	25
3.1.4	Rotary System	26
3.1.5	Circulation System	27
3.1.6	Drillstring Design	28
3.1.6.1	Bottomhole Stabilizer Design	30
3.1.6.2	Tool Joint Design	31
3.1.6.3	Incorporation of Downhole Sensor	32
3.1.7	Stabilizing Elements at Surface	34
3.1.7.1	Riser	34
3.1.7.2	Surface Stabilizer	35
3.1.7.3	Drill Deck Bushing	37
3.1.8	Measurement, Control and Instrumentation System	38
3.1.8.1	Measurement and Sensors	40
3.1.9	Construction Cost	43
3.2	Power Consumption	46
3.2.1	Top Drive Motor	46

TABLE OF CONTENTS

3.2.2	Hoisting Motor	48
3.2.3	Fluid Pump	48
3.2.4	Computer	49
3.2.5	Summary	49
4	Pre-Study	51
4.1	Compression Analysis	52
4.1.1	Euler’s Critical Load Analysis	53
4.1.2	Weight of Drill String	55
4.1.3	Magnitude of Force F_c	55
4.1.3.1	Burst Pressure	57
4.1.3.2	Pressure Loss in Circulation System	57
4.1.3.3	Summary of Pressure Loss in Circulation System	68
4.1.3.4	Calculation of F_c	69
4.1.3.5	Constriction Diameter	70
4.1.3.6	Drill String Compression Analysis Results	71
4.1.3.7	Changes in Phase II	72
4.2	Drilling Algorithm	75
4.2.1	Drillstring and Bit Dysfunctions	75
4.2.1.1	Axial Vibrations	76
4.2.1.2	Torsional Vibrations	79
4.2.1.3	Lateral Vibrations	81
4.2.1.4	Natural Frequency	83
4.2.1.5	Interfacial Severity	85
4.2.1.6	Bit Balling	86
4.2.2	Optimization of Drilling Parameters	87
4.2.2.1	Maximizing Drilling Parameters	87
4.2.2.2	MSE	87
4.2.2.3	Founder’s Point	88

TABLE OF CONTENTS

4.2.2.4	Vibration Minimization	90
4.3	Simulator	91
4.3.1	Model	91
4.3.1.1	Drillstring Model	91
4.3.1.2	Hoisting System Model	93
4.3.1.3	Circulation System Model	96
4.3.1.4	Formation Model	97
4.3.2	Control System	97
4.3.2.1	Top Drive Motor	98
4.3.2.2	Hoisting Motor	98
4.3.2.3	Pump	99
4.3.3	Logics	99
4.3.4	State Machine	100
4.3.5	Learnings from the Simulations	101
5	Testing of the Drilling Machine	103
5.1	Hardware Testing (Factory Acceptance Test)	104
5.1.1	FAT Plan	104
5.1.2	FAT Results	105
5.1.2.1	Sensors	105
5.1.2.2	Top Drive Motor	105
5.1.2.3	Hoisting Motor	106
5.1.2.4	Pump	106
5.1.2.5	Safety System	106
5.1.2.6	Emergency Stop	106
5.1.2.7	Operating Range	106
5.2	Data Infrastructure Testing	107
5.2.1	Data Infrastructure Testing Plan	107
5.2.2	Data Infrastructure Testing Results	107

TABLE OF CONTENTS

5.3	Control System Testing	108
5.3.1	Testing Description and Results	109
5.3.1.1	Getting to Know the System and its Challenges	109
5.3.1.2	Estimation of Maximum Limits	110
5.3.1.3	Safety Functionality Testing	115
5.3.1.4	Identification Testing	115
6	Automation	123
6.1	Control System	123
6.1.1	Programmable Logic Controller	124
6.1.2	Actuator Drives	124
6.1.3	Simulink Model	124
6.1.3.1	Proportional-Integral-Derivative Controller Theory	125
6.1.3.2	PID-Controllers in this System	127
6.1.3.3	Scaling	128
6.1.3.4	Safety Limits	129
6.1.3.5	Overview of Simulink Model	130
6.2	Chosen Optimization Function	138
6.2.1	Data Analysis	139
6.2.2	Implementation of the Optimization Function in Simulink	143
6.2.3	Results of using T_{ds} as an Optimization Parameter	147
6.3	Data Collection and Handling	149
6.3.1	Communication	149
6.3.2	Storage	149
6.3.3	Data Visualization	149
6.3.3.1	Dashboard	149
6.3.3.2	Response Time	151
7	Competition	155
7.1	Provided Equipment from DSATS	156

TABLE OF CONTENTS

7.1.1	PDC Bit	156
7.1.2	Rock Sample	157
7.2	Setup on the Competition Day	158
7.3	On-Site Drilling Test	159
7.4	Results and Analysis from the Test Day	163
7.4.1	Drillstring Twist-Off	164
7.4.2	Bit Wear	165
7.4.3	Borehole Quality	165
7.4.4	Formation Detection from Drilling Data	167
8	Construction Challenges and Solutions	171
8.1	Challenges Related to Hardware	171
8.2	Challenges Related to Project Management	174
8.3	Challenges Related to Automation	175
8.4	Challenges Related to the Drilling Operation	176
9	Evaluation and Reflection	179
9.1	Small-Scale Drilling Rig Compared to Conventional Drilling	179
9.2	Theoretical Calculations versus Reality	181
9.3	Rig Structure	182
9.4	Weight on Bit	183
9.5	Vibrations	183
9.6	Control System	184
9.7	Understanding of Drilling Dysfunctions and Bit-Rock Interaction	185
9.8	Project Management	186
9.9	Further Work	186
10	Summary	189
A	Safety	197
A.1	Risk Assessment	197

TABLE OF CONTENTS

B Hardware	201
B.1 Hoisting Motor Specifications	201
B.2 Top-Drive-Specifications	208
B.3 BHA design	209
B.4 Swivel	215
B.5 Load Cell Specifications	221
B.6 Lyng Miniature Drill Bit Design	224
B.7 Rig Design	225
C Automation	239
C.1 Control System Architecture	239
D Testing	241
D.1 Factory-Acceptance-Testing	241
D.2 Rock Samples use for Testing	243
E Competition	249
E.1 Drillbotics™ Guidelines	249
E.2 NTNU Monthly Reports Phase II	277

TABLE OF CONTENTS

List of Tables

- 3.1.1 Evaluation of stabilizers 30
- 3.2.1 System power distribution 49
- 4.1.1 Input data for Euler’s critical load 54
- 4.1.2 This table summarizes the results of Re-calculations (in the right column) for dif-
ferent q in m^3/s (the left column) 61
- 4.1.3 Pressure loss in circulation system 69
- 4.1.4 Input data for hydraulic force calculations 70
- 4.1.5 Estimated values for F_c , weight of drill string and maximum WOB. 71
- 4.1.6 F_c and maximum WOB for a constriction diameter of 1.40 mm 74
- 4.1.7 F_c and maximum WOB for a constriction diameter of 1.50 mm 74
- 4.1.8 Estimated values for F_c , weight of drill string and maximum WOB. 74
- 4.3.1 Drillability coefficients 95
- 5.3.1 Estimation of maximum limits 115
- B.1.1 Technical data for the hoisting motor (Lenze GST03-2M VBR 063C42) [23]. 201

LIST OF TABLES

List of Figures

1	From upper left to lower right: Astrid Lescoeur, Martin Aagaard Olsen, Mayuran Vasantharajan, Runa Linn Egeland, Alexey Pavlov, John-Morten Godhavn, Noralf Verner, Sigve Hovda, Stian W. Moen and Tor Berge Gjersvik	viii
2.1	Caster with foot-activated lift mechanism	10
2.2	Demonstration of the handling of the rock sample	11
2.3	Electrical cabinet to keep the electrical system separated from water	12
2.4	Stopping mechanism on the extremities of the rail	13
2.5	Emergency stop button attached to the electrical cabinet	15
2.6	Plexiglass mounted to the derrick, isolating high pressure zones from working personnel	16
3.1.1	Overall rig view	20
3.1.2	Side view of the rig in upright position (dimensions in mm)	22
3.1.3	Front view of the rig in upright position (dimensions in mm)	23
3.1.4	Illustration of the rig in folded position	24
3.1.5	Side view of the rig in folded position (dimensions in mm)	24
3.1.6	Illustration of the complete ball screw package (KGT16x5 FGR RH 1 S 1500 G9 AEG) that was used for the hoisting system [8]	25
3.1.7	Illustration of linear roller guide (HGR20R-C-KAPP, HGW20CC-ZO-C VOGN) for hoisting system [7]	26

LIST OF FIGURES

3.1.8	Illustration of circulation circuit with swivel and pressure reducing valve	27
3.1.9	Overall rig view showing the hoisting motor, top drive motor, electrical swivel, swivel and drill string.	28
3.1.10	Drill string designs used during testing phase and on the competition day	29
3.1.11	Illustration of the stabilizer, showing a side cut on the left hand side. Designed by Noralf Vedvik.	31
3.1.12	Hydraulic connections used as tool joints between BHA and pipe, and between pipe and swivel	32
3.1.13	Illustration of the BHA design, showing where and how the sensors are mounted inside the BHA. The sensors are attached to the plate inside the red circled area (3.1.13) and mounted to the sensor-protector shown inside the green circle. The blue circle shows how the sensor-protector is attached from above. Designed by Noralf Vedvik.	33
3.1.14	Another illustration of the BHA design, showing where the four wires from the sensors are lead trough the "sensor-protector" into the drill pipe. Designed by Noralf Vedvik.	34
3.1.15	Illustrations of roller bearings	35
3.1.16	Picture showing the bottomhole configuration	36
3.1.17	Landing of the surface stabilizer inside the riser. Picture from on-site test day. . .	37
3.1.18	Drill string running through drill deck bushing	38
3.1.19	Picture of the AC500 PLC [2]	39
3.1.20	Control system flow chart	40
3.1.21	Load cell, HBM S2M [18]	41
3.1.22	Pressure transducer, Keller Druck PA-25EI [3]	41
3.1.23	Downhole sensor, MPU-6000 [20]	42
3.1.24	Picture of implemented downhole sensor	43
4.1.1	End conditions of pipe [28]	54
4.1.2	Illustration of force F_c counteracting the WOB and increasing the tension in the drill pipe wall	56

LIST OF FIGURES

4.1.3	Illustration of the circulation system consisting of a mud pump, hose, swivel, drill pipe, BHA, bit nozzles and flowline.	58
4.1.4	Graph showing the pressure loss in bar through the hose on the y-axis for different flow rates on the x-axis	62
4.1.5	Graph showing the estimated pressure loss in bar through the swivel on the y-axis for different flow rates on the x-axis	63
4.1.6	The graph showing the pressure loss in bar through the drill pipe on the y-axis for different flow rates on the x-axis	64
4.1.7	Graph showing the pressure loss in bar over the BHA on the y-axis for different flow rates on the x-axis	65
4.1.8	Graph showing the pressure loss in bar through the bit on the y-axis for different flow rates on the x-axis	66
4.1.9	Graph showing the pressure loss in bar over the bit nozzle on the y-axis for different flow rates on the x-axis	67
4.1.10	Graph showing the pressure loss in bar over the annulus on the y-axis for different flow rates on the x-axis	68
4.1.11	Graph showing the effect of flow rate on pressure loss. The slotted line shows the total system pressure loss for different flow rates, and the dashed line shows the resulting maximum pressure in the drill pipe. The red arrows show the burst pressure for the pipe with safety factors of 1, 2 and 3, with burst pressure of 52.6 bar, 78.9 bar and 157.8 bar respectively.	72
4.1.12	Figure showing the pressure inside the drill pipe (z-axis), the constriction diameter, d_c (x-axis) and flow rate, q (y-axis).	73
4.2.1	Illustration of the three types of drillstring vibrations [37]	76
4.2.2	Illustration of the procedure for mitigating axial vibrations[36]	78
4.2.3	Illustration of the procedure for mitigating torsional vibrations [36]	80
4.2.4	Illustration of the procedure for mitigating lateral vibrations [36]	82

LIST OF FIGURES

4.2.5	Graph illustrating the founder point. Point 1 is the point at which the critical depth of cut occurs and point 2 is the founder point. Phase 1 is before point I occurs, phase II is between point 1 and 2, and phase III is after point 2 [24]	89
4.3.1	Illustration of the RPM model from the Simulink model	91
4.3.2	Illustration of the ROP model from the Simulink model	94
4.3.3	Illustration of the pressure model from the Simulink model	96
4.3.4	Illustration of the PID controllers from the Simulink model	98
4.3.5	Illustration of the high-level control	100
4.3.6	Illustration of the possible states in a state machine	101
5.3.1	Pictures of test holes drilled in asphalt, marble, slate and soapstone	109
5.3.2	Relationship between load cell signal (kg) and weight on scale	111
5.3.3	Demonstration of twist-off test	112
5.3.4	Graph of hoisting motor torque during buckling test	113
5.3.5	Picture of pipe after running buckling test	114
5.3.6	Graph of WOB and RPM versus time showing resonance around 800 RPM.	117
5.3.7	Graph of WOB and RPM versus time showing resonance around 800 RPM.	118
5.3.8	Graph of WOB and RPM versus time showing resonance and unstable drilling conditions when drilling with RPM above 1100.	119
5.3.9	Poor borehole quality after experiencing bit bouncing	120
5.3.10	Twist-off at the connection between the BHA and the drill string when drilling asphalt	121
6.1.1	Illustration of a PID control loop [41]	125
6.1.2	”Rig Data” subsystem	131
6.1.3	”Enable Operations” data subsystem	132
6.1.4	”From HMI” data subsystem	133
6.1.5	”From HMI” data subsystem	134
6.1.6	Inputs and outputs to the ”PID Controllers” subsystem in Simulink	135
6.1.7	”PID Controllers” data subsystem	136

LIST OF FIGURES

6.1.8	Variable PID gains in the WOB PID controller	137
6.1.9	”Write Data” subsystem	138
6.2.1	Test results from drilling in soapstone with a constant RPM of 1000. MSE plotted against time on the primary y-axis and WOB against time on the secondary y-axis. [17]	139
6.2.2	Test results from drilling in marble with a constant RPM of 1000. MSE plotted against time on the primary y-axis and WOB against time on the secondary y-axis. [17]	140
6.2.3	Test results on asphalt with a constant RPM of 1000. MSE plotted against time on the primary y-axis and WOB against time on the secondary y-axis. [17]	140
6.2.4	Test results from drilling in soapstone with a constant RPM of 1000. ROP plotted against time on the primary y-axis and WOB against time on the secondary y-axis. [22]	141
6.2.5	Results from drilling in marble with a constant RPM of 1000. ROP plotted against time on the primary y-axis and WOB against time on the secondary y-axis. [22]	142
6.2.6	Test results on asphalt with a constant RPM of 1000. ROP plotted against time on the primary y-axis and WOB against time on the secondary y-axis. [24]	142
6.2.7	Illustration of the operating window.	143
6.2.8	Illustration of the use of drill string torque as a process variable	144
6.2.9	Illustration of the updated operating window.	145
6.2.10	Details of the stateflow chart	146
6.2.11	Graph of T_{ds} and WOB vs depth showing how the control system reacts to peaks in T_{ds} by reducing the WOB	147
6.3.1	Simulink dashboard	151
6.3.2	The graph above shows a response time of 1.5 to 3 seconds on the top drive motor, where the desired set points are shown in blue and the measured values are shown in green	152
6.3.3	Graph of WOB PID controller response, where the desired set points are shown in green and the measured values are shown in blue	153

LIST OF FIGURES

7.1.1	PDC bit provided by DSATS	156
7.1.2	Rock sample provided by DSATS	157
7.2.1	Overall rig view on the on-site test day	159
7.3.1	Early phase drilling on the on-site testing day	160
7.3.2	The first twist-off	161
7.3.3	The second twist off	162
7.3.4	Return flow from annulus	163
7.4.1	Drilled rock sample on competition day	164
7.4.2	Wear on the bit cutters and bit body	165
7.4.3	Picture of the drilled hole on the on-site test day	166
7.4.4	Plotted results from the downhole survey performed by one of the DSATS judges (Kurt West), showing a maximum inclination of 2 degrees	166
7.4.5	Table of detected formations based on the drilling data and actual formation depths	167
7.4.6	Drilling data from the competition day	168
7.4.7	Drilled rock sample on competition day with formation depths. Measuring tape positioned next to the drilled well.	169
8.4.1	Steel cylinder placed inside the pipe at connection point to increase strength	177
B.1.1	Dimensions specifications for the hoisting motor (Lenze GST03-2M VBR 063C42) [23]	202
B.1.2	Mechanical drawings for the hoisting motor (Lenze GST03-2M VBR 063C42) [23].	203
B.1.3	Ball screw [8]	204
B.1.4	Ball screw nut [8].	205
B.1.5	Ball screw [8].	206
B.1.6	Complete linear roller guide package [7].	207
B.2.1	Top drive motor (3GAA091520-ASJ).	208
B.3.1	Sensor cover inside BHA.	209
B.3.2	Holder for the sensor inside BHA.	210
B.3.3	Top of BHA.	211

LIST OF FIGURES

B.3.4	Middle section inside BHA.	212
B.3.5	BHA Body.	213
B.3.6	Cross section of the BHA body.	214
B.4.1	Top- and bottom part of the swivel.	215
B.4.2	Shaft for sensor wiring.	216
B.4.3	Electrical housing for sensor.	217
B.4.4	Holder for the swivel.	218
B.4.5	Middle section of the swivel.	219
B.4.6	Hollow shaft for water circulation.	220
B.5.1	Load cell (HBM S2M 500 N, CLIP AE301) dimensions. [18].	221
B.5.2	Load cell (HBM S2M 500 N, CLIP AE301) dimensions. [18]	222
B.5.3	Load cell (HBM S2M 500 N, CLIP AE301) dimensions [18].	223
B.6.1	Miniature drill bit from Lyng Drilling AS.	224
B.7.1	Substructure of rig. All dimensions in mm.	225
B.7.2	Derrick. All dimensions in mm.	226
B.7.3	Carriage. All dimensions in mm.	227
B.7.4	Moveable plate with riser. All dimensions in mm.	228
B.7.5	Tabletop. All dimensions in mm.	229
B.7.6	Rig viewed from front and side. All dimensions in mm.	230
B.7.7	Assembled rig.	231
B.7.8	Drilldeck.	232
B.7.9	Strut for carriage.	233
B.7.10	Hinge part 1.	234
B.7.11	Hinge part 2.	235
B.7.12	Top mount for hoisting motor.	236
B.7.13	Bottom mount for hoisting motor.	237
B.7.14	Carriage mount for top drive motor.	238
C.1.1	Control system.	239
C.1.2	Drilling algorithm.	240

LIST OF FIGURES

D.2.1	Picture of the collected rock samples from Nidaros Domkirke Restaureringsarbeider. A mix of marble, granite and different types of clay stones.	244
D.2.2	Picture of a homemade "sandstone" in the making. The mixture of sand, water and cement is poured into the forms and is ready to solidify.	245
D.2.3	Picture of the finished product. Some of the rock samples were sawed, so it could be easier to study the distribution of the sand and the cement within the rock samples.	245
D.2.4	Picture of black shale collected in Laanke in north Stjordal.	246
D.2.5	Picture of the rock sample made of shale with finer grain in the upper part, quartz in the middle and shale with coarser grains at the lower part.	246
D.2.6	Picture of the rock samples provided by SINTEF. Marble in the right, two different types of sandstones in the middle and dolomite in the left.	247

List of Abbreviations

Abbreviation	Explanation
A_t	Cross-sectional area
BHA	Bottom Hole Assembly
C_d	Discharge coefficient
d_i	Inner diameter
DSATS	Drilling System Automation Technical Section
ϵ	Efficiency
F	Force
l	Length
N	Revolutions per Minute
NTNU	Norwegian University of Science and Technology
P	Power
p	Pump pressure
p_{br}	Burst pressure
P_P	Pump power
PDC	Polycrystalline Diamond Compact
PLC	Programmable Logic Controller
ρ_f	Fluid density
Q	Flow rate
MSE	Mechanic Specific Energy

LIST OF FIGURES

ROP	Rate Of Penetration
RPM	Revolutions Per Minute
SPE	Society of Petroleum Engineers
T	Torque
T_{crit}	Critical torque
τ_{crit}	Critical shear stress
T_{ds}	Drill string torque
T_h	Hoisting motor torque
WOB	Weight on Bit
ω	Angular velocity
ω_h	Hoisting motor speed

Introduction and Overview

The oil and gas industry is continuously looking for new solutions to reduce costs and improve safety and efficiency. As a result of this, the interest in drilling automation has grown during the last decades as oil and gas prospects have become more complex and more challenging. An increased level of automation can provide a more accurate and rapid response to drilling anomalies, as well as reduce the need for human intervention during drilling operations.

As a response to this, the Society of Petroleum Engineers (SPE) formed the sub-committee Drilling System Automation Technical Section (DSATS) to accelerate the uptake of automation in the drilling industry. During the last 2 years, DSATS has organized an international student competition called Drillbotics™[10]. The aim of the competition is to design a drilling rig and related equipment to autonomously drill a vertical well as quickly as possible while maintaining borehole quality and integrity of the drilling rig and drill string [10]. The only manual intervention allowed is to press a button to start the drilling operation.

Several requirements were stated in a set of guidelines, shown in Appendix E, and they formed the basis and limitations of the design. The most important limitations were related to the pipe, drill string design, mobility of the rig, and, downhole and surface measurements of drilling variables. In addition to this, the evaluation committee listed a set of different grading criteria. This included safety, mobility of the rig, design considerations and lessons learned, mechanical design

and functionality/versatility, simulation/model/algorithm and control scheme.

The drill pipe and the drill bit were provided by DSATS and their dimensions were stated in the guidelines. The drill pipe was made of aluminum, had a length of 914 mm, an outer diameter of 9.53 mm and an inner diameter of 7.75 mm. The bit was a polycrystalline diamond compact (PDC) bit and had an outer diameter of 28.6 mm. The total maximum length of the stabilizers was limited to 90 mm. The total power consumption was limited to 25 hp and the WOB was unlimited. The properties of the formation rock for the test day were unknown, but the dimensions were given (approximately 30cmx30cmx60cm).

Another limitation to the project was the rig and material cost. The budget was limited to US\$ 10,000 and had to be covered through funding. Equipment could be provided by the university or by companies that were interested in supporting the project and the cost of this was not included in the budget. The source of funding for this project was the Department of Geoscience and Petroleum at the Norwegian University of Science and Technology (NTNU) and Statoil. ABB sponsored the team with a programmable logic controller (PLC).

Since this was the first time a team from NTNU participated in the Drillbotics™ competition, all parts of the rig were designed in Phase I of the competition (fall semester 2016) and the construction was done in Phase II (spring semester 2017). This report therefore contains many design features already presented in the design report delivered in the fall semester 2016 [34]. Large parts of the literature review and gathering of background information for the design also revolved around the examination of the previously delivered design reports from the different universities [11].

Throughout this study, four main concerns were identified: building a rig structure that could provide the required stability whilst being mobile; being able to provide sufficient weight on bit (WOB); keeping vibrations under control; designing an efficient and safe control system.

1.1 Rig structure

The main purpose of the rig structure was to provide stability for the planned drilling operations. The rig was constructed in hollow steel pipes, both to ensure the strength needed, but also to provide

enough weight so that the rig could keep itself at bay. It was also very important to provide vertical motion for lowering and hoisting of the drill string, torque to rotate the bit and fluid circulation.

The hoisting system consisted of a ball-screw combined with a linear roller guide system, driven by an AC-motor. The ball screw translated the rotary motion from the motor to vertical motion. This allowed to increase the weight applied to the drill string by increasing the torque or the speed of the AC-motor. The rotary motion of the drill pipe was provided by an AC-motor. This motor was mounted on a carriage attached to the ball screw. The combination of the hoisting system and the rotary system provided the required torque to the drill bit.

Finally, a single-acting triplex pump provided fluid flow to circulate out cuttings.

1.2 Weight on Bit

The weight that could be applied at the top of the string was expected to be greatly limited by the weakness of the drill pipe. If too much weight was applied, the pipe would enter a state of compression and if it reached a critical load, it could buckle and fail. The weight added at the top directly affected the force exerted by the bit on the formation. This force was equal to the force exerted by the formation on the bit, commonly referred to as weight on bit (WOB), which meant that insufficient weight at the top reduced the ability to drill efficiently through the formation. As one of the main goals of the competition was to drill as fast as possible, it was crucial to optimize the WOB while staying within the critical load criteria.

Inspired by the University of Oklahoma's design report from 2015 [31], a nozzle was added in the bottom hole assembly (BHA) to increase the internal pressure of the drill string. The background for this decision was that the nozzle would lead to an increase in tension and geometrical stiffness which would counteract the compressional forces when applying WOB. The desired internal pressure of the pipe was established at the burst limit of the pipe to maximize the tension force and thereby maximize the WOB. This solution was expected to be the main way to maximize WOB, but the set-up was unfortunately not tested to a large enough extent to be used on the test day. However, being such an important part of the design phase and still having the potential to improve

the drilling operation, it will be reviewed in detail in this thesis.

1.3 Vibrations

Large and destructive pipe vibrations were expected to occur while drilling and were of great concern due to the fragility of the pipe. The rig was designed to minimize the magnitude of these vibrations and thus reduce their impact on the equipment.

A point of support was provided through a fixed plate positioned under the top drive, simulating a drill deck with a bushing. A steel cylinder attached to a plate was positioned over the formation block to guide the bit and provide an additional point of stabilization to the drill pipe during operations.

Vibrations were also taken into consideration when designing the drill string. To minimize the amplitude of the vibrations the total length of the drill string was kept as short as possible and the BHA included a welded spiral blade stabilizer.

In addition to this, resonance frequencies were identified during the testing phase and were used to determine the drilling operating window.

1.4 Control System

The main goal of the competition was to construct a drilling machine that could operate entirely autonomously. It was therefore of great importance to develop a control system that could ensure a safe, efficient and entirely autonomous drilling operation.

One of the objectives was to create an algorithm that continuously tried to determine the optimal drilling parameters. They were the amount of weight applied on the string and the rotational speed of the string, referred to as input variables in the rest of the text. Adjusting these variables caused a change in other drilling variables that were monitored by downhole and surface sensors, referred to as output variables. An optimization function was developed with the goal being to increase the speed of drilling, but also, respond to drilling dysfunctions and ensure that all drilling variables

were within a pre-defined safe range to ensure a vertical borehole and maintain the integrity of the drilling rig and the drill string.

Safety

The main part of the risk assessment of this project was conducted during the design phase, but it was continuously updated as the project progressed. This was done to identify hazards and risk factors that have the potential to cause harm, in particular harm to personnel. The risks were analyzed and evaluated, before appropriate ways to eliminate and control them were determined.

One of the main concerns during any operation, regardless of its scale or scope, is the health and safety of the personnel. By automating the drilling process, the need for manual intervention decreased which reduced risk related to personnel. The improved safety, as well as the increased efficiency and reduced costs, are some of the main advantages of automated drilling processes.

Although manual intervention was not required for an automated drilling operation, the construction, installation and transportation of the rig required physical labor which increased the risk of hazardous situations. Any unplanned incidents requiring manual intervention during drilling therefore also had to be considered.

Most accidents on a full-scale platform occur on the drill floor, especially during pipe handling [6]. Because of the scale of the rig, this was however not an issue. It was therefore important to bear in mind that if this design was to be used for a full-scale operation, the safety hazards would be of a different nature.

The main safety hazards during the construction and operation of this drilling rig were identified

and safety precautions have been proposed in the sections below. A full risk assessment can be found in Appendix A. The level of risk involved has been estimated and the acceptable level of risk has been determined.

2.1 Safety Hazards during Construction

2.1.1 Rig Construction

During the period of construction of the rig the hazardous situations were expected to be mostly mechanical. The handling of equipment, material and debris were the main concerns.

To minimize the risk of any accidents occurring, safety glasses and protective footwear were worn. Hearing protection, gloves and coveralls were also required during construction activity. In addition to this, the construction area was kept off limits to people not involved in the project.

As mentioned in the introduction, because of the small scale of the rig and the light weight of the equipment, the risk of any severe accidents occurring was very small.

2.1.2 Electrical Practices

Safety related work practices were followed during the construction phase to prevent the occurrence of injuries resulting from electrical shock. No power was to be supplied while connecting wires and components. All electrical connections had to be secured and wiring had to be insulated. Qualified personnel was responsible for the high voltage setup of the rig, while all low voltage setups could be arranged by the team members [29].

2.2 Safety Hazards during Testing Phase

During the testing phase, the most severe risks were expected to be related to the failure of the pipe because some of the tests aimed to reach the failure limits of the pipe. The tests were conducted in a controlled manner, but it was important to keep in mind that no matter which precautions were taken, working so close to failure limits increases the risk of accidents.

One of the main safety concerns during that phase was being able to accurately estimate critical values and to study how the system behaved close to its limits without putting personnel and equipment in danger.

Although the tests were conducted in a controlled manner, there is always a certain risk that equipment can fail unexpectedly. In the occurrence of an unexpected or uncontrolled event it therefore had to be possible to manually stop the process by pressing an emergency button. This safety measure would mitigate injury to personnel and damage to equipment.

Leakage as a result of pipe failure was also identified as a risk. The consequence of this can be a pressure drop followed by an increase in pump speed to compensate for the loss. Safety features therefore had to be included in the control system to ensure that the pump would stop if the pipe breaks.

Safety glasses had to be included to mitigate all cases related to spilling of high pressure fluid and debris, isolating personnel from high pressure zones.

2.3 Storage and Maintenance

Although chemicals were not expected to be used, it was decided that in the case that they were, the use had to be documented. Disposal of waste also had to be controlled and done as stated in regulations.

2.4 Safety During Transportation

The rig was designed to ensure safe transportation. The derrick could be folded down to increase maneuverability and stability by lowering the center of mass. Jack-up casters were put on each leg to avoid heavy lifts for personnel and ensure easy rolling movement of the rig.



(a) Wheel in up position



(b) Wheel in down position

Figure 2.1: Caster with foot-activated lift mechanism

2.5 Safety Hazards During Operation

2.5.1 Unloading and Handling of Rock Sample

The rig was designed to operate with the rock sample placed on the ground. This meant that the rig could be maneuvered in place, instead of moving the rock sample around. No heavy lifting during rig up/down and operation was needed, thereby reducing the risk of personnel injury and equipment damage.



Figure 2.2: Demonstration of the handling of the rock sample

2.5.2 Electrical System

The water and the electrical system were kept separate from each other to avoid shorting and electrical hazards. All electrical components were stored inside waterproof housing. Electrical cables followed the motion of the carriage and were exposed to wear because of bending and twisting. The state of the cables were therefore continuously monitored.



Figure 2.3: Electrical cabinet to keep the electrical system separated from water

2.5.3 Safety Factors and Dimensioning

Safety factors were applied to all calculations regarding failure of equipment. The motors and the pump were dimensioned to fit the required criteria, such as operating RPM intervals and pump rate. The selected pump for the system had a higher pressure rating than required during the operation, a safety valve was therefore included to ensure that the pressure did not exceed the critical values of the system.

2.5.4 Hoisting System

Because the top drive was attached to a carriage moving vertically along a set of rails, two stopping mechanisms were added at each of the extremities to avoid running off the rails.

The lower stopping mechanism was placed at the bottom of the rail. The upper stopping mechanism was limited by the length of the pipe. This was due to the roller bearing on the drill deck, which

had an inner diameter that was smaller than the outer diameter of the BHA. The BHA therefore always had to be below the drill deck, this was ensured by placing the stopping mechanism 85 cm above it.



Figure 2.4: Stopping mechanism on the extremities of the rail

2.5.5 Circulation System

As the rig design did not have a closed-loop fluid circulation system, a containment system was included to collect the circulating fluid and guide it to a drainage area to avoid slips and trips, as well as electrical shorts due to wet floor.

2.5.6 Control System

The control system ensured that the system operated within safe intervals for weight on bit, top drive and hoisting motor torque and speed, and pump pressure. These values were estimated to avoid failure due to buckling, twist-off, burst and vibrations. Safety limits had the highest priority

in the control system. The operating variables were continuously monitored to check that they were within safe ranges. If the variables were outside the safe interval, the system responded accordingly.

It was also very important to have a control system that was highly accurate and responsive. Because the machine was automatic, there were risks related to how the drilling parameters were controlled. Typical problems with control signals were overshooting, slow response and instability. These issues with the control system could have large and dangerous consequences for the system. They could cause slow response to problems, too rapid increases in values or too large variations in parameters to obtain smooth and stable drilling.

2.5.7 Emergency Shutdown of System

Although the drilling process was fully automated, there is always the possibility that uncontrolled situations occur. A manual stop button therefore cut the power supply to the top drive and pump in case of emergency.

The high internal pressure within the drill pipe allowed the drill pipe to withstand the force applied from the hoisting system (This is explained in chapter 3.2.3). One of the concerns when the pump was stopped, was the reduction of the internal pressure within the drill pipe, reducing the drill pipes ability to withstand the force applied by the hoisting motor. It was planned to program the control system to reset the force applied from the hoisting motor on to the drillstring when the emergency button is pressed. This would mitigate injury to personnel and damage to equipment.



Figure 2.5: Emergency stop button attached to the electrical cabinet

2.5.8 Safety Measures Related to Drill Pipe Pressure

As explained in the design, the pressure in the drill pipe was planned to be around 40 bar during operation in order to maintain the drill string in tension. If the drill pipe burst, loose parts could injure personnel and equipment. Plexiglass was therefore set up around the rig structure, isolating the high pressure zones from the working personnel, shown in Figure 2.6. It was also important to have as few people as possible close to the machine and to keep a distance from the machine while it was operating.



Figure 2.6: Plexiglass mounted to the derrick, isolating high pressure zones from working personnel

2.6 Project Risk

Project risk is defined as the possibility that project events do not occur as planned or that events with a negative impact on the project occur. Risk identification in the project is critical in order to manage and complete the project successfully. The earlier the risk can be identified, the earlier the plan can be made to mitigate the effects of the potential risks.

Personnel availability risks were highly significant because the project depended on the expertise and work availability of key personnel. If a person from the team with critical knowledge became unavailable it could cause reduced efficiency, quality and time delay. Each team member had different roles, responsibilities and tasks to complete. To mitigate the risk of reduced personnel availability there was therefore always given an update and a good summary of what had been done to at least one other team member.

Logistics and building risks, such as equipment not being delivered in time or problems with the integration of the different components, can endanger timely delivery and quality of the end product. Taking time to research, plan and organize was a good way to make sure that all equipment was compatible and arrived in time. Having a good backup plan was also useful for worst case scenarios, for example having a local supplier with short delivery time if the equipment is not delivered in time.

A critical project risk that was identified was that components could be found to be unreliable or fail during the testing phase close to the on-site testing date. This could have caused major time delays and a low quality end product. To mitigate this risk it was important to make sure that operations occurred within the safe operating windows and that if a component failed, there were local suppliers that could deliver the equipment on short notice. This was the case for many components, but some of the components could not have been easily replaced.

Poor time management can delay projects severely and in the worst case it may lead to the project not being finished on time. Effective time planning strategies, like time schedules, priority lists and weekly team meetings, were therefore important to make sure that the rig was ready at on-site testing day.

Hardware

In this chapter, the design of the hardware, the reason behind the different design choices and the construction challenges will be presented.

The first section reviews the design of the rig structure itself. The different systems ensuring the functionality of the rig are then presented one by one. The hoisting system provides the vertical movement of the travelling block which applies weight directly on the drill string. The rotary system provides torque to the bit through rotation of the drill string. Finally, the circulation system provides fluid flow to remove cuttings, and cool and lubricate the bit. It also provides pressure in the drill string to increase its geometric stiffness and increase the allowable WOB.

The two following sections present the drill string design and the stabilizing elements at surface designed to reduce the impact of drill string vibrations. Finally, the measurement, control and instrumentation system is reviewed.

Following the rig design, the power consumption of the system is estimated as it is limited to 25 hp by the competition guidelines.

3.1 As-Built Rig Design

The rig design was based on the criteria in the competition guidelines and industry norms. Mobility, functionality, versatility, stability, and safety were the main concerns while designing the rig. The focus was on having a hoisting system and a rotary system with high precision and functionality to ensure an efficient drilling operation. It was important to use equipment that was already available in the university workshop to make the project as cost efficient as possible.

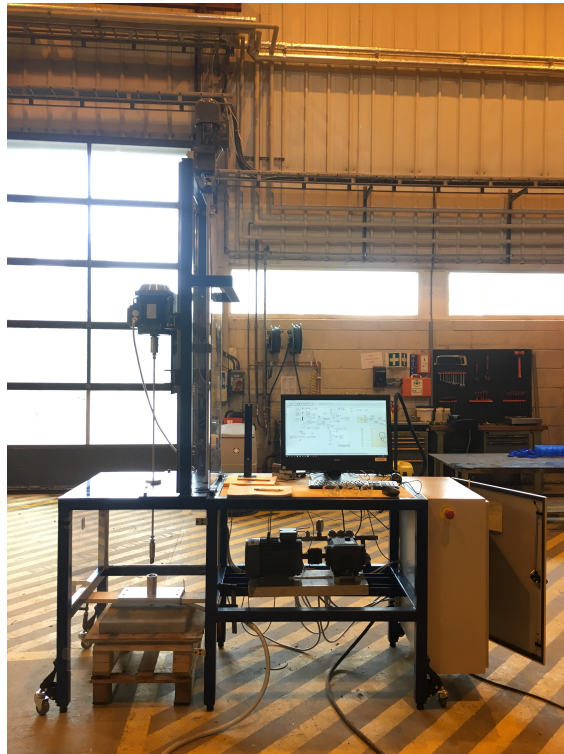


Figure 3.1.1: Overall rig view

3.1.1 Rig Structure

Steel was chosen as construction material for the main structure of the rig to ensure rigidity and stability. It also had the benefit of being cost efficient and easily accessible. Aluminum profiles were also considered, but were not chosen due to their high cost. The total weight of the rig structure was approximately 170kg.

The height of the drilling rig was chosen based on the rock sample height (60 cm) and the total length of the assembled drill string (105.8 cm). Since no making or breaking of connections was required, the length of the drill string was customized to drill through the block in one go. The total length of the drillstring could accommodate a full length of drill pipe (91.4 cm), the BHA (8.0 cm) and the drill bit (13.5 cm). Refer to Figure 3.1.2 and 3.1.3 for illustrations and dimensions of the rig structure.

Because versatility was important when designing the rig, the height and the width of the structure were chosen to allow for a formation height up to 85 cm dependent on the drill string and riser configuration, and a width and length up to 60 cm.

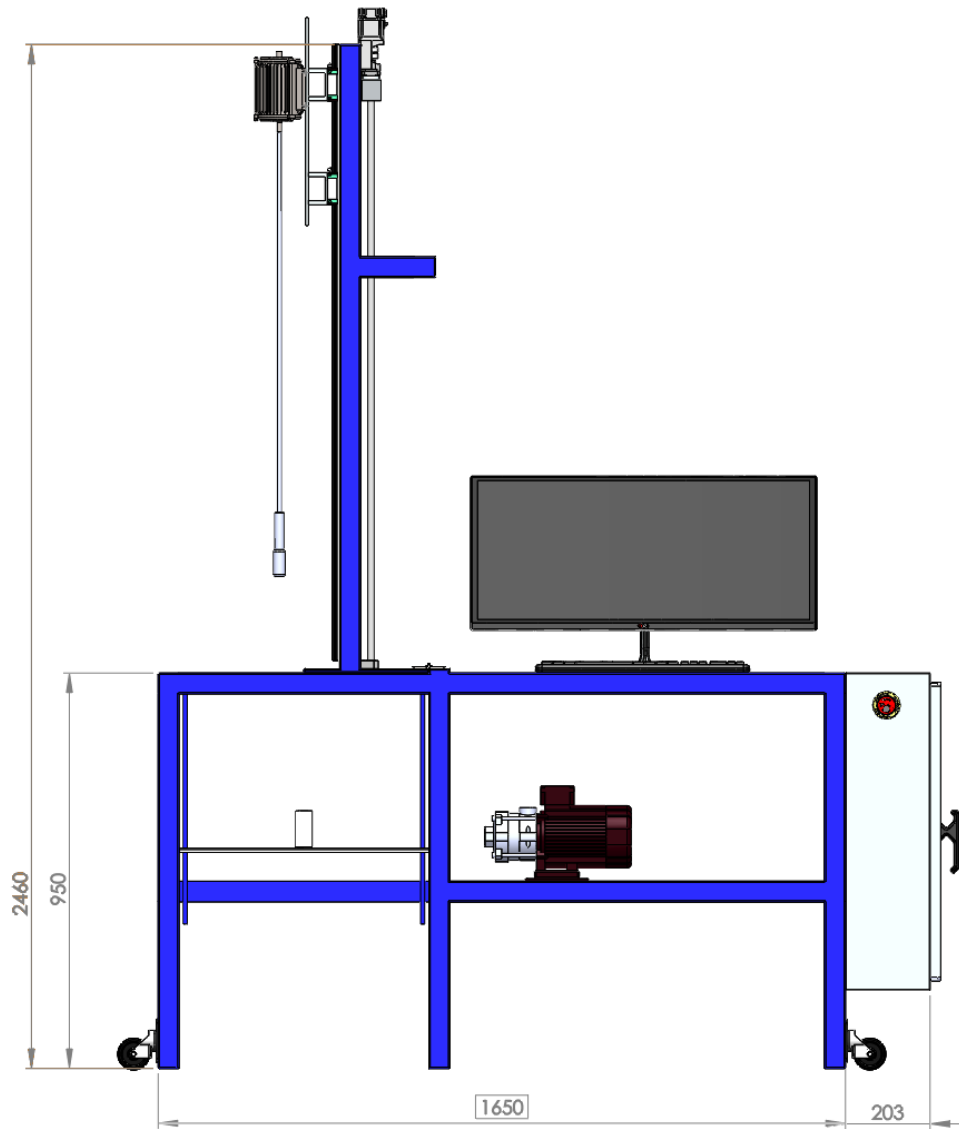


Figure 3.1.2: Side view of the rig in upright position (dimensions in mm)

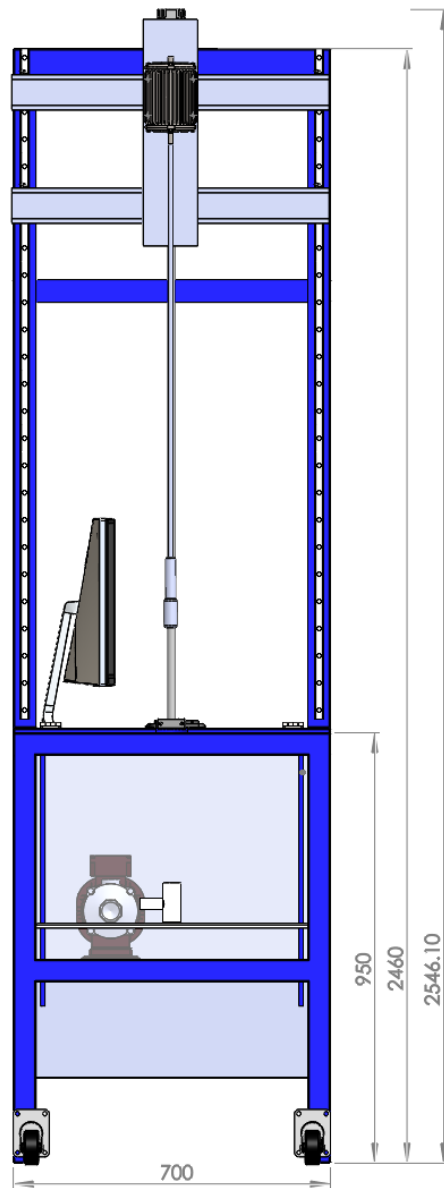


Figure 3.1.3: Front view of the rig in upright position (dimensions in mm)

3.1.2 Mobility of Rig

The drilling rig was designed to be easily moved around, as well as to ensure quick rig up and rig down. Jack up casters were used on each leg so that the rig could effortlessly be operated by one person. The casters also made it possible to put the structure down on its steel legs to ensure stability during operation. The derrick was attached to the rest of the structure by hinges and bolts,

and could be folded down for a steady and safe transport. The structure was designed to be able to pass through a standard doorway, with a folded down height and width of 1.38 m and 0.7 m, respectively. Figures 3.1.4 and 3.1.5 illustrate the folded position of the rig with dimensions.

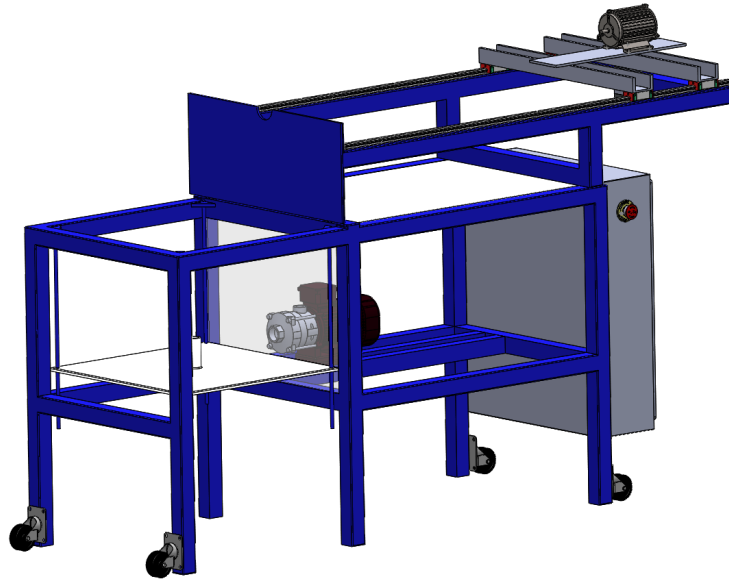


Figure 3.1.4: Illustration of the rig in folded position

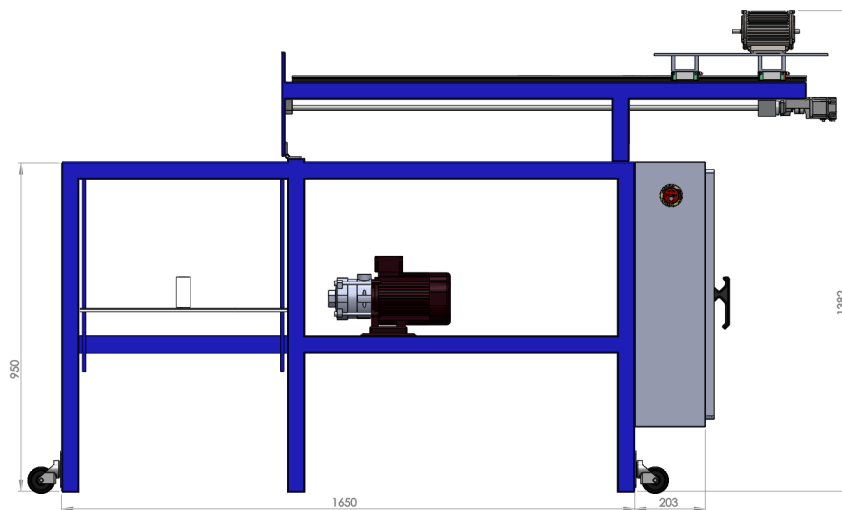


Figure 3.1.5: Side view of the rig in folded position (dimensions in mm)

3.1.3 Hoisting System

The system that provided vertical movement to the drill string to perform the drilling operation will be referred to as a hoisting system. Unlike the traditional hoisting system used in the industry where the weight of the drill string alone provides sufficient WOB, this system needed to be able to push down on the string to add additional weight on the bit. A traditional hoisting system with drawworks was considered during the design phase, but found to be inapplicable because of its complexity and lack of precision. Using a rack and pinion drive was weighed against ball screw drive, where the ball screw was selected due to a higher accuracy and step resolution.

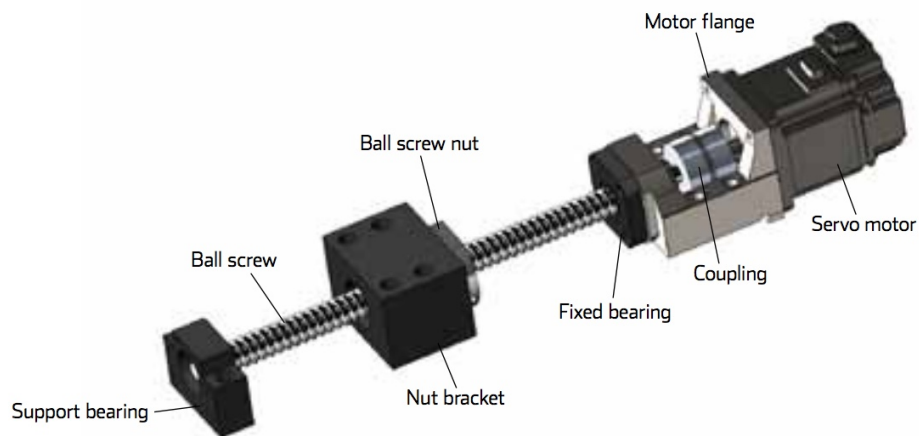


Figure 3.1.6: Illustration of the complete ball screw package (KGT16x5 FGR RH 1 S 1500 G9 AEG) that was used for the hoisting system [8]

The ball screw was driven by an AC-motor. Because of the mechanical advantage of the ball screw, this motor did not need a high torque-output, but rather a high RPM. The power calculations for the motor are shown in section 4.3.

A linear roller guide system was combined with the ball screw to provide stable vertical motion and eliminate horizontal movement.

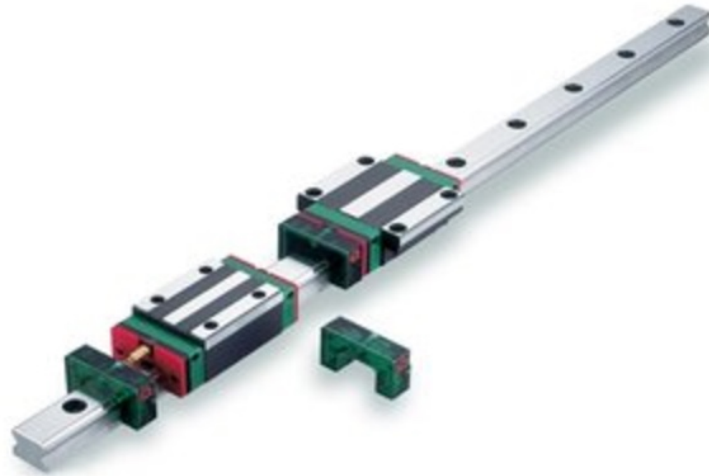


Figure 3.1.7: Illustration of linear roller guide (HGR20R-C-KAPP, HGW20CC-ZO-C VOGN) for hoisting system [7]

A linear roller guide is a low friction system which was able to ensure accurate WOB-measurements and provide stability and high rigidity to the structure. The lead of the ball screw, together with the appropriate motor selection, made it possible to choose the hoisting speed and accuracy. An accurate hoisting system, with a low-lead ball screw, facilitated small incremented and precise WOB changes.

A carriage was attached to the ball screw which translated the rotational motion of the motor to linear motion. To make sure the motion was smooth and stable, the carriage was guided by a set of vertical rails. The purpose of this was to be able to attach a motor to the carriage which provided rotary motion to the drill string while the carriage moved downwards.

3.1.4 Rotary System

The main function of the rotary system was to provide torque to the bit through the drillstring. Both a rotary table and a top drive system were considered during the design phase, where the top drive system was chosen as the best solution. Even though the rotary table system would have made it easier to design the circulation system, top drive systems contain less components and provide higher power efficiency since the motor is directly connected to drill pipe.

The top drive system consisted of a 400 V AC-engine, and the required motor power was discussed in section 3.5. The motor was a 3-Phase squirrel cage motor (3GAA091520-ASJ).

The vertical position of the top drive motor could be adjusted to fit the requirements of the set-up.

3.1.5 Circulation System

The function of the circulation system was to provide fluid flow to remove the cuttings from the borehole and cool and lubricate the bit. In this project it was also used to provide additional pressure in the pipe in order to avoid buckling.

The circulation system consisted of a pump with a water inlet and outlet. It was a single-acting triplex pump, Hawk HC980A, and provided the required pressure to the system. The inlet was connected to a standard water outlet using a conventional garden hose and the outlet was connected to a high pressure hydraulic hose which guided the drilling fluid from the pump to the drill string. The hose was directly connected to a swivel which provided the required rotation to let the drill string rotate while the fluid circulated through the pipe.

To make the swivel withstand the required pressure, a back pressure of 8 bar on the seals had to be applied. This was obtained using a pressure reducing valve from the circulation pump, see Figure 3.1.8.

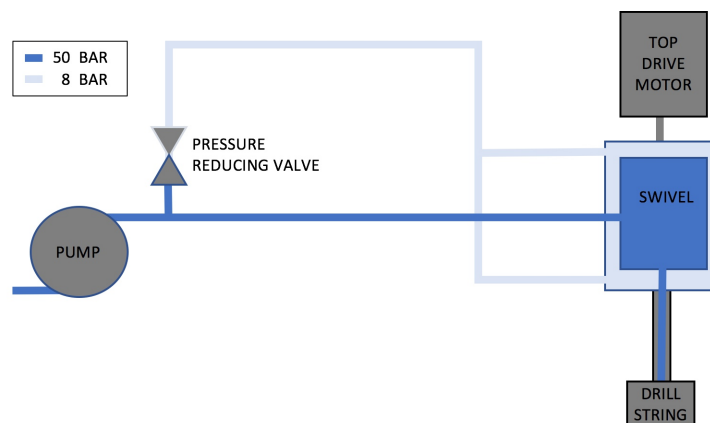


Figure 3.1.8: Illustration of circulation circuit with swivel and pressure reducing valve

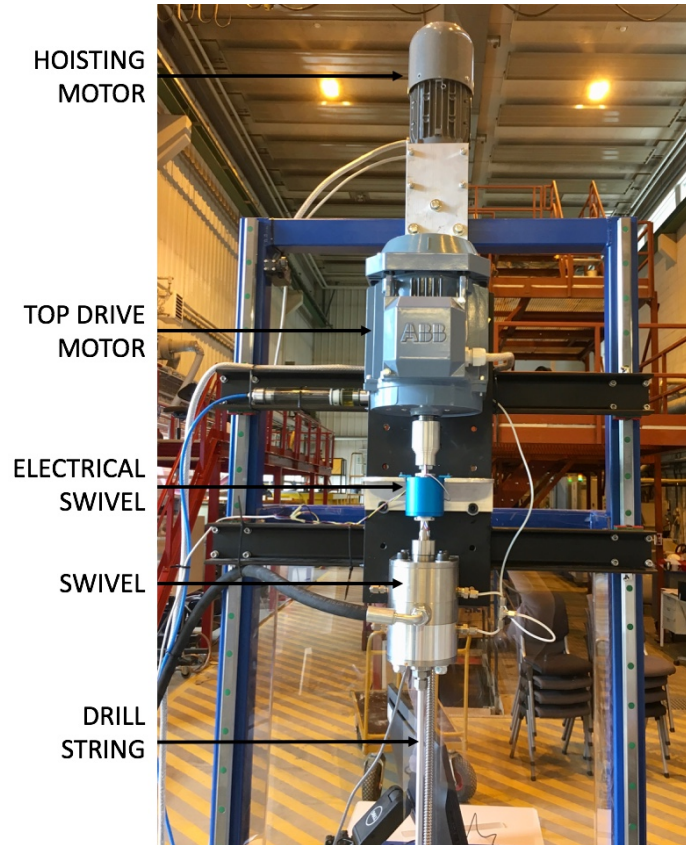


Figure 3.1.9: Overall rig view showing the hoisting motor, top drive motor, electrical swivel, swivel and drill string.

3.1.6 Drillstring Design

The drillstring consisted of a drill pipe and a BHA. The combined length of the drill string was kept as short as possible to mitigate vibrations. It was stated in the competition guidelines that at least one length of drill pipe (91.4 cm) had to be used. The BHA was optimized to fit both the sensors and stabilizer, and had a length of 80 mm. It was also stated in the guidelines that the maximum combined length of stabilizers could not be more than 90mm, where sections within 10% of the bit diameter were considered a stabilizer. Since the surface stabilizer had a length of 15 mm, the stabilizer in the BHA was limited to a length of 75 mm to fulfill the requirements. The drill bit used during the on-site test had a length of 13.5 cm. However, as the guidelines stated that the bit should be less than 6.4 cm, the bit used during the testing phase was 5 cm.



(a) Picture of the bit and BHA used during testing phase



(b) Picture of the bit and BHA used on competition day

Figure 3.1.10: Drill string designs used during testing phase and on the competition day

Figure 3.1.10 shows pictures of the two different bit and BHA configurations that were used. The choice of BHA will be reviewed in Section 3.1.6.1.

3.1.6.1 Bottomhole Stabilizer Design

One of the main judging criteria was the verticality of the borehole. Stabilizers were used to control the hole deviation and counteract vibrations. Several types of stabilizers were considered during the design phase, shown in Table 3.1.1, where the integral blade stabilizer was chosen as the best suited solution due to its durability and strength.

Table 3.1.1: Evaluation of stabilizers

Type	Description	Pros	Cons
Integral blade	Blades are an integral part of the tool body	No risk of leaving components in the wellbore	Difficult to machine, expensive
Welded blade	Blades are welded onto the tool body	Easy to make, cheap	Weak points in welding
Sleeve type	Replaceable sleeve mounted onto the tool body	Replaceable	Needs threading
Non-rotating	Rubber sleeve remains stationary while the string rotates	Less wear on the blades, good for hard formations	Difficult to make, expensive

The main body of the BHA had an outer diameter of 22.9 mm. To minimize frictional forces, the stabilizer blades were designed with an outer diameter of 28 mm, which was slightly smaller than the diameter of the wellbore being drilled. Spiral blades were used, and the distance between the

blades provided enough space to transport cuttings and avoid pressure build-up in the wellbore. An illustration of the stabilizer is shown in Figure 3.1.11.

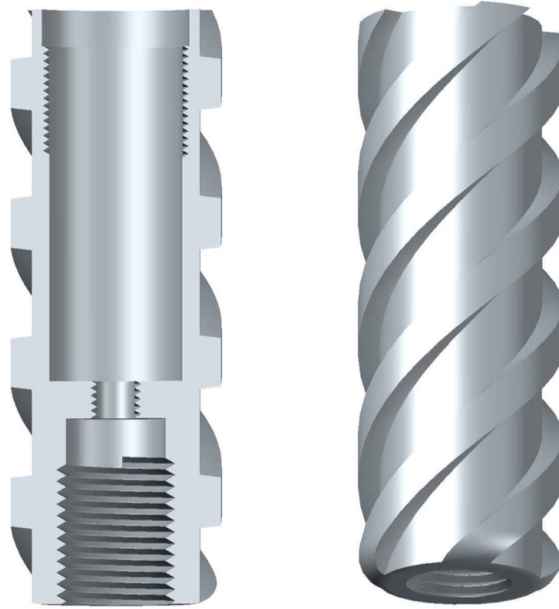


Figure 3.1.11: Illustration of the stabilizer, showing a side cut on the left hand side. Designed by Noralf Vedvik.

3.1.6.2 Tool Joint Design

Hydraulic connections were used as tool joints between the BHA and the pipe as well as between the pipe and the swivel. Since the internal pressure in the drill string was in some cases high, hydraulic connections were chosen. See Figure 3.1.12



Figure 3.1.12: Hydraulic connections used as tool joints between BHA and pipe, and between pipe and swivel

3.1.6.3 Incorporation of Downhole Sensor

It was important to design a BHA that could protect the downhole sensors from the high internal pressure and the flow of water within the pipe. Figure 3.1.13 and Figure 3.1.14 display the design of the BHA. The chosen solution was to put the sensors inside the red circled area in Figure 3.1.13 and mount it to the part below, which served as a sensor-protector (green circle). The main objective of the sensor-protector was to withstand the high internal pressure and protect the sensors placed inside of it. The black O-shaped rubber ring was used to protect the sensors by preventing fluids to flow in. A second device (blue circle), was attached from above. The drill pipe was mounted on the top of it and interconnected the whole system.

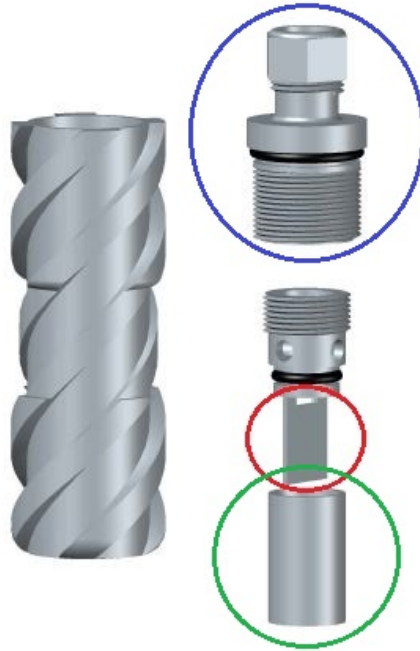


Figure 3.1.13: Illustration of the BHA design, showing where and how the sensors are mounted inside the BHA. The sensors are attached to the plate inside the red circled area (3.1.13) and mounted to the sensor-protector shown inside the green circle. The blue circle shows how the sensor-protector is attached from above. Designed by Noralf Vedvik.

An important feature was how the wires were connected to the sensors. The small space and the high internal pressure narrowed down the possible solutions. A single cable would have had a good chance to withstand the high internal pressure, but would take up space and reduce the fluid flow area. The space needed to accommodate four small wires would on the other hand be far less than for a single large wire, but the ability to withstand pressure would be reduced. The preferred solution was to use four small wires out of the BHA, but gather them into one cable through the drill pipe to make it easier to change if something got broken. Figure 3.1.14 illustrates how the four wires were lead through four small holes inside the BHA.

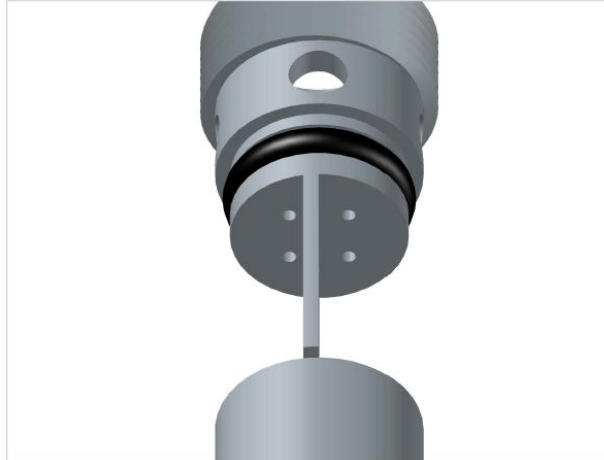


Figure 3.1.14: Another illustration of the BHA design, showing where the four wires from the sensors are lead trough the "sensor-protector" into the drill pipe. Designed by Noralf Vedvik.

An electrical swivel was included in the design to avoid twisting of the sensor wires.

3.1.7 Stabilizing Elements at Surface

Because large and destructive pipe vibrations were expected to occur while drilling, great importance was given to the implementation of features in the design to reduce the magnitude of these vibrations. It was therefore, in addition to the stabilizers in the BHA, added surface stabilizing elements at the surface in the form of a riser, surface stabilizer and drill deck bushing. These features will be presented in the following sections.

3.1.7.1 Riser

A steel plate with a thickness of 10 mm connected to a steel cylinder with a length of 90 mm made up the riser. The riser was attached to the top of the formation by screws. The steel cylinder had an inner diameter of 45 mm in the top 7 mm, an inner diameter of 35 mm in the next 18 mm and an inner diameter of 28.75 mm in the bottom part was welded to the plate. It was centered on the plate and worked as a guiding shoe for the bit. Because the steel cylinder was referred to as a riser in the guidelines, this term will be used in the rest of the text. See Figure 3.1.16 for a picture of the riser.

3.1.7.2 Surface Stabilizer

A linear motion bearing and a radial ball bearing were attached to the drill string on top of the BHA to provide low friction stability. See Figure 3.1.15 for illustrations of the roller bearings.



(a) Illustration of radial ball bearing [19]



(b) Illustration of linear motion bearing [9]

Figure 3.1.15: Illustrations of roller bearings

A hollow cylinder providing weight was placed above the surface stabilizer to keep the stabilizer at bay when drilling. See Figure 3.1.16

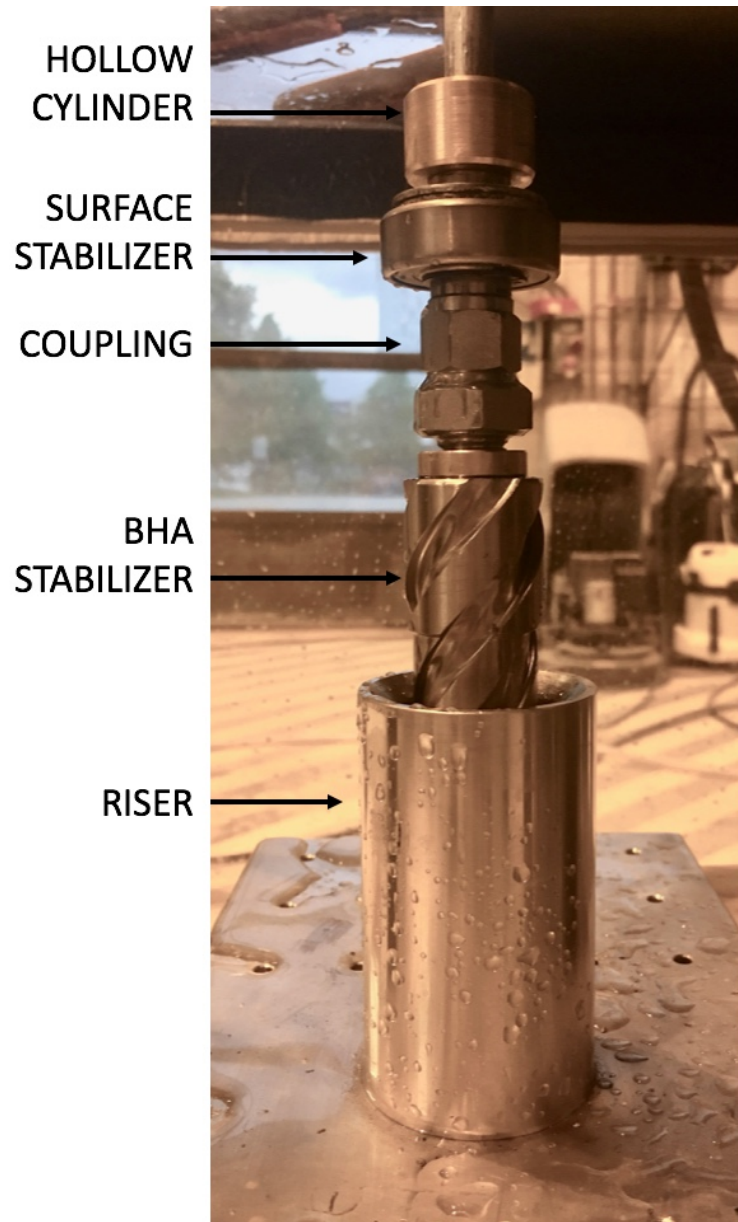


Figure 3.1.16: Picture showing the bottomhole configuration

As the drill string moved through the riser, the two roller bearings were deposited inside the riser. This provided stability for the drill string once the BHA and the bit had entered the formation, and will therefore be referred to as a surface stabilizer. The combination of the riser and the surface stabilizer provided stability during the entire drilling operation. See Figure 3.1.17 for an illustration of this.



Figure 3.1.17: Landing of the surface stabilizer inside the riser. Picture from on-site test day.

3.1.7.3 Drill Deck Bushing

A drill deck bushing, in the form of a linear motion bearing and radial ball bearing, was attached to the drill deck floor and served as a stabilizing element to prevent excessive lateral vibrations and also imitated the actual drilling operation as much as possible. The inner diameter of the roller bearing was slightly larger than the outer diameter of the drill pipe. The pipe was guided through the linear bearing before the BHA and the bit were attached to the string. See Figure 3.1.18 for an illustration.

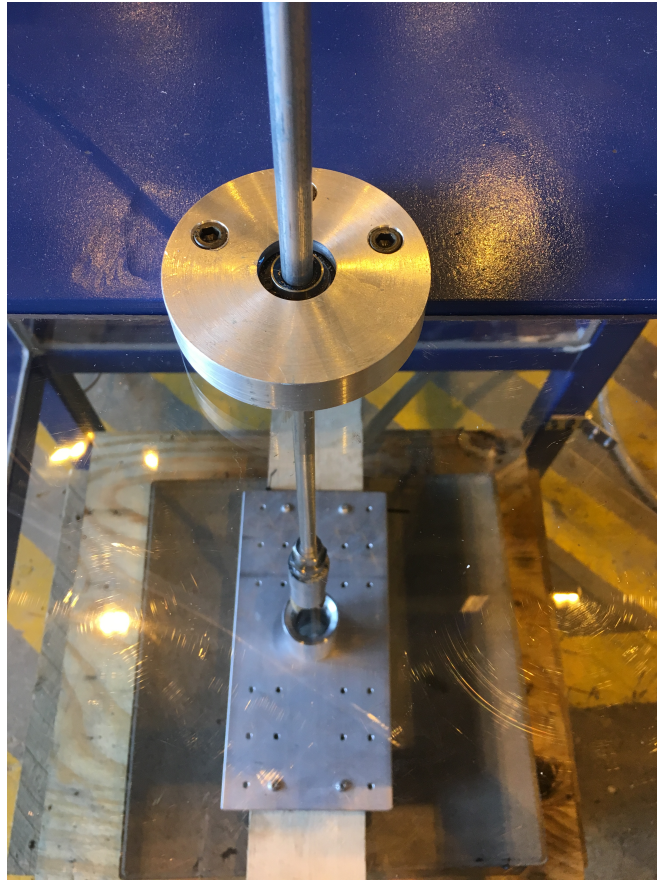


Figure 3.1.18: Drill string running through drill deck bushing

3.1.8 Measurement, Control and Instrumentation System

The drilling operation was controlled by a programmable logic controller (PLC). The PLC received input variables from the sensors and the actuators and transmitted these signals to the PC. The control algorithm in Matlab processed the signals and sent output variables back to the PLC. The PLC could then transmit the output variables to the actuator drives in order to control the motor.

The PLC was provided by ABB and was the Basic Training Case for the AC500 PLC and the CP600 Control Panel.



Figure 3.1.19: Picture of the AC500 PLC [2]

The PLC was programmed using CodeSys and the control algorithm was developed using Simulink in Matlab. The control system and algorithm are reviewed more in depth in chapters 6.1 and 4.2.

The aim of the sensors included in the control system was to measure key drilling variables. Vibration, temperature, inclination and azimuth were measurements planned to be monitored by a downhole sensor. Torque, pump pressure, pump flow rate and carriage position were suggested surface measurements. The measurements were going to be continuously transmitted to and processed by the PLC which in turn would send signals to the hoisting motor, top drive and pump to adjust the WOP, RPM and pressure.

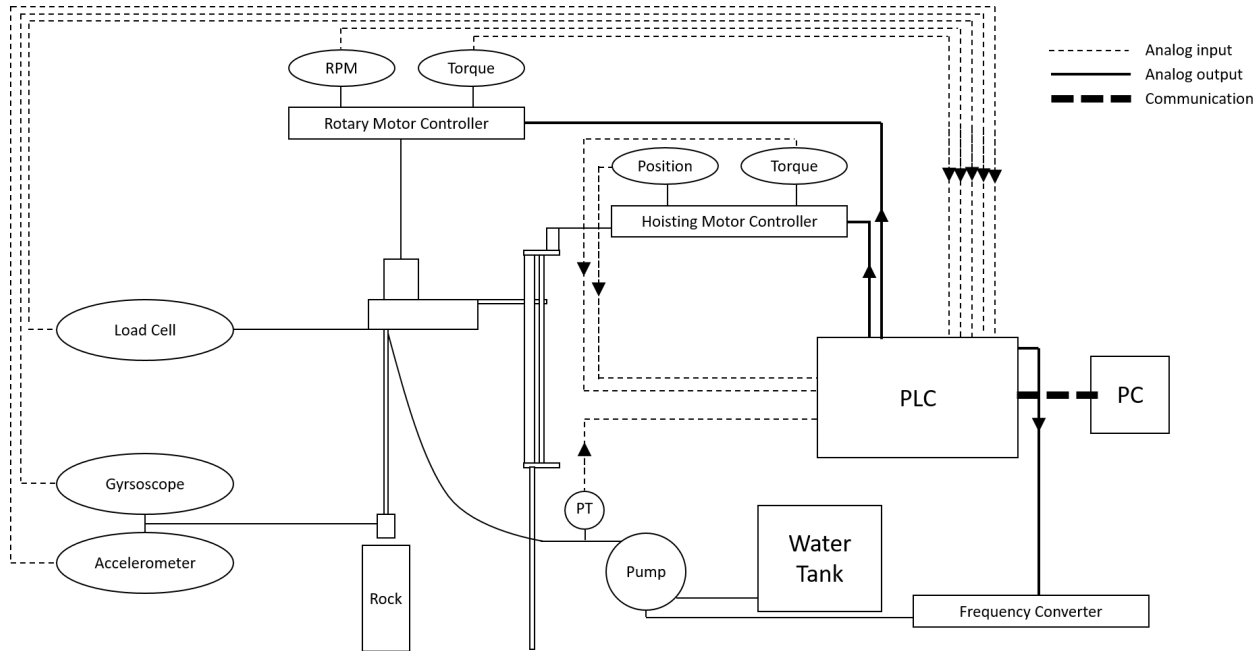


Figure 3.1.20: Control system flow chart

3.1.8.1 Measurement and Sensors

The analog data from the sensors was planned to be transmitted to the PLC through wires which were placed inside the drill pipe, along the pipe wall. Wireless transmission was considered, but the water in the drill pipe, the thickness of the pipe wall and the rotation of the string, were expected to cause noise which would have made the data unreliable.

No sensor is perfect and even sensors from the same manufacturer can yield different readings. In addition to this, the sensors may change response if they are subjected to varying conditions like heat, humidity and shocks. Calibrating the sensors was therefore important to build and operate a complete automated drilling system.

Direct output from motors The RPM and the torque were direct outputs from the top drive motor. ROP was estimated from the direct position output of the hoisting motor.

Surface sensors The following sensors were the sensors that made measurements at surface. Some of these measurements approximated downhole measurements.

Load cell A load cell is a transducer which converts force into a measurable electrical output. It

measures the tension in the drill string at surface, but the WOB can be estimated by suspending the bit off bottom. As the bit is lowered and touches bottom, the hook load decreases by an amount equal to the WOB. It was positioned between the ball screw nut and the carriage. The load cell that was used was the model S2M from HBM and was supplied by the university [18].

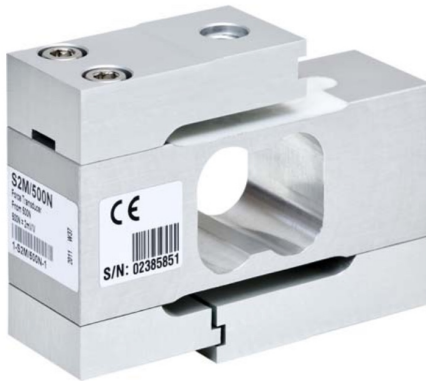


Figure 3.1.21: Load cell, HBM S2M [18]

Pressure transducer A pressure transducer converts pressure into an analogue electrical signal. The main benefit of including this sensor was to be able to estimate the pressure in the different components of the circulation system. The pressure transducer that was planned to be used was the model PA-25EI from Keller Druck and was supplied by the university [3].



Figure 3.1.22: Pressure transducer, Keller Druck PA-25EI [3]

Downhole sensors An accelerometer and a gyroscope were included in the same sensor in the BHA which was placed over the constriction. This was expected to cause some difficulty for both the integration of the sensor in the BHA due to its small diameter and for data telemetry due to the fluid circulation in the drill string and the small diameter of the drill pipe.

Accelerometer The accelerometer measured vibration, or acceleration, in the BHA. Its main use was going to be monitoring the amplitude of the vibrations.

Gyroscope The gyroscope was going to provide estimates of inclination and azimuth by measuring the angle of deflection from the vertical. As the verticality of the borehole was an important factor during the competition, it was a valuable measurement.

The downhole sensor that was used was the model MPU-6000 from InvenSense, which is the first 6-axis motiontracking device; combining a 3-axis gyroscope and a 3-axis accelerometer [20].

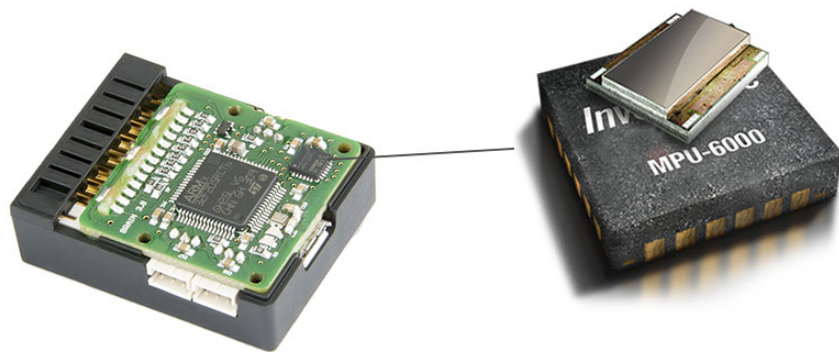


Figure 3.1.23: Downhole sensor, MPU-6000 [20]



Figure 3.1.24: Picture of implemented downhole sensor

3.1.9 Construction Cost

The cost of the rig and materials for 2016-2017 Drillbotics™ competition was limited to US\$ 10,000. The total rig cost was approximately 7,500 USD. The cost estimate from the design phase and the actual total cost are shown in Figure 3.1.9.

Components that were already owned by the university or borrowed from companies are not included in the total expenses as they are free of cost.

The total expenditures were covered by funding from the Department of Geoscience and Petroleum at NTNU and Statoil.

Description	Cost Estimate				Actual Cost		Comment	Source
	Cost per Unit	Amount	Total Cost		Total Cost			
Rig Structure								
Steel pipe (50x50x3 (mm))		17,9 m	1 127,52	NOK	1 311,65	NOK		E. A. Smith AS
Steel pipe (50x80x3 (mm))		0,7 m	489,02	NOK	-		Provided by NTNU	
Steel pipe (100x40x3 (mm))		0,7 m	542,59	NOK	-		Provided by NTNU	
Steel plate (600x600x10 (mm))		0,36 m	138,24	NOK	-		Provided by NTNU	
Hinge	200,00	2	400,00	NOK	-		Provided by NTNU	
Table top (wood)		2	600,00		350,00	NOK		Byggmakker
(Powertech 17000 Workbench Caster Kit)	120,00	6	720,00	NOK	2 186,14	NOK		Amazon
Hydraulic System								
Pump (HAWK HC980A)		1	-		-	NOK	Owned	
Hose		2,5 m	925,00	NOK	925,00	NOK		TESS
Safety Valve	400,00	1	400,00	NOK	-	NOK	Owned	
Electrical swivel					2 508,30	NOK		Senring
Sealing Swivel primary (ASL-610R-0200-C-2413)	1 940,00	1	1 940,00	NOK	1 990,00	NOK		Otto Olsen AS
Sealing Swivel secondary (B2PT-20x30x7-10/FS6101)					690,00	NOK		Otto Olsen AS
Swivel Sealing DBS					149,83	NOK		TESS
Swivel O-Ring					732,00	NOK		Abra Kulelagersenter AS
Linear Motion and Rotating Equipment								
Hiwin rail (HGWR20R-C-KAPP, 1.48m)	938,80	2	1 877,50	NOK	2 270,00	NOK		Aratron
Hiwin wagon (HGW20CC-ZO-C)	686,90	2	1 373,80	NOK	1 680,00	NOK		Aratron
Ball screw (KGT16X5 FGR RH 1 S 1500 G9 AEG)	3 294,40	1	3 294,40	NOK	5 216,25	NOK		Aratron
Bearing fix					1 097,50	NOK		Aratron
Bearing support					302,50	NOK		Aratron
Hoisting servomotor (NX620MC-3+PLE060+CC051F-USB)	8 000,00	1	8 000,00	NOK	21 887,50	NOK		Aratron
Shaft coupling					385,00	NOK		Aratron
Top drive frequency converter (ACS880-01-05A6-3+K473)	9 000,00	1	9 000,00	NOK	8 600,00	NOK		ABB/KYMAR
Top drive motor (3GAA091520-ASJ)	5 625,00	1	5 625,00	NOK	1 950,00	NOK		ABB/KYMAR
Sensors								
Accelerometer, gyroscope and temperature sensor		1	70,00	NOK	70,00	NOK		
Load cell		1	-	NOK	-	NOK	Owned	
Other								
Machining/raw materials					-	NOK	Provided by NTNU	
Electrical cables					-	NOK	Provided by NTNU	
Drill pipes	200,00	3	600,00	NOK	48,58	NOK		Hobbylink
Plexi glas					1 295,00	NOK		VINK Norway AS
Tool joint (SS-600-1-8)	300,00	1	300,00	NOK	241,00	NOK		Swagelok
Signal/control cable					457,50	NOK		Ahlsell
Rubber cable					352,41	NOK		Ahlsell
Cam Switch P1-32/EA/SVB					863,24	NOK		Ahlsell
Circuit breaker iC60H 4P 20A/C					322,41	NOK		Ahlsell
Electrical cabinet (80x60x30 (cm))					2 649,00	NOK		Ahlsell

Ball bushing linear motion bearing 3/8 inch 0.375 inch ID					933,00	NOK		Ebay
Radial ball bearing (5/8in bore x 35 mm x 1 mm rubber seal shield)					352,00	NOK		Ebay
JB J-B Weld 8265-SS Original					219,00	NOK		Ebay
PLC (TA512 - BAS Basic Training Case - 1SAP182400R0001)					-	NOK	Provided by ABB	
Computer		1		-	-	NOK	Owned	
Equipment for cementing rock samples					700,00	NOK		Byggmakker

TOTAL			37 423,07	NOK	62 734,81	NOK		
			4 447,58	USD*	7 455,78	USD*	*currency 04.06.2017	

3.2 Power Consumption

The power system consisted of a top drive motor, a hoisting motor, a fluid pump and a computer. As stated in the guidelines [13], the total power consumption could not exceed 25 hp, equivalent to 18.64 kw. This is a large value which meant that the fatigue of the system components was the limiting factor rather than the electric power available. However, the operation should be as energy efficient as possible and the expected electrical loads were therefore calculated.

3.2.1 Top Drive Motor

The top drive motor, which was the main element of the rotary system, was dimensioned from the pipe torque limit, as the drill pipe was considered to be the weakest element in the system. The torque limit for the drill pipe was calculated using the triaxial failure criterion showed in equation (3.2.1) [5]. The critical point was set to be at the top of the drill pipe, where the largest axial force and internal pressure were felt.

$$(\sigma_{\theta} - \sigma_z)^2 + (\sigma_r - \sigma_{\theta})^2 + (\sigma_z - \sigma_r)^2 = 2\sigma_{ys}^2 \quad (3.2.1)$$

σ_{θ} is the tangential stress (Pa) given by equation (3.2.2), σ_r is the radial stress (Pa) given by equation (3.2.3), σ_z is the axial stress (Pa) given by equation (3.2.4), τ is the shear stress (Pa) and σ_{ys} is the yield strength of aluminum (Pa).

$$\sigma_{\theta} = \frac{\left(\frac{d_o}{2}\right)^2 + \left(\frac{d_i}{2}\right)^2}{\left(\frac{d_o}{2}\right)^2 - \left(\frac{d_i}{2}\right)^2} \quad (3.2.2)$$

$$\sigma_r = -P_i \quad (3.2.3)$$

$$\sigma_z = \frac{\left(\frac{d_i}{2}\right)^2 P_i}{\left(\frac{d_o}{2}\right)^2 - \left(\frac{d_i}{2}\right)^2} \quad (3.2.4)$$

P_i is the internal pressure in the pipe (Pa), d_o is the outer diameter of the pipe (m) and d_i is the inner diameter of the pipe (m).

The torque limit for the pipe was then calculated using equation (3.2.5) [5].

$$T_{crit} \approx \tau_{crit} \frac{\pi}{4} (d_o^2 - d_i^2) \frac{d_o + d_i}{4} \quad (3.2.5)$$

T_{crit} is the critical torque limit (Nm) and τ_{crit} is the critical shear stress (Pa).

The yield strength of the aluminum pipe provided by DSATS was 120 MPa (1200 bar) [1], the outer diameter of the pipe was 9.53 mm, the inner diameter of the pipe was 7.75 mm and the internal pressure was 5.26 MPa (52.6 bar) which was calculated in section 4.1.3.1. The result of the pipe critical shear stress calculation was 55.66 MPa (556.6 bar). This gave a critical torque limit of 5.80 Nm.

Shaft power for the top drive motor can be estimated using equation (3.2.6) [4].

$$P = \omega T \cdot \frac{1}{\varepsilon} \quad (3.2.6)$$

P is the power which in this case was the shaft power for the top drive motor (W), ω is the angular velocity of the shaft (rad/sec) given by equation (3.2.7), T is torque (Nm) and ε is the efficiency factor (dimensionless).

$$\omega = \frac{2\pi N}{60} \quad (3.2.7)$$

N is the number of revolutions per minute (RPM).

Since this system was small scale compared to a real drilling rig, and had a very unconventional bit size, it was hard to give a good estimate of the RPM interval limits. To give a rough estimate of the upper limit, a 1.125 bit would have 2,000 RPM to get the same tangential speed as a 12.25 bit with a rotational speed of 300 RPM. Critical RPM values for the system had to be avoided to reduce the

impact of large vibrations.

Using the critical torque value of 5.80 Nm, an RPM of 2,000 and an efficiency factor of 0.9, the power consumption of the top drive motor was calculated to be 1,350 W. This was not a fixed value and RPM had to be adjusted according to the critical values for the system.

3.2.2 Hoisting Motor

The hoisting motor power was calculated in the same way as for the top drive motor, using equation (3.2.6). Torque was estimated using equation (3.2.8), which was given in the ball screw specifications [8].

$$T = \frac{F \cdot l}{2\pi \cdot \varepsilon_{BS}} \quad (3.2.8)$$

F is the force acting on the ball screw (N) and l is the lead of the ball screw (m). The total force acting on the ball screw, from weight of drill string, stiffening force, top drive motor and carriage, was estimated to be 491 N. To ensure precision while drilling, the lowest available ball screw lead was chosen. Aratron was chosen as supplier and their smallest available lead was 5 mm. The efficiency factor for the ball screw was set as 0.90 [8]. Torque was then estimated to be 0.43 Nm.

To provide a rough estimate of the power consumption of the hoisting motor, the carriage was estimated to be able to move from top to bottom of the guide system within 10 seconds, which resulted in an RPM of 1,440. The efficiency factor for the hoisting motor was set as 0.9 [15], and the motor power required was calculated to be 73 W using equation (3.2.6).

The power consumption varied according to the required carriage speed, but as this was only a rough estimate, the exact speed was not required.

3.2.3 Fluid Pump

The fluid pump supplied power to the circulation system to ensure proper hole cleaning and to provide geometric stiffness by increasing the internal pressure of the drill string.

The power of the pump was calculated using equation (3.2.9).

$$P_P = pQ \cdot \frac{1}{\varepsilon} \quad (3.2.9)$$

P_P is the power of the pump (W), p is the pump pressure (Pa) and Q is the flow rate (m³/s).

The factors limiting the power of the pump were the maximum pump pressure and minimum pump flow rate. The maximum pressure was estimated from the burst pressure of the pipe, as calculated in section 4.1.3.1, and was found to be 5.26 MPa (52.6 bar). The flow rate was estimated from hole cleaning requirements, as calculated in section 4.1.3.2, and was found to be 0.00014 m³/s. The pump efficiency was set to be 0.9, which is a typical value for piston pumps [32]. The power of the pump was then calculated to be 775 W.

3.2.4 Computer

The computer used for the control system used approximately 70 W, which is a maximum value for a general laptop.

3.2.5 Summary

The power distribution for the two motors, the pump and the computer is presented in table (3.2.1). The total estimated power consumption was 2.27 kW, which was only 12% of the power consumption limit of 18.64 kW.

Table 3.2.1: System power distribution

Component	Power [kW]
Top Drive Motor, P_{TD}	1,350
Hoisting Motor, P_H	73
Fluid Pump, P_P	775
Computer, P_C	70

Pre-Study

Several different topics had to be reviewed before starting implementing the control system or test drilling in order to understand the strengths and limitations of the system.

The physical limitations related to the requirement to use a thin-walled aluminum pipe will be reviewed first. It is expected that buckling will occur easily in such a weak pipe and calculations have therefore been conducted to try to estimate how easily the pipe will fail and how this can be prevented.

To build and operate a fully automated drilling system it was important to have a reliable control system. This included developing a good control algorithm and ensuring fast and accurate data handling.

To be able to develop a control algorithm that would ensure a safe and efficient drilling operation a pre-study on typical drilling dysfunctions and drilling optimization was conducted.

To get an idea of how the control system should operate, a simulator was developed in the early phase of construction. An overview of the choices made and the lessons learned from running simulations is presented in the last section.

4.1 Compression Analysis

Buckling was expected to be one of the main sources of pipe failure based on the weakness of the pipe provided by DSATS [13] and reports from previous contests. The drill string was therefore designed to address this issue and thus limit the risk of buckling.

Buckling occurs when too much weight is applied at the top of the drill string. This puts the pipe in a state of compression where it starts to deflect laterally and becomes prone to increased metal fatigue failure. Furthermore, the body of the drill pipe wears rapidly due to abrasion along the wall. The worst-case scenario is that the pipe fails because of buckling.

The buckling limit can be estimated using Euler's buckling load. However, because there was a high risk of experiencing drilling dysfunctions related to the weakness of the pipe, the aim was to completely avoid entering a state of compression.

Buckling can be prevented by increasing the tension of the drill string and thus avoiding entering a state of compression. There were two ways to achieve this, one was to reduce the weight applied at the top and the other was to increase the weight in the lower part of the string.

Although reducing the weight applied by the top drive was a simple and effective solution, it limited the amount of weight applied on the bit and thus slowed down the drilling speed. Increasing the weight in the lower part of the string, in this case the BHA, was therefore chosen as the best solution.

In the industry, the weight of the BHA is increased by adding drill collars and heavy-weight drill pipes, however, the scale of this project made it difficult to add sufficient weight in this manner. The proposed solution was therefore to increase the tension in the pipe wall by increasing the internal pressure of the pipe. This could be achieved by adding a nozzle in the BHA which increased the internal pressure and resulted in a force, F_c , acting downwards on the constriction area.

The sum of the weight of the drill string and the force F_c defined the limit of the weight that could be applied by the top drive. It also enabled the estimation of the required diameter of constriction. In addition to this, Euler's critical load was estimated to provide the absolute maximum weight that

could be applied to the top drive. After having performed these calculations, the pressure drop in the circulation system was calculated to be able to determine the force F_c . Following this, the estimation of the constriction diameter was made.

A summary of the drill string compression analysis is given in Section 4.1.3.6. Finally, an overview of the changes made during Phase II are presented in Section 4.1.3.7.

4.1.1 Euler's Critical Load Analysis

Even though the main goal was to keep the drill string completely in tension, it was not possible to predict how much WOB would be required to drill through the formation before testing the machine. To set a theoretical absolute upper limit for WOB, Euler's equation (4.1.1) for critical load was therefore used. This enabled the estimation of the maximum load the pipe could theoretically bear without experiencing lateral deflection [28].

$$F_{cr} = \frac{\pi^2 EI}{(KL)^2} \quad (4.1.1)$$

where F_{cr} is the critical compression load (N) on the drill pipe, E is the modulus of elasticity of pipe material (Pa), I is the minimum area moment of inertia of the cross section of the pipe (m^4) given by Equation 4.1.2[38], L is the unsupported length of the pipe (m) and K is the effective length factor determined by the end conditions of the pipe given in Figure 4.1.1.

$$I = \frac{\pi}{64}(d_o^4 - d_i^4) \quad (4.1.2)$$

where d_o and d_i is the outer and inner diameter of the pipe respectively.





End Condition:	Pinned-Pinned	Fixed-Fixed	Fixed-Pinned	Fixed-Free
Illustration:				
Theoretical Effective Length Factor, K:	1	0.5	$1/\sqrt{2}$	2
Recommended Effective Length Factor, K:	1	0.9	0.9	2.1

Figure 4.1.1: End conditions of pipe [28]

Due to the implementation of a riser above the formation, the end conditions were *fixed-fixed*, which yielded a recommended effective length factor, K , of 0.9.

Input data for Equation 4.1.1 can be found in Table 4.1.1.

Table 4.1.1: Input data for Euler’s critical load

E [Pa]	$6.9 \cdot 10^{10}$
I [m ⁴]	$2.27 \cdot 10^{-10}$
K	0.9
L [m]	0.91

The critical load was found to be 230.7 N, equivalent to a weight of 23.5 kg. It was therefore estimated that the pipe would enter a state of compression when the WOB passed 23.5 kg, when no internal pressure is added. When the internal pressure was added, it was estimated that the drillstring would not buckle until it reached the sum of F_c , the drill string weight and the critical load, in this case 46.9 kg. This is described in the next sections.

4.1.2 Weight of Drill String

The weight of the drill pipe may be estimated using Equation 4.1.3.

$$m_{DP} = \frac{\pi}{4}(d_o^2 - d_i^2)\rho_{al}L \quad (4.1.3)$$

m_{DP} is the total mass of the drill pipe (kg), d_o is the outer diameter of the drill pipe (m), d_i is the inner diameter of the drill pipe (m), ρ_{al} is the density of the aluminum (kg/m^3) and L is the length of the pipe (m).

The outer diameter of the drill pipe was 9.53 mm, the inner diameter was 7.75 mm, the density of aluminum was assumed to be $2,750 \text{ kg/m}^3$, and the length was 91.4 cm. This gave a total drill pipe weight of 0.061 kg.

To be able to make design choices, the weight of the BHA was estimated to be 0.227 kg and the weight of the bit to be 0.300 kg. These weights were based on initial estimations and were not the exact weights of the BHA and bit that were used during the competition. The total weight of the drill string was therefore initially estimated to be 0.588 kg.

The buoyed weight of the string can be calculated using Equation 4.1.4 [5].

$$m_B = m_{DP}\left(1 - \frac{\rho_w}{\rho_{al}}\right) + (m_{BHA} + m_{bit})\left(1 - \frac{\rho_w}{\rho_{steel}}\right) \quad (4.1.4)$$

The density of steel was assumed to be $7,750 \text{ kg/m}^3$ which resulted in a total buoyed weight of 0.498 kg.

4.1.3 Magnitude of Force F_c

The magnitude of F_c was determined to be able to estimate how much weight could be applied through the top drive without putting the drill pipe in a state of compression. This is illustrated in Figure 4.1.2.

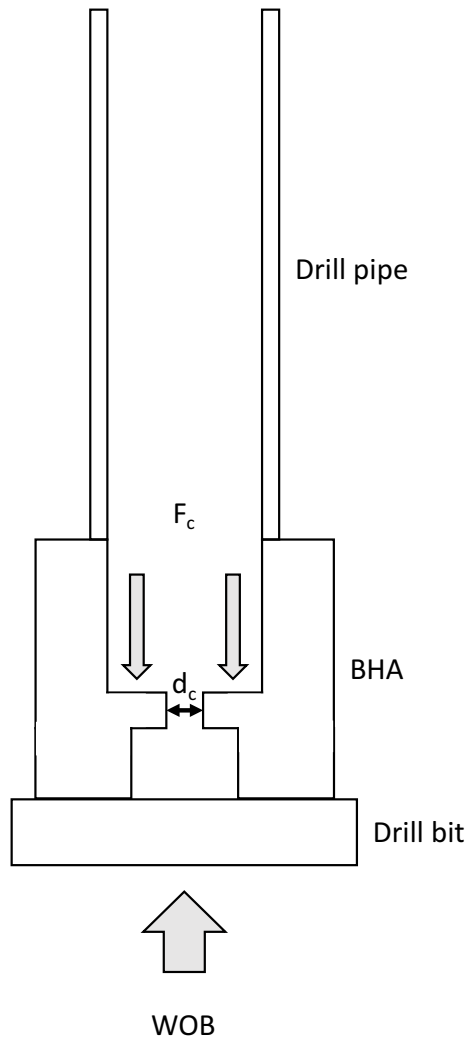


Figure 4.1.2: Illustration of force F_c counteracting the WOB and increasing the tension in the drill pipe wall

The first step was to calculate the burst pressure of the pipe as it is the limiting factor of the system. Following this, the minimum fluid velocity was estimated in order to calculate the pressure losses through the different components in the circulation system. These results made it possible to estimate the maximum value of F_c and thus the maximum pump pressure. Finally, estimating the pressure drop over the constriction enabled the dimensioning of the constriction.

4.1.3.1 Burst Pressure

The limiting factor of the system was the risk of burst in the aluminum drill pipe due to the increased pressure used to counteract the WOB. Barlows formula, Equation 4.1.5, was used to determine the ultimate burst pressure [5].

$$p_{br} = 0.8 \frac{2\sigma_{ys}t}{d_o} \quad (4.1.5)$$

p_{br} is the maximum internal pressure the pipe can withstand (Pa), σ_{ys} is the yield strength of aluminum (Pa), t is the wall thickness of the pipe (m) and d_o is the outer diameter of the pipe (m).

The yield strength of aluminum was assumed to be 96.5 MPa (965 bar), the safety factor was chosen as 3, the thickness of the pipe wall was 0.89 mm and the outer diameter of the pipe was 9.53 mm. The burst pressure of the drill pipe was estimated to be 5.26 MPa (52.6 bar).

4.1.3.2 Pressure Loss in Circulation System

The main purpose of the circulation system of this drilling rig was to provide additional internal pressure in the drill pipe to increase its geometric stiffness and reduce the risk of buckling. In addition to this, the circulation system facilitated the removal of cuttings, cooled and lubricated the drill string and bit.

Fresh water was selected as drilling fluid to enable the circulation of cuttings out of the well. The use of mineral oil was considered, but due to the limited distance of transportation and the expected low pore pressure, it was concluded that fresh water was a better choice. This was a cheaper and more accessible alternative to standard drilling muds used in the industry.

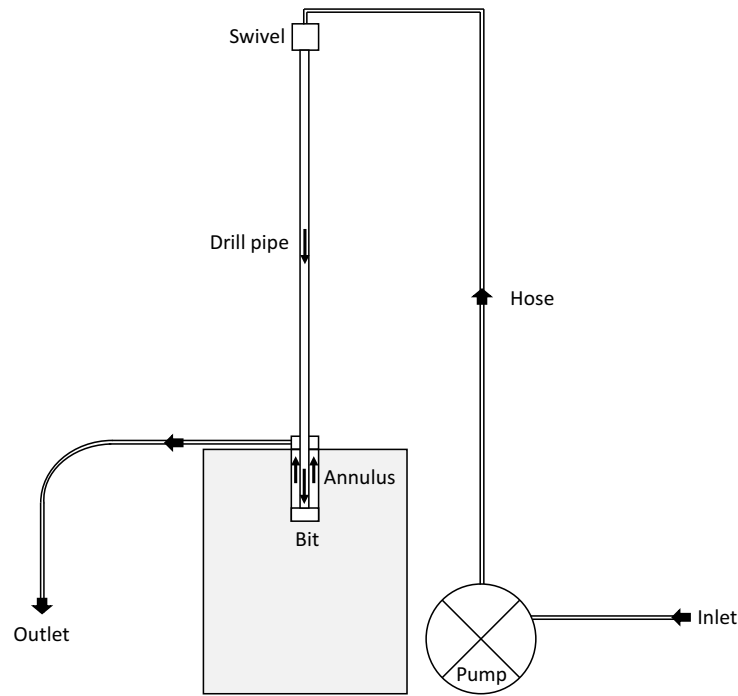


Figure 4.1.3: Illustration of the circulation system consisting of a mud pump, hose, swivel, drill pipe, BHA, bit nozzles and flowline.

A pump was used both to circulate the drilling fluid through the system and increase the internal pressure of the drill string. The re-circulation of drilling fluid was not included in this design as it required an advanced solid removal system. The fluid was conducted out of the well and into a separate tank for storage or to a drain.

A density of 998.2 kg/m^3 and dynamic viscosity of 0.001002 Pas were used in the pressure loss calculations. This was chosen based on the properties of water at a temperature of 20 [40].

The fluid velocity through the different components was determined based on the minimum required flow velocity in the annulus to circulate the cuttings out of the well. It was decided that the flow rate would be maintained constant during the drilling operation.

Fluid flow velocity To remove cuttings from the wellbore, the annular velocity had to be greater than the cutting slip velocity. The cutting slip velocity was estimated using equation (4.1.6) which is valid for all Reynolds numbers [4].

$$v_{sl} = \sqrt{\frac{d_s (\rho_s - \rho_f)}{f \rho_f}} \quad (4.1.6)$$

d_s is the particle diameter (m), ρ_s is the solid density (kg/m³), ρ_f is the fluid density (kg/m³) and f is the friction factor.

The maximum particle diameter was in this case assumed to be half the distance between the borehole wall and the outer diameter of the BHA, resulting in a particle diameter of 0.7 mm. The solid density was assumed to be 2,640 kg/m³ (based on the density of granite). The friction factor f could be estimated using an empirical relationship between Re, the sphere diameter and the sphericity. Because Re is dependent on the unknown slip velocity, an initial simplifying assumption was made. To calculate the initial Reynolds number, the slip velocity v_{sl} was approximated by Stokes relation for creeping flow around a spherical particle given by Equation 4.1.7 [4].

$$v_{sl} = \frac{d_s^2 (\rho_s - \rho_f)}{\mu} \quad (4.1.7)$$

The initial guess for the particle slip velocity was 0.42 m/s. Re was then calculated based on the input data and the particle slip friction factor based on the empirical friction factor chart [4]. Assuming a sphericity factor of 1, the friction factor was expected to be 0.6. This resulted in a cutting slip velocity of 0.16 m/s.

Iterations were then performed until a good approximation was found. The final cutting slip velocity was found to be 0.12 m/s. Based on the assumption that is usually desirable to have a transport efficiency, Equation 4.1.8 [4], of 50% or higher, the aim was to have an annulus fluid velocity of 0.25 m/s.

$$v_a = \frac{v_{sl}}{\text{transport efficiency}} \quad (4.1.8)$$

Assuming a constant flow rate throughout the system, the minimum flow rate delivered by the pump was determined by multiplying the annulus velocity by the annulus cross-sectional area. The

borehole diameter was approximated by the bit diameter, 28.6 mm, and the outer diameter of the pipe was 9.53 mm, this yielded a cross-sectional area of 570.1 mm². The minimum flow rate in the system was estimated to be 0.00014 m³/s based on these calculations.

The fluid velocity in the different components of the circulation system could then be calculated based on the above results.

Pressure loss in hose The first step in the process of calculating the pressure drop through the hose was to determine the type of flow regime. This was done by estimating Reynolds number given by Equation 4.1.9 [4].

$$Re = \frac{\rho v d_i}{\mu} \quad (4.1.9)$$

Re is Reynolds number (dimensionless), ρ is the fluid density (kg/m³), v is the fluid velocity (m/s), d_i is the inner diameter of the pipe (m) and μ is the fluid viscosity (Pas). The density and the viscosity were presented in Section 4.1.3.2.

The inner diameter of the hose was assumed to be 7.75 mm, the same as for the pipe. This was an initial estimate as the exact dimensions were not known during the design phase.

Flow with $Re < 2,500$ is defined as laminar, $2,500 < Re < 4,000$ as transitional and $Re > 4,000$ as turbulent [4]. Table 4.1.2 shows Reynold's number for flow rates in the interval 0.0001 - 0.0002 m³/s which was estimated to be the range of flow rates valid for this case.

Table 4.1.2: This table summarizes the results of Re-calculations (in the right column) for different q in m^3/s (the left column)

q [m^3/s]	Re
0.00010	14,600
0.00011	16,000
0.00012	17,450
0.00013	19,000
0.00014	20,400
0.00015	21,800
0.00016	23,300
0.00017	24,750
0.00018	26,200
0.00019	27,700
0.00020	29,100

As seen in Table 4.1.2, Reynolds' number was estimated to be above 4,000, and therefore turbulent, for every single case of different flow rates. In the case of turbulent flow, the friction factor must be determined using an empirical correlation. Colebrook's equation, which is widely used in the field of fluid dynamics, was chosen as a good approximation and is given by Equation 4.1.10 [4]. It is an implicit equation and it was therefore solved numerically using Excel.

$$\frac{1}{\sqrt{f}} = -4 \log \left(\frac{0.269\varepsilon}{d} + \frac{1.255}{Re\sqrt{f}} \right) \quad (4.1.10)$$

f is the friction factor (dimensionless) and ε is the roughness of the hose (m).

The friction factor was then used in the Fanning Equation given by Equation 4.1.11 [4] to calculate the frictional pressure drop in the hose.

$$\Delta p_f = \frac{f \rho v^2 L}{25.8d} \quad (4.1.11)$$

Δp_f is the frictional pressure loss (Pa) and L is the length of the hose (m). In the case of laminar flow, a simpler set of equations may be used [4].

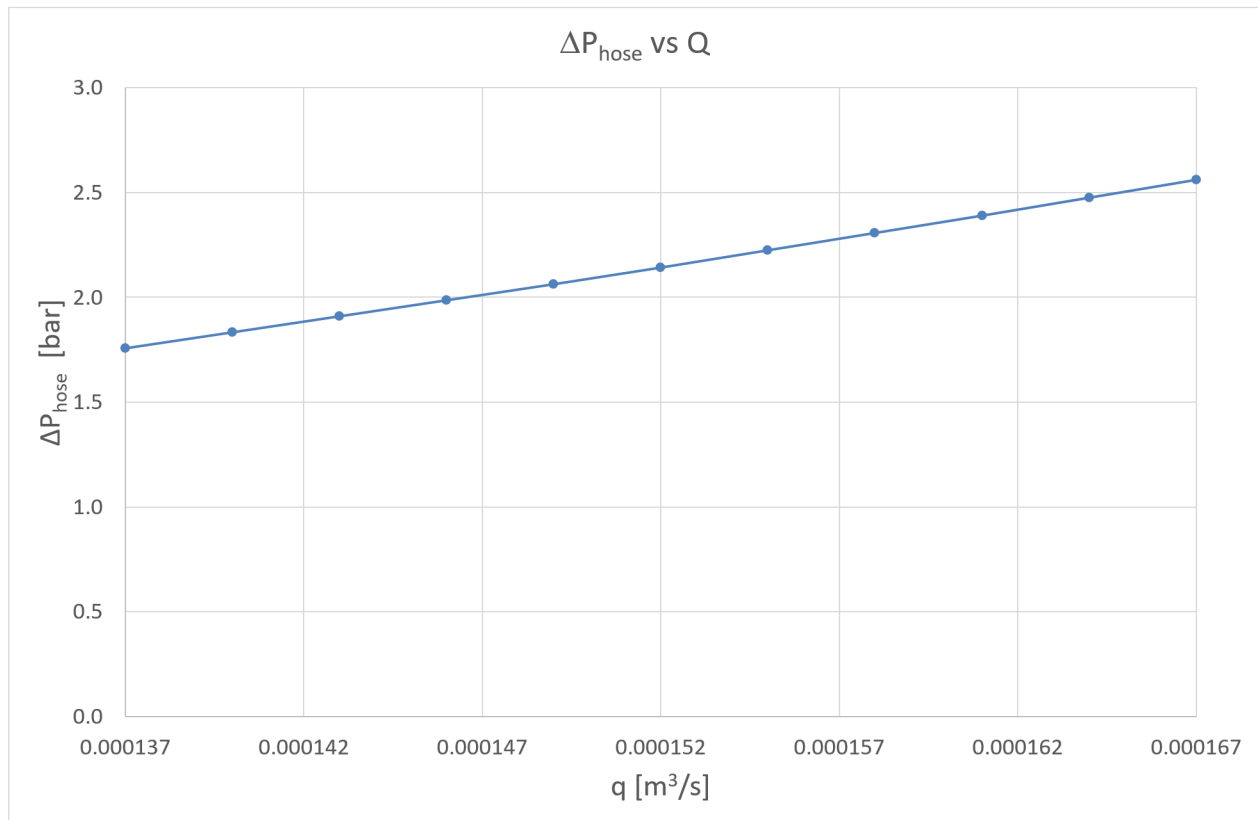


Figure 4.1.4: Graph showing the pressure loss in bar through the hose on the y-axis for different flow rates on the x-axis

The pressure drop through the hose, Δp_1 , with a flow rate of 0.000143 m³/s (8,6 l/min) was estimated to be 190 kPa (1.90 bar).

Pressure loss in swivel It was assumed that the pressure loss through the swivel could be approximated by calculating the pressure loss through a regular 90 °elbow with screwed fittings. The same method as for the pressure loss in a pipe could be used for this calculation, however, the length had to be substituted by an equivalent length. Based on a pipe diameter of 7.75 mm, the equivalent length was 0.9 m [40].

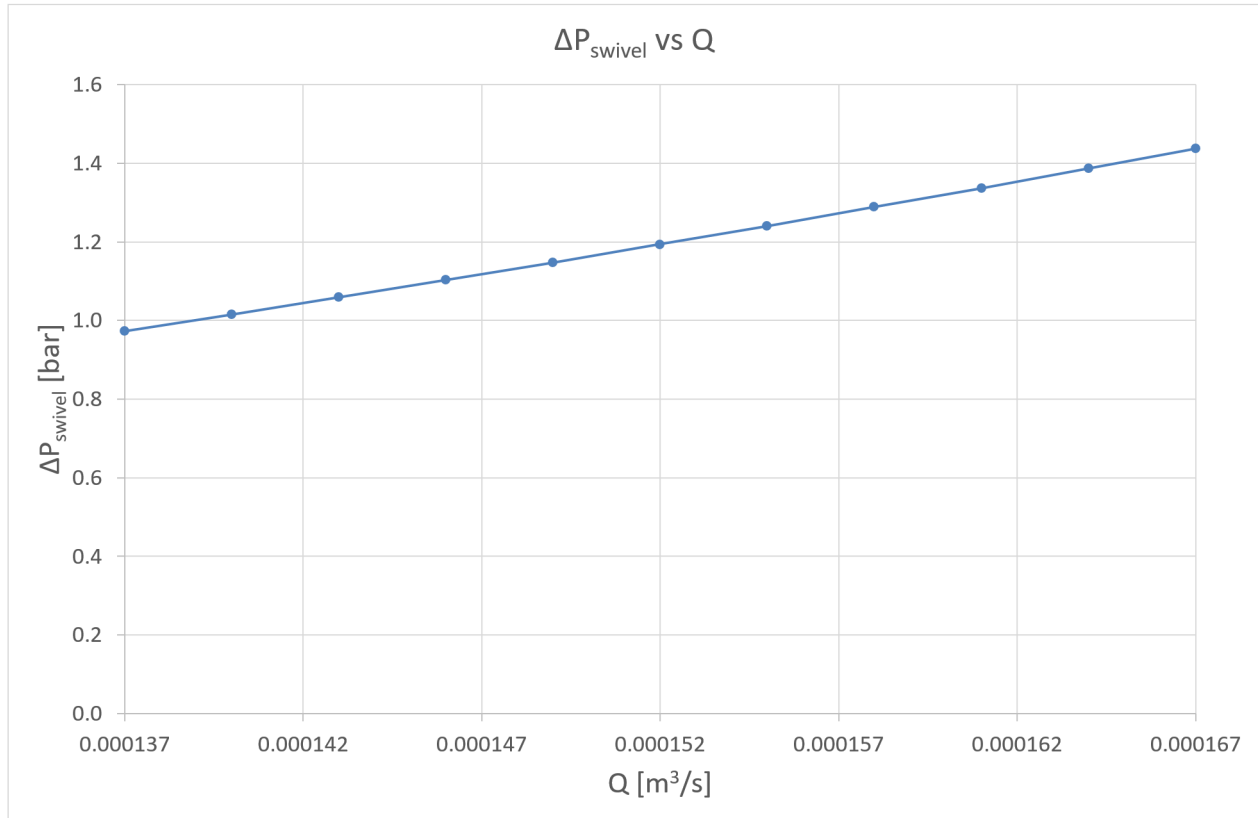


Figure 4.1.5: Graph showing the estimated pressure loss in bar through the swivel on the y-axis for different flow rates on the x-axis

The flow through the swivel was found to be turbulent and the total pressure drop through the swivel, Δp_2 , with the same flow rate as above was estimated to be 105 kPa (1.05 bar).

Pressure loss in pipe and BHA The pressure loss in the drill pipe and in the BHA was calculated in the same way as the pressure loss in the hose. The inner diameter of the drill pipe was 7.75 mm and the inner diameter of the BHA was 18 mm. The length of the drill pipe was 914 mm and the length of the BHA was 80 mm.

From Equation 4.1.9 it was determined that the flow through both the pipe and the BHA would be turbulent. Equation 4.1.10 was used to determine the friction factor and, finally, Equation 4.1.11 was used to estimate the pressure drop.

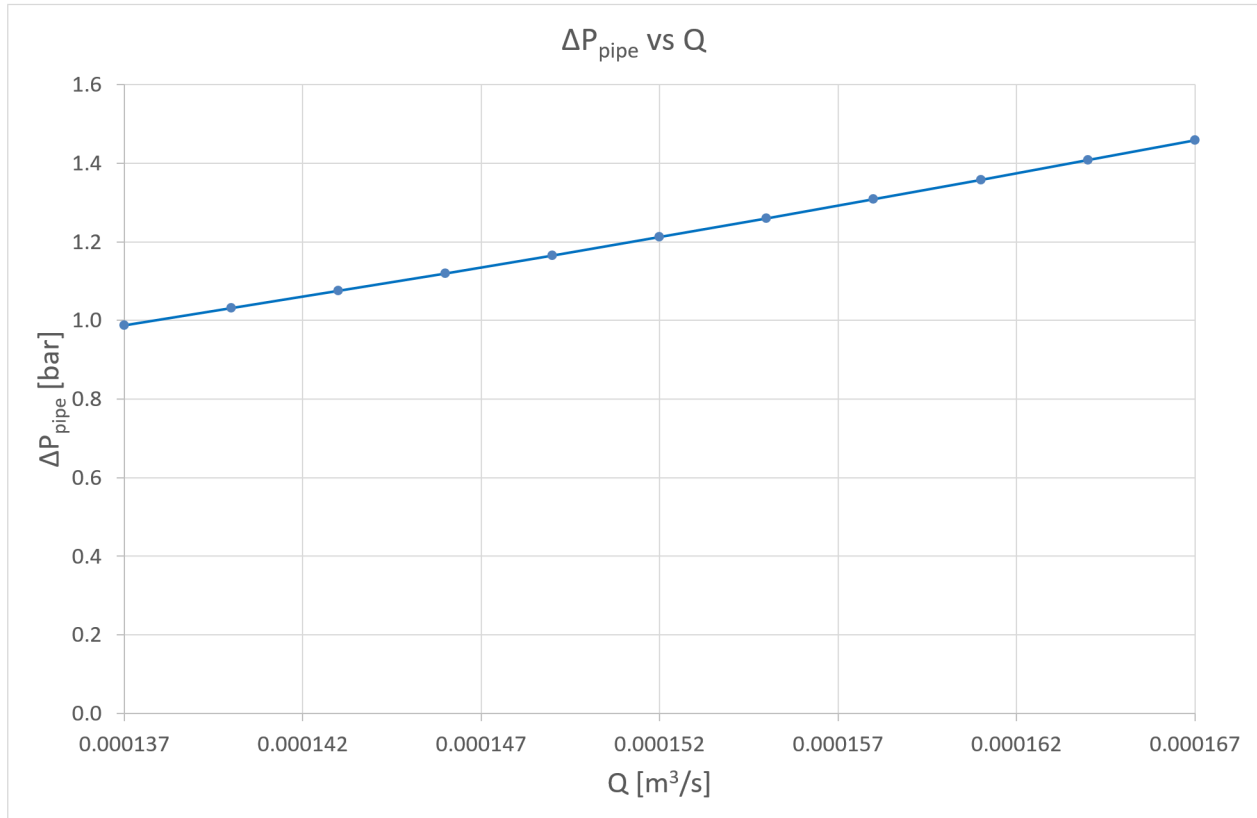


Figure 4.1.6: The graph showing the pressure loss in bar through the drill pipe on the y-axis for different flow rates on the x-axis

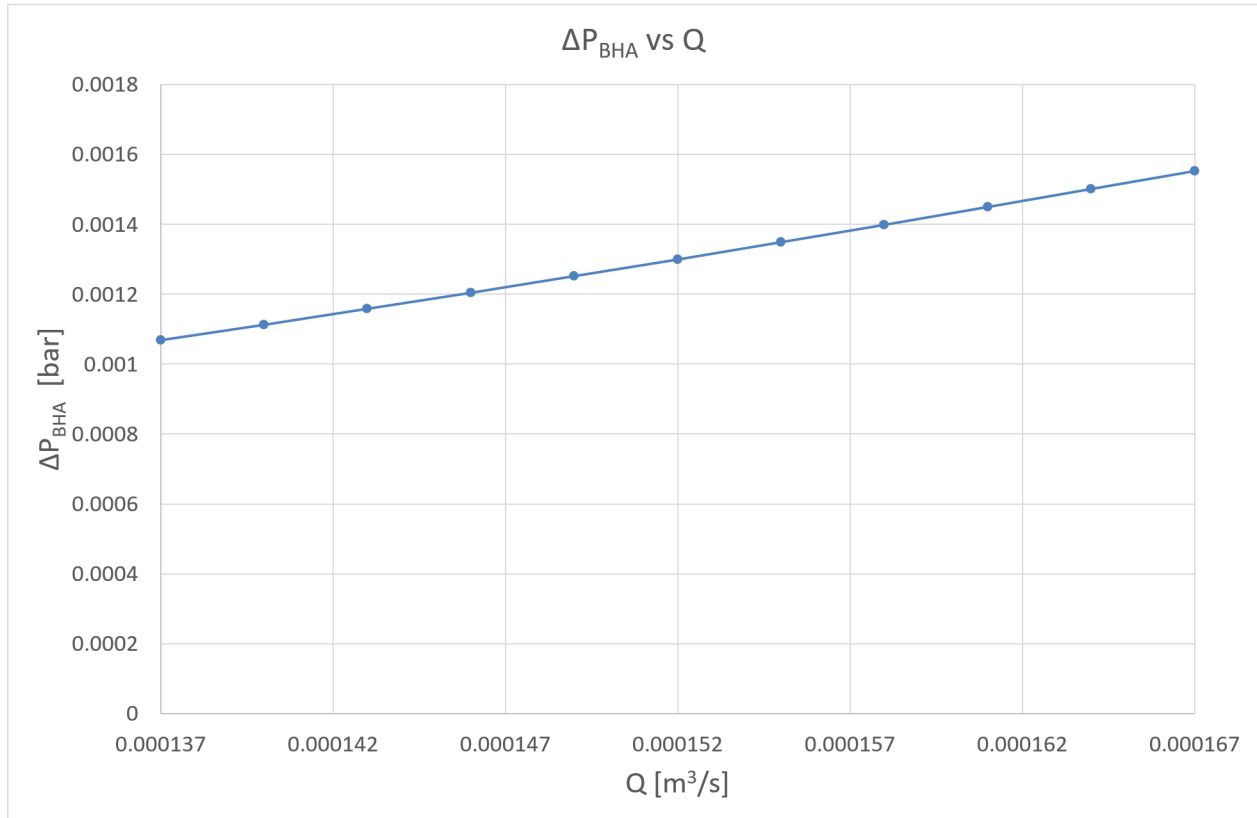


Figure 4.1.7: Graph showing the pressure loss in bar over the BHA on the y-axis for different flow rates on the x-axis

The pressure drop through the drill pipe, Δp_3 , was estimated to be 107.0 kPa (1.07 bar) and the pressure drop through the BHA, Δp_4 , was estimated to be 0.11 kPa (0.0011 bar).

Pressure loss in bit and nozzle The pressure loss in the bit was calculated in the same way as for a pipe (Equations 4.1.9, 4.1.10 and 4.1.11), but the pressure loss through the two nozzles was based on Equation 4.1.12 [4].

$$\Delta p_n = \frac{\rho Q^2 L}{C_d^2 A^2} \quad (4.1.12)$$

Q is the fluid flow rate (kg/m³), C_d is the discharge coefficient (dimensionless) and A is the cross-sectional flow area (m²). The discharge coefficient was estimated to be 0.95 and the flow area was determined assuming it consisted of two nozzles with circular area, each with a diameter of 4.34

mm².

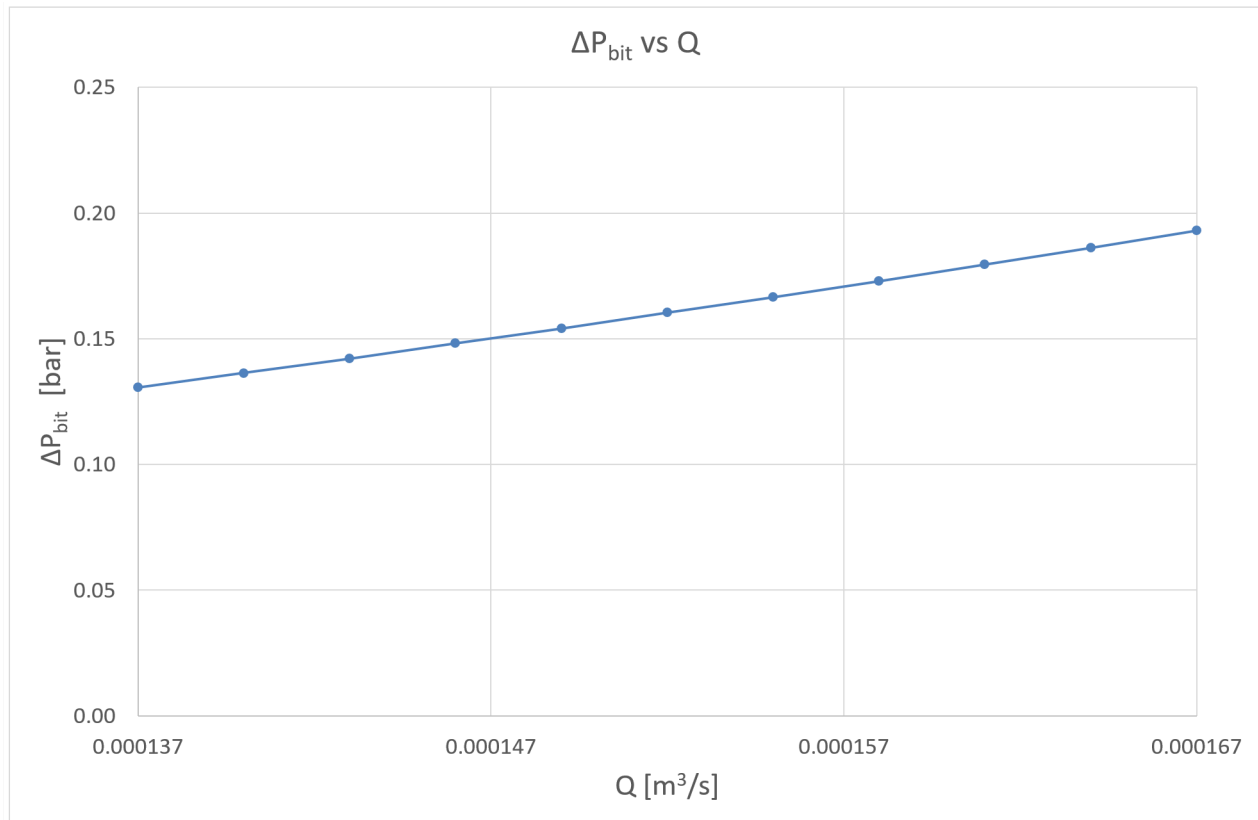


Figure 4.1.8: Graph showing the pressure loss in bar through the bit on the y-axis for different flow rates on the x-axis

The pressure drop through the bit, Δp_6 , was estimated to be 15 kPa (0.15 bar).

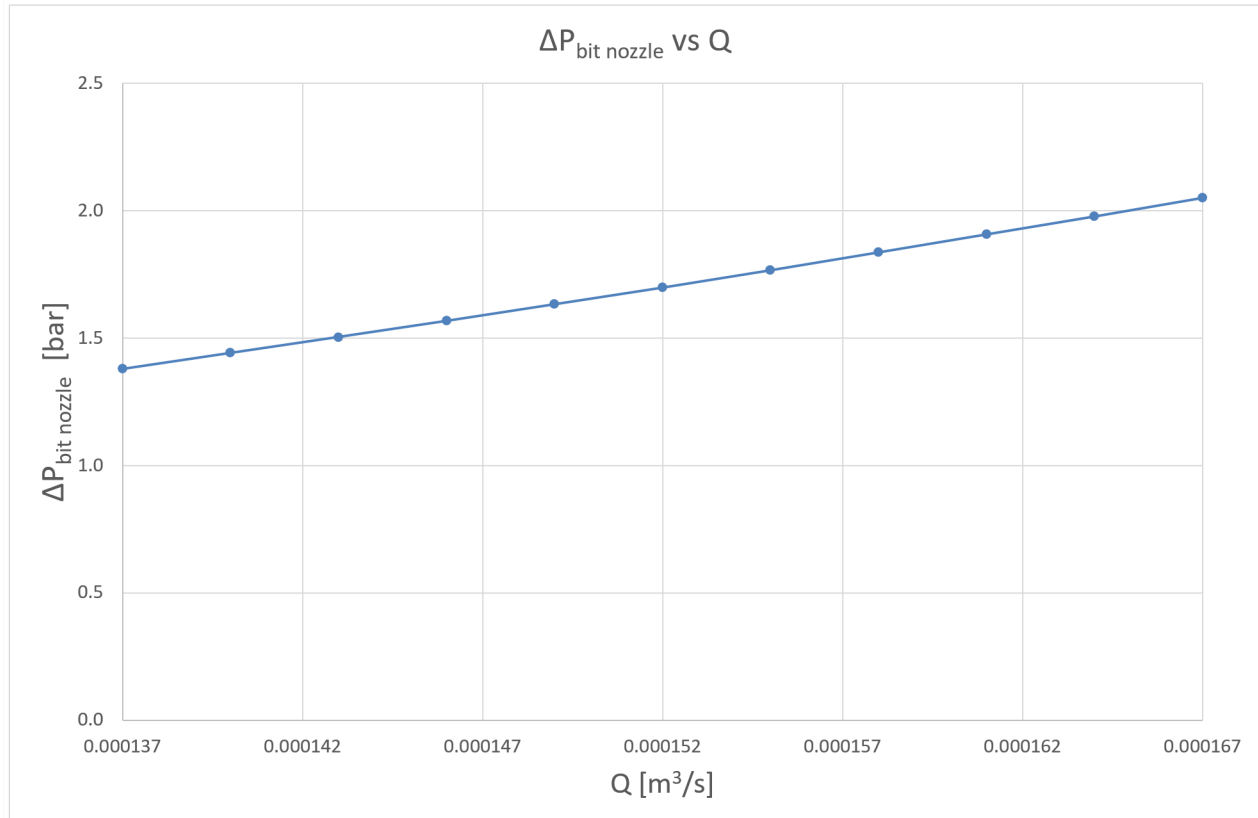


Figure 4.1.9: Graph showing the pressure loss in bar over the bit nozzle on the y-axis for different flow rates on the x-axis

The pressure drop through the bit nozzle, Δp_7 , was estimated to be 150.3 kPa (1.503 bar).

Pressure loss in annulus The pressure loss through the annulus was based on Equations 4.1.9, 4.1.10 and 4.1.11. The value of the diameter used in these equations was an equivalent diameter calculated using Equation 4.1.13 [4].

$$d_{eq} = \sqrt{d_a^2 - d_o^2} \quad (4.1.13)$$

d_a is the diameter of the annulus and d_o is the outer diameter of the pipe (m).

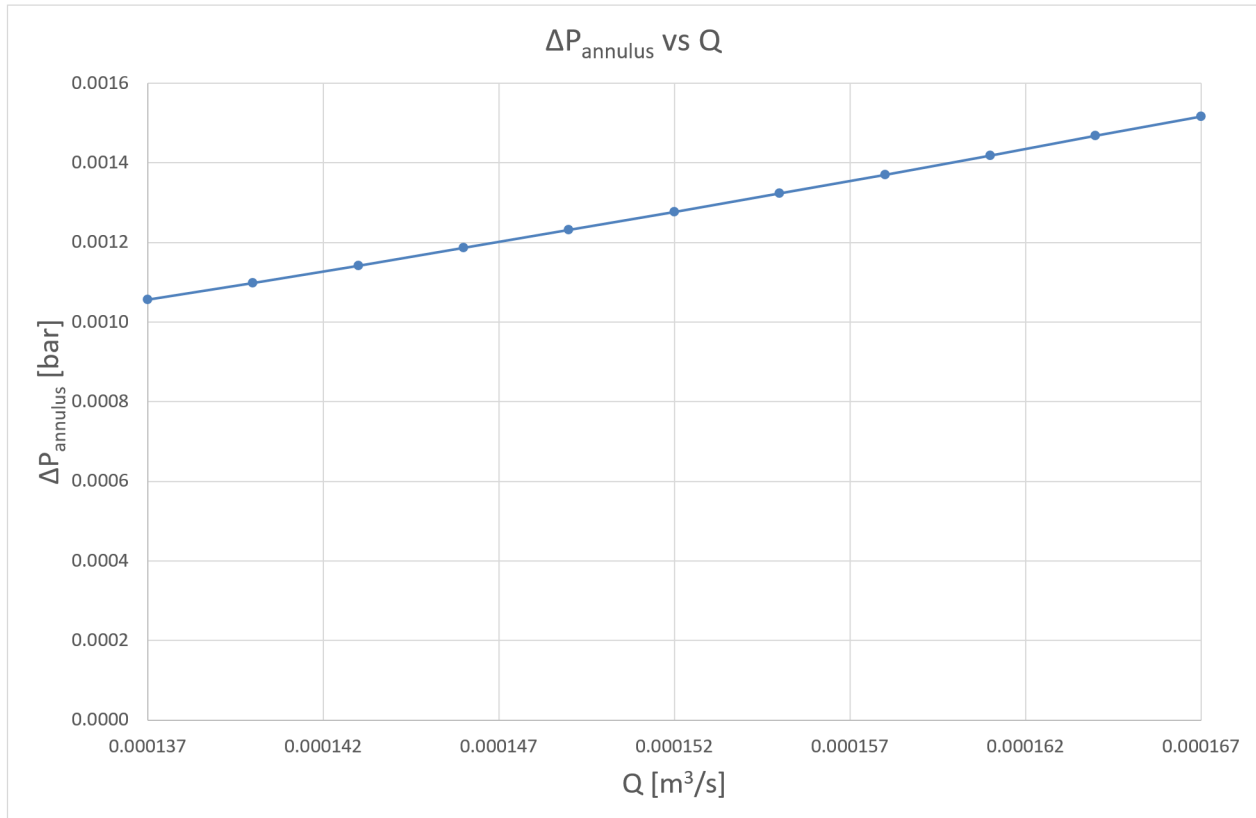


Figure 4.1.10: Graph showing the pressure loss in bar over the annulus on the y-axis for different flow rates on the x-axis

The flow rate was estimated to be turbulent through the annulus as well and resulted in a pressure drop, Δp_8 , of 0.11 kPa (0.0011 bar).

4.1.3.3 Summary of Pressure Loss in Circulation System

The results from the pressure loss calculations are presented in Table 4.1.3. The different pressure drops have been numbered from 1-8 starting with the hose and ending with the annulus. Δp_5 is not present in the table as it represents the pressure loss over the constriction and will be calculated in the next section.

Table 4.1.3: Pressure loss in circulation system

Component	Pressure Loss [bar]
Hose, Δp_1	1.90
Swivel, Δp_2	1.05
Drill Pipe, Δp_3	1.07
BHA, Δp_4	0.001
Bit, Δp_6	0.15
Bit Nozzles, Δp_7	1.503
Annulus, Δp_8	0.001
Total, Δp_{tot}	5.675

The pressure drop through the different components of the circulation system were then used to determine the force acting on the constriction.

4.1.3.4 Calculation of F_c

To determine the force acting on the constriction, an equation describing the pressure loss components in the system is shown in equation (4.1.14).

$$p_{pump} = \sum_{i=1}^8 \Delta p_i \quad (4.1.14)$$

The parameter that dimensioned the pressure drop over the constriction was the burst pressure of the pipe. The internal pressure of the pipe was within this limit as long as the pressure at the top of the pipe was less than p_{br} . The pressure drop over the constriction may be determined by subtracting the pressure loss in the entire system from the maximum burst pressure as shown in equation (4.1.15).

$$p_c = p_{br} - (\sum_{i=3}^4 \Delta p_i + \sum_{i=8}^6 \Delta p_i) \quad (4.1.15)$$

From the previous section, the sum of the pressure drops is 567.5 kPa (5.675 bar) and based on this the pressure drop over the constriction can be assumed to be 4,692 kPa (46,9 bar).

To determine the magnitude of the tension force F_c , the area the force was acting on had to be calculated. For the sake of simplicity, the area was assumed to be the complete cross sectional area of the drill pipe. It may be calculated using equation (4.1.16).

$$A_t = \frac{\pi}{4} d_i^2 \quad (4.1.16)$$

The inner diameter of the drill pipe was 7.75 mm which yields a cross-sectional area of 47.1 mm².

The hydraulic force could then be calculated by multiplying ΔP_c by A_t . This resulted in a force F_c of 220.5 N, equivalent to a weight of 22.5 kg.

4.1.3.5 Constriction Diameter

To dimension the size of the nozzle, Equation 4.1.17 [4] was solved for the diameter of the nozzle using Excel.

$$\Delta p_c = \frac{1}{2} \rho_f (1 - \beta^4) \left(\frac{q}{C_d A_t} \right)^2 \quad (4.1.17)$$

Where $\beta = \frac{d_n}{d_i}$.

Input data for Equation 4.1.17 can be found in Table 4.1.4.

Table 4.1.4: Input data for hydraulic force calculations

Density of fluid [kg/m ³]	998.2
Flowrate [m ³ /s]	0.00014
C_d	0.95
Pressure drop at constriction [kPa]	4,692
Inner diameter of pipe [mm]	7.75

Table 4.1.5: Estimated values for F_c , weight of drill string and maximum WOB.

F_c [kg]	22.5
Weight of Drill String [kg]	0.5
Maximum WOB [kg]	23.5
Critical WOB [kg]	46.5

The diameter of the constriction was found to be 1.425 mm.

4.1.3.6 Drill String Compression Analysis Results

After the analysis, it was found that the flow rate should be at least 8.4 l/min (0.00014 m³/s), so the velocity of the circulation fluid through the annulus was 2.4 m/s so an efficient cuttings removal may take place.

It was estimated that a total of 23.5 kg could be applied on the drillstring through the hoisting system without internal pressure and rotation. By using a constriction with a flow diameter of 1.425 mm in the BHA, the total weight of 46,5 kg could be applied on the drillstring by the hoisting system. The estimation above is without surface stabilizing elements.

Having a constriction with a flow diameter of 1.425 mm did not allow the flow rate to be changed while staying within a burst safety factor of 3 in the drill pipe, shown in Figure 4.1.11. It was decided that a lower value of safety factor or/and changing the constriction diameter could be accepted if a variable flow rate became necessary.

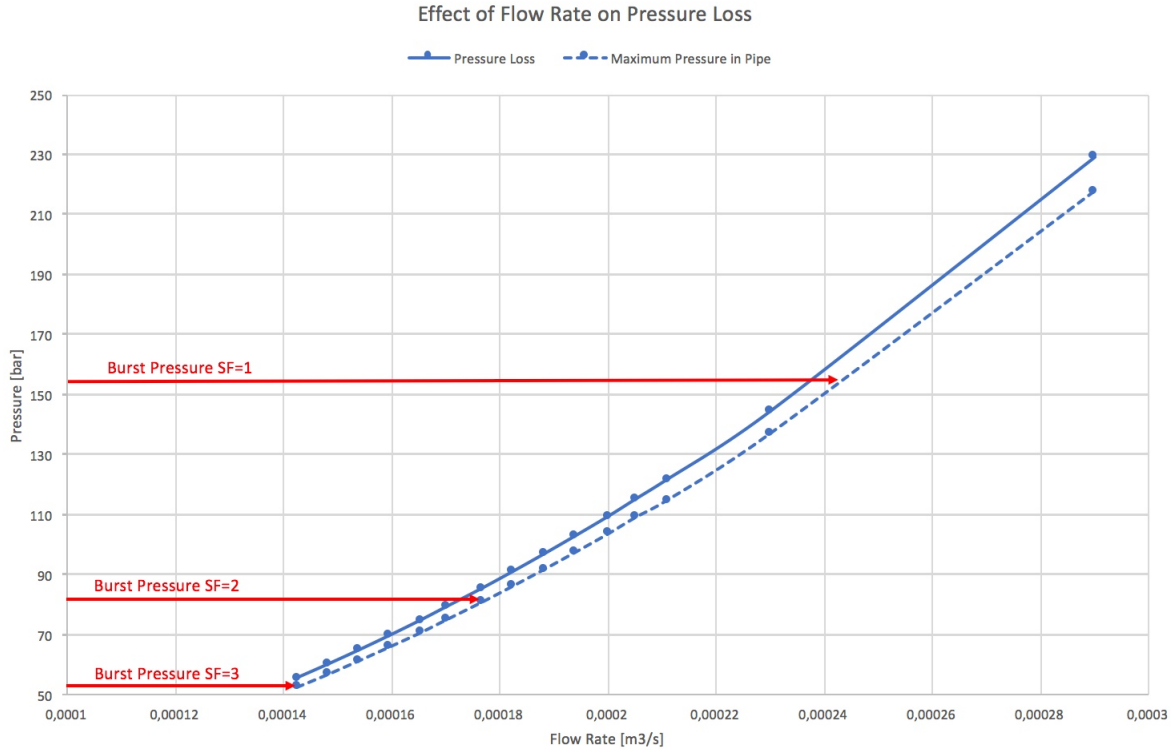


Figure 4.1.11: Graph showing the effect of flow rate on pressure loss. The slotted line shows the total system pressure loss for different flow rates, and the dashed line shows the resulting maximum pressure in the drill pipe. The red arrows show the burst pressure for the pipe with safety factors of 1, 2 and 3, with burst pressure of 52.6 bar, 78.9 bar and 157.8 bar respectively.

4.1.3.7 Changes in Phase II

At a later time in Phase II, some changes were made to the size of the constriction diameter due the availability of drill bits in the lab. A variety of constriction diameters were chosen (1.2 mm, 1.3 mm, 1.4 mm and 1.5 mm) and a similar pressure loss analysis as the one conducted in the previous section was conducted for each constriction diameter.

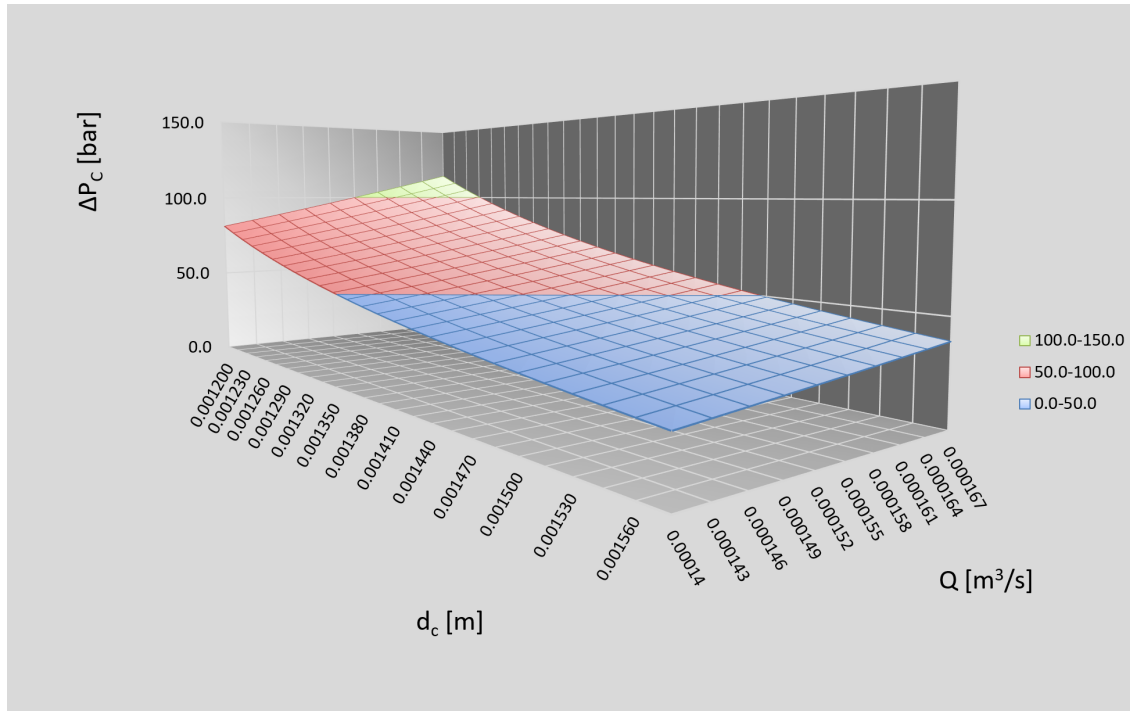


Figure 4.1.12: Figure showing the pressure inside the drill pipe (z-axis), the constriction diameter, d_c (x-axis) and flow rate, q (y-axis).

From the analysis, it was found that neither constriction diameters of 1.2 mm or 1.3 mm would be suitable as the pressure loss in the system would become too high for the chosen flow rates. To overcome the pressure loss, the pressure into the drill pipe had to be so high that it would surpass the burst pressure. Therefore, it was concluded that these constriction diameters would be unsuitable for the required purpose. This can be seen in Figure 4.1.12. The constriction diameters of 1.4 mm and 1.5 mm were a better choice because the pressure needed to overcome the pressure loss in the system was below the burst pressure and fulfilled the desired minimum fluid flow velocity inside the annulus.

By taking a closer look at the analysis, it could be seen that the constriction diameter and the pressure loss over the constriction were inversely proportional. In this case, it means that for a bigger constriction diameter, less force could be applied to the drill pipe before the drill pipe entered a state of compression. In other words, the maximum allowable WOB would be reduced when increasing the constriction size. By using Equation 4.1.16, the allowable weight on bit can be

calculated. The flow rate was assumed to be 8.4 L/min and constant, and the constriction diameters were 1.4 mm and 1.5 mm. The results from the calculations are presented in Table 4.1.6 and Table 4.1.7.

Table 4.1.6: F_c and maximum WOB for a constriction diameter of 1.40 mm

d_c	1.40 mm
F_c	224.6 N
Maximum WOB	22.9.9 kg

Table 4.1.7: F_c and maximum WOB for a constriction diameter of 1.50 mm

d_c	1.50 mm
F_c	170.5 kN
Maximum WOB	17.3 kg

To achieve the greatest possible WOB, the smallest constriction diameter had to be used, in this case 1.4 mm. By choosing a constriction diameter of 1.4 mm, a additional force of 224.6 N (22.9 kg) could be applied to the drill string by the hoisting motor while maintaining tension in the entire drill string.

Table 4.1.8: Estimated values for F_c , weight of drill string and maximum WOB.

F_c [kg]	22.9
Weight of Drill String [kg]	0.5
Maximum WOB [kg]	23.5
Critical WOB [kg]	46.9

The corresponding absolute maximum allowable WOB (based on the buckling limit) was estimated to be 46.9 kg.

Another important change was made to the design of the machine in Phase II. Because of the expected vibrations and the buckling limit of the pipe, a drill deck bushing was added to increase the

stability to the pipe. This changed the behaviour of the drill string and especially the buckling limit. However, because this point was fixed and the pipe moved, the dynamics of the string vibrations and failure limits changed continuously as the length of the pipe changed. It was therefore too complex to model the string vibrations and change in buckling limit in the limit amount of time available.

4.2 Drilling Algorithm

One of the main goals for an automated drilling machine, is that its control algorithm should be able to select optimal drilling parameters for changing downhole conditions and detect and mitigate problems that occur while drilling.

To learn more about problems that occur during a drilling operation, some of the most common drilling dysfunctions were studied and are presented in the sections below. The focus was to implement this in the design of the rig in order to reduce the probability that dysfunctions should occur and then to understand how it would be possible to detect and mitigate them.

Several ways to optimize drilling parameters were considered when developing the optimization algorithm, these methods are reviewed in Section 4.2.2. The first one is the simplest one and aims to maximize the two drilling parameters that are controlled by the motors in the drilling machine: WOB and RPM. This is based on the belief that drilling efficiency is directly proportional to the drilling parameters. The second method is based on minimizing the amount of energy required to remove a certain volume of rock, which is described by the function of Mechanic Specific Energy (MSE). A third method looks at how ROP changes with increasing WOB and RPM and detects any deviation from the normal trend. Another possibility is to try to detect increased string vibration amplitude.

4.2.1 Drillstring and Bit Dysfunctions

A goal for the drilling algorithm was that it should be able to detect the most common drilling dysfunctions. These dysfunctions occur as a result of the interaction between the drill string and the formation.

A general description has been given of several different types of dysfunctions, as well as ways to detect and mitigate them. The first four are related to vibrations in the drillstring.

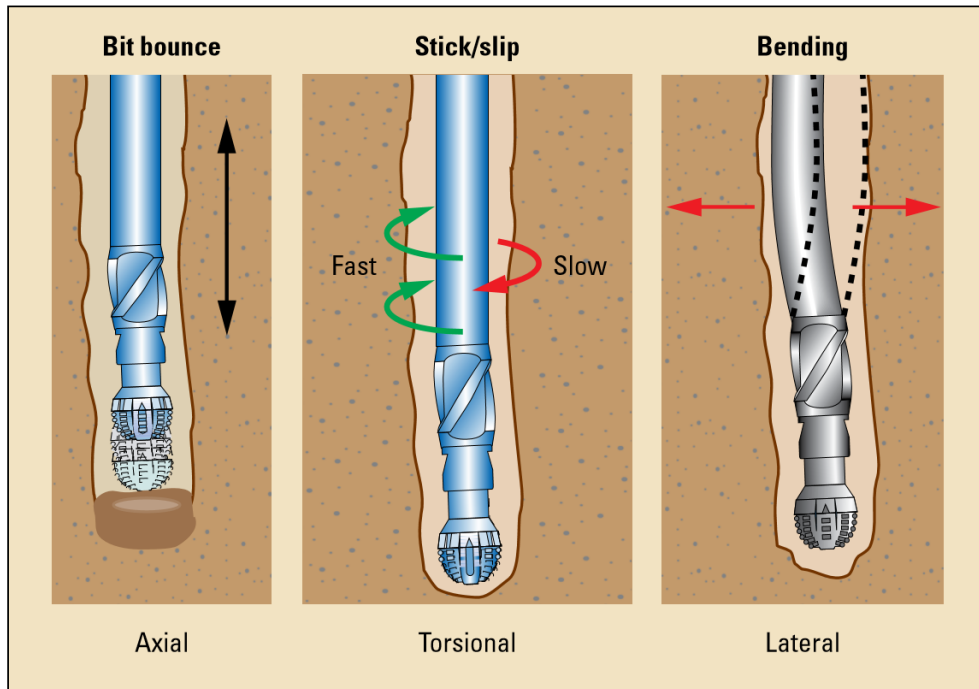


Figure 4.2.1: Illustration of the three types of drillstring vibrations [37]

4.2.1.1 Axial Vibrations

Three types of drillstring vibrations were identified, one of them was axial vibrations which are also known as longitudinal vibrations. Axial vibrations are most likely to occur when drilling through hard spots in the formation or when there are changing characteristics causing uneven drilling. Drilling through formations like this may cause a periodical displacement of the drillstring and bit. If the periodical displacement increases in severity the bit can start to loose contact with the bottom of the hole and bit bounce can be initiated.

Axial vibrations are more likely to occur when drilling a vertical or a low inclined well and when drilling with a three-cone bit. It may however also happen when drilling with a PDC-bit. Although this mode of vibrations is generally not expected to have a large impact on the overall drilling performance, long term axial vibrations may result in premature wear or in the worst case, equipment

damage (to the drill bit cutters, bearings, downhole tools or the drillstring itself). It is therefore important to detect these vibrations at an early stage and try to avoid or reduce their impact as much as possible [35].

Axial vibrations usually cause significant WOB fluctuations, rig or top drive shaking, irregular movement of the drillstring along its axis and reduced ROP [36] [35].

In this section the different steps that can be performed to avoid axial vibrations will be discussed. There are practical strategies to mitigate or avoid drillstring vibrations through empirical methods based on tuning surface controlled drilling parameters. Some of these parameters are the viscosity and the density of the drilling fluid used in the drilling operation, the flow of the drilling fluid through the drillstring, the WOB and the rotational speed of the drillstring (RPM) [35]. In this project, tap water was used as drilling fluid which resulted in both constant density and viscosity. There were two surface controlled parameters left that could be modified during the drilling operation: RPM and WOB.

When axial vibration are encountered, RPM should be reduced and WOB increased, each by a certain percentage. If the vibrations stop, drilling can resume with the new WOB and RPM. If the vibrations persist, the first step should be repeated until the vibrations are reduced or the maximum WOB is reached. If the maximum WOB is reached and the vibrations are still a problem, the bit must be picked off-bottom and the string torque must be allowed to unwind. The RPM should then be set to 40-50 % of the original value and the WOB should be increased by 10 % of the original value. Drilling must start again with these new variables and increase the RPM gradually to the original RPM. If axial vibrations still occur, the procedure above should be repeated again, but instead of increasing the RPM gradually to the original RPM, it should be increased gradually to 25 % of the original rpm [36].

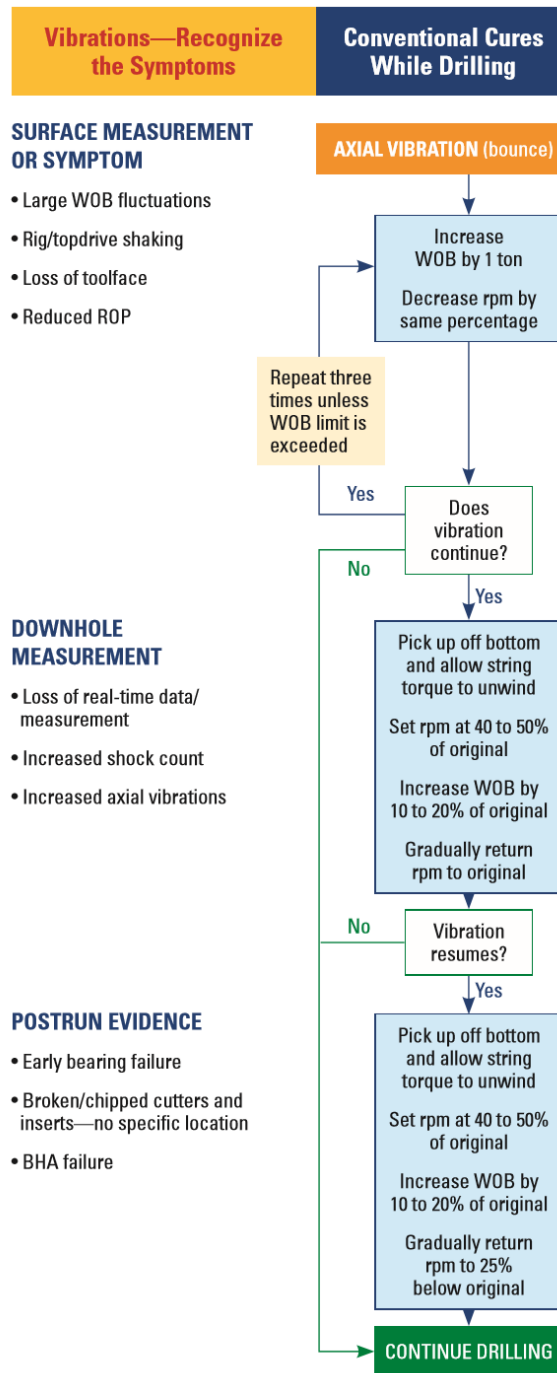


Figure 4.2.2: Illustration of the procedure for mitigating axial vibrations[36]

The main idea for detecting severe axial vibrations was to use an algorithm implemented in Matlab. The critical limit for the amplitude or frequency of axial vibrations should be estimated from experiments, and the function should then be able to detect any measurements above this critical value. It

was expected that there would be oscillations in the load cell measurements, so the function had to be able to differentiate between oscillations occurring due to measurement errors and oscillations due to axial vibrations.

4.2.1.2 Torsional Vibrations

Torsional vibrations are mainly due to the vibrational mechanism called stick/slip [39], where irregular drillstring rotation leads to fatigue of the components. The bit stops rotating at regular intervals causing the string to periodically torque up. To overcome the resistance, an increase in torque from the motor is applied. The increase in torque leads to greater twisting of the drillstring and storage of energy. When the applied torque is high enough to overcome the resistance, the bit spins free, and all the stored energy in the pipe will be transferred over to the BHA and bit. This can cause the BHA to accelerate up to 15 times the current rotary speed.

In normal scale drilling, torsional vibrations can lead to severe damage to both the bit and the BHA. In this case however, the drill pipe was expected to be the weak link as it had a low yield point and torque limit. Torsional vibrations were therefore suspected to cause the pipe to twist off close to the connection with the BHA if the torque got to high, instead of damaging the bit and the BHA.

Torsional vibrations can be identified by a cyclic increase in torque while the ROP remains constant or even decreases. Another way to detect torsional vibrations could be to compare the downhole rotational speed with the rotational speed of the top drive motor. Both a positive and a negative difference could imply torsional vibrations in the system.

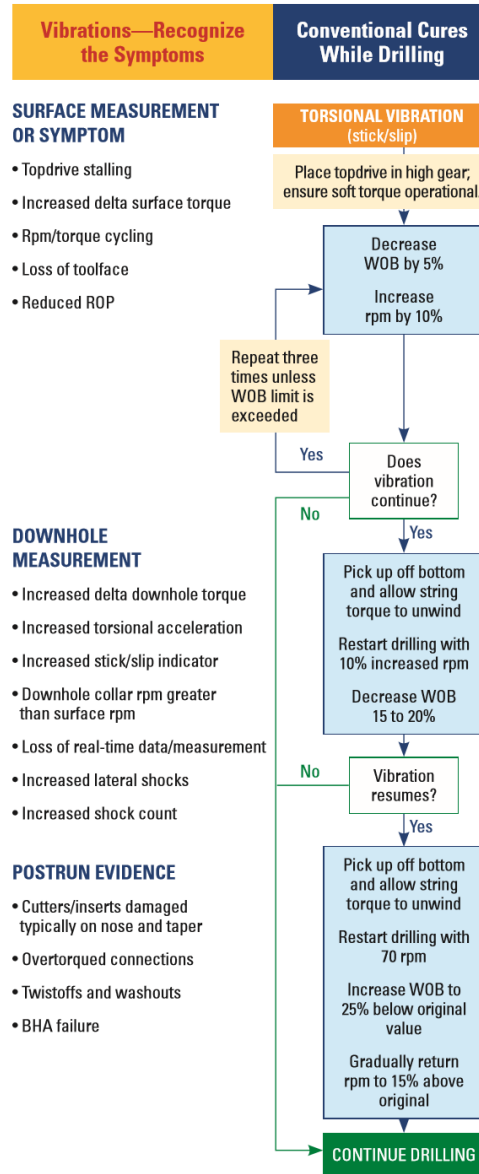


Figure 4.2.3: Illustration of the procedure for mitigating torsional vibrations [36]

This type of vibration could be detected using monitored parameters like: the torque of the top drive motor; the rotational speed of the top drive motor; the ROP; and the rotational speed of the BHA. There was no direct measurement of RPM in the BHA, but there was a possibility to calculate it from the combination of data from the gyroscope and the accelerometer. A possible way to implement this in the drilling algorithm could be to continuously monitor the parameters and look for indications of torsional vibrations.

The most conventional response to torsional vibrations is to place the top drive in high gear and ensure a low-torque operation. This could be achieved by reducing the WOB while increasing the RPM in small increments until the vibrations are mitigated. If the top drive stalls, i.e the torque increases to maximum while the RPM goes to zero, the bit should be picked off bottom to let the string unwind, and drilling with high RPM and low WOB will commence.

Due to the small scale of the drilling rig in this project, torsional vibrations were not expected to cause any damage of importance. However, stick/slip was certainly expected to occur. To avoid twist off in the pipe connection, a maximum torque of the top drive motor should be limited to the torque limit of the drillstring.

4.2.1.3 Lateral Vibrations

Lateral vibrations are the most destructive type of vibrations, and are, together with axial vibrations, more violent in vertical wells. Lateral vibration shocks are caused by the interaction between the BHA and the wellbore and may cause a high-frequency, large-magnitude, bending moment which can lead the system into whirl.

As the system is lead into whirl, the center of rotation is offset from the center of the hole, resulting in a drillstring that walks around the hole as it is rotating around itself. Whirl is a result of bit vibrations and a misalignment of the drillstring and BHA. It creates a fatigue damage in the drillstring through bending stress cycles which may lead to failure of connections [37].

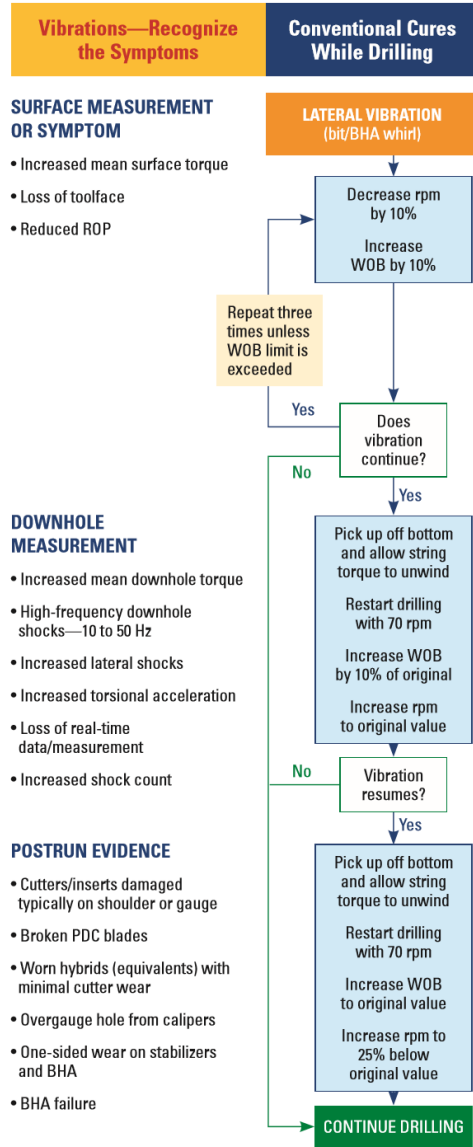


Figure 4.2.4: Illustration of the procedure for mitigating lateral vibrations [36]

Lateral vibrations could be detected using a downhole accelerometer. A defined critical value for the acceleration should be defined and any measurement above this value should be "noted". A response from the control system would then occur if there was more than a given number of critical measurements within a defined time interval. This could for example be more than 5 measurements within an interval of 3 seconds.

A way to mitigate vibrations could be to reduce the RPM using the top drive and then stepwise

increase the WOB using the hoisting motor. If the value of accelerations did not decrease and the problem persisted, the bit would then have to be picked up off bottom to unwind the torque and then drilling could resume. WOB would then have to be increased stepwise again.

4.2.1.4 Natural Frequency

After having reviewed the different types of vibrations, it was important to look into the possibility of experiencing resonance due to the natural frequency of the system. Natural frequency is the frequency at which a system tends to oscillate in the absence of any driving or damping force. When drilling through a formation, the drilling operation leads to vibrations that pass from the bit through the BHA and finally to the drill pipe. If the vibrations reach the same natural frequency as that of the drilling equipment, resonance is established.

Resonance is a phenomenon that occurs when a vibrating system drives another system to oscillate with greater amplitude at a specific frequency. In this case, it was expected that it could result in a higher amplitude displacement of the equipment, thus damaging it even more.

Rotation of the bit causes vibrations that spread through the equipment [37]. It is therefore critical to find the rotation speed, RPM, that does not create vibrations with the same frequency as the drilling equipments natural frequency. By avoiding the critical RPM, the lifetime of the equipment could be increased and the drilling operations would be optimized.

An analysis of the harmonic response for a rotating pipe was done for lateral and for axial vibrations in order to estimate if resonance would be a problem during the drilling operation.

The analysis of lateral vibrations was simplified by assuming that the pipe behaved like a uniform beam. The tension of the drillstring had a significant effect on the vibrations and was therefore included in the analysis. In this case, the tension force was estimated to be 0 since F_c neutralized the compression force. The natural frequency of the system is defined by Equation 4.2.1 [25].

$$w_n^2 = \left(\frac{n\pi}{l}\right)^2 \frac{T}{A\rho} + \left(\frac{n\pi}{l}\right)^4 \frac{EI}{A\rho} \quad (4.2.1)$$

n is the mode number which varies from 1 and upwards, l is the length between the top drive and

the top of the riser which varied between 91.4 cm 31.4 cm, T is the tension within the drill pipe, A is the cross sectional area of the pipe which was 24.1 mm^2 , ρ is the density of aluminum, $2,800 \text{ kg/m}^3$, E is Young's modulus, 68 GPa and I is the second moment of inertia, $7.3 \cdot 10^{-9} \text{ mm}^4$.

The lowest occurring natural frequency for this system was expected to occur for the first mode and when the length between the top drive and the riser was at its maximum, which was 160 Hz . This is equivalent to a rotational speed of around $10,000 \text{ RPM}$. This was far outside what was expected to be a normal operating range of rotational speeds and resonance was therefore not expected to be a significant issue when drilling.

The natural frequency of longitudinal vibrations was estimated using Equation 4.2.2.

$$w_n = \frac{\alpha_n c}{l} \quad (4.2.2)$$

where α is determined from Equation 4.2.3, c is the sonic speed, $4,928 \text{ m/s}$, and l is the length of the drill pipe (91.4 cm).

$$\alpha_n \tan \alpha_n = \beta \quad (4.2.3)$$

β is determined from Equation 4.2.4.

$$\beta = \frac{m}{M} \quad (4.2.4)$$

m is the weight of the drill pipe (0.062 kg), and M is the weight of the BHA and the drill bit (0.223 kg). This resulted in a natural frequency of 435.7 Hz . This is equivalent to a rotational speed of $26,144 \text{ RPM}$. As for the lateral vibrations, this was far out of the range of operating rotational speeds. Resonance was therefore not expected to be an issue during drilling.

From these results, it could be concluded that resonance would most probably would not occur because the natural frequency of lateral and axial vibrations were much higher than the expected operating frequency. Vibrations were however still expected to be a significant issue.

Since resonance occurs when a system drives another system to oscillate with greater amplitude, the natural frequency of the rig structure should also have been estimated. The vibrations in the drill string could lead the rig structure to oscillate at a certain frequency which, if the oscillations are large enough, could cause damage to the equipment.

Since the system was a lot more complex than what could be modeled using simple equations, it was decided that tests should be run to find out if resonance could occur or not.

4.2.1.5 Interfacial Severity

Interfacial severity occurs when a harder rock, a new layer or an inclusion in the current layer, is encountered in the formation. The force on the bit is then concentrated on the part of the bit in contact with the hard rock instead of the entire surface area of the bit. This can cause reduced drilling efficiency and wear on the equipment.

Interfacial severity may be detected through an increase in compression of the drillstring without having an increase in ROP. The torque is expected to increase as the bit is unable to remove rock efficiently at the current drilling regime.

As a harder layer is detected, the best response would be to lower the WOB, increase the RPM, and then stepwise increase WOB again.

The aim of the drilling algorithm was to detect a change in rock properties and respond in order to optimize drilling efficiency and prevent bit damage. A possible functionality the drilling algorithm could have had could have been to identify a new, harder, formation layer by detecting when WOB increased by a certain percentage of its "initial value" and ROP decreased by a smaller percentage of its "initial value" at the same time or within a given time interval. The number of events that exceeded these predetermined maximum and minimum values for WOB and ROP, respectively, would have been counted. If the events were within the same time interval, and the number of these events had exceeded a maximum tolerated limit, the algorithm would have responded by reducing WOB at the same time as RPM was increased.

4.2.1.6 Bit Balling

Bit balling is a drilling dysfunction characterized by cuttings sticking to the surface of the bit. It can happen when drilling through water reactive shale or clay formations in which electrochemical and mechanical sticking are the two main mechanisms that contribute to bit balling. If poor hydraulic design is used or the mud flow is stopped, an electrostatic force may cause cuttings to stick on the surface of the bit, and once initiated, it is easier for cuttings to build up and eventually ball up the bit.

Bit balling may be detected by a sudden reduction in ROP, without any significant change in other drilling variables [12]. The torque is usually lower than normal since the cutters are covered up by cuttings and there may also be a sudden increase in standpipe pressure because balling reduces the annular flow area which increases the pressure.

As soon as bit balling is detected, the best way to mitigate the problem is to reduce the WOB and increase the flow rate. By doing this, the cuttings stuck on the drillstring may be washed out.

If bit balling occurs during drilling, the drilling algorithm should be able to detect it and the control system must respond in order to mitigate the problem.

As described above, bit balling may be detected by a sudden reduction in ROP together with a slight reduction in torque. A way to detect bit balling could therefore be detecting when ROP decreases by a certain percentage of its "initial value" and torque decreases by a smaller percentage of its "normal value" at the same time or within a given time interval.

A proposed mitigation technique was to reduce the WOB using the hoisting motor and increase the flow rate of the pump. If ROP does not increase significantly, the bit could be lifted off bottom for a certain amount of time before continuing drilling.

Bit balling was not expected to occur as the chance of having water reactive shale or clay formations was considered low, and the total length being drilled was only 60 cm.

4.2.2 Optimization of Drilling Parameters

Another important part of the drilling algorithm was to be able to optimize the drilling parameters. The choice of which method to use in the final algorithm was based on time available and on the outcome of the testing phase. If drilling was considered efficient enough by maximizing the output variables, it would not be necessary to implement a different optimization function. If however, it was clear that drilling was not necessarily optimal at maximum values, but rather at lower values, the other methods would be considered.

4.2.2.1 Maximizing Drilling Parameters

The output variables would be optimized if they were not at their maximum limit or if there was a significant reduction in ROP. The aim would be to increase WOB and/or RPM stepwise to increase ROP. This process would have a lower frequency than the monitoring process.

The general idea was that the two output variables would be increased by a certain percentage. This would continue until the critical limit of any input variable was reached.

4.2.2.2 MSE

A possible optimization function that could be used in this case is the function of MSE. MSE is a measure of how much energy is required to remove a unit volume of rock and it is usually expressed in terms of drilling variables such as WOB, torque, ROP and RPM. Choosing the optimum combination of input variables to minimize the MSE would result in optimizing the drilling efficiency [17].

MSE is defined by Equation 4.2.5.

$$MSE = \frac{\textit{Total Energy Input}}{\textit{Volume Removed}} \quad (4.2.5)$$

There are two forces acting on the bit during drilling: WOB (axial force) and torque (rotational force). MSE can be expressed in terms of these forces, as shown in Equations 4.2.6 and 4.2.7.

$$MSE = \frac{\textit{Vertical Energy Input}}{\textit{Volume Removed}} + \frac{\textit{Rotational Energy Input}}{\textit{Volume Removed}} \quad (4.2.6)$$

$$MSE = \frac{WOB \Delta h}{Area \Delta h} + \frac{Torque 2\pi \textit{Numbers of rotations}}{\textit{Volume Removed}} \quad (4.2.7)$$

Because the distance travelled by the bit is the ROP divided by the RPM, Equation 4.2.7 can be rearranged to give Equation 4.2.8.

$$MSE = \frac{WOB}{Area} + \frac{2\pi RPM Torque}{Area ROP} \quad (4.2.8)$$

As shown in Equation 4.2.8, MSE is a function of drilling variables that were monitored continuously through the drilling process. Using MSE as an optimizing function was therefore thought to be a possible solution to ensure an effective drilling operation [17].

However, an important factor that was considered was that MSE would be a measure of energy efficiency which was not necessarily the highest priority.

4.2.2.3 Founder's Point

Another way to model drilling efficiency is to use the concept of the founder point.

The main concept behind this model is that when drilling through the same formation, with constant WOB, RPM and mud weight, the ROP should also be constant. When increasing the WOB and/or RPM, the ROP should increase proportionally if the set of variables is efficient[30].

On the other hand, if the ROP does not increase proportionally, it means something is making the drilling operation inefficient. Different drilling dysfunctions may be the cause for this inefficient drilling, some of these were presented in section 4.2.1 [24].

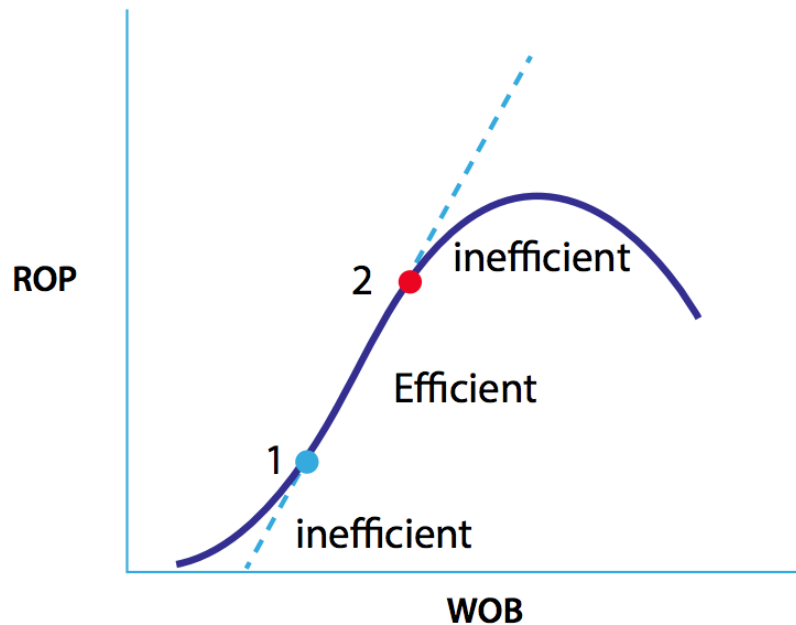


Figure 4.2.5: Graph illustrating the founder point. Point 1 is the point at which the critical depth of cut occurs and point 2 is the founder point. Phase 1 is before point I occurs, phase II is between point 1 and 2, and phase III is after point 2 [24]

The drilling response of the bit can be analyzed as three different operating phases [22]. Phase I occurs at low WOB, where the contact area between the bit wear and the rock slowly increases until a critical depth of cut is reached.

In phase II, after the critical depth of cut has been reached, any increase in WOB directly affects the cutting of the rock. The ROP increases proportionally with increasing WOB until the founder point is reached. At this point, the volume of cuttings produced is too large compared to what is circulated out of the hole by the drilling fluid.

Phase III is the phase after the founder point. During this phase the trapped cuttings reduce the flow path of the drilling mud which results in a low cuttings production than at the founder point. Since the cutting production rate is proportional to the depth of cut, the depth of cut decreases after the founder point.

The founder point is therefore the value of the drilling variables right before the drilling operation becomes more inefficient. This is illustrated in Figure (4.2.5). Detecting the founder point may

make it possible to define a safe and efficient operating range.

The main goal of the procedure is to drill the well with an optimal ROP for a given layer with a systematically chosen WOB and RPM based on the detection of the founder point.

4.2.2.4 Vibration Minimization

A third way to optimize the drilling efficiency was reviewed and it was to minimize the waste of energy. When drilling, the goal is that all the energy provided by the top drive should be used to remove rock. However, large amounts of energy contribute to the propagation of vibrations. To ensure that the operation is as efficient as possible, the goal could be to minimize the waste of energy.

Vibrational motion can be understood in terms of the conservation of energy. When the pipe is displaced from its center, some potential energy is stored in the pipe. When it is released and returns to its neutral state, its mass is accelerated and the potential energy is transformed into kinetic energy. The mass then decelerates and transfers the kinetic energy back to its potential. Oscillation of the drillstring therefore amounts to transferring back and forth from kinetic energy to potential energy.

To quantify the amplitude of the vibrations, the amount of energy in the oscillation can be calculated. By using an accelerometer downhole, continuous measurements of the movement can be made and this can enable the calculation of the waste of energy through vibrations.

The waste of energy could then be minimized by creating an optimization algorithm that uses the accelerometer measurements to monitor the vibration energy, and the input variables to reduce the vibration amplitude.

As the chosen optimization function was largely determined based on test results, it will be reviewed in Section 6.2.

4.3 Simulator

Ideally, several tests and analyses should be performed to achieve the required knowledge to optimize the control system. This was the first year NTNU competed in the Drillbotics™ competition and the rig therefore had to be built from scratch. As a consequence of this, all the materials and components had to be ordered and delivered, which again caused great time losses for testing and optimization. Therefore, a simulator was constructed in Simulink, a graphical programming environment in Matlab, to simulate the real drilling operation. Through this simulator it was possible to run tests and develop the control algorithm, as well as becoming familiar with Simulink, which in the end was used to program the real rig.

The simulator consisted of four main models that together described the total drilling system: the Drillstring Model, the Hoisting System Model, the Circulation System Model and the Formation Model.

4.3.1 Model

4.3.1.1 Drillstring Model

The drillstring model was developed with the aim of describing the relationship between the torque applied by the top drive motor and the rotational speed of the drillstring. The top drive motor was controlled by torque which was the input value for the model.

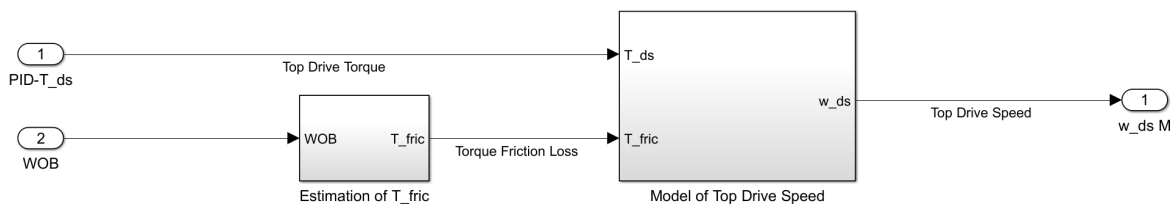


Figure 4.3.1: Illustration of the RPM model from the Simulink model

The relationship between the torque and the angular speed of the drill string was developed based on equation 4.3.1. This equation determines the change of the body angular momentum for unbalanced

torque on a body along the axis of rotation.

$$\tau_{net} = \frac{dL}{dt} \quad (4.3.1)$$

τ_{net} is the sum of the torque acting on the body (Nm), L is the angular momentum vector (kg·m²/s) and t is time (s).

For rotation about a fixed axis equation 4.3.2 yields,

$$L = I\omega \quad (4.3.2)$$

I is the moment of inertia (kg/m²) and ω is the angular velocity (rad/s).

Combining Equations 4.3.1 and 4.3.2 resulted in Equation 4.3.3,

$$\tau_{net} = \frac{d(I\omega)}{dt} \quad (4.3.3)$$

Since multiple torques were acting on the body, it was the net torque that determined the rate of change. In this case the net torque was the sum of the torque applied by the top drive motor and the friction torque from the interaction between the drill bit and the formation.

$$\tau_{net} = \tau_{ds} - \tau_{fric} \quad (4.3.4)$$

τ_{ds} is the torque applied by the top drive motor (Nm) and τ_{fric} is the torque loss due to friction (Nm) from the interaction between the bit and formation.

τ_{fric} was estimated based on the torque friction of a rotating disk [33]. The exact definition used is showed in equation .

$$\tau_{fric} = \frac{2}{3}M\mu gR \quad (4.3.5)$$

Equations 4.3.3 and 4.3.4 together give the equation for the angular speed of the drill string shown in equation 4.3.6.

$$\omega = \frac{1}{I} \int (\tau_{ds} - \tau_{fric}) dt \quad (4.3.6)$$

The moment of inertia, I, had to be calculated for the three parts of the drillstring (pipe, BHA and bit) and added together. The following equation can be used to estimate the moment of inertia.

$$a = \Sigma I_z = \Sigma \frac{\pi \rho h}{2} (r_{OD}^4 - r_{ID}^4) \quad (4.3.7)$$

This gave a general equation that required the drillstring torque (Nm) as an input and gave the rotational speed of the drillstring as an output (RPM).

$$\omega = \frac{1}{\Sigma \frac{\pi \rho h}{2} (r_{OD}^4 - r_{ID}^4)} \int (\tau_{ds} - \frac{2}{3} M \mu g R) dt \quad (4.3.8)$$

4.3.1.2 Hoisting System Model

The hoisting system model aimed to describe how the vertical movement of the travelling block was related to the torque applied from the hoisting motor. The hoisting motor was, in the same way as for the top drive motor, controlled by torque as an input value. The goal for this model was to obtain a measure of ROP and the drilled height.

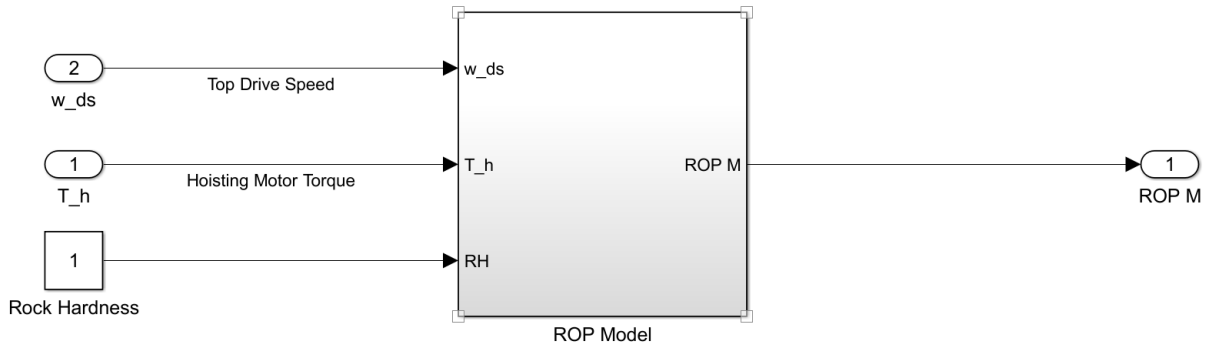


Figure 4.3.2: Illustration of the ROP model from the Simulink model

The Bourgoyne an Young ROP model, shown in equation 4.3.9, was used as an approach to calculate ROP. This model considered the effect of depth, the characteristics of the formation being drilled, the drill-bit size, the mechanical factors of the drilling process (i.e. WOB and RPM) and the mud system properties, and allowed each one to be adjusted by drillability coefficients.

$$ROP = f_1 \cdot f_2 \cdot f_3 \cdot f_4 \cdot f_5 \cdot f_6 \cdot f_7 \cdot f_8 \quad (4.3.9)$$

f_1 is the formation strength, f_2 is effect of depth and compaction, f_3 is effect of pore pressure, f_4 is effect of differential pressure, f_5 is effect of drill-bit diameter and WOB, f_6 is effect of rotary speed, f_7 is effect of drill-bit tooth wear, and f_8 is effect of bit hydraulic jet impact force.

Since the height of formation that was to be drilled in the competition was only 60 cm, the effect of compaction was assumed to be negligible. The effect of pore pressure and differential pressure was neglected as it was stated in the guidelines that the formation would not have any overpressured zones and because the rig setup gave a differential pressure in annulus to be close to zero. The effect of drill bit wear was also neglected due to the short distance being drilled. The hydraulic jet impact force through the bit was considered small because of the large pressure drop across the constriction inside the BHA, and therefore neglected.

Neglecting f_2 , f_3 , f_4 , f_7 and f_8 reduced Equation 4.3.9 to 4.3.10,

$$ROP = f_1 \cdot f_5 \cdot f_6 \quad (4.3.10)$$

Equation 4.3.10 can be broken down to three subequations as follows

$$f_1 = e^{2.303a_1} \quad (4.3.11)$$

a_1 is the coefficient for the effect of formation strength shown in Table 4.3.1.

$$f_5 = \left[\frac{\left(\frac{WOB_{sf}}{OD_{bit}} \right) - \left(\frac{WOB_{sf}}{OD_{bit}} \right)_t}{\left(\frac{WOB_{sf}}{OD_{bit}} \right)_N - \left(\frac{WOB_{sf}}{OD_{bit}} \right)_t} \right]^{a_5} \quad (4.3.12)$$

$\left(\frac{WOB_{sf}}{OD_{bit}} \right)$ is weight on bit measured at surface divided by outer diameter of the drill bit (kg/m), $\left(\frac{WOB_{sf}}{OD_{bit}} \right)_t$ is the weight on bit measured at surface divided by outer diameter of the drill bit at which the bit begin to dig in the formation (kg/m), and $\left(\frac{WOB_{sf}}{OD_{bit}} \right)_N$ is weight on bit measured at surface over outer diameter of the drill bit normalization value (kg/m). a_5 is the coefficient for the effect of bit diameter and WOB shown in Table 4.3.1.

$$f_6 = \left[\frac{RPM_{sf}}{(RPM_{sf})_N} \right]^{a_6} \quad (4.3.13)$$

a_6 is the coefficient for the effect of rotary speed shown in Table 4.3.1.

Table 4.3.1: Drillability coefficients

Parameter	Lower Boundary (unitless)	Upper Boundary (unitless)
a_1	0.50	3.91
a_5	0.10	2.00
a_6	0.40	2.23

Since the hoisting motor was controlled by torque, it was essential to find a formula that related torque to WOB. Assuming that there would be no buckling or friction loss, the WOB would be

proportional to the torque applied by the motor. The torque-force relation, shown in equation 4.3.14, was obtained from the product catalog for the ball screw that would be used for the hoisting system.

$$F_h = WOB = \frac{0.9\Delta 2000\Delta\pi\Delta\tau_h}{l} \quad (4.3.14)$$

F_h is the force (N) exerted by the ball screw onto the drill string and equals the weight on bit (N), τ_h is the torque applied by the hoisting motor (Nm), and l is the lead of the ball screw (m).

4.3.1.3 Circulation System Model

To implement the circulation system in the simulator it was first suggested to use a differential equation to model the pump pressure as a function of the difference in outflow and inflow of the system. However, due to the small volume of the system and the extremely low compressibility of water, the circulation system was instead implemented through static conditions.

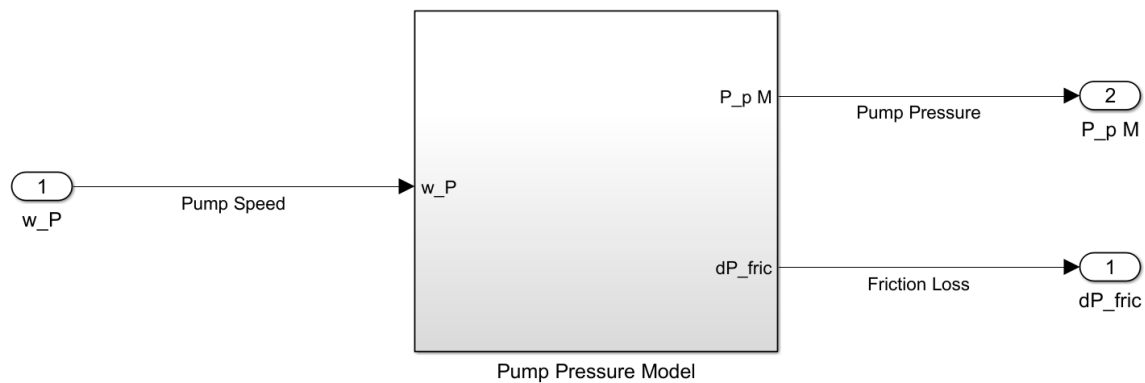


Figure 4.3.3: Illustration of the pressure model from the Simulink model

The pump was a single acting triplex pump, and was to be controlled by the angular velocity of its motor. The flow rate from the pump is shown in Equation 4.3.15.

$$q_p = \gamma_p \cdot \omega_p - leakage(\omega_p, p_p) \quad (4.3.15)$$

q_p is the flow rate from the pump, γ_p is the cylinder volume i.e. the volume pumped pr. stroke, and ω_p is the number of strokes pr. min (RPM).

The leakage term, which is a function of both pressure and flowrate, had to be found experimentally, but while working on the simulator, it was set to zero. The pump had an operating envelope of 0-140 bar, while the simulation and the actual experiment was never expected to be run at any higher pressure than 50 bar. Operating at 50 bar and 8.4 L/min, the pump would only be working at 35 % of its maximum pressure and 20 % of its maximum flow rate, which should make neglecting the leakage an acceptable assumption.

4.3.1.4 Formation Model

As the hoisting system required an effect of formation strength when calculating ROP, a formation model was implemented to simulate different formation layers using different rock hardness values. The model was created as a signal in Simulink MatLab that stepped between a range of predefined values for hardness at a specified time. The formation model took drilled height as an input value, and gave the corresponding rock hardness for that height as an output value.

4.3.2 Control System

The control system in the simulator consisted of three PID-controllers, one for each of the three motors (pump, top drive motor, hoisting motor). These controllers aimed to reduce the errors between the set point and the measured value of a process variable by adjusting a control variable over time.

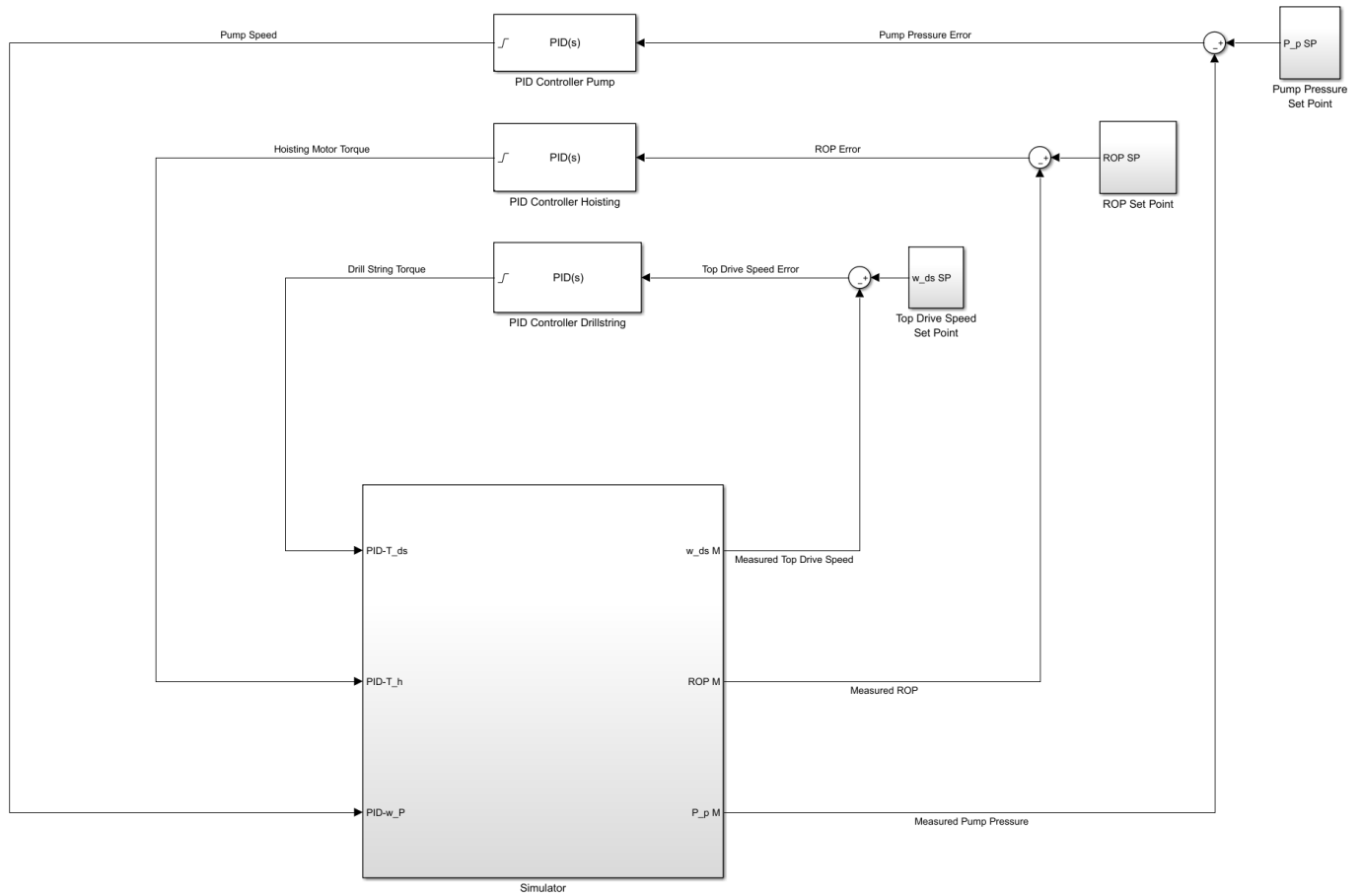


Figure 4.3.4: Illustration of the PID controllers from the Simulink model

4.3.2.1 Top Drive Motor

The rotational speed of the drillstring was used to control the torque of the top drive motor. The set point in the simulator was chosen to be 60 RPM and the PID-controller varied the torque in order to maintain the error between the measured value and the set point as close to zero as possible.

4.3.2.2 Hoisting Motor

An estimation of ROP was used to control the hoisting motor. The set point of the ROP was chosen to be an unreachable high value, as it was not supposed to limit the ROP. However, the value could not be set too high, as it would speed up the motor if any air gaps in the formation were encountered, which again would prevent a smooth transition between the formation layers. The limitation was

in this case the torque of the hoisting motor which directly controlled the WOB. The WOB was, as explained previously, limited by the buckling limit of the pipe.

4.3.2.3 Pump

The pump pressure was used to control the rotational speed of the pump. The set point in the simulator was set to 50 bar and the PID-controller then controlled the rotational speed of the pump in order to keep the error between the measured value and the set point as small as possible.

4.3.3 Logics

After having set up the low-level control system, implementing high-level logics was considered. The idea was that in addition to having PID-controllers, the control system should be able to optimize the drilling efficiency based on measurements from the drilling machine.

One of the situations simulated was encountering a harder layer which caused a reduction in ROP. The basic logic was that if the ROP decreased below a certain value, the RPM of the top drive should be increased to be able to maintain a certain ROP. The RPM was increased by changing the set point for the drill string speed.

This was implemented by creating a rock hardness vector with a stepwise increase in value. The torque and RPM of the motors, as well as the ROP, could then be monitored to see if the control system reacted to the increase in rock hardness.

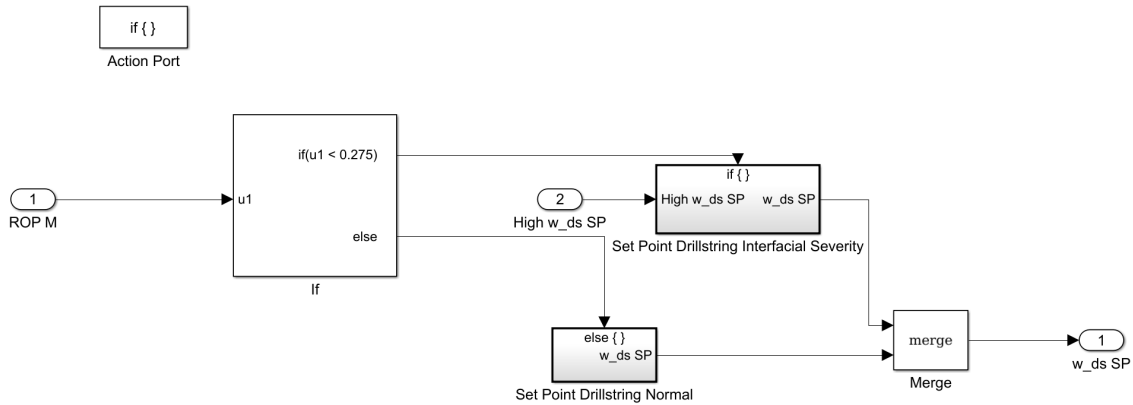


Figure 4.3.5: Illustration of the high-level control

Figure 4.3.5 shows the logic block used to implement a change in drill string speed set point due to an increase in rock hardness.

The biggest difficulty in this case was simulating the measurements. One issue was creating the dysfunction itself, but an even more problematic issue was deciding what would happen once the dysfunction had been detected and a change in set point had been made. Several solutions were considered, but it was finally decided that a finite state machine should be used.

4.3.4 State Machine

The theory behind a state machine is that an abstract machine can be in exactly one of a finite number of states at a given time. It consists of a set of states, a set of input events, a set of output events and a state transition function [16].

In the case of interfacial severity, the initial state would be "Normal Drilling", then, a transition function would cause a change of state if the ROP decreased below a certain level and the state machine would transition into "Hard Layer Drilling" for example. This new state would have a new set of set points specific for drilling through a hard layer.

The problem with using ROP as a condition was that when the problem was solved and ROP increased again, the state machine automatically transitioned back to "Normal Drilling" even if the

layer was still hard. A solution to this was to have a different condition for transitioning out of the "Hard Layer Drilling" state. This would make it possible to keep the machine in the "Hard Layer Drilling" state until the formation was soft again even if the ROP went back to a normal.

Implementing a state machine could easily be done in Simulink using the Stateflow environment [27].

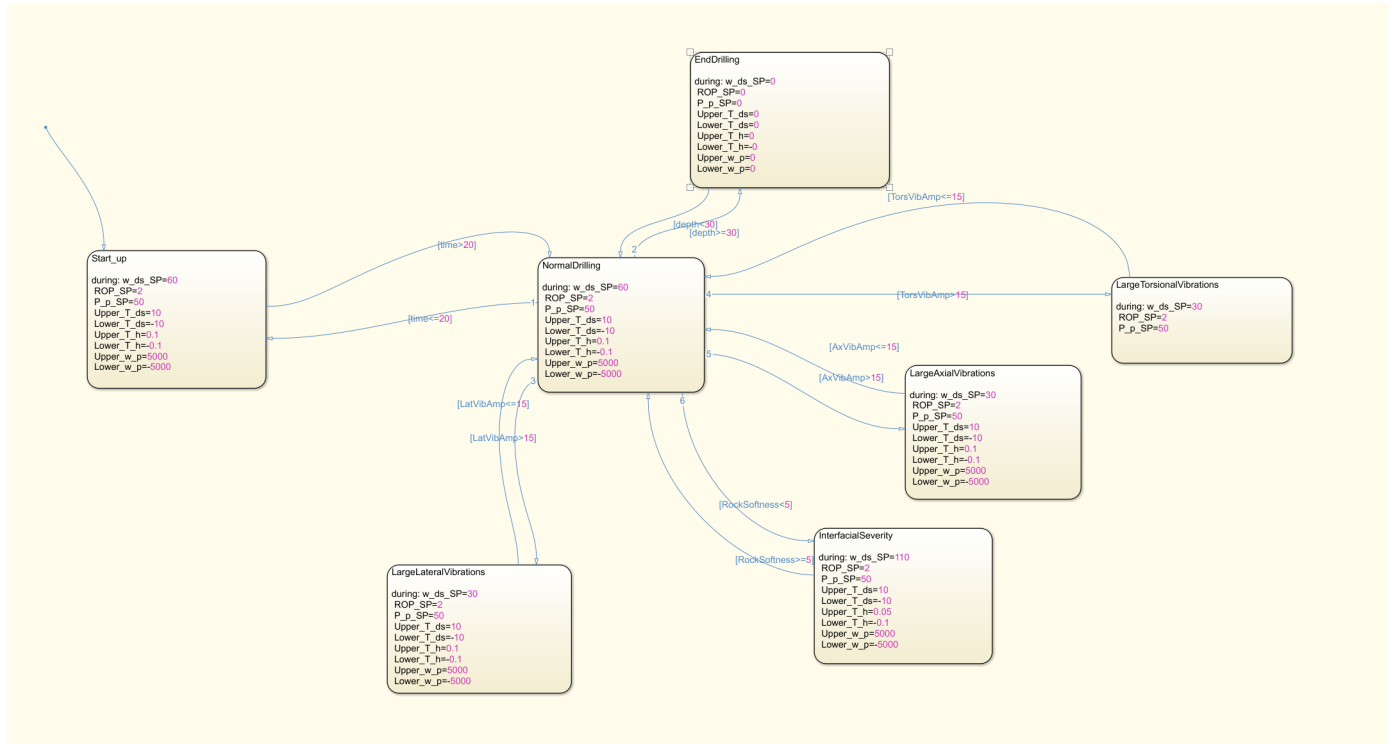


Figure 4.3.6: Illustration of the possible states in a state machine

As seen in Figure 4.3.6, many states could be defined for different drilling dysfunctions. One state could be defined as the starting state which was the default state when starting the simulation. One of the most important things was that none of the states overlapped and that both the transition into and out of the state was well defined.

4.3.5 Learnings from the Simulations

Several important points were taken from what was learned while working in Simulink.

The first point was the choice of low-level controllers. It was decided early on that PID-controllers

should be used and simulating this in Simulink confirmed that this could be a good choice. It was relatively easy to change the set points and the limits which was very useful when wanting to optimize the drilling operation.

While simulating in Simulink, different types of set points and control methods were considered and final choices were made based on what was the most effective way of controlling the motors.

The required inputs and outputs could then be determined based on what was required to control the motors. The units of the different variables were also reviewed in this phase.

Working with simulating high-level logics also gave a good idea of what would be easy and what would be difficult to implement in the real-time model.

Another issue that was discussed in this phase was noisy data. From the simulations it could be seen that it would be very important to smooth out the data before sending output signals to the motors in order to enable a smooth transitions between the different states. This was achieved by using transfer functions as shown in Equation 4.3.16.

$$f = \frac{1}{s + 1} \quad (4.3.16)$$

Finally, using Stateflow was concluded to be a good way to create a state machine in Simulink. The definition of the different states and the conditions for transitioning between them required more work and study when the machine was set up, but the simulator gave a good start.

Testing

To be able to run a fully autonomous drilling operation, it was essential to run tests on the hardware, the data infrastructure and the control system. It was also very important to test the system as a whole in order to determine its operating window and its limitations.

In the first phase of testing, the hardware was verified. This is often called a Factory Acceptance Test (FAT) which is a test conducted to determine if the requirements of a specification or contract are met. In this case the contract was the set of guidelines of the Drillbotics™ competition. The tests consisted of checking that all components of the drilling machine worked as expected and that the drilling machine was ready for use.

After having set up the system, tests had to be conducted to check that the data infrastructure of the rig had the desired functionality. This ensured that the control system could operate in real time as required by the guidelines.

The final phase of testing consisted of testing the control system. In the first part this consisted of estimating the maximum limits of the drilling variables. Following this, the safety functionality of the control system was checked. Finally, the optimizing procedure of the control system was verified.

5.1 Hardware Testing (Factory Acceptance Test)

The main objective of a factory acceptance test (FAT) is to test the safety instrumented system, where the logic solver and associated software are being tested together. It is a procedure that is normally executed during the final part of the design and engineering phase before the final installation at the plant. The test is used to verify the functionality of the system, where the goal is to make sure that the equipment is working as it should and that it delivers what is needed for the subsequent use which in this case is drilling with automatic control.

The point is to check that everything that would be needed during the operation is working and to do this through tests that would uniquely identify the problem if they fail. Some tests may involve several functionalities acting together and due to that, if the test fails, it may not clear which functionality caused the problem.

5.1.1 FAT Plan

During the FAT, it was, as far as possible, ensured that:

1. When the system is powered on, the equipment does not give any errors.
2. Sensors: The sensor signals that are received, displayed and logged by Simulink are observed physically and are in accordance with reality. Check that the signals are not too noisy, as it may be an indication of a connection problem or some external distortion.
 - (a) Pressure transducer: Pump is powered on, check readings from pressure transducer.
 - (b) Load cell: Hoisting motor is powered on, supplying weight on bit, check readings from load cell.
 - (c) Gyroscope and accelerometer: Top drive motor is powered on, supplying rotation of the drill string, check readings from downhole sensor.
3. Actuators: The torque or speed set-point for the motor being tested (hoisting, top drive or pump) is set to a certain value in Simulink. Observe physically that there is a corresponding

change in the motor and that its operation, according to the received sensor data in Simulink, is according to the set-point.

4. Accuracy: Check that the torque/RPM control is accurate. Set different set-points and observe that the motor follows that set-point.
5. Safety system: Check that the safety system stops the operation when the rig goes out of its safe operational range (e.g. max torque, max/min values for position, etc.).
6. Emergency stop: Check the functionality of the emergency stop button.
7. Operating range: Check that the hoisting system can move freely within its operating range (max/min position).

The full FAT procedure and check list is shown in Appendix D. A review of the FAT result for each component is given below.

5.1.2 FAT Results

5.1.2.1 Sensors

Due to delays and limited time for testing in the last part of the project, only measurements from the load cell were processed in Simulink.

To ensure that the load cell readings were correct and accurate, the hoisting motor was powered on and while it was supplying WOB, readings from the load cell were checked. Comparing with the weight on a scale, the load cell readings were accepted as realistic.

5.1.2.2 Top Drive Motor

The drive was successfully connected to the PLC and the PC. Using simple Simulink blocks, the top drive motor could be started, stopped and controlled. Both torque control and speed control were tested, and both were working as expected.

The input variables were received and plotted in Simulink. Given a maximum torque limit, increasing the friction caused an increase in torque and a reduction in RPM which could be viewed in real

time. Changing the output variables in Simulink resulted in the wanted response from the motor.

The communication frequency was satisfactory.

5.1.2.3 Hoisting Motor

The drive was connected to the PLC and the PC. The connection was successful and both input and output signals gave the expected results. Changes in setpoint successfully controlled the hoisting motor.

5.1.2.4 Pump

The drive was connected to the PLC and the PC, but setting up the communication was unsuccessful. Due to limited time, additional efforts were not made to fix this issue. The pump was run manually to ensure fluid circulation.

5.1.2.5 Safety System

To test the safety system, set points above the maximum limits set in the drives were sent from the PC to the PLC. It could be seen that the measured value would saturate at the maximum limit and not go above it. This tested had positive results for both the hoisting and the top drive motor.

5.1.2.6 Emergency Stop

The emergency button was tested and successfully stopped all motion in the hoisting and top drive motor. When released, the operation continued. It was therefore important to make sure that the required settings were chosen when releasing the emergency stop button.

5.1.2.7 Operating Range

It was made sure that the hoisting system could move freely within its operating range by moving it up to its zero position at the upper stopping mechanism and then down to the lower stopping mechanism.

5.2 Data Infrastructure Testing

The data infrastructure of the rig had to be tested in order to ensure its functionality. One of the requirements from the competition committee was that the control system should operate in real-time, it was therefore extremely important that the system was effective and accurate.

5.2.1 Data Infrastructure Testing Plan

The functionality of the data infrastructure was tested through the following steps:

1. Running the Simulink model in real time and checking the communication with the PLC.
2. Checking that the output value set in a Simulink block is received in the PLC with the same value.
3. Verifying that input values set in a PLC register is received in Simulink with the same value.
4. Check that signals sent by Simulink and by the PLC are of correct scale.
5. Ensure that the communication frequency is sufficiently high.
6. Test that the logging solution is satisfactory.

5.2.2 Data Infrastructure Testing Results

A Simulink model was created to monitor and process the input signals from the PLC and to respond by sending out control signals to the PLC. The first step was to check that the model could be run in real-time and that communication with the PLC was successful. There were some challenges with connecting the hoisting motor to the PLC, but after a while everything was connected and the model was running.

Next it was made sure that output values set in Simulink were received by the PLC with the same value. This could be seen by how the actuators reacted to changes in set points. It was easy to start and stop the actuators, as well as increase and reduced the set points and change the direction of rotation.

The next part that was checked was the scaling of the signals. Some of them were scaled in the PLC, but a few of them had to be converted in Simulink. This was done by using Simulink gain blocks to multiply or divide the signal by the right factor.

Communication frequency quickly became an important issue because the Simulink model started to run very slowly. By going through all the signals and their sampling rate, it was decided that most signals should have a sampling rate of 10 per second. The output signals had the same sampling rate as the input signals.

In addition to this the Pseudo Real Time option in the OPC Configuration Block was enabled which made one time step in the simulation equal to one second in "real-time". The end time of the simulation was also set to a finite number instead of infinite in order to solve problems with memory allocation.

To view the signals after the end of a run, the Simulation Data Inspector in Simulink was used. This provided graphs that could easily be viewed and compared. Chosen logs could then be exported to the Matlab Workspace for further analysis.

5.3 Control System Testing

Once the rotary system, the hoisting system, the circulation system and the control system were set up, the drilling machine needed to be tested to determine the safe ranges of the different variables and to optimize the drilling operation.

The tests were divided in two different categories. The first category of tests aimed to determine the absolute maximum values of the critical variables that were not defined directly in the PLC or the drives. The second category tested the safety functionality of the control system and its optimization algorithm.

5.3.1 Testing Description and Results

5.3.1.1 Getting to Know the System and its Challenges

Initially, a test phase was planned to get to know the system. The idea behind this "pre-testing" drilling was to get some understanding of the range of values the drilling parameters would be in, which challenges would limit the drilling parameters and if the design of the rig needed any minor modifications to ensure a safe and efficient drilling operation. The main goal of this part was to give some experience to the students as to where work should be done.

When the hoisting motor and the top drive were successfully connected to the PLC and the PC and the signals were scaled and accurate, a few tests were run. Experiments were carried out on different rock samples to analyze the reaction of the system to various operating conditions. Some of the formations drilled are shown in Figure 5.3.1,

The first rock sample was a relatively hard shale. The RPM was increased up to 700 RPM and the WOB up to 50 kg without any significant vibrations or problems. The ROP was relatively low, but drilling was smooth and stable.

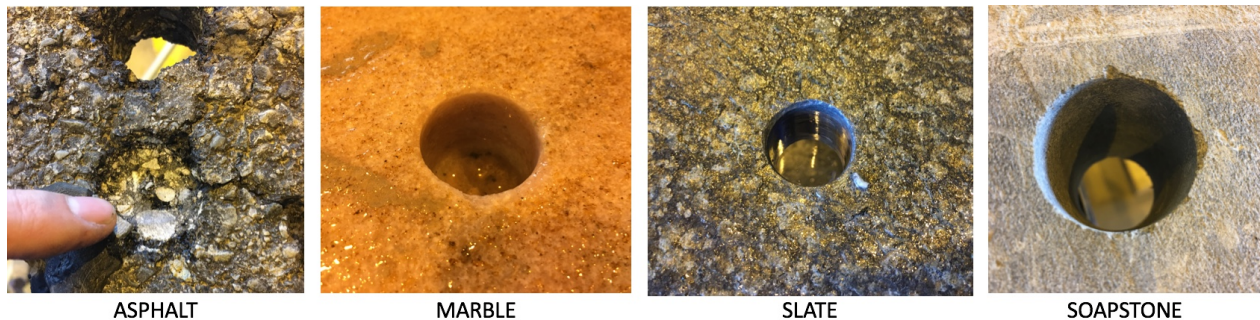


Figure 5.3.1: Pictures of test holes drilled in asphalt, marble, slate and soapstone

The second rock sample was a softer, black shale. Drilling was faster and it was easier to achieve a higher ROP, but vibrations quickly became a problem. The vibrations in the drill string propagated to the carriage and the hoisting system. After stopping the drilling operation and looking at the drill string it could be seen that the BHA and the joints were not completely aligned. In addition to this, the pipe seemed to be a little bit bent. This could have occurred before or even during drilling.

Solutions to this problem were discussed and one of the ideas was to use a lathe in the workshop to ensure that everything was aligned.

Bit wear, pipe wear and its impact on drilling performance were considered during testing phase as bit/rock interactions downhole and lateral and axial vibrations were highly anticipated. As the length being drilled was 60 cm, it was important to be able to test and set critical limits for tolerated vibrations to avoid pipe and bit fatigue. The early drilling phase (first 30 cm) was expected to experience the highest vibration impact, as the drill string was the least supported by the rock sample, and critical limits for acceptable vibrations were therefore planned to be set lower compared to the late drilling phase.

5.3.1.2 Estimation of Maximum Limits

The aim of these tests was to obtain an operating envelope (T_{ds} versus WOB). It was initially planned to perform several additional tests in order to test the pipe when pressure was increased in the pipe, but because the circulation system was set up very late, only two tests were run and they were run without water.

1. T_{ds}^{max} : increase drill string torque until pipe failure. The bit should be fixed. High priority.
2. WOB_{max} : increase WOB without rotation and without fluid until failure. Medium priority.

To be able to get information from the tests, the load cell needed to be scaled from an analogue signal to the WOB in kg. To do this, the torque and the speed of the hoisting motor were increased until the carriage landed on a weighing scale and then the weight on the scale was noted together with the value of the signal from the load cell. This relationship is shown in Figure 5.3.2.

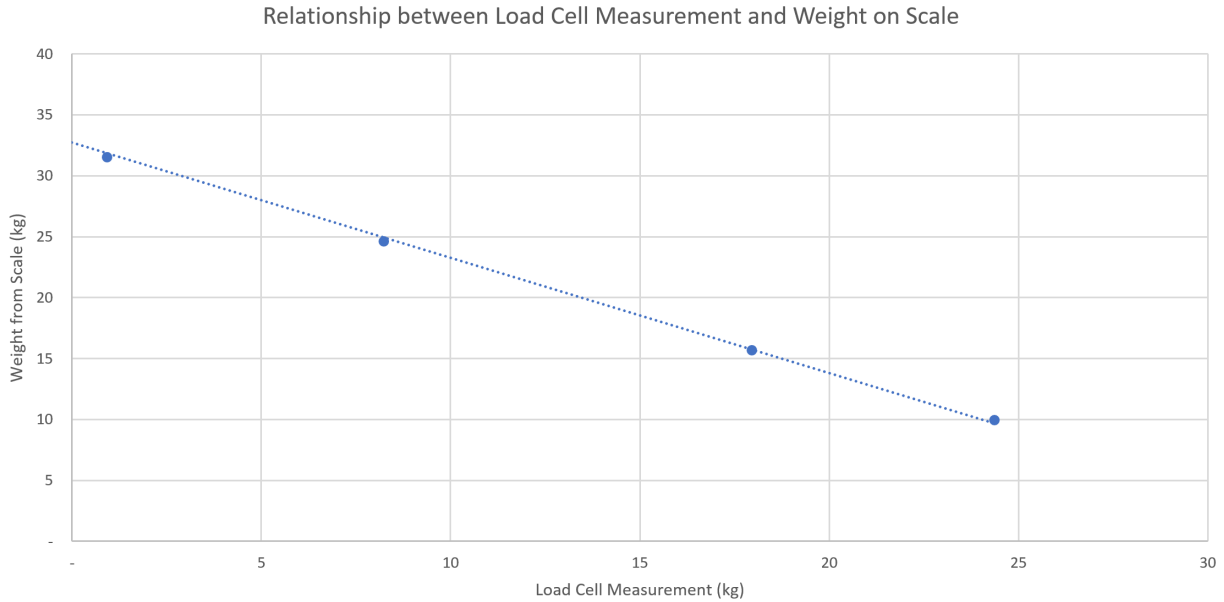
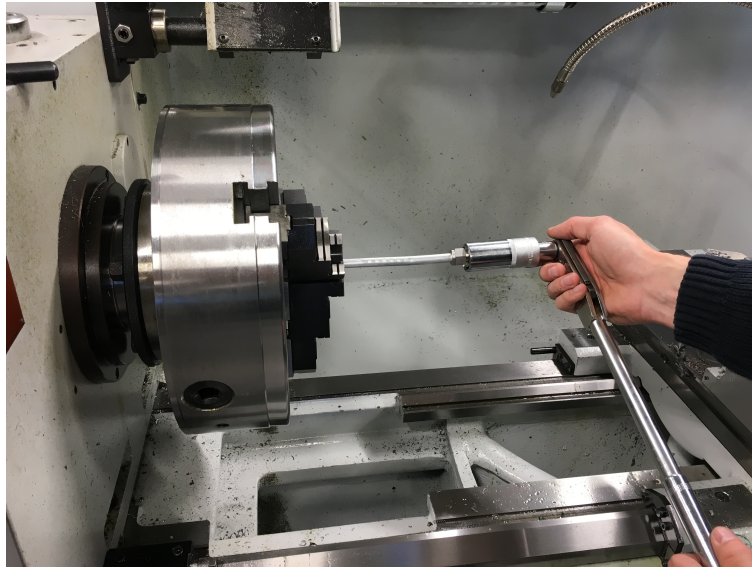


Figure 5.3.2: Relationship between load cell signal (kg) and weight on scale

Twist-off test The twist-off test was run on the pipe without the BHA or the bit. A torque wrench was used to conduct the test by gradually increasing the torque until failure. Twist-off occurred at 17 Nm.

A limitation to this test was that only the torque limit of the pipe was tested, not the limit of the entire string. The hydraulic connections used to connect the BHA to the pipe and the pipe to the top drive had a severe limitation in the way they were connected. They were connected manually and applying too much force damaged the pipe and applying too little could cause unscrewing during the operation. Therefore, the torque limit of the drill string was more limited by the connections than the actual torque limit of the pipe itself.



(a) Demonstration of torque wrench used to conduct twist-off test



(b) Twist-off

Figure 5.3.3: Demonstration of twist-off test

Buckling Test A buckling test was run without fluid circulation, fluid pressure or rotation. It did however have the drill deck bushing and the riser in place. This provided some additional stability.

A plot of hoisting motor torque versus time can be seen in Figure 5.3.4. It can be seen that the hoisting motor torque increases until 130 s and falls after that. The buckling limit for the pipe

without fluid pressure or rotation was 0.22 N.m.

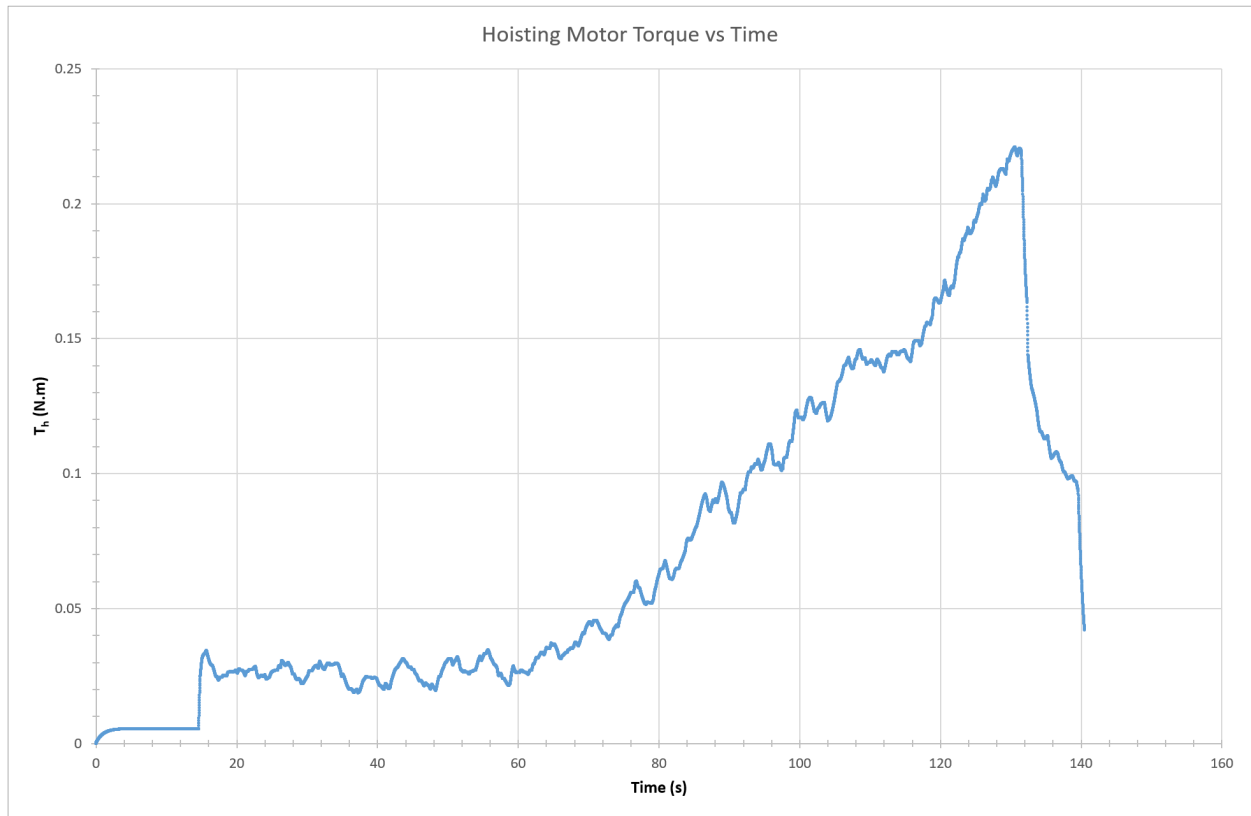


Figure 5.3.4: Graph of hoisting motor torque during buckling test

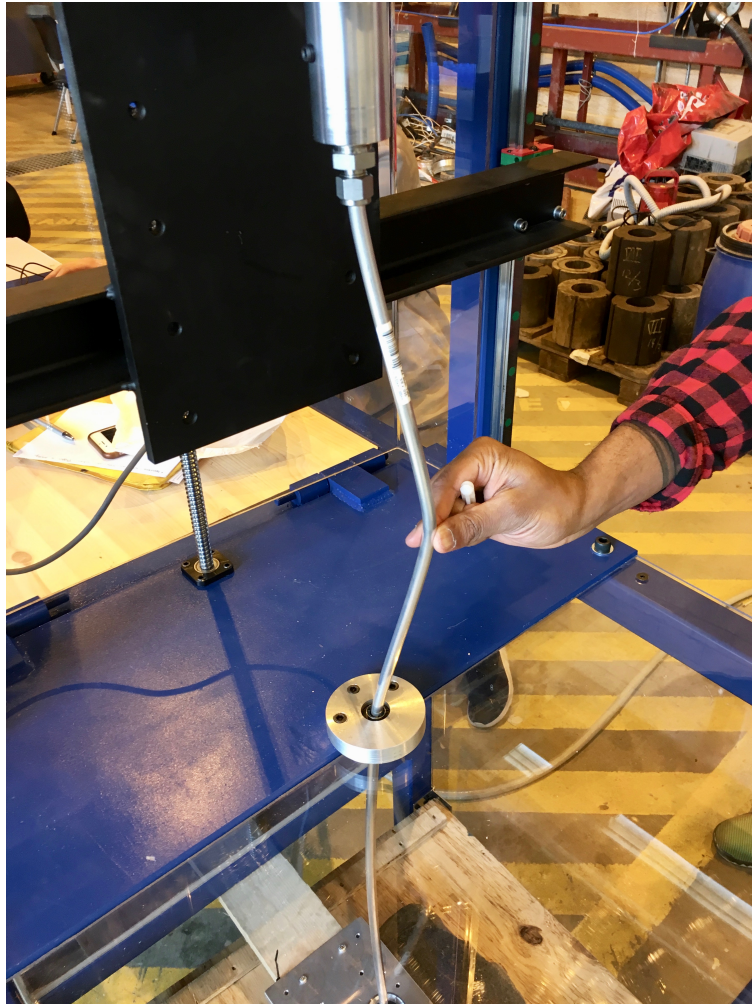


Figure 5.3.5: Picture of pipe after running buckling test

Summary The results from the two different maximum limit tests are shown in Table5.3.1

Table 5.3.1: Estimation of maximum limits

Test	Parameter	Result	Comment
T_{ds}^{max}	T_{ds}	17 Nm	Only tested on pipe, not entire drill-string
T_h^{max}	T_h^{max}	0.22 Nm	Tested with drill deck bushing

5.3.1.3 Safety Functionality Testing

These tests were performed to check that the control system worked and that the safety functionality was "according to standard".

1. Gradually increase drill string torque, and check that the system respects the limit. Also check that it is possible to change this limit during operation. High priority.
2. Gradually increase hoisting motor torque, and check that the system respects the limit. Also check that it is possible to change this limit during operation. High priority.

For both the top drive and the hoisting motor the system successfully respected the limits set in the drives and in the Simulink model. It was possible to change the limits in Simulink during the operation. It was not checked whether or not it was possible to change the limits in the drives while operating. However, since these limits were absolute limits they should not be changed.

5.3.1.4 Identification Testing

The aim of these tests was to increase the understanding of the system and its interactions with rock formations. Ultimately, this gave a basis for choosing the optimal operating parameters.

One way to do this was to for example to try to determine the optimal values for WOB and RPM. This was done by measuring ROP/vibrations/... at different combinations of RPM and WOB for

one formation This should give an indication of the optimal drilling parameters. If time allows, several formations will be tested.

Resonance An interesting observation was made when conducting the identification tests. When increasing the WOB and the RPM, large vibrations that propagated to the rest of the structure started occurring at a certain point which was initially thought to be the limit of the operating range. After some more testing it was however discussed if this could be the natural frequency of the system.

To test this idea, the RPM was increased quickly past the point where vibrations were the most violent. This proved to be a good idea because the amplitude of the vibrations were greatly reduced at higher RPM.

It was then discussed if the same frequencies would cause resonance at different WOBs. Tests were therefore conducted for WOB=15 kg, WOB=25 kg, WOB=35 kg, WOB=45 kg and WOB=55 kg. For each WOB the RPM was gradually increased as high as possible. When analyzing the data from the tests it was observed that the vibrations at the resonance frequencies could be observed on the load cell measurements. The resulting graphs for WOB=15 kg and WOB=25 kg can be seen below. In addition to this, a graph of WOB=14.3 kg was added to show resonance at 1100 RPM.

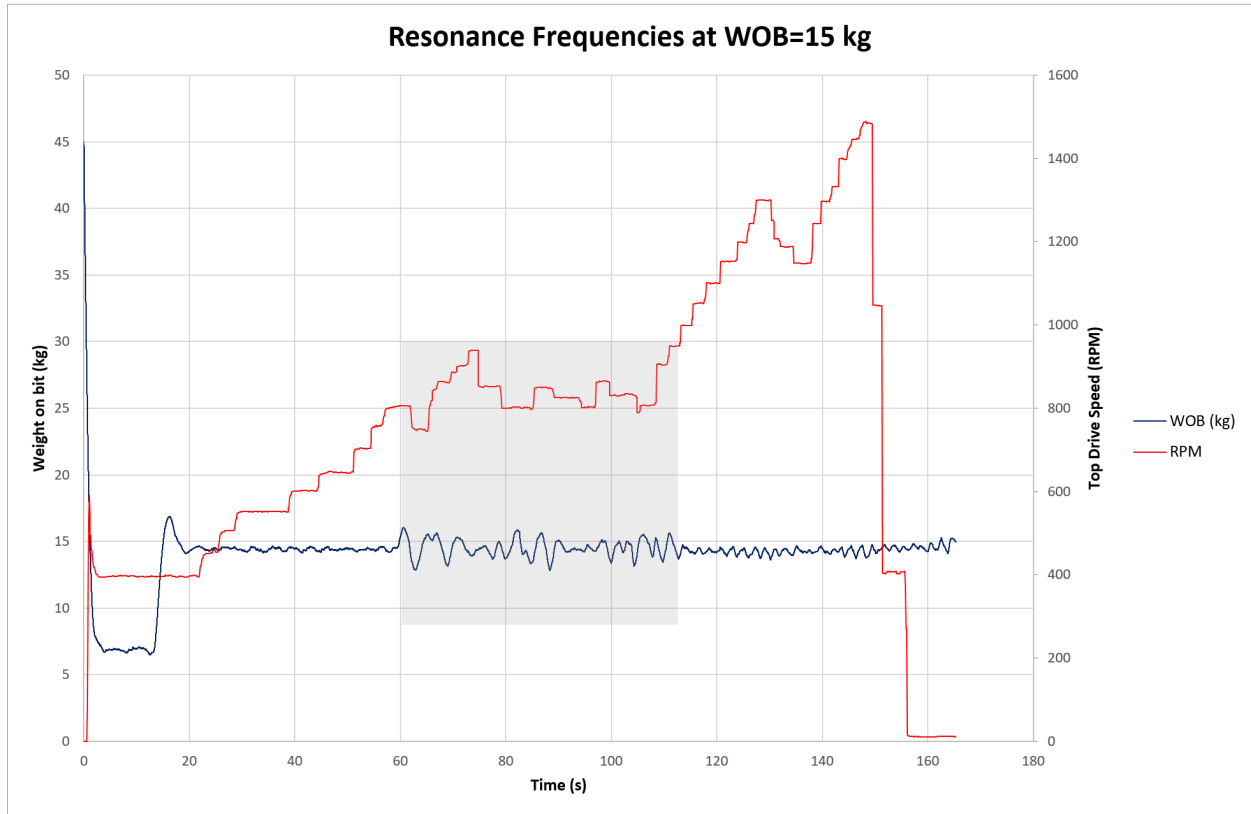


Figure 5.3.6: Graph of WOB and RPM versus time showing resonance around 800 RPM.

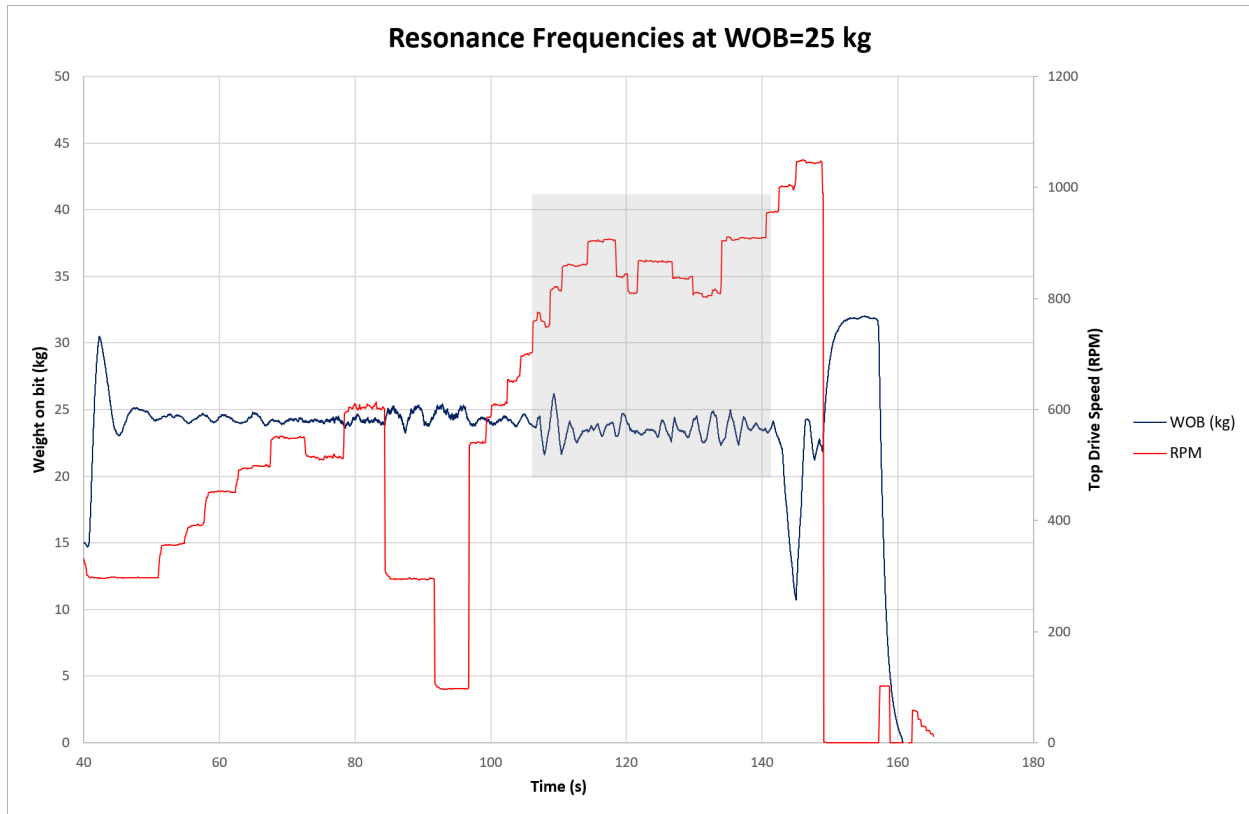


Figure 5.3.7: Graph of WOB and RPM versus time showing resonance around 800 RPM.

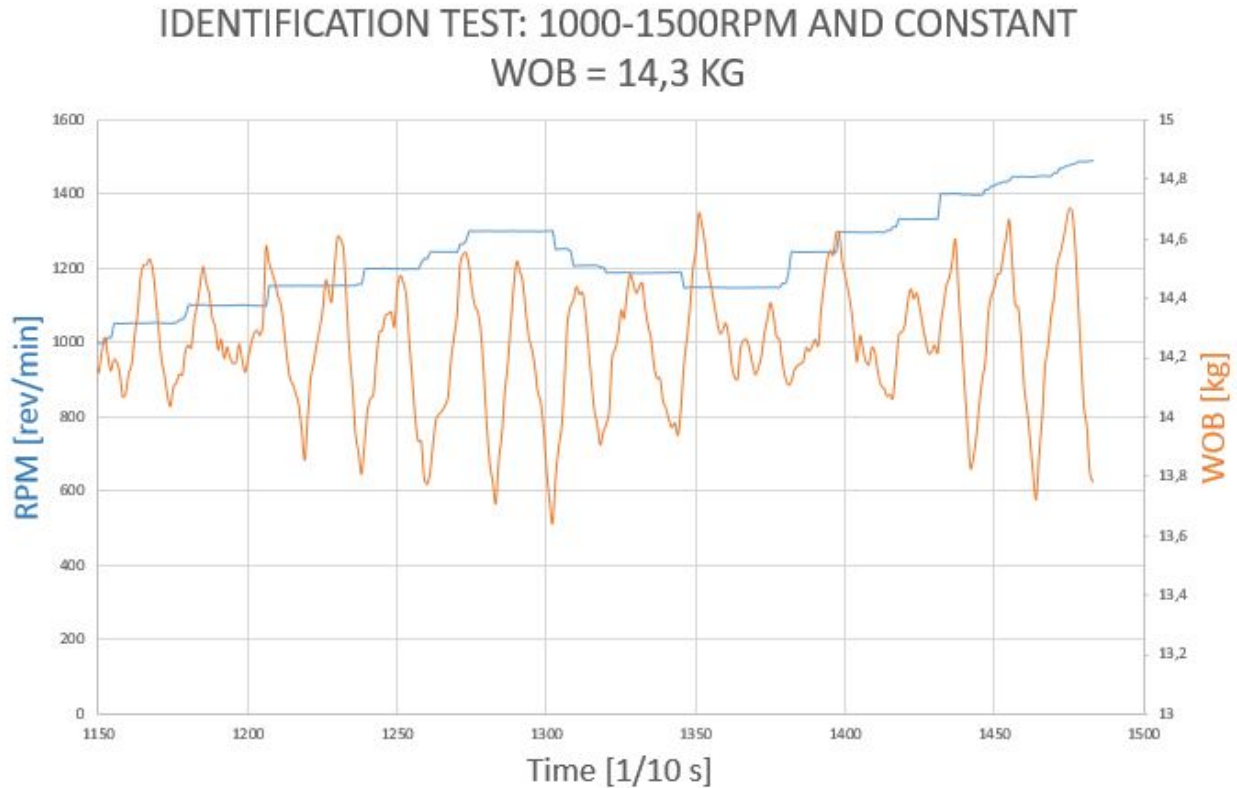


Figure 5.3.8: Graph of WOB and RPM versus time showing resonance and unstable drilling conditions when drilling with RPM above 1100.

The resonance frequencies were finally estimated to be around 600 RPM, 840 RPM and 1100 RPM.

Discovering this made it possible to push the efficiency of the drilling operation even further and increase the ROP above what was previously expected to be the maximum.

Bit bouncing Another important observation that was made when conducting the identification tests was bit bouncing at low drilling RPM. Bit bouncing resulted in poor borehole quality which was difficult to recover.

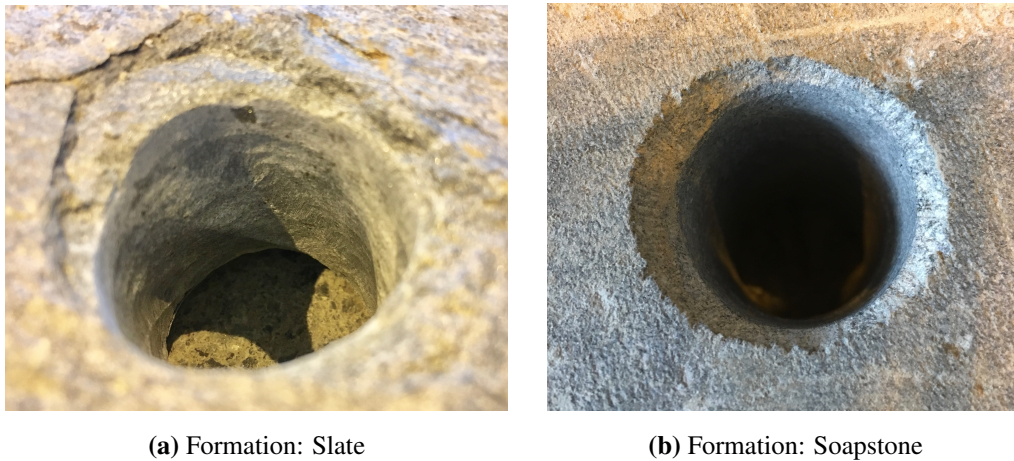


Figure 5.3.9: Poor borehole quality after experiencing bit bouncing

The results related to resonance, unstable drilling conditions and bit bouncing lead to the final decision that the RPM of the top drive should be kept constant. The final chosen value was 1000 RPM which, from the performed tests, was found to almost always ensure a stable drilling operation.

Weakest link of the design The weakest link of the design was found to be the connection between the BHA and the drill string. This connection point suffered from excessive drill string torques and torque peaks. It was therefore important to set a max drill string torque limit in the control system drive to avoid twist-off. Based on several test, this limit was set to 4 Nm. The control drill string torque was set to a set-point below safety limit to avoid excessive peaking of the drill string torque.



Figure 5.3.10: Twist-off at the connection between the BHA and the drill string when drilling asphalt

Internal drill string pressure Due to the limited amount of time before the competition day, and the difficulties with the machining and making of the high pressure swivel, the required testing to obtain the desired results could not be performed. Together with all this, a minor leakage in the swivel would have made the results somewhat untrustworthy.

However, to at least get a subjective impression of the effect of the internal pressure, 40 bars of operating pressure was applied to the circulation system on the night before the competition. When the bit was off-bottom and the pressure was applied, it was possible to see that the drill string would straighten out. When drilling, it was also possible to see that the drill string vibrations would reduce with increasing circulation pressure.

Automation

To be able to drill automatically, several components and elements from the discipline of control engineering had to be implemented. In this chapter, the components, the design, the optimization and the data infrastructure will be presented.

The first section reviews the components used to make the the control system work as a whole. It presents the PLC, the drives of the actuators, and the Simulink model.

The subsequent section explains the structure of the optimization function and why it was chosen. It demonstrates the in-depth study of how the different drilling parameters change in different drilling conditions, the limitations of the system and the final state machine used on the competition day.

The last section describes the data infrastructure and the data handling of the system. The communication between the different components, the storage of the data, data visualization and response time will all be presented and explained in detail.

6.1 Control System

A PLC provided by ABB was used to control the drilling operation. The PLC communicated with the PC where a Simulink model ran a control algorithm.

A feedback control system was used to control the drilling process. This means that the error

between the control signal and the output from the drilling process was used to bring the output from the drilling process closer to the control signal. PID controllers are common and effective for control loops including sensors, actuators and control algorithms and were therefore chosen as controllers for the drilling machine.

In addition to the PID controllers, the Simulink model ensured that all input and output variables were within the safety limits, signal units were converted to the right unit, an optimization function selected the right drilling parameters and that drilling dysfunctions were detected and mitigated.

6.1.1 Programmable Logic Controller

The PLC provided by ABB was programmed using CodeSys. 12 analogue inputs and 5 analogue outputs were required to provide sufficient information for the control system. The input ports received signals from the sensors and the motors and the output ports sent signals to the motors.

6.1.2 Actuator Drives

The actuator drives had an important role when it came to the safety of the system. The absolute limits of the output variables were set in the drives to make sure that no matter how the control system acted, these limits would never be violated.

If signals from the control system violating the limits were sent from the PC, a warning appeared on the screen.

The hoisting motor was limited by a maximum torque and a maximum RPM estimated during the testing phase. This meant that no matter what the set point was set as in Simulink, the drives would never output a control signal over the limit set in the drive. The top drive motor also had a maximum torque and a maximum RPM which were also estimated during the testing phase.

6.1.3 Simulink Model

PID controllers were proposed as a possible control loop feedback mechanism for the control system. The basic idea behind this type of controller is to read a sensor, then compute the desired

actuator output by calculating the proportional, integral and derivative responses and summing those three components to compute the output [21].

In this control system there were two PID controllers incorporated in the drives using the hoisting motor speed and the top drive speed as process variables. In Simulink there were two PID controllers used to control the hoisting motor. These two controllers had the two following process variables: the WOB and the torque of the drill string. Sensors and outputs from the drive encoders were used to measure these variables and provide feedback to the control system. The set points were the desired values of the process variables and were in most cases the maximum value for that variable. Because of the optimization function, the set point could however vary depending on the formation being drilled. At all time the difference between the measured process variable and the set point was used by the control system algorithm to determine the desired actuator output to drive the system.

6.1.3.1 Proportional-Integral-Derivative Controller Theory

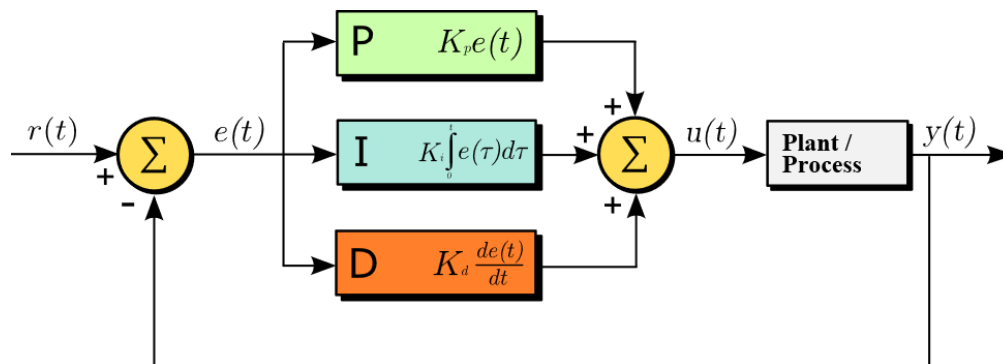


Figure 6.1.1: Illustration of a PID control loop [41]

General definition The proportional response depends only on the difference between the value of the set point and the value of the process variable which is referred to as the error term. The proportional gain determines the ratio of output responses to the error signal which generally means that increasing the proportional gain will increase the speed of the control response. However, if the proportional gain is too large it may cause the process variable to oscillate. It can be defined by Equation 6.1.1.

$$u_p(t) = k_c(y_s(t) - y(t)) \quad (6.1.1)$$

$u_p(t)$ the proportional term of the control output of the PID controller, k_c is the proportional gain, $y_s(t)$ denotes the desired setpoint and $y(t)$ the value of the process variable, .

The integral component sums the error term over time which results in a growing integral term component over time even if the error is very small. It can be defined by Equation 6.1.2.

$$u_I(t) = \frac{k_c}{\tau_i} \int_0^t (y_s(\tau) - y(\tau)) d\tau \quad (6.1.2)$$

$u_I(t)$ is the integral term of the control output of the PID controller and τ_i is the integral time. The steady-state difference is the final difference between the process variable and the set point. Since the integral response will continuously increase over time unless the error is zero, the effect is to drive the steady-state error to zero.

The derivative response is proportional to the rate of change of the process variable and causes the output to decrease if the process variable is increasing rapidly. Increasing the derivative time parameter will cause the control system to react more strongly to changes in the error term and will increase the speed of the overall control system response. The derivative term can be defined by Equation 6.1.3.

$$u_D(t) = k_c \tau_d \frac{d(y_s(t) - y(t))}{dt} \quad (6.1.3)$$

$u_D(t)$ is the derivative term of the control output of the PID controller and τ_d is the derivative time.

The output of the PID controller is the sum of the three parts described above. It is shown in Equation 6.1.4.

$$u(t) = u_p(t) + u_I(t) + u_D(t) = k_c(y_s(t) - y(t)) + \frac{k_c}{\tau_i} \int_0^t (y_s(\tau) - y(\tau))d\tau + k_c\tau_d \frac{d(y_s(t) - y(t))}{dt} \quad (6.1.4)$$

Tuning Tuning is the process of setting the optimal gains of P, I and D to get an ideal response from the control system where the goal is to achieve a stable and responsive loop with minimal overshooting. The gains of a PID controller can be obtained through trial and error. This is done by first setting the I and D terms to zero and gradually increasing the P term until the output of the loop oscillates. When P has been set to obtain a desired fast response, the I term is increased to stop the oscillations. The I term reduces the steady-state error but increases the overshoot (amount that process variable overshoots the final value). The I term is tweaked to achieve a minimal steady state error. Finally, the D term is increased until the loop is acceptably quick to its set point.

Gain scheduling When the value of gains and time constants vary according to the current value of the process value, the system is said to be non-linear. The problem of non-linearity can be solved by defining different operating points and linearising the problem about these points. In control theory this is called gain scheduling.

A gain-scheduled control system is a controller whose gains are automatically adjusted as a function of time, operating condition or plant parameters [26]. This is a common strategy for controlling systems whose dynamics change with such variables. This was the case in this project because the dynamics of the system changed when the properties of the formation changed. The WOB and RPM did not for example have the same set point in a soft sandstone as in a hard granite.

6.1.3.2 PID-Controllers in this System

The hoisting motor was controlled by a PID-controller in the drive and two PID-controllers implemented in the Simulink control system. The top drive motor was only controlled by the PID-controller in the drive.

The PID-controller of the hoisting motor drive was speed controlled. This meant that the speed set point was an output from the PC and controlled the torque of the motor. There was a possibility to

switch to torque control, but it was a slower signal and not as easy to control. In addition to this, when the motor was torque controlled it tried to achieve the highest possible speed for the given torque. This could have been dangerous if the WOB increased too much.

In the simulink model there were two PID-controllers that enabled the hoisting motor to be either WOB or torque controlled. When using WOB control, the set point was chosen based on the buckling limit of the pipe and the vibrations in the system. The saturations of the PID-controller made it possible to limit the speed during landing or gaps in the formation.

When using torque control, the torque set point was chosen based on experimental results. The output from the torque PID-controller was WOB which was then used as an input to the WOB PID-controller. After some testing it was found that a value of 2.4 Nm was a safe value and would reduce the risk of twist-off.

The top drive motor was controlled by torque in the drive and its set point was given by the RPM of the motor. There was a possibility to switch to speed control, but because of the torque limit of the pipe it was decided that torque control was safer. The RPM set point was not limited by the system, it could in theory be very high. Tests were therefore conducted to see how the system reacted to an increase in RPM.

The PID-controllers needed to be tuned in order to get a stable and accurate control. If overshooting was too high, there was a large risk related to buckling of the pipe. If the reaction was too slow, situations with too high vibrations or too high load would maybe not be mitigated fast enough.

The final gains used in the two PID controllers in the Simulink model were $P=2$, $I=1.2$ and $D=0$ for the torque PID controller and $P=80$, $I=0.1$ and $D=0$ for the WOB PID controller.

6.1.3.3 Scaling

The analogue and digital signals were either in volt or in Boolean values and therefore had to be converted to SI units. There was a scaling block in the PLC which enabled almost all unit conversions to be done there. This meant that Simulink would mainly handle regular SI units.

Torque values from the top drive motor were given in percentage of the nominal torque value (7.2

Nm), and later converted from percentage to Nm in Simulink.

The torque values of the hoisting motor first had to be converted to volts (0-10 V range) and then converted to Nm (0-4.68 Nm).

The speed values of the hoisting motor also had to be converted to RPM by first converting the signal to a 0-10 V signal and then to a 0-3,400 RPM signal.

The load cell also required a conversion to N. After having been converted to V, it could be converted to N as 0-10 V scale was equivalent to a 0-500 N scale. This signal was then converted to kg in order to compare it with the buckling limits that were calculated during the design phase. This signal then showed the amount of stress the load cell felt which was inversely proportional to the WOB. A relationship between Load Cell values and WOB was then found by pressing the top drive down on a scale and measuring how much weight was measured by a scale for a given Load Cell value. The relationship was approximately:

$$WOB = -1\Delta LoadCell - 38 \quad (6.1.5)$$

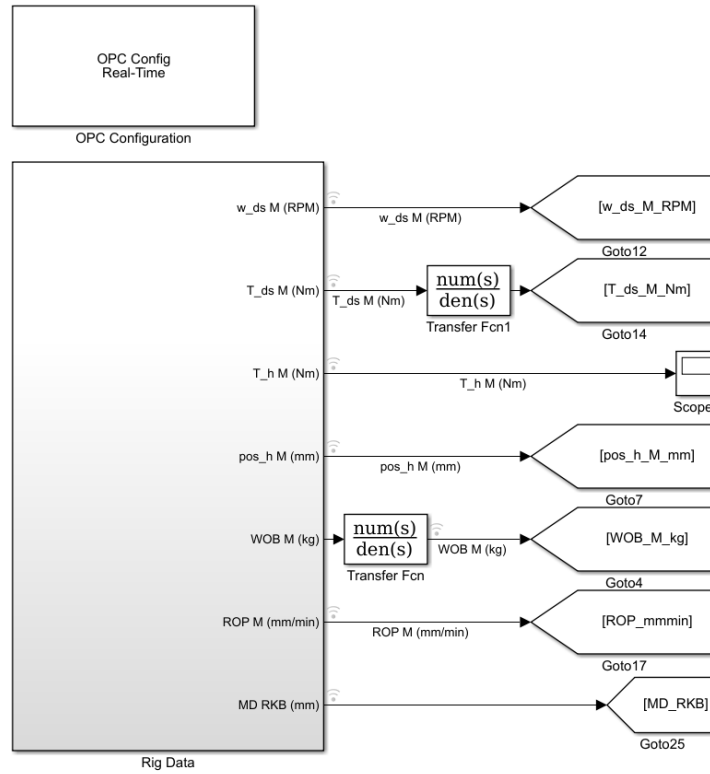
An offset of 38 kg had to be used which was equivalent to the weight of the top drive and the carriage. When the swivel was added, this offset was increased to 56 kg due to the additional weight on the carriage.

6.1.3.4 Safety Limits

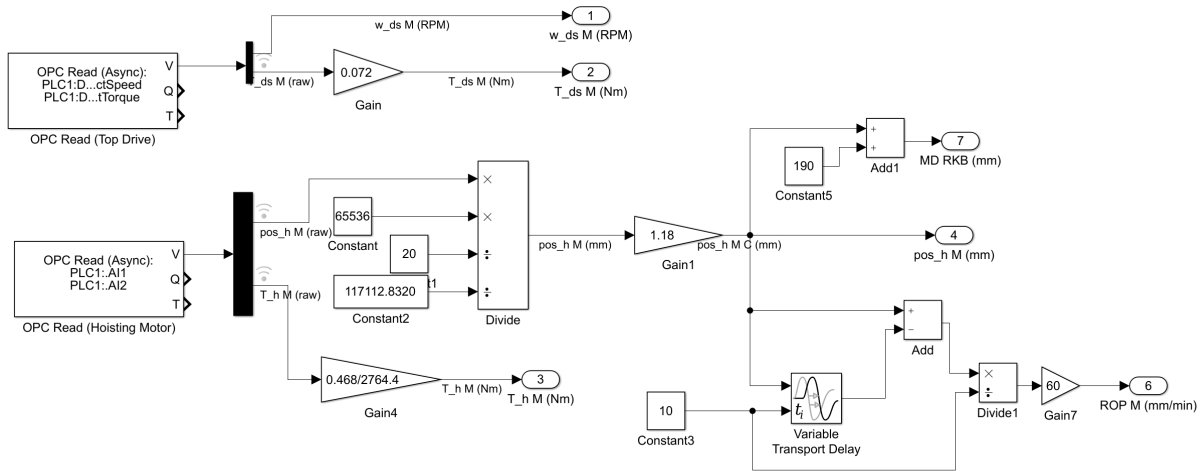
While drilling, several processes were running at the same time to keep the operation safe and efficient. One of the processes was continuously monitoring input variables. The critical limits for all the input variables were defined, this was both minimum and maximum values. The maximum values were critical, crossing this limit could cause pipe damage, wear and/or failure. The minimum value was defined based on what was thought to be an acceptable value to maintain efficient drilling. Any values below the minimum limit would lead to low ROP. These limits were based on testing which was presented in Chapter 5.

6.1.3.5 Overview of Simulink Model

The Simulink model was divided into several subsystems to make it easier to keep track of the different signals, different modes of operation and set points. The signals from the PLC were read from OPC Read blocks in a subsystem named "Rig Data". The signals were scaled inside the subsystem, but the filters were added on the signals outside the subsystem.



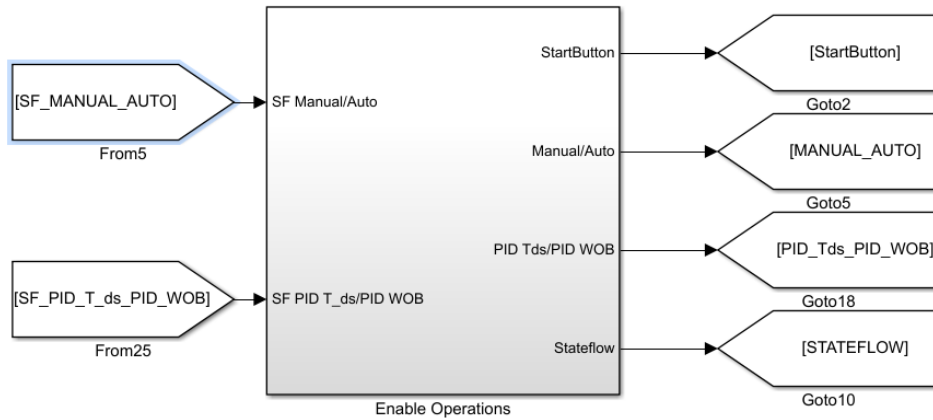
(a) Inputs and Outputs to the "Rig Data" subsystem in Simulink



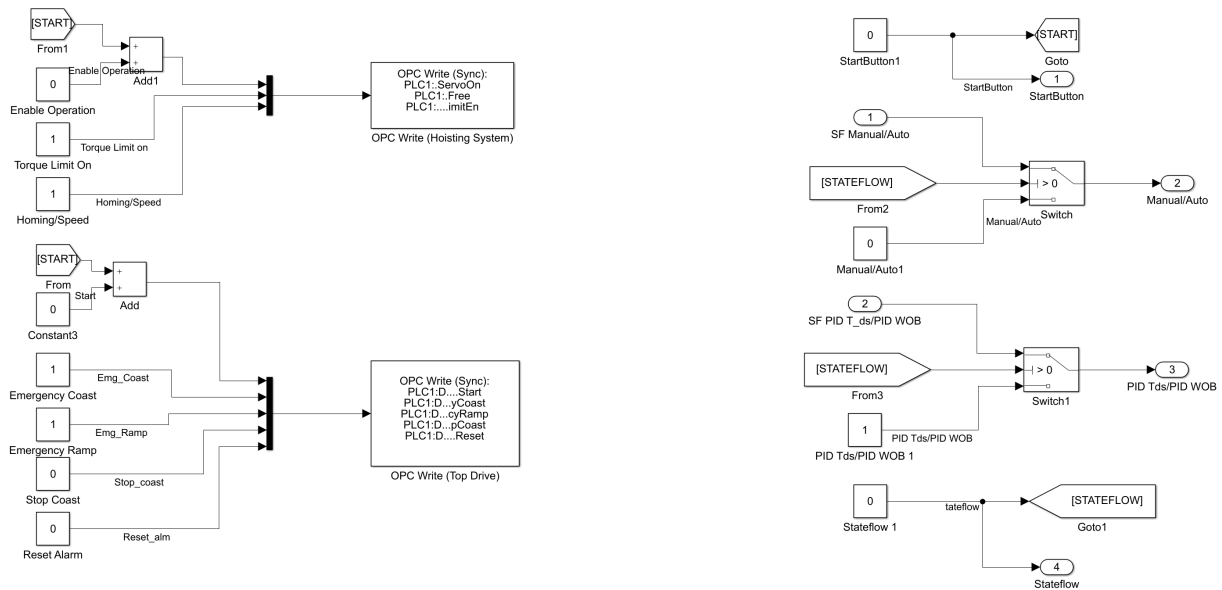
(b) "Rig Data" subsystem

Figure 6.1.2: "Rig Data" subsystem

The digital signals used to enable operations in the drives were gathered in a subsystem called "Enable Operations".



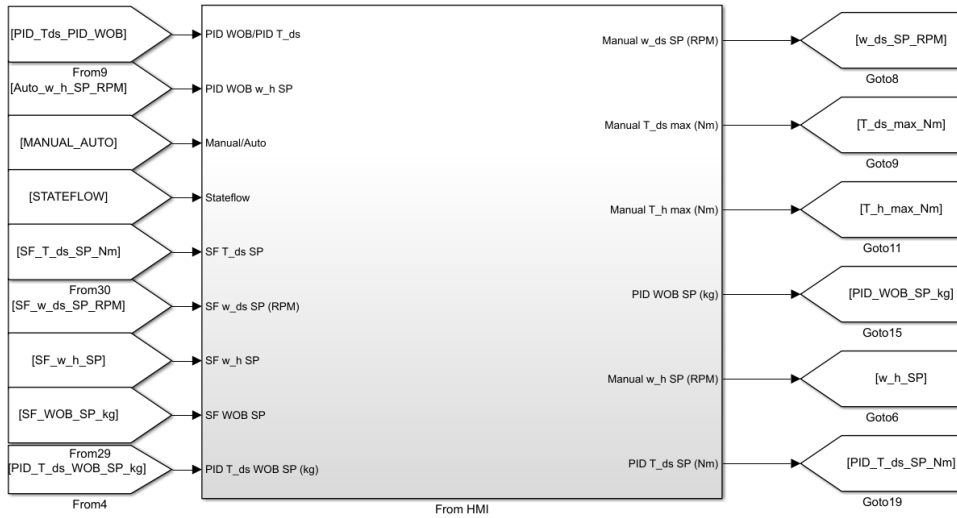
(a) Inputs and outputs to the "Enable Operations" subsystem in Simulink



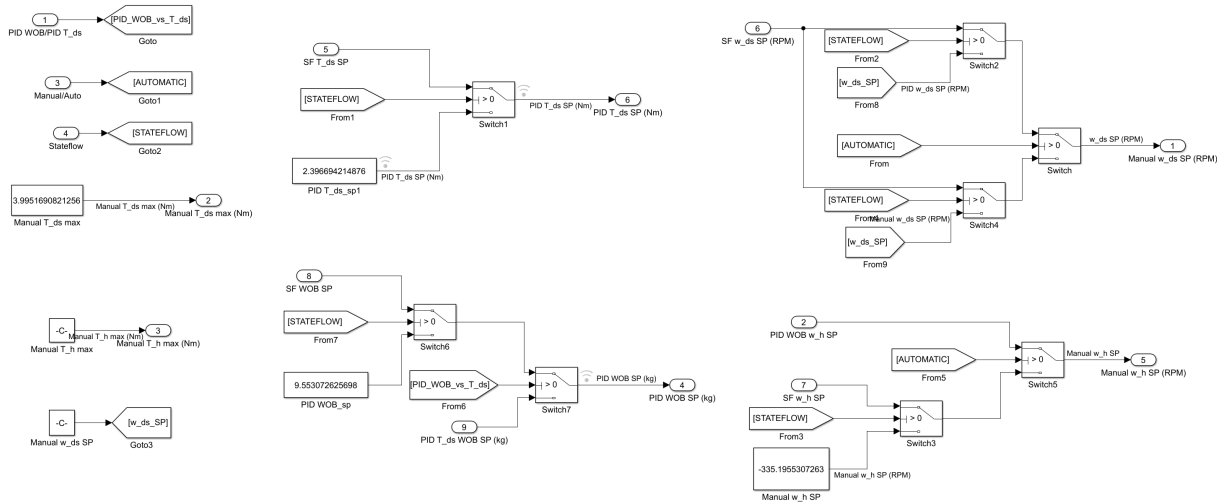
(b) "Enable Operations" subsystem

Figure 6.1.3: "Enable Operations" data subsystem

The different set points were put in a subsystem named "From HMI". The inputs were set points from the automatic controls, the set points chosen from the HMI were inside the subsystem and the outputs were the final set points chosen depending on the mode of operation (manual/automatic, PID/Stateflow).



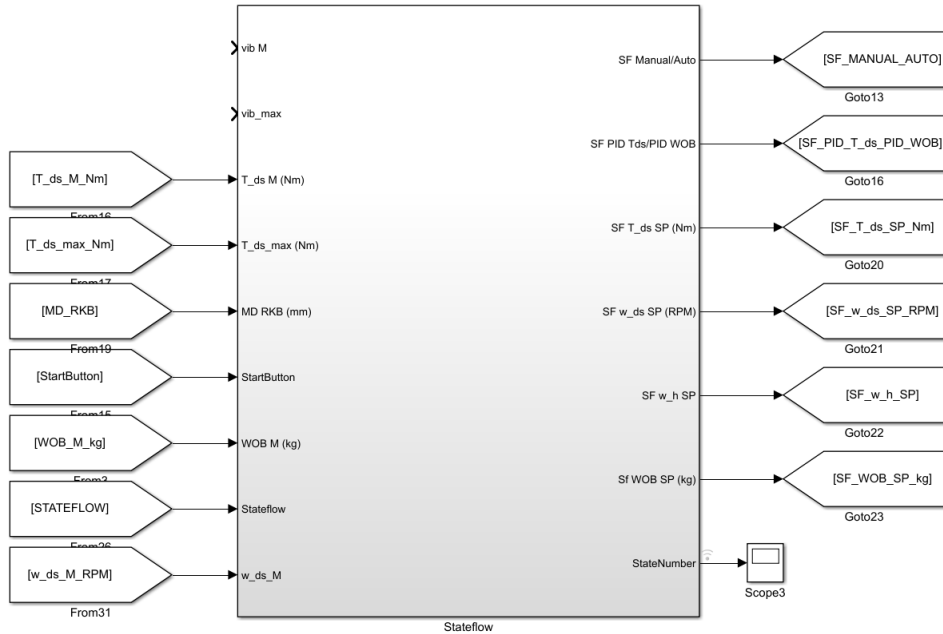
(a) Inputs and outputs to the "From HMI" subsystem in Simulink



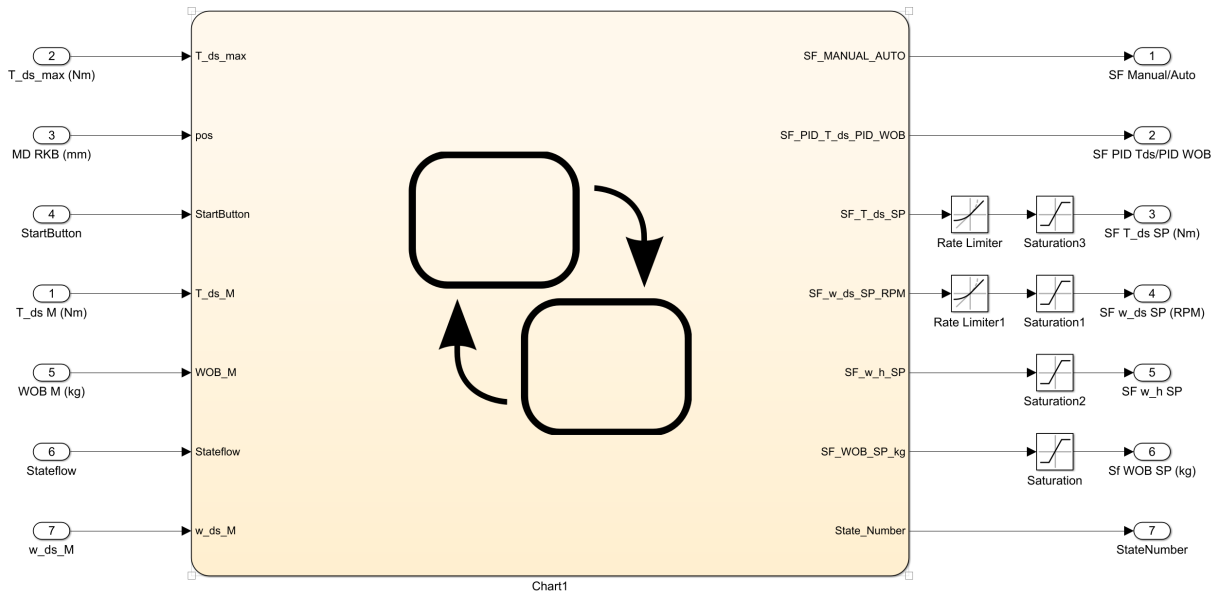
(b) "From HMI" subsystem

Figure 6.1.4: "From HMI" data subsystem

The Stateflow chart was put in the subsystem called "Stateflow". Inputs to this subsystem were different measurements required to automate the operation (position, WOB...) and the outputs were set points.



(a) Inputs and outputs to the "Stateflow" subsystem in Simulink



(b) "Stateflow" subsystem

Figure 6.1.5: "From HMI" data subsystem

The two PID controllers were gathered in a subsystem called "PID Controllers". The main inputs were the drill string torque set point and the WOB set point and the most important output was the

hoisting motor speed.

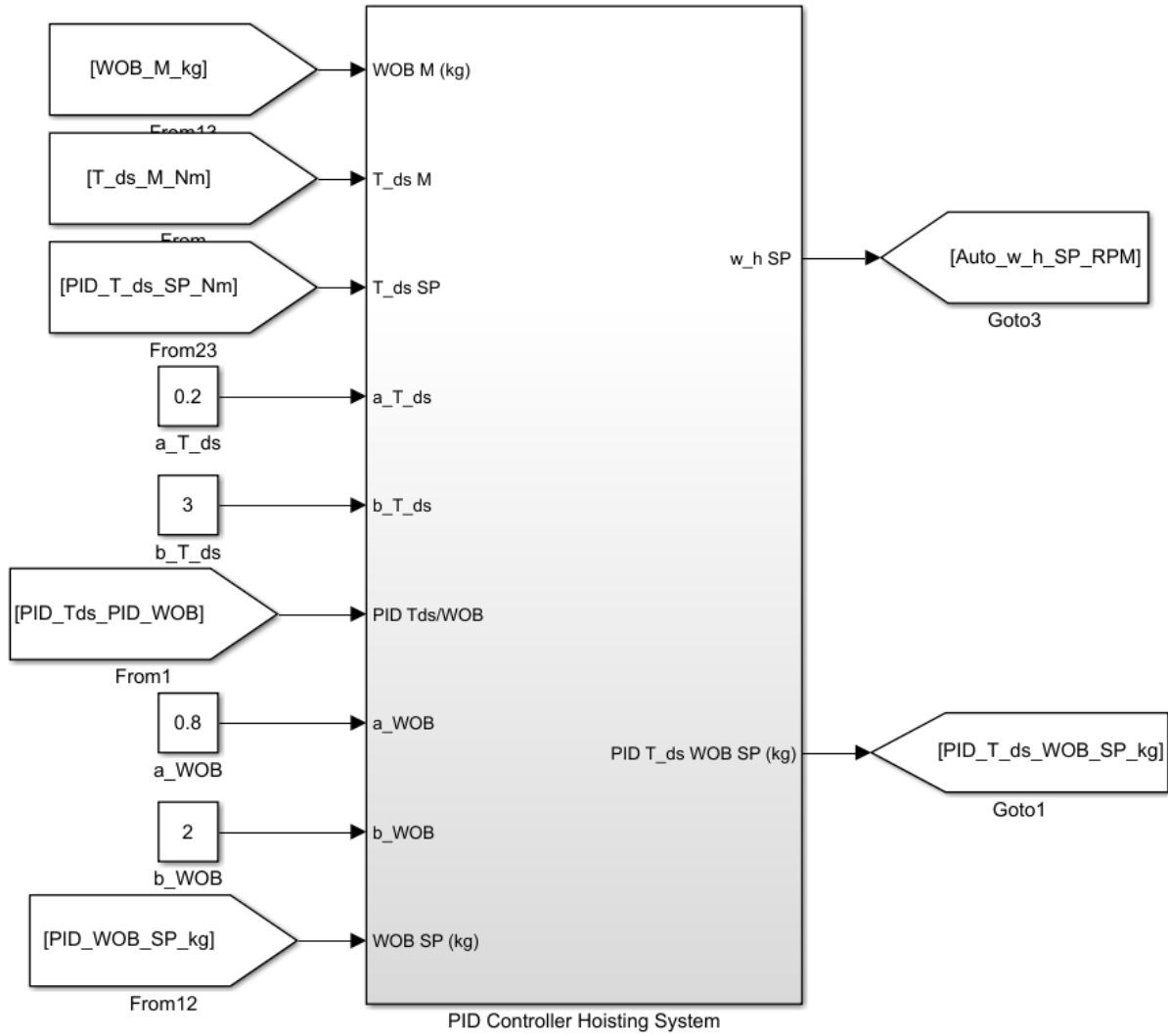
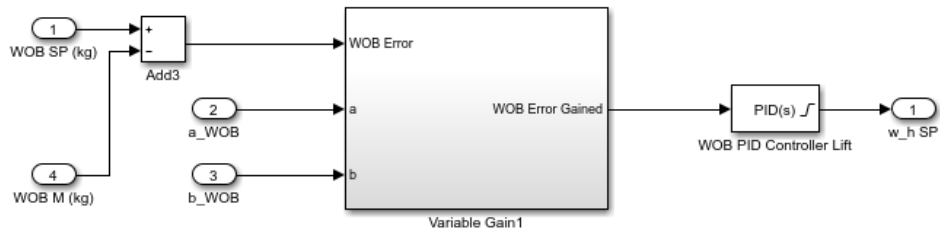
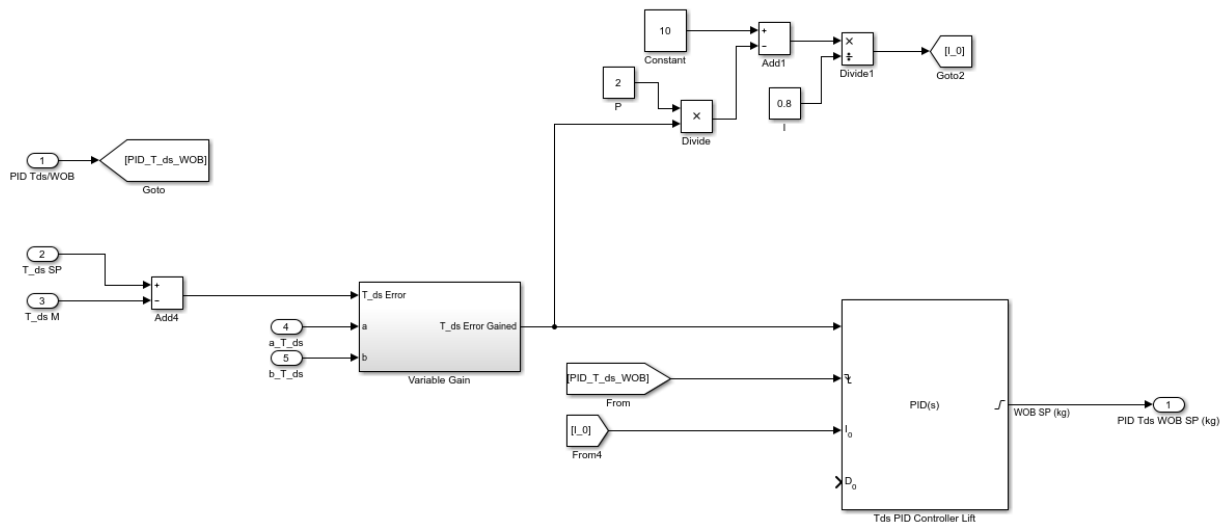


Figure 6.1.6: Inputs and outputs to the "PID Controllers" subsystem in Simulink



(a) "WOB PID" subsystem



(b) "Tds PID" subsystem

Figure 6.1.7: "PID Controllers" data subsystem

Variable gains were added to the PID controllers in order to reduce the rate at which the the set point was reached when the measured value was lower than the set point, and increase the rate of change when the measured value was higher than the set point.

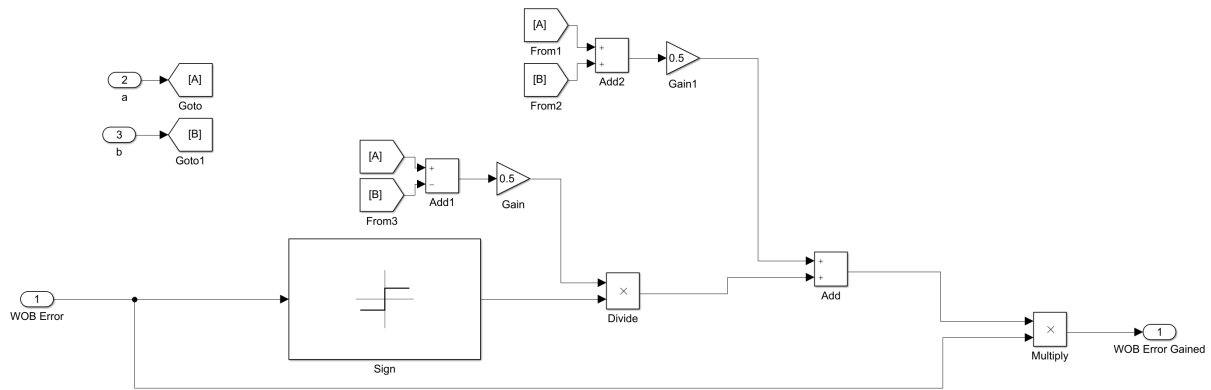
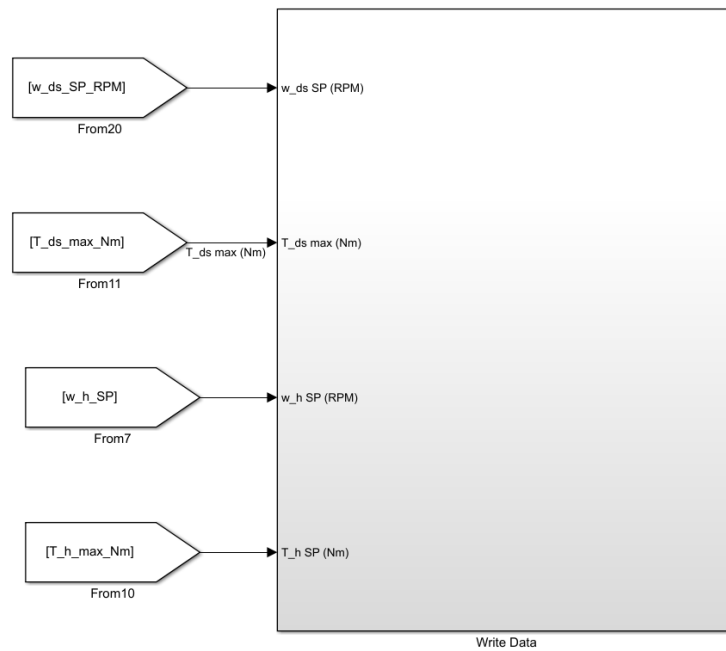
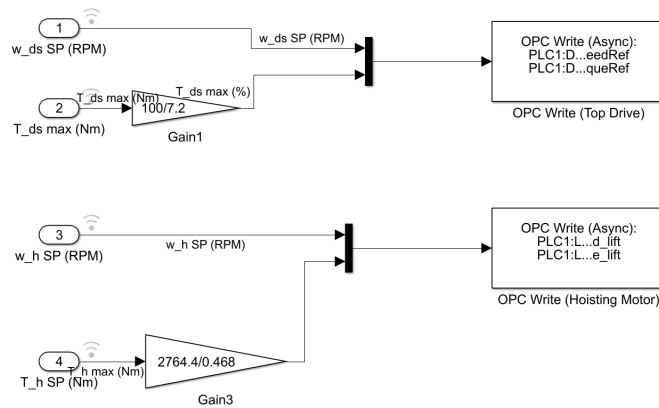


Figure 6.1.8: Variable PID gains in the WOB PID controller

The final subsystem was the "Write Data" subsystem with the OPC Write blocks, enabling the the communication from the PC to the PLC and then to the drives.



(a) Inputs and outputs to the "Write Data" subsystem in Simulink



(b) "Write Data" subsystem

Figure 6.1.9: "Write Data" subsystem

6.2 Chosen Optimization Function

When the optimization function was finally developed, it was based on experience from testing the rig, advice from the supervisors, literature studies and the limitations/possibilities of the drilling machine.

6.2.1 Data Analysis

After running several tests on different types of rock samples, data analysis of the test results was performed to get a better understanding of the drilling operation. For the optimization of the drilling operation, ROP and MSE were studied for different types of rock samples ranging from hard rocks, such as marble and cement blocks, to softer rocks, such as black slate and soapstone. Several tests were conducted on asphalt as well.

Because a decision was made to drill with a constant RPM, a more in-depth study of the effect of a changing WOB on ROP and MSE in different rock samples was done. The results are shown in Figure 6.2.1, 6.2.2, 6.2.3, 6.2.4, 6.2.5 and 6.2.6.

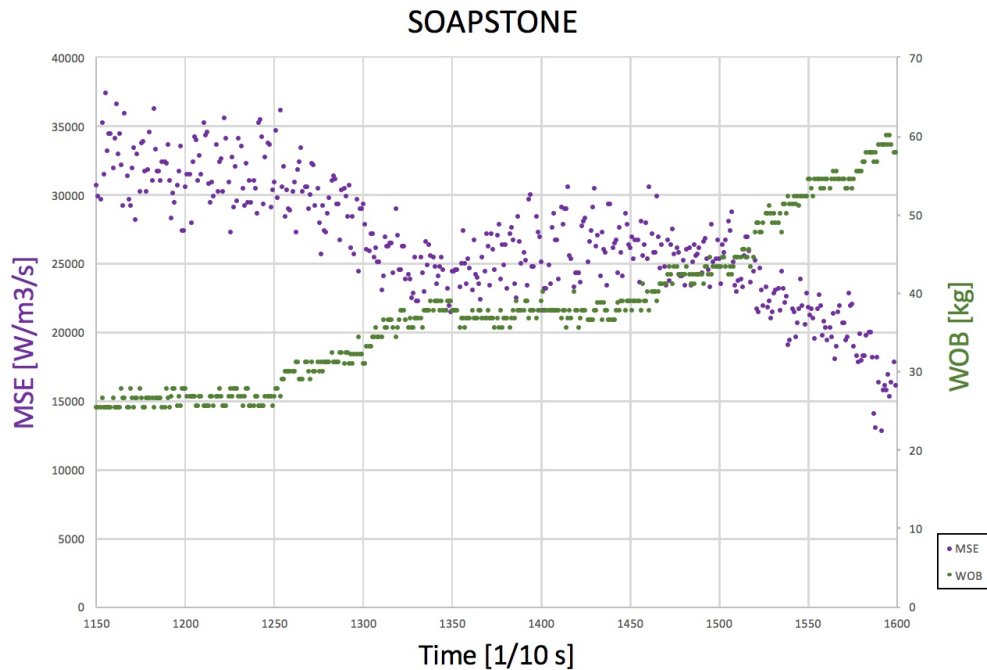


Figure 6.2.1: Test results from drilling in soapstone with a constant RPM of 1000. MSE plotted against time on the primary y-axis and WOB against time on the secondary y-axis. [17]

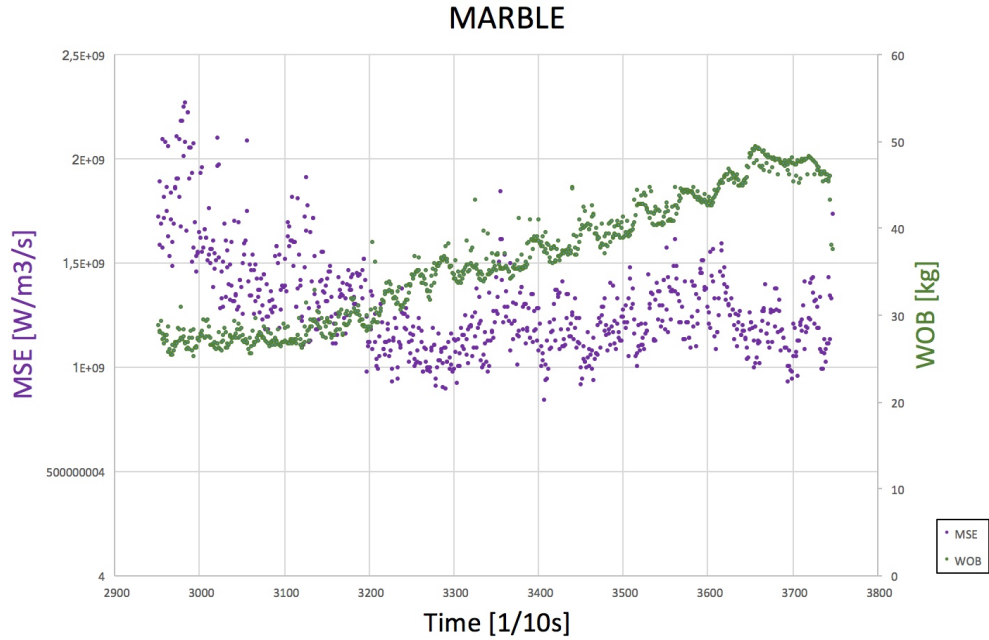


Figure 6.2.2: Test results from drilling in marble with a constant RPM of 1000. MSE plotted against time on the primary y-axis and WOB against time on the secondary y-axis. [17]

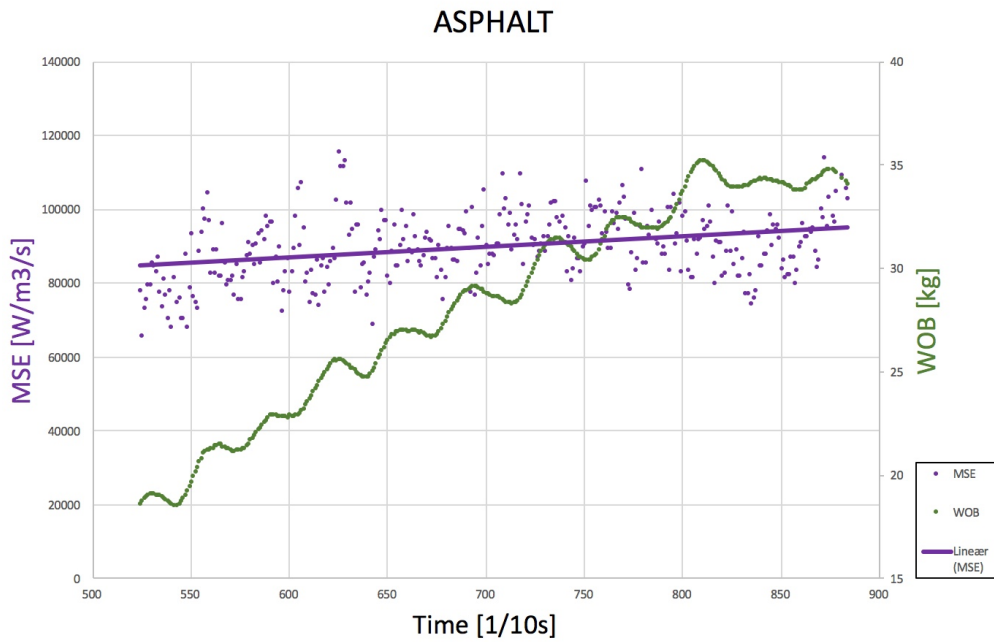


Figure 6.2.3: Test results on asphalt with a constant RPM of 1000. MSE plotted against time on the primary y-axis and WOB against time on the secondary y-axis. [17]

To ensure an energy efficient drilling operation, the smallest possible MSE is the preferable choice.

From the data analysis, it was found that for harder rocks, the MSE became higher compared to softer rocks. This can be seen in Figure 6.2.1 and Figure 6.2.1. MSE calculation could possibly be used to estimate the hardness of the drilled rock.

In most cases, increasing WOB resulted in a decrease in the MSE, meaning more energy efficient drilling. This can be seen in Figure 6.2.2 and Figure 6.2.1. This did however not apply for asphalt, Figure 6.2.3. When drilling through asphalt, increased vibrations were observed in both the drill string and the entire structure. It was also observed that the cutting size was relatively large, making it difficult to circulate it out from the bottom due the small area between the annulus and the BHA. A result of this was cutting accumulation in the bottom of the hole and inefficient drilling. A combination of both of this may be the reason for the increase of MSE when WOB was increased.

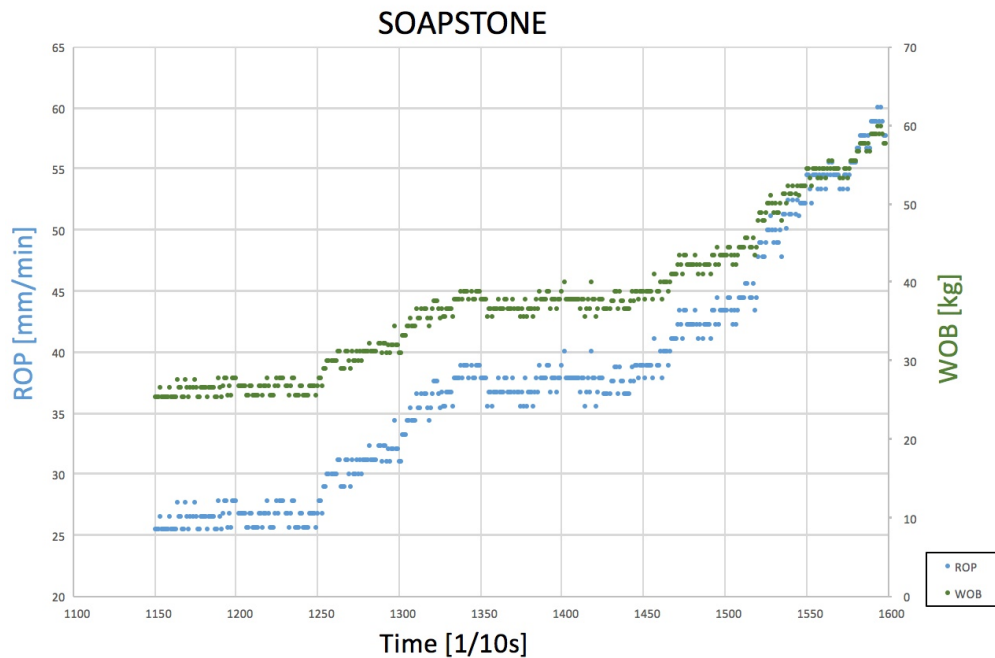


Figure 6.2.4: Test results from drilling in soapstone with a constant RPM of 1000. ROP plotted against time on the primary y-axis and WOB against time on the secondary y-axis. [22]

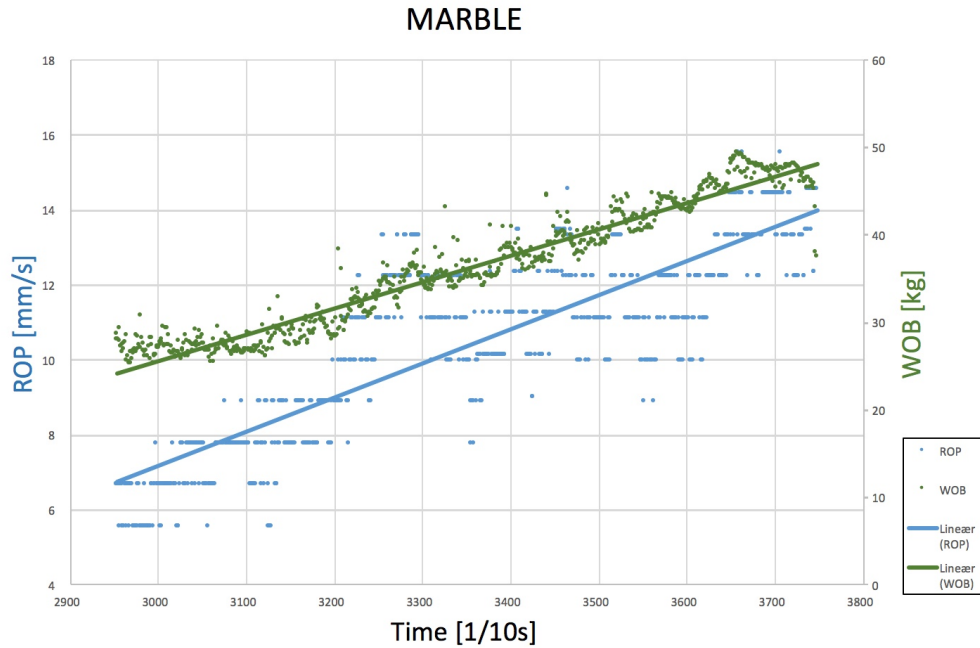


Figure 6.2.5: Results from drilling in marble with a constant RPM of 1000. ROP plotted against time on the primary y-axis and WOB against time on the secondary y-axis. [22]

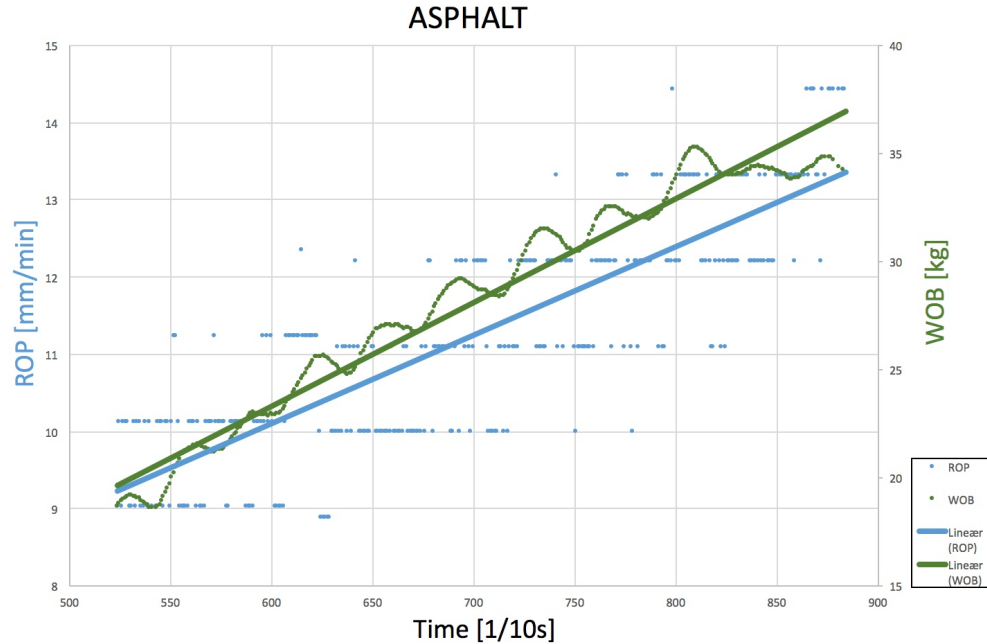


Figure 6.2.6: Test results on asphalt with a constant RPM of 1000. ROP plotted against time on the primary y-axis and WOB against time on the secondary y-axis. [24]

From Figure 6.2.4, 6.2.5 and 6.2.6, it appears clearly that the ROP is proportional to WOB. One of the main objectives of this project was to drill fast and there was no energy restriction, therefore, ROP was the preferable optimization parameter.

6.2.2 Implementation of the Optimization Function in Simulink

The drilling machine had two control variables: WOB and RPM. ROP is a function of both variables, but the exact relationship is unknown. ROP is also a function of the formation being drilled which means that the relationship between ROP, RPM and WOB varies depending on the formation.

ROP can be optimized within an operational window limited by different factors. In this case, because of the weak pipe, they were expected to be vibrations and buckling. This means that combinations of WOB and RPM could be optimized within a window defined by buckling and vibration limits. To optimize the ROP, the values of the drilling variables should lie close to these limits. This is illustrated in figure 6.2.7 where the operating window is described by a hoisting motor parameter and a top drive motor parameter. The exact parameter is not yet specified as this will be discussed later.

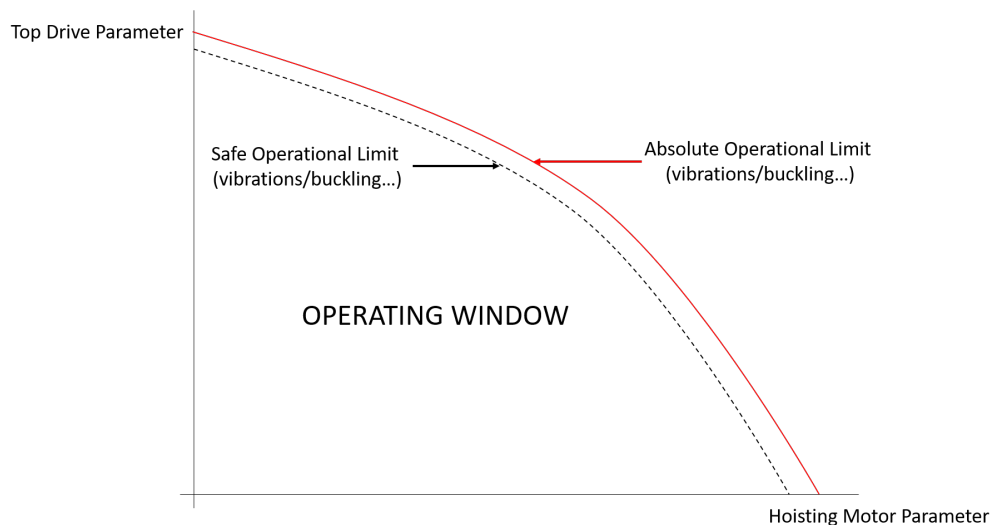


Figure 6.2.7: Illustration of the operating window.

To determine the limits of the operating parameters, extensive testing was conducted in different

rock formations and different operating parameters 5.3.1.4. During testing, several cases of twist-off and stick-slip were experienced and it therefore became clear that buckling was not the biggest limitation, but rather the drill string torque. When the drill string torque peaked due to a change in a formation or hard inclusions in the rock, the WOB PID controller did not react accordingly because the WOB did not necessarily change. It therefore became important to include the drill string torque in the control algorithm in some way.

After some reflection and analysis, it was proposed that two PID controllers could be connected in series with the first one having the drill string torque as a process variable and the required WOB as an output and the second using the WOB from the first PID as a process variable and controlling the hoisting motor speed by sending a speed set point signal to the drives.

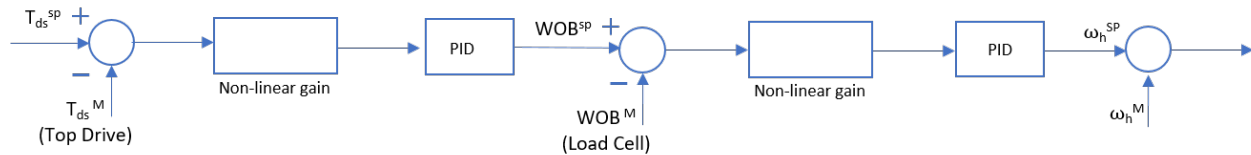


Figure 6.2.8: Illustration of the use of drill string torque as a process variable

An illustration of the new optimization strategy is shown in Figure 6.2.9. The idea is that the speed of drilling should be optimized by maximizing T_{ds} as a function of w_h .

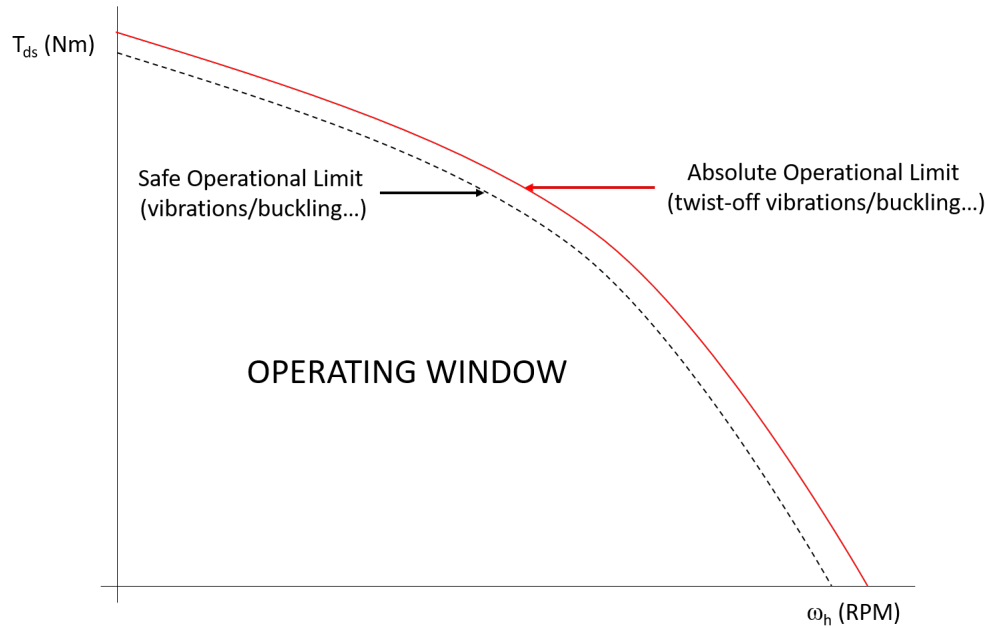


Figure 6.2.9: Illustration of the updated operating window.

A constant RPM (1000 RPM) and a constant drill string torque (2.4 Nm) were chosen for the drilling operation. The idea was that as long as the drill string torque was limited, the machine would be able to transition between different layers by adjusting the WOB through reducing or increasing the downward vertical speed to keep a constant drill string torque.

Following this, a decision was made to implement the drilling machine as a state machine in which the operation changed between different, discrete drilling states. The drilling strategy implemented was based on experiences from the testing phase. One of the priorities was to keep the strategy as simple as possible and "fit for purpose".

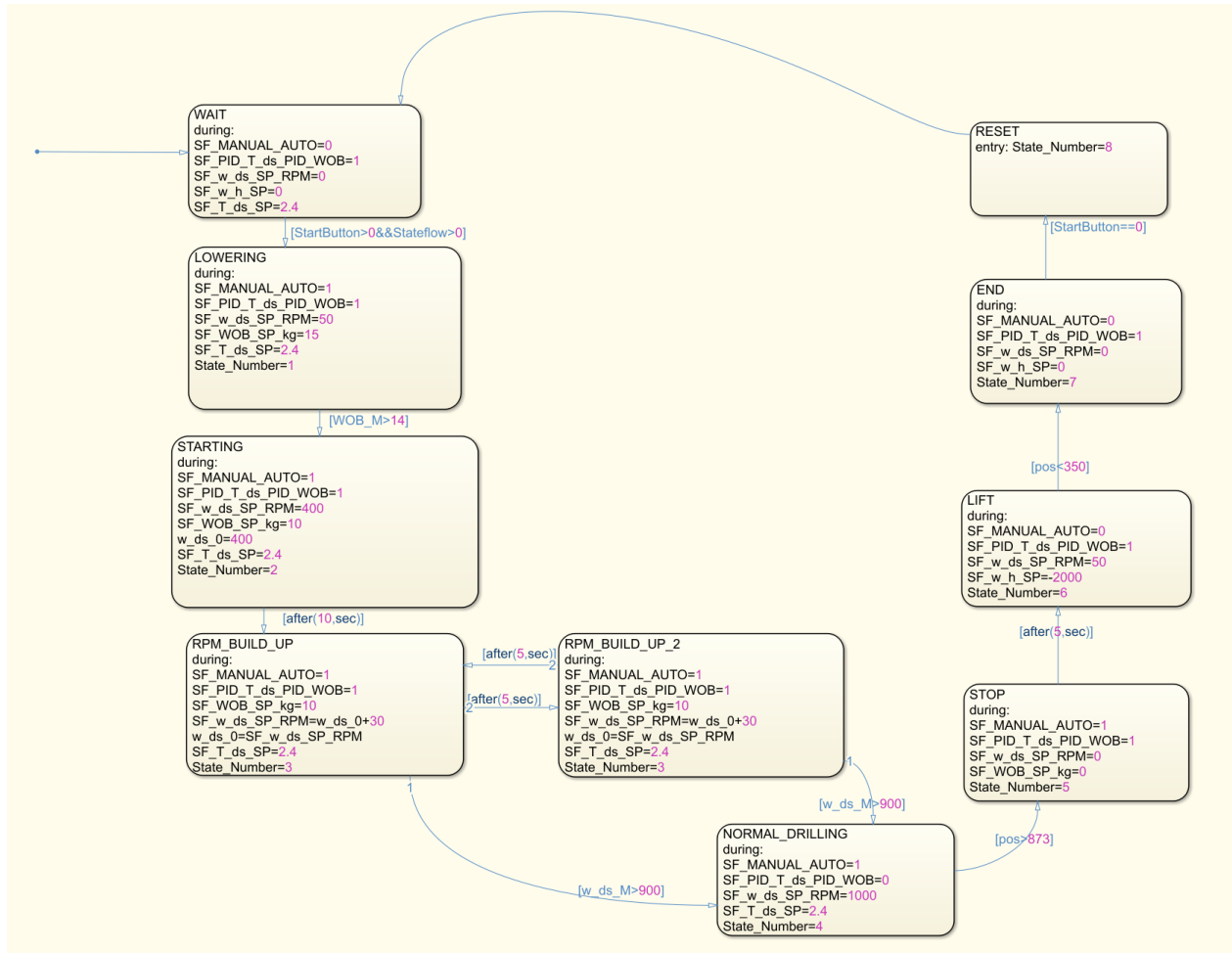


Figure 6.2.10: Details of the stateflow chart

The main drilling states were "Lowering", "Initializing", "Drilling", "End Reached", "Tripping Out" and "End of Operation". In the "Lowering" state the bit was lowered at a constant speed and low RPM (50 RPM) using the manual mode until an increase in WOB was detected. When the WOB reached a certain value (14 kg) the machine transitioned to the "Initializing" state where the machine switched to WOB Control Mode. The WOB set point was set to a low value (10 kg) and the RPM was increased to a safe value (400 PRM). After 20 seconds the machine transitioned into the "Drilling" state where it switched to Drill String Torque Control. The top drive speed was slowly increased to the chosen operating value (1000 RPM) and the top drive torque set point was chosen (2.4 Nm). Before starting the drilling, the end point had to be calibrated as the "End Reached" state was initiated when a certain depth was reached. In this state all set points were set

to 0. After a certain time period the machine transitioned into "Tripping Out" mode where it was in manual control. At a certain speed and RPM the bit was lifted up to the surface. At a certain depth all set points were again set to zero in the "End of Operation" mode.

6.2.3 Results of using T_{ds} as an Optimization Parameter

Using T_{ds} to control the WOB proved to be a good solution when trying to fully automate the drilling operation. The control system managed to ensure good and stable transitions when drilling through formations with different properties. It was also able to react to problems with high drill string torque in rocks with high friction coefficient. The graph in Figure 6.2.11 shows how the control system reacts to peaks in drill string torque by reducing the WOB.

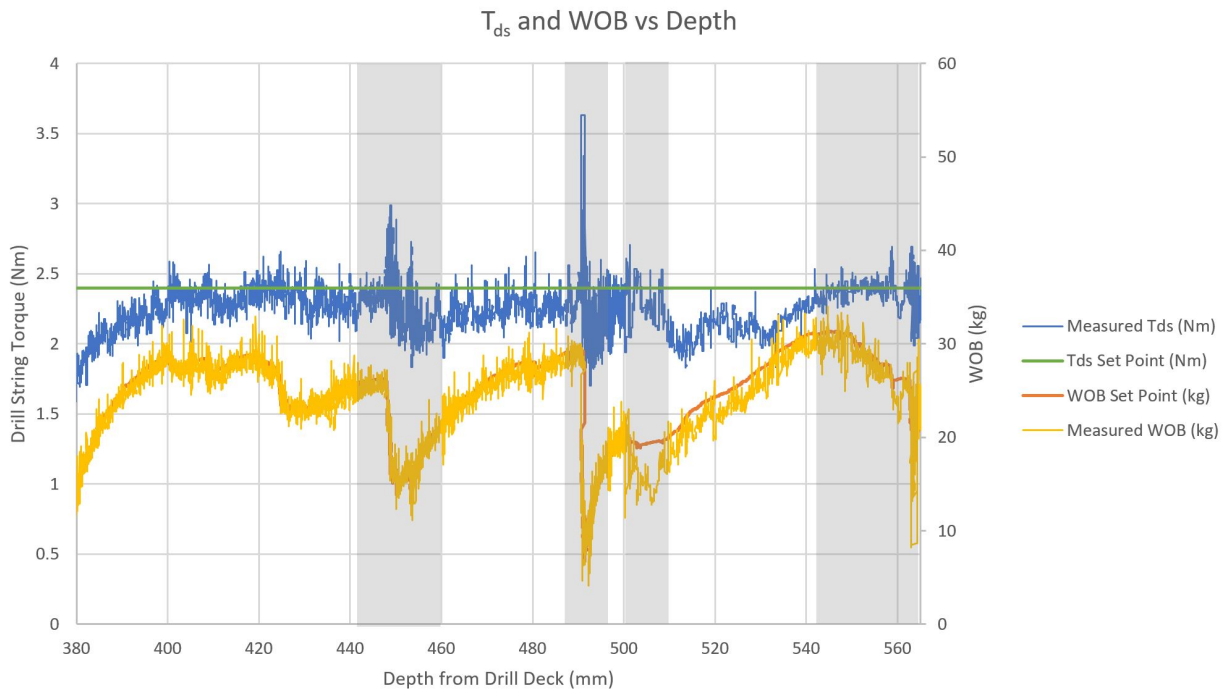


Figure 6.2.11: Graph of T_{ds} and WOB vs depth showing how the control system reacts to peaks in T_{ds} by reducing the WOB

6.3 Data Infrastructure

6.3.1 Communication

The control system was dependent on receiving reliable and accurate real-time data from the actuators and the sensors, as well as sending controls to the actuators. This was done by connecting all sensors and actuators to the PLC and connecting the PLC to the PC. Connections were made using analogue input and outputs in the PLC.

Another important point to consider was how the units of the input and output signals had to be scaled as the units required by the actuator drives and the Simulink model were different. A scaling block in the PLC was used to convert the signals, however, not all required scalings were available. The signals that were not converted to the desired unit in the PLC had to be converted using blocks in the Simulink model.

6.3.2 Storage

It was also important to evaluate the different ways to log and store data. Relevant input/output signals and control system variables had to be stored in files to enable post-operation analysis.

This was done using the Simulation Data Inspector in Simulink which exported the signal data to the Matlab Workspace. The variables containing the signal data could then be saved to files.

6.3.3 Data Visualization

6.3.3.1 Dashboard

Dashboard blocks in Simulink were used to design the display for monitoring and visualizing the overall operation. The main dashboard contained a collection of the most important parameters related to the rotary system and hoisting system. Some of the most important parameters to monitor were the time, the depth from the drill deck, the WOB, the torque of the top drive, the RPM, the ROP and the MSE.

Switches to enable drilling in different modes were placed in the upper left corner of the screen. The sliders used to change the different set points for the drilling modes were placed on the right hand side.

Important drilling parameters such as the duration of the drilling operation and the drilled depth were continuously displayed as numerical values during the entire drilling operation.

The process variables used to control the hoisting system were displayed graphically. The measured torque was displayed together with its set point and its maximum value, and the measured RPM and WOB were plotted together with their respective set points.

Drilling parameters used to quantify the drilling efficiency were also displayed graphically. The two chosen parameters were the ROP and the MSE.

Some of the most important values were also displayed numerically or in semi-circular gauges.

A display of the current drilling state was also added as a function of the current state in the Stateflow chart.

Two subsystems were also added to enable manual control of the hoisting motor and the top drive.

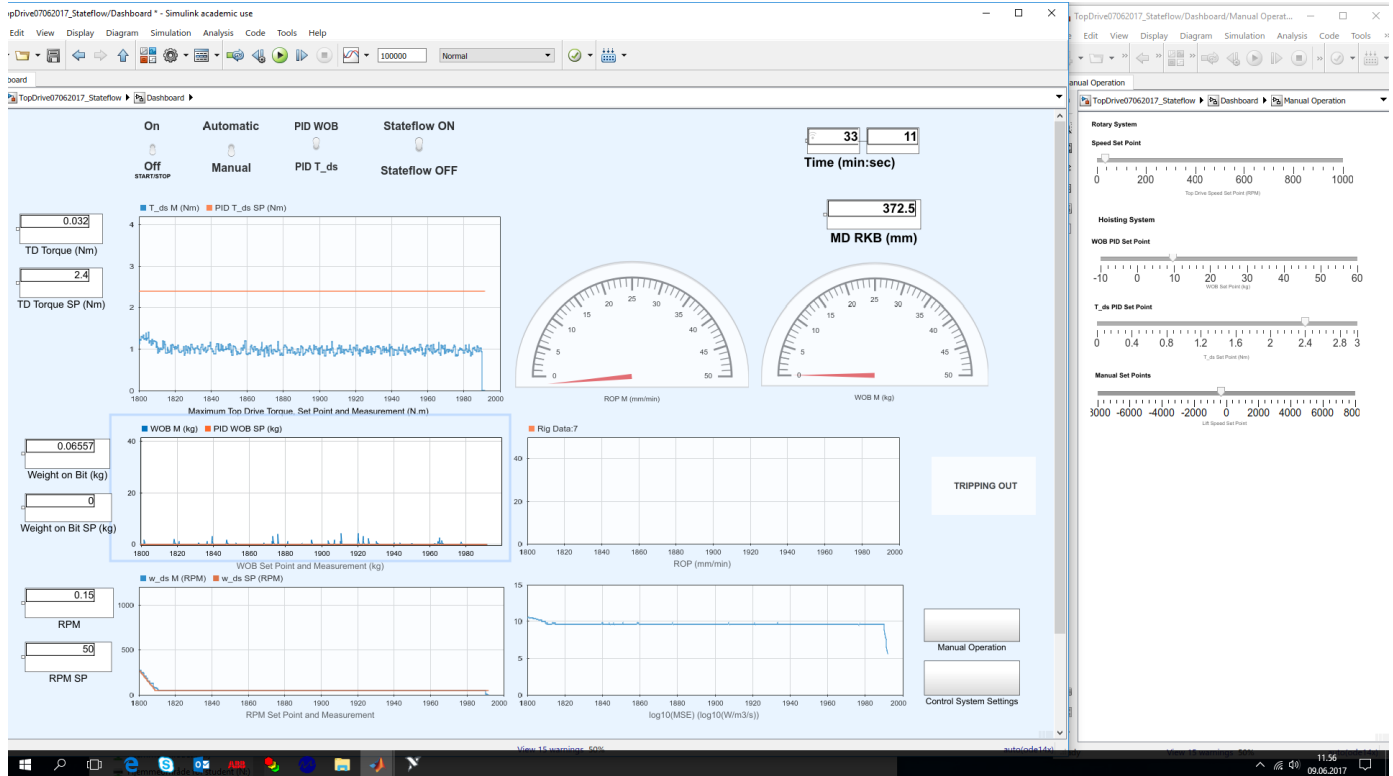


Figure 6.3.1: Simulink dashboard

6.3.3.2 Response Time

Response time of a measurement is defined as the elapsed time between an inquiry on the system and the response to that inquiry. Speed of response is an important measure of how quickly the system respond and of how well the system is performing. Figure 6.3.2 shows a response time of 1.5 to 3 seconds for the top drive motor.

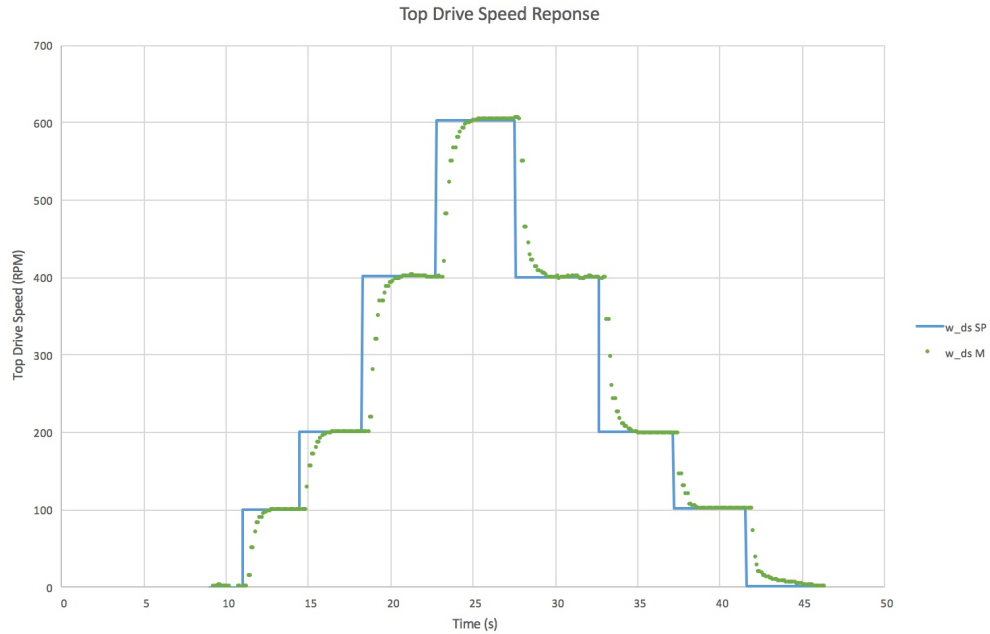


Figure 6.3.2: The graph above shows a response time of 1.5 to 3 seconds on the top drive motor, where the desired set points are shown in blue and the measured values are shown in green

Figure 6.3.3 shows the response time for the WOB PID controller (hoisting motor).

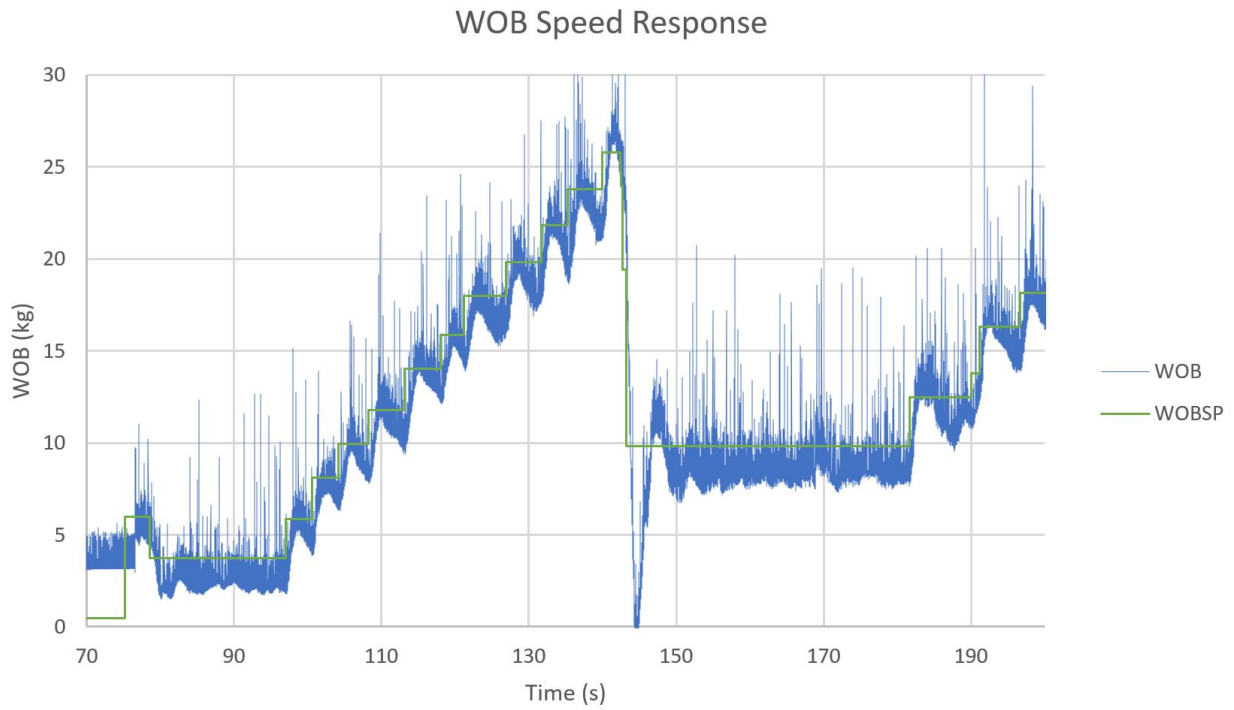


Figure 6.3.3: Graph of WOB PID controller response, where the desired set points are shown in green and the measured values are shown in blue

Competition

In the fall of 2016, student teams from ten different universities joined a design competition where the aim was to design a drilling rig and related equipment to autonomously drill a vertical well as quickly as possible while maintaining borehole quality and integrity of the drilling rig and drill-string.

In the spring term of 2017, seven universities were qualified and selected by DSATS to proceed to the second phase, where the students were to build the rig and use it to drill the provided rock sample.

The performance of the rig design and control algorithms were demonstrated through a test conducted at each university. The on-site test day at NTNU was scheduled by the competition committee to be on June 8th 2017.

As the judges arrived, a team and project presentation was given by the students followed by questions from the judges. The presentation highlighted the key areas of the design, noting the changes that had been made since the design phase, stating why and how they they were made. Key findings, construction challenges and lessons learned were presented, as well as an overview of actual expenses compared with the initial estimate.

After the presentation, DSATS members were invited to attend and witness the drilling operation. A pilot hole of 25 mm had been pre-drilled, and the stopwatch was started as the main drilling

began. The test continued until the final depth of the formation block was reached, and the final drilling time was noted.

The winning team was selected by the committee based on a scoring system that weighted certain criteria including performance, safety, mobility, design considerations and functionality. The control system and drilling algorithm were significant factors, in addition to data handling and visualization.

7.1 Provided Equipment from DSATS

7.1.1 PDC Bit

A PDC micro-bit was provided by DSATS to be used on the on-site testing day. The bit had an outer diameter of 28.6 mm, brazed cutters and two nozzles. The cutter backrake was 20 degrees and the cutter diameter was 13.4 mm. The two nozzles had a diameter of 2.35 mm. The length of the bit was approximately 12.5 cm without the threads. A picture of the provided PDC bit is shown in Figure 7.1.1.

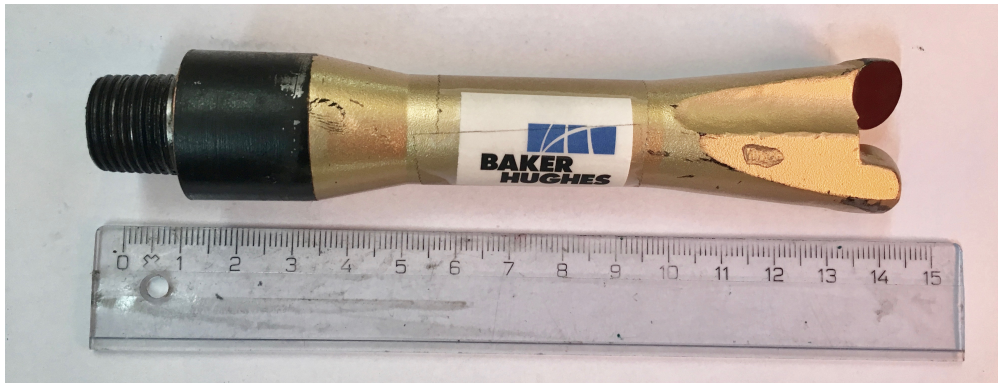


Figure 7.1.1: PDC bit provided by DSATS

7.1.2 Rock Sample

Laboratory rock built samples were prepared and packed by DSATS before the formation block was shipped to the university for the actual drilling test. The composite-rock block was manufactured to be as homogeneous as possible so no student team was disadvantaged with a different formation. The box contained layers of sandstone, cement, floor tiles, and an asphalt patch material, to imitate unusual downhole conditions experienced in some drilling programs. The box had dimensions of 153x305x610 mm and a weight of approximately 39 kg. The crate was not to be opened or tampered with prior to the on-site test day, as the rock formations, thickness and potential formation dip were to remain unknown until after the test.



Figure 7.1.2: Rock sample provided by DSATS

7.2 Setup on the Competition Day

Due to problems with time management and implementation of the pump into the control system, the circulation system had to be run manually during the competition.

The swivel had a minor leakage in the top section. This fault was not crucial, and was not prioritized to be fixed in the limited time prior to the competition. To mitigate the leakage, the pump was run at 7.4 bars of operating pressure instead of the desired pressure at 50 bars. This reduced the geometrical stiffness of the drill string by a certain amount, but since buckling of the string had not previously been a problem, the pressure reduction was seen as an acceptable action.

The implementation of the down-hole sensor chip also turned out to be more challenging than expected, because even though the sensor was installed in the BHA, there was not enough time to implement the readings into the control algorithm.

The autonomous functionality with respect to both the top drive motor and the hoisting system through the Simulink model worked smoothly. The control system had the desired response to peaks and drops in drill string torque which enabled stable transitions between rock formations of different properties.



Figure 7.2.1: Overall rig view on the on-site test day

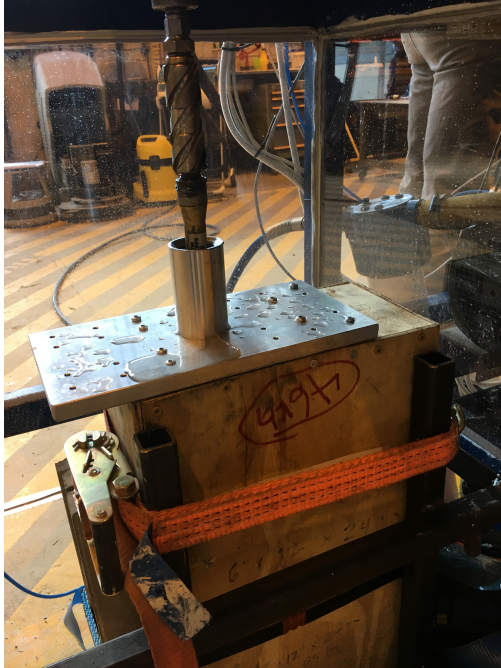
7.3 On-Site Drilling Test

The pump was manually started and the rig start button was pressed to start the drilling process. The rig autonomously started the top-drive with a set point of 50 RPM and the hoisting system began lowering the carriage slowly through the riser towards the formation top. The bit landing went smoothly and once the set point of 10 kg WOB was reached, the state machine entered the optimization algorithm. The RPM gradually increased to 1000 RPM, and the WOB was continuously changing set point to maintain the desired set point of the drill string torque.

As a result of the length of the Baker Hughes competition bit, the stabilizers on the BHA were not engaged inside the riser in the initial phase of the drilling. This caused high amplitude vibrations, which led to stress and material fatigue to the pipe.

When the drilled depth was large enough to make the BHA enter the riser, the drilling went

smoothly with very little vibrations. Once the stabilizing roller bearing module had landed in the riser, the drilling went even better.



(a) Initial phase of drilling with BHA and stabilizers outside of the riser



(b) BHA and roller bearing stabilizers landed inside the riser

Figure 7.3.1: Early phase drilling on the on-site testing day

The first section, which contained normal construction concrete, was drilled easily with only minor instances of bit bouncing and vibrations. The inclined transition zone from concrete to the sandstone did not seem to be a problem for the drilling rig. The remaining part of the sandstone was drilled without any major problems and with relatively high ROP.

In the transition zone between the inclined sandstone layer and the ceramic tile, the rig started having problems with maintaining the ROP. After some minutes with almost zero ROP, a high frequent squeaking noise was heard, and the measurements of the drill string torque and WOB started oscillating. The drilling continued a couple of more minutes, but the ROP remained at zero. The system was then switched to manual mode and the drill string was pulled out. A twist-off, seen in Figure 7.3.2, had happened, and the bit was still inside the formation box. The bit was fished out

of the hole, a new string was attached, and the drilling was restarted in the ceramic tile.



Figure 7.3.2: The first twist-off

After a new and long period with very low ROP, the bit had passed through the tile and entered the next layer which contained construction concrete with small pebbles inside. The ROP had a certain increase in this layer, but the pebbles caused a lot of problems with axial vibration. Whenever the bit encountered the pebbles, the torque readings would show tall peaks, and the control system would struggle to keep it constant by changing the WOB set point.

The following layer consisted of a limestone tile. Both the transition and the drilling of this went very smoothly because the limestone was much softer than the ceramics. This gave an immediate increase in the ROP and a reduction in vibrations.

A new layer of sandstone was then entered, which resulted in an even higher ROP than in the previous layer. The MSE readings revealed a very efficient stage in the drilling sequence.

The subsequent layer was made up of asphalt putty, a very soft and sticky material with limited amount of shear strength. In this layer the rig was not able to reach its set point on drill string

torque, which made the control system continuously increase the WOB set point towards the upper limit. As a result of this, the speed of the hoisting motor went to its maximum limit, which resulted in a very high ROP.

The last two layers consisted of a rubber door mat and a new section of construction concrete, before entering the plywood in the bottom of the formation box. The rubber mat was drilled without any problem, with just some minor peaks on drill string torque, while the concrete was drilled with about the same parameters as the first layer. However, in the plywood some problems started arising. The ROP continued on a stable value and the position measurement showed that bit should have exited the box and be visible. Despite this, the bit was nowhere to be seen. The drilling continued like this for several minutes, before it was decided to pull out and check the integrity of the drill string. A second twist off, seen in figure 7.3.3, had happened. Unlike the first twist off where the cut was clean, the end of the drill string now looked like a lump of steel wool.



Figure 7.3.3: The second twist off

Since the rig did not have a closed loop circulation system, it was possible to analyze the return

flow from annulus as it moved towards the drainage area. The color and cutting size of the return flow gave an impression of what the possible formation that were drilled could be. The initial guess of drilling through sandstone and asphalt from data analysis (torque, WOB, ROP and MSE) were confirmed by analyzing the return flow together with input from the judges.



(a) Return flow from annulus indicating sandstone was being drilled



(b) Return flow from annulus indicating asphalt was being drilled

Figure 7.3.4: Return flow from annulus

7.4 Results and Analysis from the Test Day

After testing the performance of the automatic rig, drilling data was analyzed, drill bit and drill pipe were recovered and carefully examined, and the quality of the wellbore was evaluated. The drilled rock sample box was opened and the formations were analyzed, see Figure 7.4.1.



Figure 7.4.1: Drilled rock sample on competition day

7.4.1 Drillstring Twist-Off

During the test, two twist-offs were encountered. After having a close look at the twist-off point, it was possible to see that the failure had happened just over the connection point between the BHA and drill string. A possible explanation was the weight imbalance between the bit and the drill string, and therefore a large difference in moments of inertia during rotation. This could have caused wobbling of the drill string and bit walking, which eventually could give rise to material fatigue failure to the pipe.

A possible reason why the drill pipe ended up looking like a lump of steel wool, was suggested

to be that the pipe had twisted off and slipped in between the formation and the BHA, causing a milling effect against the sharp edges of the BHA. The reason why the ROP and position readings showed positive ROP and increase in position, was that the drill pipe continuously was milled down against the BHA due to the applied rotation and WOB.

7.4.2 Bit Wear

After drilling, bit wear was clearly visible on the cutters and on the bit body, see Figure 7.4.2. High instantaneous impact force and vibrations might be a possible explanation of the experienced bit wear.



Figure 7.4.2: Wear on the bit cutters and bit body

7.4.3 Borehole Quality

After the final depth of the formation block was reached, the string was pulled out of the hole and a visual analysis of the borehole quality was performed. The quality of the borehole was considered good, having a smooth stable surface throughout the entire depth, see Figure 7.4.3.



Figure 7.4.3: Picture of the drilled hole on the on-site test day

One of the judges also run a survey tool through the borehole to measure the borehole verticality. The results from this survey showed a maximum inclination of two degrees, see plot shown in Figure 7.4.4.

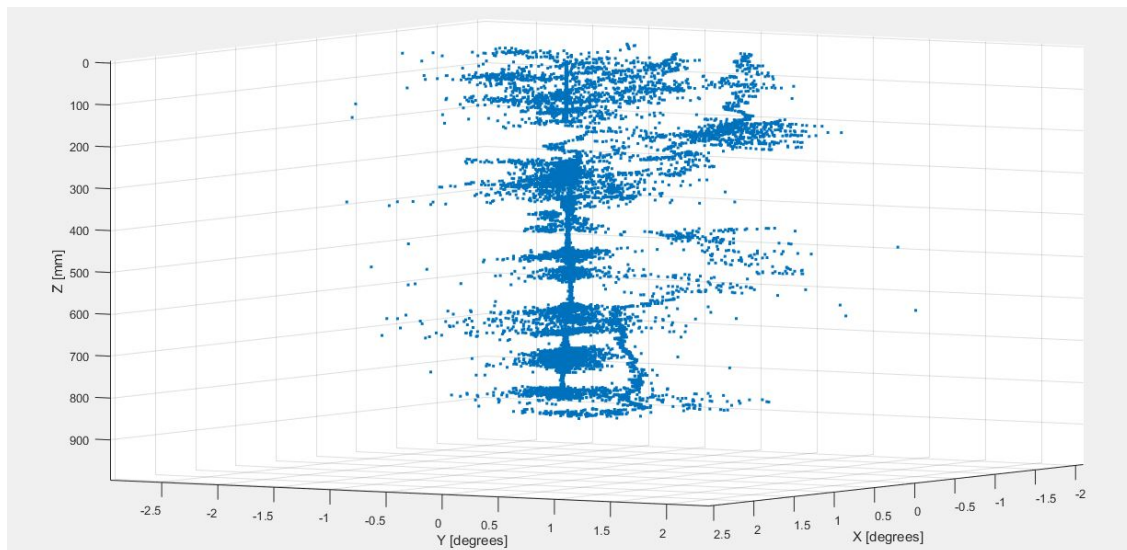


Figure 7.4.4: Plotted results from the downhole survey performed by one of the DSATS judges (Kurt West), showing a maximum inclination of 2 degrees

The early drilling phase was quite problematic due to the unengaged stabilizers and BHA. Bit walking and large amplitude vibrations resulted in an over-gauged borehole with poor quality. This could have been mitigated by using a shorter bit or increasing the distance between the bottom of the riser and the formation top, and in that way increase the stability of the drillstring. However, to be sure the design was within the rules stated in the guidelines and avoid any chance of, it was chosen not to change the setup.

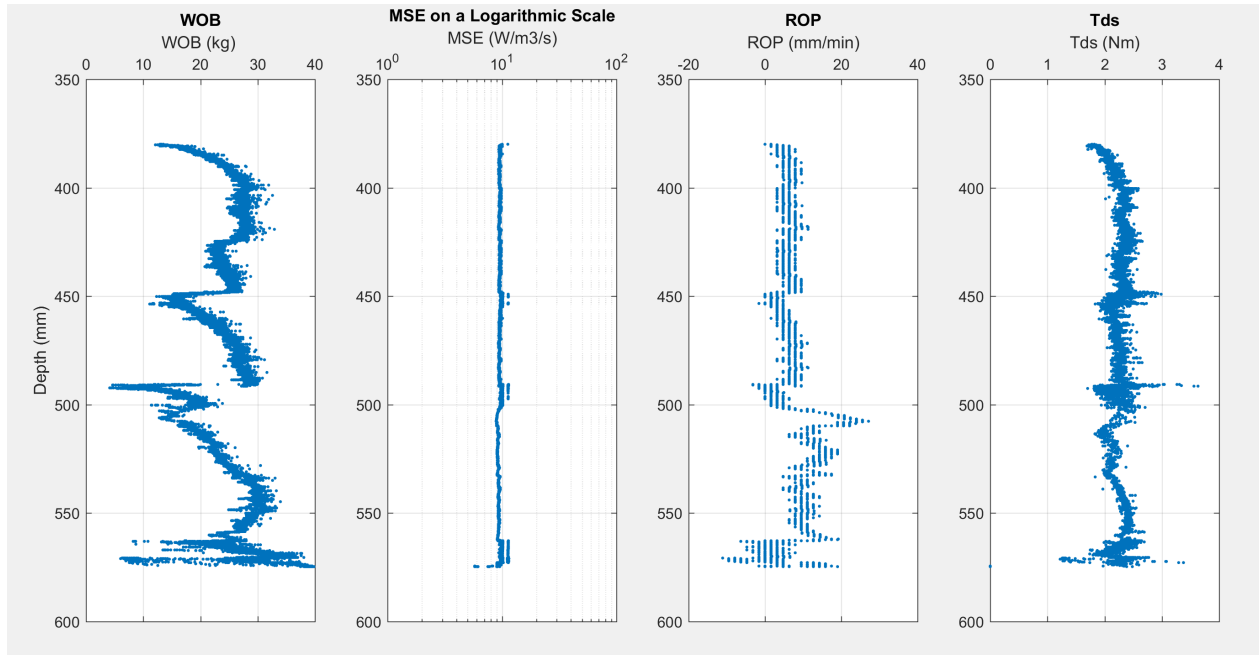
7.4.4 Formation Detection from Drilling Data

From the drilling data, shown in Figures 7.4.6a and 7.4.6b, a clear correlation can be seen between peaks and drops in drillstring torque, ROP, MSE and WOB. Based on these peaks and drops, a possible new formation layer can be detected.

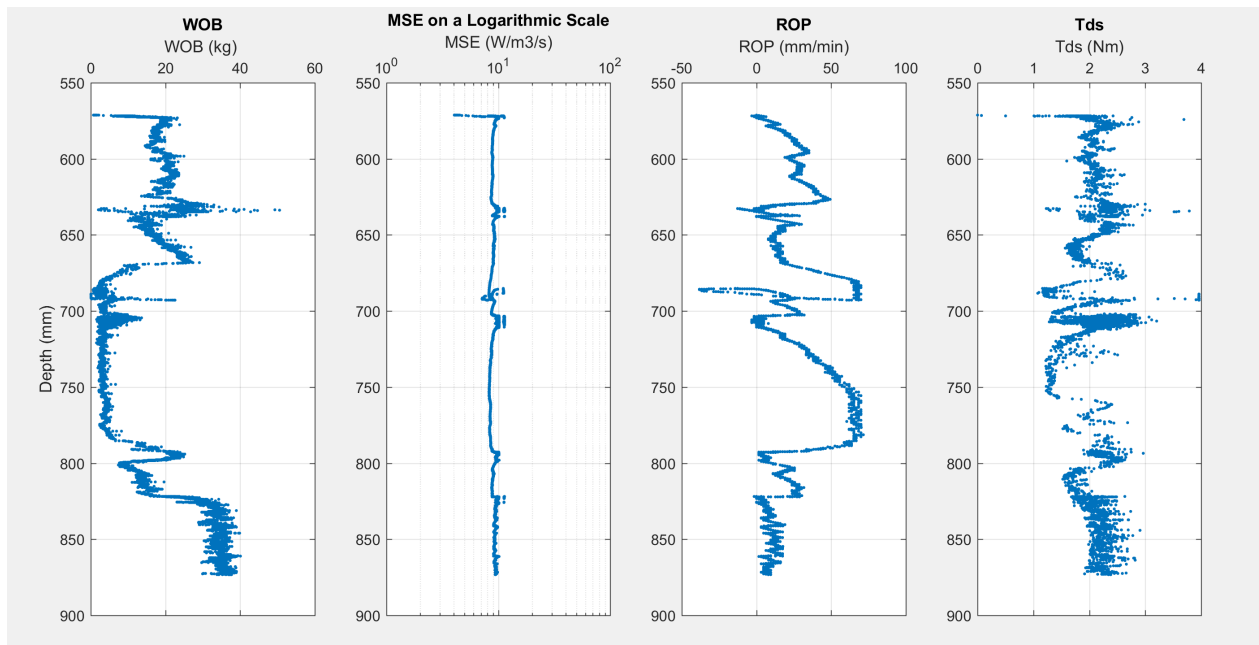
Using the drilling data from the two runs together with the formation rock sample, shown in Figure 7.4.7, the formation depth and composition could be determined. A 25 mm pilot hole was drilled prior to the competition. The drilling test started at 380 mm on the drilling data, which corresponded to 45 mm on the measuring tape. The actual formation depths were set using a measuring tape on the rock sample. The measurements from the measuring tape and the drilling data were correlated to be able to compare the results. The results are presented in Figure 7.4.5, and they show a good correlation between the results from the data analysis and the reality.

Formation	Measuring tape [mm]	Calibrated measuring depth to drilling data depth [mm]	Drilling data [mm]	Error [mm]
Test Start	45	380	380	0
Cement	170	505	490	15
Sandstone	220	555	560	5
Ceramic tile	230	565	570	5
Aggregate concrete	290	625	625	0
Limestone tile	300	635	640	5
Sandstone	310	645	645	0
Asphalt	350	685	680	5
Rubber mat	450	785	780	5

Figure 7.4.5: Table of detected formations based on the drilling data and actual formation depths



(a) Drilling data from first run



(b) Drilling data from second run

Figure 7.4.6: Drilling data from the competition day



Figure 7.4.7: Drilled rock sample on competition day with formation depths. Measuring tape positioned next to the drilled well.

Construction challenges and solutions

Like in any other project, unforeseen challenges and problems occurred during the period of the construction. Especially when taking a product from the design phase to the actual construction, many details are easily overlooked. Since the student team mainly consisted of petroleum engineers, electrical components and design was notably difficult to get a good overview of. Mistakes, negotiations, decision making, vacations and misunderstandings were all factors that notoriously delayed the progress, and even though they were accounted for to some extent, they consumed much more time than expected.

8.1 Challenges Related to Hardware

The main challenges related to the hardware were long delivery time and delays on the equipment, as well as lack of knowledge and experience among the students in order to keep an overview of what was needed of system components at all times. This resulted in unforeseen components having to be ordered, which in turn led to delays in the construction phase.

Linear Guides In the original design proposal, the carriage was designed with only one steel beam mounted to the linear guides by a wagon on each side. However, after several discussions with both the personnel in the workshop and the supplier of the linear guide system, it was decided to use two steel beams and two pairs of wagons to increase stability and to ensure smooth vertical movement

of the carriage. To still be able to provide the required length of movement to drill the block, the length of the linear rails had to be increased, which again meant that the height of the derrick had to be changed correspondingly. These considerations were done before ordering the linear guide system, so that no unnecessary expenses were made. However, extra steel had to be ordered, which resulted in some delay of the construction.

Motor Drive Problems During the process of ordering the frequency converter for the top drive motor, there were some communication problems between the workshop and the team. Instead of the converter for 3-phase 400V that was actually needed, a unit that required 3-phase 230V was ordered and delivered. Seeing the 3-phase input connection, the drive was connected without any further thought. There was no bang or smoke when the drive was connected, and it would still start, but it gave an error due to over-voltage. Neither the producer or the supplier would exchange the drive unit, so a new unit had to be ordered and paid for. This increased the delay of the rig construction even more.

The top drive motor experienced sudden stops. The reason for these sudden stops was somewhat unclear, but it was thought to most likely be due to a failure in the drive. It was a reoccurring problem during the testing phase, which was temporarily resolved by resetting the system back to a previous back-up.

When trying to connect the hoisting motor to the PLC and the PC, a problem regarding the resolution of the analogue signal was discovered. With the current drive it was only possible to send and receive signals in increments of 1 volt. Because of the fragility of the drill string, it was crucial to be able to control the torque of the hoisting system much more accurately. It was necessary to change the hoisting motor, which resulted in some delay of the construction. Luckily, a suitable motor was available from the lab, as ordering a new motor would have taken two weeks.

Circulation system Attempts were made to find a swivel that would fit the system and its requirements, but none could be found. The swivel therefore had to be machined by the personnel working in the Department's workshop. Being able to design a swivel that could withstand the high operating pressure was a challenge and the design had to be carefully thought through. Together with the challenging design, delayed delivery of seals slowed down the construction of the swivel, resulting

in a severe time loss for the project as a whole.

A regular water hose was used as a simplified, temporary circulation system during the testing phase, ensuring, to some extent, bit cooling and hole cleaning. Poor borehole cleaning was experienced during test drilling of rock samples with a height of over 10 cm and it was therefore made a priority to set up the circulation system with water running through the drillstring. The formation block for the on-site test day had a depth of 60 cm and it was therefore critical to have an efficient circulation system for the on-site test day.

The swivel and the pump were installed the day before the on-site test day, which provoked an insufficient testing phase. The swivel was suffering from a leakage, which was not prioritized to be fixed in the limited time prior to the competition. This resulted in a lower operating pressure than initially planned.

However, the circulation system provided more fluid flow than the hose previously did, so even if it could not provide a very high pressure, it improved drilling efficiency considerably.

Limited Range of Measurement for the Load Cell The range of the load cell used in the set-up had a range of -500 to +500 N which is approximately equivalent to 100 kg. When running the buckling test this range was not large enough as buckling occurred at a WOB higher than 100 kg. However, the hoisting motor torque measurement was used to define a safety limit against buckling in the PID-controller. The small range of the load cell was therefore not a great limitation, but it could have been improved.

Downhole sensor Limited amount of space, high pressure and water inside the aluminum drill pipe made the wire design and installation of the downhole sensor challenging and the design had to be carefully thought through.

Plexiglass Due to the highly pressurized drill string (approximately 40 bar), it was decided to implement plexiglass in the design. The plexiglass was mounted around the drilling area and hoisting system on the rig. This was done both to provide another measure with respect to human safety and protect the electrical system.

Transportation The design of the rig with respect to transportation was thoroughly investigated,

however one challenge was forgotten in the phase. The rig did not fit the small elevator in the workshop. This was not a critical problem, but made some parts of the construction slightly inconvenient.

Changes in the guidelines In November last year the pipe size was changed from a tubing wall thickness of 0.016” to 0.035”. This was relatively late in the design phase and calculations had to be redone.

In addition to this, one of the main features of the rig design became less important because of this change. Because of the initially very thin pipe wall, buckling of the pipe was expected to be the biggest issue. It was therefore decided that this should be the main focus and a solution was found for this. When the pipe wall was increased, this solution seemed less important and time was spent to discuss new problems with the rig design.

Another challenge was the stated length of the bit. It was written in the competition FAQs that the bit should be shorter than 64 mm. The drill string design, height of the derrick, height of the drill deck bushing and the positioning of the riser was based on this given length. The competition bit was received late in the construction phase and had a length of 125 mm, which affected the rig set-up. Adjustments like moving the riser higher up to improve stabilization of the extended drill string was considered, but not completed because it was unclear from the guidelines whether the riser had to be placed directly on the formation block or not. The initial rig set-up was used due to lack of time.

8.2 Challenges Related to Project Management

Time management Some of the mechanical parts of the drill string design took longer time to machine than estimated.

The swivel had to be designed and machined in the workshop. The estimated time for the production of the swivel was initially two weeks, but delayed delivery time on the seals severely slowed down the construction. As a result, the testing phase had to be done without circulation system.

The design of the BHA with stabilizers was also a crucial factor, and had the same production time

as the swivel. A temporary BHA with a simpler design was constructed in order to let the testing phase begin earlier.

The delivery time of the top drive motor was underestimated, which led to the postponement of the rig construction and set up.

8.3 Challenges Related to Automation

Communication between PLC and PC A major problem that was encountered was the communication between the PLC and the PC. After some help from ABB and extensive work in the workshop, the communication with the PLC was obtained through the OPC-server package in Simulink.

Limited number of inputs and outputs in the PLC The PLC was ordered with a certain number of analogue inputs and outputs early on in the construction phase. When the actuator drives were connected to the PLC it however became clear that more inputs and outputs than initially expected were required. ABB was contacted but the delivery time for the ports was long and changes therefore had to be made to the number of signals that were required in the model.

It was for example decided that only torque and speed would be outputs from the hoisting motor drive, while torque and position were inputs in the model. In addition to this, because the flow rate and the pressure of the pump were going to be constant, the outputs and inputs related to this were also removed.

Running real-time in Simulink Another severe challenge that was encountered when creating the Simulink model was running in real-time. The first problem was to simulate real-time by setting the simulation time step size equal to a second. This was solved by enabling Pseudo Real-Time Simulation in the OPC Configuration block parameter.

Another problem related to real-time simulation was that after a while the model slowed down. This was thought to be related to problems with memory allocation. This problem was solved by reducing the simulation time from infinite to 100000.

Downhole sensor The downhole sensor was successfully placed inside the BHA, with wires con-

necting it to the PC. Setting up the communication was, on the other hand, unsuccessful, and because of time limitation fixing this was not made a priority.

8.4 Challenges Related to the Drilling Operation

Propagation of vibrations During the drilling operation, large vibrations quickly occurred in the drill string and propagated up to the carriage and top drive motor and even to the PC and table. This caused fatigue, not only in the drill string, but also in the railing and carriage, and the rest of the equipment. Solutions to mitigate this issue were proposed, such as implementing maximum limits in the control system based on visual results from the experiments.

Bit bouncing was experienced throughout the testing phase at low drilling RPMs, and ended up being a severe bottleneck resulting in poor borehole quality which was difficult to recover. Operational RPM was therefore set sufficiently high to avoid this problem.

Material fatigue Twist-off at the connection between the BHA and the drill string was a severe challenge throughout the testing phase. The pipe seemed to experience abrasion at the connection point due to vibrations, suffering from excessive drill string torques and torque peaks. To mitigate the problem, one idea was to add a steel cylinder inside the pipe at the connection point, see Figure 8.4.1. This was expected to increase the strength of the pipe. However, when implementing the steel cylinder, the weak point was moved further up in the pipe, causing twist-off at a new point.

It was therefore important to set a max drill string torque limit in the control system drive to avoid twist-off. Based on several test, this limit was set to 4 Nm. The control drill string torque was set to a set-point below safety limit to avoid excessive peaking of the drill string torque.

After the on-site competition day, a different explanation was proposed. The twist-off might in fact have occurred due to mass imbalance between the BHA and the pipe. A possible way of mitigating this problem could be to add heavyweight drill pipe to the drillstring design, providing a gradual transition between the BHA and drill pipe to improve fatigue resistance of the drill string.



Figure 8.4.1: Steel cylinder placed inside the pipe at connection point to increase strength

Evaluation and Reflection

The aim of this project was to construct an autonomous drilling machine and develop a control system that could detect and mitigate drilling issues, as well as optimize the drilling efficiency. This required designing and building a drilling machine, and developing skills to understand drilling dysfunctions and mitigation strategies. Although the differences between a miniature drilling rig and a full-scale drilling rig are large and numerous, the results from this project might give a fresh approach to some of the challenges the drilling industry is facing today.

In this chapter the project has been evaluated and recommendations for further work have been proposed. The degree to which the requirements in the guidelines [10] have been fulfilled have also been looked at.

9.1 Small-Scale Drilling Rig Compared to Conventional Drilling

The oil and gas industry seeks lower costs through efficiency and innovation. A solution to this is to implement autonomous systems. Delivering drilling optimization through automation requires a comprehensive understanding of the subsurface and its interactions with the downhole drilling system cutting the rock, the drill string delivering power from the rig, and the drilling fluid system.

It was important to keep in mind that the analysis done throughout this project was based on a miniature drilling rig, which attempted to simulate a full-scale drilling rig. There were several

factors that made this project differ from a real drilling operation, where the characteristics of the drill string was prominent.

The drill string used in this project was made of aluminum, and not steel which is commonly used on drilling rigs. The physical limitations related to the thin-walled aluminum drill pipe ensured that operating challenges related to buckling and failure of pipe would occur when put in compression.

Due to the small scale of the autonomous drilling rig, the method of applying weight to the bit had to be different. Unlike the normal convention where the weight on bit is obtained by slacking of the hook load and releasing tension in the drill string, the weight on bit in this case had to be applied by pushing the carriage down using a ball screw combined with a linear roller guide system and a motor. This way of applying weight on bit put the drill pipe in compression, which is unlikely to occur in a normal drilling operation where the drill pipe should always be in tension.

The drilling operation did not include any making or breaking of connections, as only one length (914 mm) of aluminum drill pipe was used in the design.

The bit used in the design was a miniature PDC bit with an outer diameter of 28.6 mm. This very unconventional bit size made it difficult to relate operating regimes, of WOB and RPM, and expected bit/rock interaction to a real drilling operation.

Drilling fluids used in the industry are typically non-Newtonian, serving many functions as providing cutting transportation, sealing permeable formations, cooling and lubricating the bit, transmitting hydraulic energy to downhole tools and bit, but perhaps most importantly maintaining wellbore stability and well control. As no well control equipment for over-pressure considerations was necessary for the miniature rig design, tap water was used as circulation fluid as it could provide the most important functions like ensuring internal pressure in the pipe and cuttings removal. Currently used drilling fluids in the industry are complex formulations, and using water for the miniature drilling rig was a huge simplification for the circulation system.

As mentioned in the introduction to this Chapter, there are many and large differences between a miniature drilling rig and a full-scale drilling. However, this project might give a different perspective to challenges faced on a full-scale rig.

One of the main results of the project was the approach to automating the drilling operation. Being able to correctly determine and estimate the limitations of the system can make it possible to fully automate a drilling operation. In this case it was discovered that the critical parameter to monitor was the drill string torque. This was observed after a long period of testing where drill pipe failures were analyzed and an effort was made to understand how the failures could be prevented and detected.

The main failures and problems were related to stick-slip and twist-off and in order to prevent these dysfunctions to occur it became important to monitor the drill string torque. After further testing, a way to mitigate this issue was proposed. The solution consisted of lifting the bit off-bottom when the drill string torque became too high.

As the proposed solution was successful, it was agreed that drill string torque was the critical parameter and that torque should be implemented in the optimization algorithm. It was also decided that WOB should be reduced to mitigate the problem of high drill string torque. This was done using a PID controller with the error between the drill string torque set point and measurement as the input and the WOB set point as the output.

This proved to be a good way to ensure safe drilling and after tuning and filtering the signals, the control system successfully managed to drill through different types of rocks and handle difficult transitions without the need of manual intervention.

9.2 Theoretical Calculations versus Reality

During the design phase, several analyses and calculations were performed to dimension the drilling machine and predict failure limits. These models were based on approximations and simplifications.

When testing the drilling machine, it became clear that the simplifications made during the design phase were too large and that the estimated limits were very different from the actual limits.

One of these limits was the buckling limit. Because the pipe was estimated to only be fixed at the extremities, the buckling limit was much higher than expected when the surface stabilizer was

added on the drill deck.

Another theoretical limit that was wrongly estimated was the natural frequency of the system. The natural frequency analysis was also based on a pipe fixed at the extremities and was also only conducted for the pipe, not for the entire structure. The resonance observed on the rig was however due to the natural frequency of the structure and not of the pipe alone.

Finally, another important calculations that was performed but that was based on the wrong assumptions was the torque limit of the pipe. The torque limit of the pipe was calculated to be able to set a limit in the top drive. A flawed assumption that was made in this case was that the weakest part of the drill string would be the pipe. When testing the system and experiencing twist-off it occurred at low torque values and at the connections between the BHA and the pipe. The weakest part of the drill string was therefore the connection between the BHA and the pipe and not the pipe itself. This turned out to be one of the largest limitations of the design.

9.3 Rig Structure

The rig structure itself had a good functionality, but its weight and dimensions made it hard to move. This was not a big limitation, but in some situations it might have been useful to be able to move it more easily.

A problem that was identified while drilling was the propagation of vibrations from the drill string to the rest of the structure. When the drill string vibrations became more violent, movement in the structure could be seen. Solutions to this issue, such as adding more legs to the derrick or adding weight to the current legs, could have been evaluated.

The proximity of the PC to the drill string and rock was identified as a possible risk. Plexiglass was added to mitigate this issue, but a different design where the driller could run the operation from further away would have reduced the risk of damage to personnel.

9.4 Weight on Bit

As presented in the start of the thesis, one of the main limitations of the drilling machine was applying sufficient weight-on-bit without buckling or damaging the drill pipe. The main solution that was proposed was to add a nozzle in the BHA to increase the internal pressure of the pipe and thereby increasing its geometric stiffness. There were many issues and complications related to this design feature such as designing a swivel that could withstand such a high pressure, making sure there were no leaks in the system and being able to test without compromising the safety of the personnel.

Another feature that increased the maximum WOB was adding a bushing on the drill deck. This was initially added to reduce vibrations in the drill string, but because the buckling load limit is inversely proportional to the square of the unsupported length of the pipe, it also highly increased the buckling limit of the pipe.

9.5 Vibrations

Another problem that was identified early in the design process was the propagation of vibrations in the system. Because it was mandatory to use an entire length of drill pipe and because the pipe itself was very weak, large and destructive vibrations were expected during operation at high RPM and WOB.

Several design choices were made to mitigate the vibrations. One of them was to add a bushing in the drill deck in the form of a linear and a radial roller bearing. This added a lot of stability to the string in the start of the operation because it was situated approximately halfway between the BHA and the top of the string.

The roller bearing in the riser also helped mitigate the vibrations.

Increasing the internal pressure of the pipe increased its geometrical stiffness and therefore also reduced the amplitude of the vibrations.

When conduction identification tests, bit bouncing was observed at low drilling RPM, below 300

RPM which resulted in poor bore hole quality which was hard to recover.

After running several tests with different rock samples and different sets of WOB, the natural frequency of the structure was found to be at approximately 600 RPM, 840 RPM and 1100RPM. When operating at these RPMs resonance was encountered, meaning large vibrations propagated through the entire structure. To avoid resonance, an increase in the top drives RPM was made to jump over the resonance frequency. This worked well, and the vibration amplitude was reduced.

When operating at an RPM above 1100, violent vibrations were detected and the drilling operation became unstable.

The result of bit bouncing, unstable drilling conditions and resonance, lead to the decision that the RPM of the top drive should be held constant at 1000 RPM.

This caused problems both in terms of energy efficiency and in equipment wear. The biggest risk in this project and this scale was that large vibrations in the start of the operation would weaken the pipe and maybe cause failure in the later phase of the operations at relatively low RPM and WOB.

9.6 Control System

Creating a control system for the drilling machine was the most challenging part of the process. Designing a robust machine reduced the fragility of the system, but without an accurate and efficient control system, the drilling operation would not have been safe, fast or precise enough.

The first phase of developing the control system consisted of making sure that the data infrastructure had the functionality that was required. The different required input and output variables were defined and it was made sure that all signals were accurate and could be processed in real-time.

There were problems related to this because there were a limited number of inputs and outputs in the PLC which resulted in a limitation on the number of signals that could be communicated to the PC. Fewer signals than initially wanted were therefore processed in the Simulink model. This was not a major weakness, but it did limit and reduce the accuracy of some of the measurements. This was particularly the case for ROP which was estimated based on the derivative of the posi-

tion measurement. This reduced the accuracy and reliability of the ROP which was an important measurement.

After having set up the system, the next step was defining the limits of the control variables both in the Simulink model and in the actuator drives. The limits in the actuator drives were the absolute limits and if output variables from the PLC increased above these limits, the drives saturated the signal at the predefined maximum.

The safety limits defined in the Simulink model were limits that were estimated based on the testing phase.

After having defined the safety limits, several different ways to measure drilling efficiency were considered and it was finally decided that ROP should be used as an optimization parameter. This had limitations, one of them being that ROP was a relatively slow measurement which slowed down the optimization process. Another limitation which would be even more important on a full-scale drilling rig is that it doesn't take into consideration how efficient drilling, only how fast it is. In a situation where you drill further and deeper, the waste of energy and wear on equipment is critical, and an optimization function should take this into consideration.

9.7 Understanding of Drilling Dysfunctions and Bit-Rock Interaction

During the design phase research was done on drilling dysfunctions and bit-rock interaction. The most common drilling dysfunctions were identified and ways to mitigate these dysfunctions were developed. It was however hard to understand how the dysfunctions occurring during a normal drilling operation would translate to a small-scale drilling rig.

When the identification tests were conducted, it became clear that many of the dysfunctions that had been identified during the design phase would not occur in this small scale project. This was largely due to the weakness of the pipe which meant that buckling and failure of the drill pipe would happen before stick-slip or bit balling could happen. There were on the other hand issues that did occur that had not been anticipated.

The understanding of drilling dysfunctions and bit-rock interaction is therefore one of the main weaknesses of the project. If a more accurate and reliable relationship between the different drilling parameters could have been developed, a better control algorithm could have been made.

9.8 Project Management

9.9 Further Work

Drillstring design A possible way of mitigating twist-off in the drillstring, due to mass imbalance between the BHA and the pipe, could be to add heavyweight drill pipe to the drillstring design, providing a gradual transition between the BHA and drill pipe to improve fatigue resistance of the drill string.

Since the PDC bit is designed to perform with respect to depth of cut, it requires high WOB to operate efficiently. Due to the fragile drill pipe and the small scale of the set-up, the required WOB is not obtainable. It is therefore proposed to change the type of bit to increase the ROP and efficiency of the drilling.

After the testing phase it was possible to conclude that the weakest element in the system was the connection between the drill pipe and the BHA. The connection used was a normal hydraulic connection. The connection would slip on the pipe if tightened to little, and would bend and eventually cut the pipe if tightened to much. When exposed to large vibrations during drilling, it would also exert abrasion on and weaken the pipe. To remove these problems, a different connection should be incorporated in the next design. A proposed solution is to use the same technology as in the chuck on a normal hand drill. This will increase the area exposed to the force exerted by the connection, and it should therefore be possible to apply a larger force to fix the pipe.

Less conservative limits Further testing should be performed in order to determine the limitations of the system with more accuracy. This would enable setting less conservative limits for the operating parameters and increasing the speed of drilling.

This is for example the case for the drill string torque limit and the WOB limit. Because the set-up

of the machine was changed the day before the test, the limits were changed based on intuition and unfortunately not on extensive testing. There is therefore a good possibility of being able to improve the drilling operation by exploring the limits of the system.

Pressurizing the drillstring Although pressurizing the drillstring was planned, it was unfortunately not implemented due to the delay of the equipment. Increasing the pressure in the pipe has the potential to increase the operating window of the drilling machine and is a possible design feature that should be looked further into.

Human Machine Interface (HMI) The HMI of the system could be greatly improved by exploring the possibilities within Simulink and Matlab or considering using an entirely different software such as Labview. Having a good HMI is essential to be able to monitor the control system and improve its performance.

Detection of drilling dysfunctions The optimization function of the control system was entirely based on trying to reach the drill string torque set point. Adding more functionality such as the detection of drilling dysfunctions would greatly improve the control algorithm.

This idea was explored during the design phase, but there was not enough time to test it. Conducting additional tests to learn how to detect, identify and mitigate drilling dysfunctions could make it possible to further optimize the drilling operation. Being able to detect dysfunctions quickly would both optimize drilling when dysfunctions occur, but it could also make it possible to increase the operating window.

Circulation system A closed-loop circulation system should be implemented to reduce the risk of any accidents happening. It could also make it possible to collect the cuttings and use them for an analysis of the formation being drilled.

Summary

As stated in the introduction, the aim of this master project was to "design a drilling rig and related equipment to autonomously drill a vertical well as quickly as possible while maintaining borehole quality and integrity of the drilling rig and drillstring." [10].

The rig was designed during the fall semester of 2016 based on the guidelines (Appendix E.1) provided by the DrillboticsTM competition committee and on research about drilling dysfunctions, dysfunction mitigation and automation. Economic considerations also largely determined the projects desirability and dictated how it should be carried out having the rig maximum allowable expenditures constrained to US\$ 10,000 or its equivalent. During the spring semester of 2017 the rig was constructed and the control architecture was developed.

After having set up the system, it was possible to start the testing phase. Experiments were carried out on different rock samples to analyze the reaction of the drill string and the rest of the rig to various operating conditions, directly related to WOB and RPM. This very quickly gave a much better understanding of the main problems that would be encountered, of the weaknesses of the design, of the areas to improve and of initial operations that required a re-design. It became clear that vibrations could potentially damage the equipment and reduce the drilling efficiency.

One of the main ideas in the project was to pressurize the drill pipe to increase the geometrical stiffness, which in turn would reduce the tendencies of buckling and thereby allowing greater WOB.

To minimize the risk of bit walking and wobbling, and mitigate the chance of destructive vibrations, several stabilizers were implemented in the mechanical design. A fixed stabilizer in the drill deck floor, a stabilizer designed as a landing module for the riser, and the conventional integral spiral blade stabilizers on the BHA were all used to reduce the risk of any drilling dysfunctions.

The performance of the rig design and control algorithms were demonstrated on the on-site test day 8th of June 2017 by drilling the block sample witnessed by DSATS members. Sub-committee members of DSATS provided the bit, composite-rock block, and drill string for the final test so that the drilling would not be a trivial problem.

Bibliography

- [1] 7329873 Canada Ltd. 3003-H14 Aluminum, 2016. URL <http://www.makeitfrom.com/material-properties/3003-H14-Aluminum>. Last accessed 12/05/2017.
- [2] ABB. *AC500 - Training Case, Product News TA512-BAS*, 2013. URL https://library.e.abb.com/public/e620676957a624e8c1257c2100539f4a/Product_News%20ACM07_2013_Basic%20Training%20Case_rev1.pdf. Last accessed 11/05/2017.
- [3] K. AG. *Intrinsically Safe Pressure Transmitters*, 2010. URL <http://www.keller-druck.com/picts/pdf/engl/23eie.pdf>. Last accessed 12/05/2017.
- [4] A.T. Bourgoyne Jr., K.K. Millheim, M.E. Chenevert and F.S. Young Jr. *Applied Drilling Engineering*. SPE Textbook Series Vol. 2. Society of Petroleum Engineers, 1986. ISBN 978-1-55563-001-0.
- [5] B. A. Brechan. *Compendium Introduction to Drilling Engineering*. NTNU Compendiums. NTNU Department of Petroleum Engineering and Applied Geophysics, 2012. ISBN 666.
- [6] D. Contractor. Automated systems increase safety and efficiency, 2002. URL <http://www.drillingcontractor.org/dcpi/2002/dc-sep0ct02/Sep2-auto.pdf>. Last accessed 02/11/2016.

BIBLIOGRAPHY

- [7] H. T. Corporation. *Linear Guideway*. URL <http://wpstatic.idium.no/aratron.no/2014/12/Hiwin-Linear-Guideway.pdf>. Last accessed 10/05/2017.
- [8] H. T. Corporation. *Ballscrews*, 2013. URL <http://wpstatic.idium.no/aratron.no/2014/12/Hiwin-Ballscrews.pdf>. Last accessed 10/05/2017.
- [9] N. C. Corporation. SW6G, 2016. URL <http://www.ebay.com/itm/NB-Systems-SW6G-3-8-inch-Miniature-Ball-Bushings-Linear-Motion-Bearing-400280248446?hash=item5d328fe07e:m:MD9-rVh4EXstSSvTxIp0k4A>. Last accessed 11/05/2017.
- [10] Drillbotics™. Autonomous Drilling with a Miniature Drilling Rig. URL <http://www.drillbotics.com/>. Last accessed 12/05/2017.
- [11] Drillbotics™. Phase i design reports, 2016. URL <http://www.drillbotics.com/phase-i-design-reports>. Last accessed 19/05/2017.
- [12] Drilling Formulas. What You Need To Know About Drilling Bit Balling Up and How To Troubleshooting It. URL <http://www.drillingformulas.com/what-you-need-to-know-about-drilling-bit-balling-up-and-how-to-troubles>. Last accessed 13/11/2016.
- [13] Drilling Systems Automation Technical Section (DSATS). Drillbotics™ Guidelines, 2016. URL http://media.wix.com/ugd/7aa25a_51340308c1734fd582e0d3e4a01b6559.pdf. Last accessed 23/10/2016.
- [14] D. S. A. T. S. (DSATS). Dsats homepage. URL <http://connect.spe.org/dsats/home>. Last accessed 12/05/2017.
- [15] Engineering ToolBox. Electrical Motor Efficiency when Shaft Output is measured in Watt. URL http://www.engineeringtoolbox.com/electrical-motor-efficiency-d_655.html. Last accessed 12/05/2017.
- [16] Free On-Line Dictionary Of Computing. Finite State Machine, 2001. URL <http://foldoc.org/finite%20state%20machine>. Last accessed 15/05/2017.

- [17] T. R. Hamrick. Optimization of Operating Parameters for Minimum Mechanical Specific Energy in Drilling. 2011.
- [18] HBM. *S-Type S2M Load Cell*, 2016. URL <https://www.hbm.com/en/3364/s2m-reliable-high-precision-s-type-force-load-cell/>. Last accessed 12/05/2017.
- [19] iCablez. 4x 6202 5/8 2RS Radial Ball Bearing 5/8in Bore x 35mm x 11mm Rubber Seal Shield, 2017. URL <http://www.ebay.com/itm/4x-6202-5-8-2RS-Radial-Ball-Bearing-5-8in-Bore-x-35mm-x-11mm-Rubber-Seal-182410833217?hash=item2a78886d41:g:KmAAAOSw5UZY~6C8>. Last accessed 11/05/2017.
- [20] I. Inc. *MPU-6000 and MPU-6050 Product Specification*, 2016. URL <http://no.rs-online.com/webdocs/1414/0900766b81414eda.pdf>. Last accessed 12/05/2017.
- [21] N. Instruments. Pid theory explained, 2011. URL <http://www.ni.com/white-paper/3782/en/>. Last accessed 12/05/2017.
- [22] Jonathan Dunlop, Rustam Isangulov, Walt Aldred, Hector Arismendi Sanchez, Jose Luis Sanchez Flores, Jose Alarcon Herdoiza, Jim Belaskie, J.C. Luppens. Optimizing ROP through automation, 2011. URL <http://www.drillingcontractor.org/optimizing-rop-through-automation-2-10696>. Last accessed 12/05/2017.
- [23] Lenze. *Lenze GST03-2M VBR 063C42*, 2014. URL https://www.lenze.com/fileadmin/lenze/documents/en/catalogue/CAT_GST_GFL_MF_15593808_en_GB.pdf.
- [24] Leon H. Robinson. Are you drilling optimized or spinning your wheels?, 2001. URL www.aade.org/app/download/7238830961/AADE+31.pdf. Last accessed 12/05/17.
- [25] MaplePrimes. The vibration of continuous structures. URL <http://www>.

BIBLIOGRAPHY

mapleprimes.com/DocumentFiles/206657_question/Transverse_vibration_of_beams.pdf.

- [26] Mathworks. Gain-scheduled control systems, 2017. URL <https://se.mathworks.com/help/control/ug/gain-scheduled-control-systems.html>. Last accessed 12/05/2017.
- [27] MathWorks. Model and simulate decision logic using state machines and flow charts, 2017. URL <https://se.mathworks.com/products/stateflow.html>. Last accessed 15/05/2017.
- [28] MechaniCalc. Column Buckling. URL <https://mechanicalc.com/reference/column-buckling>. Last accessed 12/05/2017.
- [29] Michigan Technological University. Electrical safety work practices plan, 2016. URL <http://www.mtu.edu/oshs/safety-programs/required/safety-work/>. Last accessed 25/11/2016.
- [30] I. A. of Drilling Contractors. Drilling mechanics and performance, 2015. URL <http://www.iadc.org/wp-content/uploads/2015/08/preview-dp.pdf>. Last accessed 12/05/2017.
- [31] U. of Oklahoma DrillboticsTM Team of 2015. Design report, 2015. URL http://media.wix.com/ugd/7aa25a_d6873834922740c3aa2757664c99b997.pdf. Last accessed 12/05/2017.
- [32] PetroWiki. Positive displacement pumps, 2016. URL http://petrowiki.org/Positive_displacement_pumps. Last accessed 26/10/2016.
- [33] PhysicsForum. Torque friction on a rotating disk, 2010. URL <https://www.physicsforums.com/threads/torque-friction-on-a-rotating-disk.450861/>. Last accessed 16/05/2017.
- [34] M. O. M. V. R. L. Egeland, A. Lescoeur. DrillboticsTM competition, project report.

BIBLIOGRAPHY

- [35] Saldivar Marquez, M.B., Boussaada, I., Mounier, H., Niculescu, S.I. *Analysis and Control of Oil well Drilling Vibrations*. SPE Textbook Series Vol. 2. Springer international Publishing Switzerland, 2015.
- [36] Schlumberger. Drillstring Optimization Workflow. URL https://www.slb.com/~media/Files/drilling/posters/shock_vibration_posters.ashx. Last accessed 12/05/2017.
- [37] Schlumberger. Drillstring Vibrations and Vibration Modeling, 2010. URL https://www.slb.com/~media/Files/drilling/brochures/drilling_opt/drillstring_vib_br.ashx. Last accessed 11/05/2017.
- [38] The Engineering Toolbox. Area Moment of Inertia, 2010. URL http://www.engineeringtoolbox.com/area-moment-inertia-d_1328.html.
- [39] Tomax. Stick-slip. URL <http://www.tomax.no/resources/about-stick-slip/>. Last accessed 12/05/2017.
- [40] E. ToolBox. Water - Absolute or Dynamic Viscosity. URL http://www.engineeringtoolbox.com/absolute-dynamic-viscosity-water-d_575.html. Last accessed 19/10/2016.
- [41] Wikipedia. Illustration of a pid control loop. URL https://upload.wikimedia.org/wikipedia/commons/4/43/PID_en.svg. Last accessed 11/05/2017.

Appendix A

Safety

A.1 Risk Assessment

NTNU	Risk Assessment	Prepared by	Number	Date	
		HSE section	HMSRV2603E	04.02.2011	
HSE/KS		Approved by	Page	Replaces	
		The Rector	1 out of 4	01.12.2006	

Unit: Department of Geoscience and Petroleum

Date: 21.03.2017

Line manager:


Participants in the risk assessment (including their function): Drillbotics NTNU

Activity from the identification process form	Potential undesirable incident/strain	Likelihood:	Consequence:			Risk value	Comments/status Suggested measures
		Likelihood (1-5)	Human (A-E)	Environment (A-E)	Economy/material (A-E)		
Accidents and injuries related to unpredicted burst of pipe due to overpressure	Injury to personnel caused by debris and damage to equipment	2	B	A	A	2A	Safety factors will be applied to all calculations. Safety valves should be included to ensure that pressure does not exceed the critical values of the system.
Accidents and injuries related to unpredicted breaking of the pipe related to overload and buckling	Injury to personnel caused by debris and damage to equipment	2	B	A	A	2A	The probability of breaking the pipe and the corresponding high pressure leakages is high especially during testing and determining the safety limits in the trial period. There will be a possibility to quickly stop the process through an emergency stop button and safety logics will be included in the controller.
Spilling of high pressure fluid	Injury to personnel and damage to equipment.	2	B	A	A	2A	Safety glasses (Plexiglas) will be mounted around the rig to isolate personnel from high pressure zones.
Eye irritation, burn injuries and fumes emitted from welding process	Burns to skin and clothing, inhalation of toxic gases	1	B	A	A	1A	Use welding mask, safety glasses, welding screens and welding gloves. Use

Risk Assessment



Fire	Personnel could suffer from smoke inhalation and burns.	1	B	B	A	1B	Good housekeeping. Clear work area of all combustibles. Fire extinguisher and fire blanket available at the work area. Comply with site hot work permits/rules.	welding respirators.		
Manual handling	Workers could suffer from back injury and long-term pain if regularly lifting/carrying heavy or awkward objects	2	B	A	A	2A	Trolley to be used for moving loads. All workers to be instructed not to carry materials up by hand.			
Electrical hazards	<ul style="list-style-type: none"> Electrical shocks can give rise to superficial burns on the surface of the skin, or internal burns. The burns can affect the heart and result in organ failure. Electrical shorting can cause generation of heat, which can cause sparks or a fire. 	2	B	A	A	2A	<ul style="list-style-type: none"> No power will be supplied while connecting wires and components. All electrical connections will be secured and wiring will be insulated. Qualified personnel will be responsible for high voltage setup. All electrical components should be separated from wet area. The state of the cables should be continuously monitored and changed if necessary. 			

Risk Assessment			
NTNU	Prepared by	Number	Date
	HSE section	HMSRV/2603E	04.02.2011
HSE/KS	Approved by	Page	Replaces
	The Rector	3 out of 4	01.12.2006



Falling objects hitting body	2	B	A	A	2A	Protective footwear and safety helmets supplied and worn at all times. The construction area will be kept off limits to people not involved in the project.
------------------------------	---	---	---	---	----	---

Likelihood, e.g.:

1. Minimal
2. Low
3. Medium
4. High
5. Very high

Consequence, e.g.:

- A. Safe
- B. Relatively safe
- C. Dangerous
- D. Critical
- E. Very critical

Risk value (each one to be estimated separately):

Human = Likelihood x Human Consequence
 Environmental = Likelihood x Environmental consequence
 Financial/material = Likelihood x Consequence for Economy/material

Potential undesirable incident/strain

Identify possible incidents and conditions that may lead to situations that pose a hazard to people, the environment and any materiel/equipment involved.

Criteria for the assessment of likelihood and consequence in relation to fieldwork

Each activity is assessed according to a worst-case scenario. Likelihood and consequence are to be assessed separately for each potential undesirable incident. Before starting on the quantification, the participants should agree what they understand by the assessment criteria:

Likelihood

Minimal 1	Low 2	Medium 3	High 4	Very high 5
Once every 50 years or less	Once every 10 years or less	Once a year or less	Once a month or less	Once a week

NTNU		Risk Assessment		Prepared by	Number	Date
 HSE/KS				HSE section	HMSRV/2603E	04.02.2011
				Approved by	Page	Replaces
		The Rector	4 out of 4	01.12.2006		

Consequence Grading	Human	Environment	Financial/material
E Very critical	May produce fatality/ies	Very prolonged, non-reversible damage	Shutdown of work > 1 year.
D Critical	Permanent injury, may produce serious serious health damage/sickness	Prolonged damage. Long recovery time.	Shutdown of work 0.5-1 year.
C Dangerous	Serious personal injury	Minor damage. Long recovery time	Shutdown of work < 1 month
B Relatively safe	Injury that requires medical treatment	Minor damage. Short recovery time	Shutdown of work < 1week
A Safe	Injury that requires first aid	Insignificant damage. Short recovery time	Shutdown of work < 1day

The unit makes its own decision as to whether opting to fill in or not consequences for economy/materiel, for example if the unit is going to use particularly valuable equipment. It is up to the individual unit to choose the assessment criteria for this column.

Risk = Likelihood x Consequence

Please calculate the risk value for "Human", "Environment" and, if chosen, "Economy/materiel", separately.

About the column "Comments/status, suggested preventative and corrective measures":

Measures can impact on both likelihood and consequences. Prioritise measures that can prevent the incident from occurring; in other words, likelihood-reducing measures are to be prioritised above greater emergency preparedness, i.e. consequence-reducing measures.

Appendix **B**

Hardware

B.1 Hoisting

Motor

Specifications

Technical data

Gearbox size		GST03	GST04	GST05	GST06	GST07	GST09	GST11	GST14
Max. torque	[Nm]	45	73	172	375	710	1623	2848	5920
Ratio range		2.6 - 59	1.6 - 45	1.6 - 335	2 - 435	2 - 417	2 - 412	4 - 412	4 - 412
Dimensions									
Solid shaft	[mm]	14 x 28 20 x 40	16 x 32 20 x 40	20 x 40 25 x 50	25 x 50 30 x 60	30 x 60 40 x 80	40 x 80 50 x 100	60 x 120	80 x 160
Flange	[mm]	120 140 160	120 140 160	120 140 160 200	160 200	200 250	250 300	300 350	350 400

Table B.1.1: Technical data for the hoisting motor (Lenze GST03-2M VBR 063C42) [23].

GST helical gearboxes

Technical data



	063C32 063C42	071C32 071C42	080C32 080C42	090C32	100C12	100C32	112C22	132C12 132C22 132C32
g	123	139	156	176	194	218	258	258
B ₁	MFEMAXX	100	109	150	157	166	176	195
	MFEMABR	107	118	132	137	147	158	187
k ₁	MFEMAXX	187	207	224.5	274	324	319	403
k ₂		120	145	174	180	222	265	265
	MFEMABR	40	52	73	68	76	90	109.5
Δ k	MFFMAXX		128			109	102	115
	MFFMABR	170	165	183	181	170	183	201.5
k								
GST03	329							
GST04	371	391	413					
GST05	401	421	443	503	553			
GST06	427	447	469	529	579	580		
GST07			525	585	635	636	728	
GST09				648	698	699	791	
GST11					755	756	848	
GST14						846	938	

	a	h ¹⁾	o ¹⁾	p ¹⁾
GST03	2	65	90	101
GST04	0	80	100	132
GST05	1	100	115	158.5
GST06	2	125	145	198
GST07	3	160	180	251
GST09	4	200	222	311
GST11	4	250	270	385
GST14	6	315	328	479

	d	d	d ₂	l	l ₁	l ₂	u	t	i	i ₅	o ₁	b ₅	b ₇	c ₅	e ₅	f ₅	m	n	n ₁	s ₅
	k6	m6																		
GST03	14	20	M5 M6	28 40	4 5	20 28	5 6	16 22.5	34 46	40 52	127 139	60	91	11	105	84	20			6.6
GST04	20		M6	40	5	28	6	22.5	43	53	174	76	105	18	129	112	24.5	20	36	9
GST05	25		M10	50	4	40	8	28	53	66	214	90	125	23	155	139	32.5	26	49	11
GST06	30		M10	60	6	45	8	33	64	79	243	106	160	28	196	157	38	35	52	13.5
GST07	40		M16	80	7	63	12	43	84	104	302	130	200	34	247	196	48.5	45	66	18
GST09	50		M16	100	8	80	14	53.5	105	127.5	370	165	245	44	298	239	54	48	74	18
GST11		60	M20	120	8	100	18	64	125	155	433	200	300	54	368	280	69	65	80	22
GST14		80	M20	160	15	125	22	85	165	200	533	250	380	65	460	340	85	85	91	26

¹⁾k₂ !

6.4

Figure B.1.1: Dimensions specifications for the hoisting motor (Lenze GST03-2M VBR 063C42) [23]

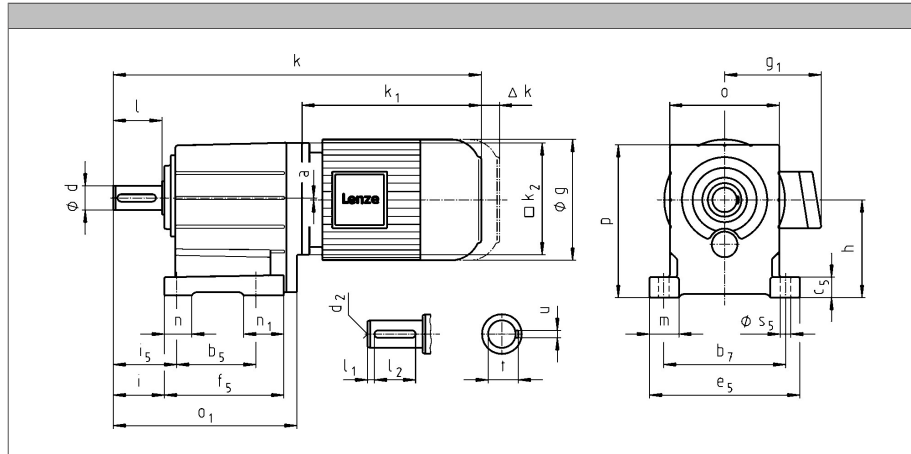
GST helical gearboxes

Technical data



Dimensions

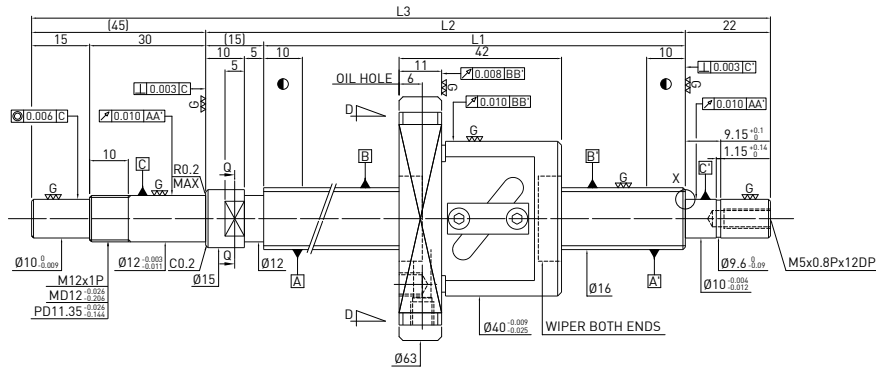
GST□□-2M VBR



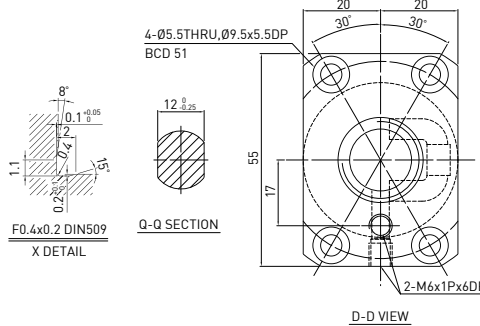
6.4

Figure B.1.2: Mechanical drawings for the hoisting motor (Lenze GST03-2M VBR 063C42) [23].

F S W TYPE (SHAFT OD 16, LEAD 5) ◀ Standard



Ballscrew Data		
Direction	Right Hand	
Lead (mm)	5	
Lead Angle	5.48°	
P.C.D (mm)	16.6	
Screw P.C.D (mm)	16.2	
RD (mm)	13.324	
Steel Ball (mm)	Ø3.175	
Circuits	2.5x1	
Dynamic Load C (Kgfl)	481	763
Static Load Co (Kgfl)	670	1399
Axial Play (mm)	0	0.005 or less
Drag Torque (Kgf-cm)	0.15~0.8	-0.2
Spacer Ball	1 : 1	-

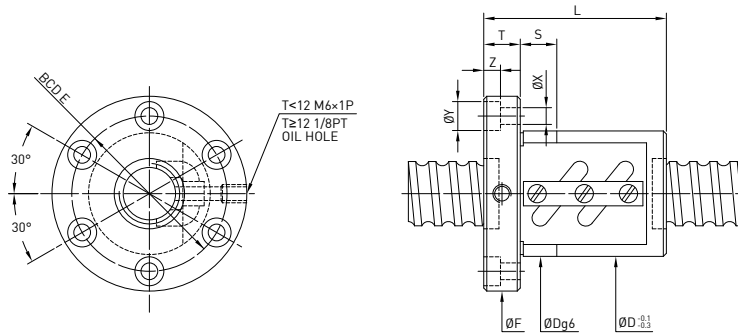


Unit : mm

Stroke	HIWIN Code	L1	L2	L3	Accuracy grade
100	R16-5B1-FSW-189-271-0.018	189	204	271	5
200	R16-5B1-FSW-289-371-0.018	289	304	371	5
300	R16-5B1-FSW-389-471-0.018	389	404	471	5
400	R16-5B1-FSW-489-571-0.018	489	504	571	5
600	R16-5B1-FSW-689-771-0.018	689	704	771	5
800	R16-5B1-FSW-889-971-0.018	889	904	971	5

Figure B.1.3: Ball screw [8]

F S W TYPE



Model	Size		Ball Dia.	PCD	RD	Circuits	Stiffness kgf / μm K	Dynamic Load 1×10^6 revs C (kgf)	Static Load Co (kgf)	Nut		Flange			Bolt			Fit
	Nominal Dia.	Lead								D	L	F	T	BCD-E	X	Y	Z	
12-4B1	12	4	2.381	12.25	9.792	2.5x1	8	383	638	30	38	50	10	40	4.5	8	4	12
12-4C1				12.25	9.792	3.5x1	9	511	893	30	44	50	10	40	4.5	8	4	12
12-5B1				12.25	9.792	2.5x1	8	383	638	30	40	50	10	40	4.5	8	4	12
14-5B1	14	5	3.175	14.6	11.324	2.5x1	10	710	1216	34	40	57	11	45	5.5	9.5	5.5	12
15-10A1				15.6	12.324	1.5x1	9	474	781	34	48	57	11	45	5.5	9.5	5.5	12
15-20A1	15	20	4	15.6	12.324	1.5x1	9	474	781	34	62	58	12	45	5.5	9.5	5.5	12
16-4B1				16.25	13.792	2.5x1	14	439	870	34	38	57	11	45	5.5	9.5	5.5	12
16-5B1	16	5	3.175	16.6	13.324	2.5x1	16	763	1400	40	45	64	12	51	5.5	9.5	5.5	12
16-5B2				16.6	13.324	2.5x2	33	1385	2799	40	60	64	12	51	5.5	9.5	5.5	12
16-5C1				16.6	13.324	3.5x1	22	1013	1946	40	50	64	12	51	5.5	9.5	5.5	12
20-5B1	20	6	3.969	20.6	17.324	2.5x1	19	837	1733	44	45	68	12	55	5.5	9.5	5.5	12
20-5B2				20.6	17.324	2.5x2	39	1519	3465	44	60	68	12	55	5.5	9.5	5.5	12
20-6B1				20.8	16.744	2.5x1	20	1137	2187	48	48	72	12	59	5.5	9.5	5.5	12
20-6C1	20	6	3.969	20.8	16.744	3.5x1	28	1512	3041	48	66	72	12	59	5.5	9.5	5.5	12
25-4B2				25.25	22.792	2.5x2	38	976	2776	46	48	69	11	57	5.5	9.5	5.5	12
25-5B2				25.6	22.324	2.5x2	46	1704	4417	50	60	74	12	62	5.5	9.5	5.5	12
25-5C1	25	5	3.175	25.6	22.324	3.5x1	35	1252	3085	50	50	74	12	62	5.5	9.5	5.5	12
25-6B1				25.8	21.744	2.5x1	24	1255	2735	53	44	76	11	64	5.5	9.5	5.5	12
25-6B2				25.8	21.744	2.5x2	48	2308	5523	56	68	82	12	69	6.6	11	6.5	12
25-6C1	25	6	3.969	25.8	21.744	3.5x1	35	1690	3844	56	55	82	12	69	6.6	11	6.5	12
25-10B1				26	21.132	2.5x1	25	1592	3237	60	65	86	16	73	6.6	11	6.5	12
25-10B2				26	21.132	2.5x2	46	2888	6472	58	97	85	15	71	6.6	11	6.5	12
25-12B1	25	12	3.969	25.8	21.744	2.5x1	24	1271	2761	53	60	78	11	64	6.6	11	6.5	12
28-5B1				28.6	25.324	2.5x1	26	984	2466	55	45	85	12	69	6.6	11	6.5	12
28-5B2				28.6	25.324	2.5x2	50	1785	4932	55	60	85	12	69	6.6	11	6.5	12
28-6A2	28	6	3.175	28.6	25.324	1.5x2	29	1150	2960	55	55	85	12	69	6.6	11	6.5	12
28-12B2				29	24.132	2.5x2	51	3060	7299	60	110	86	12	73	6.6	11	6.5	12
28-16B1				29	24.132	2.5x1	25	1686	3649	62	84	89	12	75	6.6	11	6.5	12
32-5B2	32	5	3.175	32.6	29.324	2.5x2	55	1886	5666	58	60	84	12	71	6.6	11	6.5	12
32-5C1				32.6	29.324	3.5x1	39	1388	3967	58	50	84	12	71	6.6	11	6.5	12
32-6B2				32.8	28.744	2.5x2	56	2556	7020	62	68	88	12	75	6.6	11	6.5	12
32-6C1	32	6	3.969	32.8	28.744	3.5x1	39	1888	4936	62	55	88	12	75	6.6	11	6.5	12
32-8B2				33	28.132	2.5x2	59	3284	8453	66	86	100	16	82	9	14	8.5	15
32-8C1				33	28.132	3.5x1	41	2428	5948	66	70	100	16	82	9	14	8.5	15
32-10B2	32	10	6.350	33.4	26.91	2.5x2	60	4810	11199	74	98	108	16	90	9	14	8.5	15
32-10C1				33.4	26.91	3.5x1	44	3519	7785	74	78	108	16	90	9	14	8.5	15
32-12A2				33.4	26.91	1.5x2	37	3051	6612	74	97	108	18	90	9	14	8.5	15
32-12B2	32	12	6.350	33.4	26.91	2.5x2	59	4810	11199	74	110	108	18	90	9	14	8.5	15

Remark: Stiffness values listed above value are derived from theoretical formula while axial load is 30% of dynamic load rating without preload.

Figure B.1.4: Ball screw nut [8].

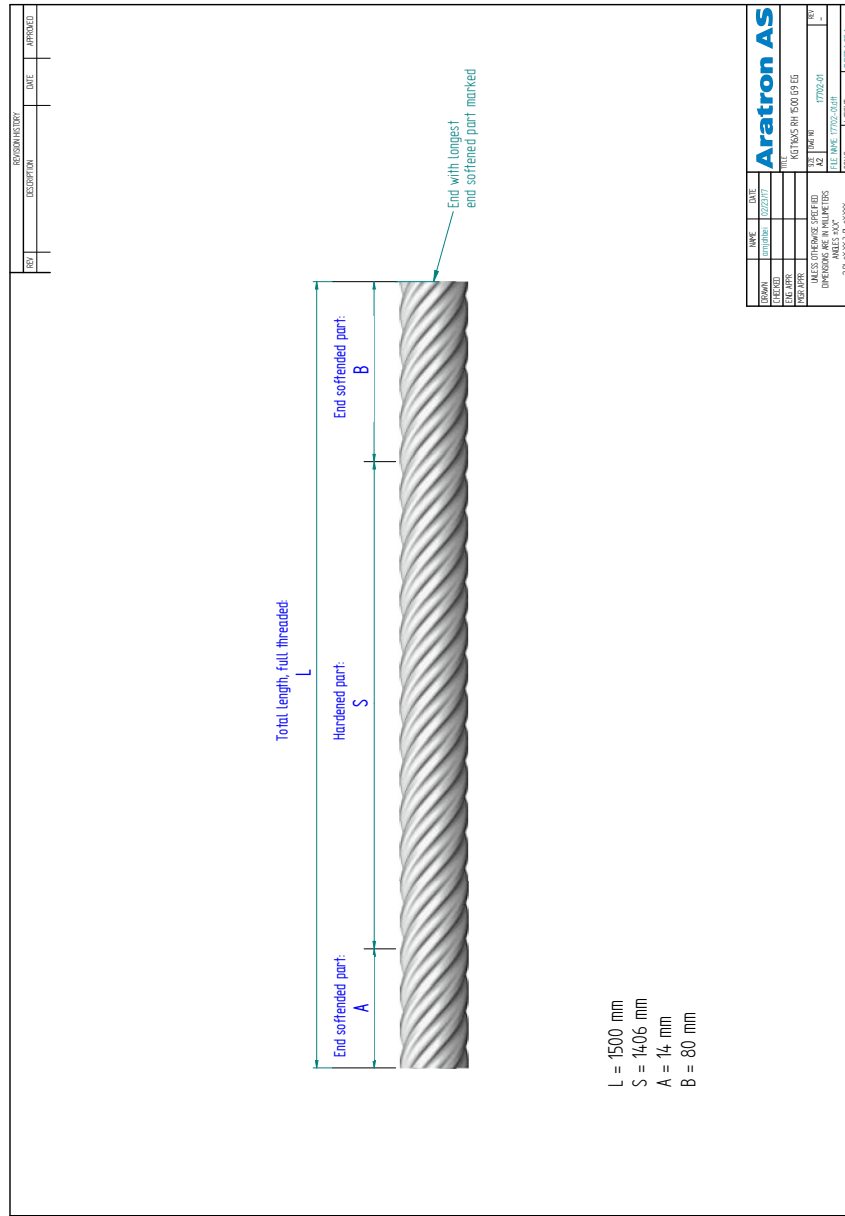
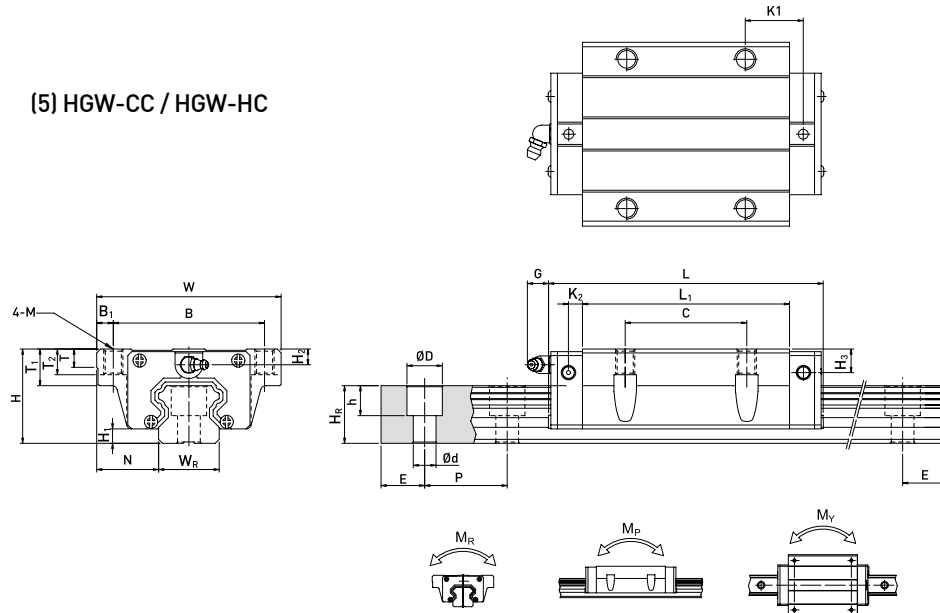


Figure B.1.5: Ball screw [8].

(5) HGW-CC / HGW-HC



Model No.	Dimensions of Assembly (mm)		Dimensions of Block (mm)														Dimensions of Rail (mm)					Mounting Bolt for Rail (mm)	Basic Dynamic Load Rating C(kN)	Basic Static Load Rating C ₀ (kN)	Static Rated Moment			Weight						
	H	H ₁	N	W	B	B ₁	C	L ₁	L	K ₁	K ₂	G	M	T	T ₁	T ₂	H ₂	H ₃	W _R	H _R	D				h	d	P	E	M _R	M _P	M _Y	Block	Rail	
	kgf	mm	mm	mm	mm	mm	mm	mm	mm	mm	mm	mm	mm	mm	mm	mm	mm	mm	mm	mm	mm				mm	mm	mm	mm	mm	kN-m	kN-m	kN-m	kg	kg/m
HGW 15CC	24	4.3	16	47	38	4.5	30	39.4	61.4	8	4.85	5.3	M5	6	8.9	6.95	3.95	3.7	15	15	7.5	5.3	4.5	60	20	M4x16	11.38	16.97	0.12	0.10	0.10	0.17	1.45	
HGW 20CC	30	4.6	21.5	63	53	5	40	50.5	77.5	10.25	6	12	M6	8	10	9.5	6	6	20	17.5	9.5	8.5	6	60	20	M5x16	17.75	27.76	0.27	0.20	0.20	0.40	2.21	
HGW 20HC								65.2	92.2	17.6																								
HGW 25CC								58	84	11.8																								
HGW 25HC	36	5.5	23.5	70	57	6.5	45	78.6	104.6	22.1	6	12	M8	8	14	10	6	5	23	22	11	9	7	60	20	M6x20	32.75	49.44	0.56	0.57	0.57	0.80	3.21	
HGW 30CC								70	97.4	14.25																								
HGW 30HC	42	6	31	90	72	9	52	93	120.4	25.75	6	12	M10	8.5	16	10	6.5	10.8	28	26	14	12	9	80	20	M8x25	47.27	69.16	0.88	0.92	0.92	1.44	4.47	
HGW 35CC								80	112.4	14.6																								
HGW 35HC	48	7.5	33	100	82	9	62	105.8	138.2	27.5	7	12	M10	10.1	18	13	9	12.6	34	29	14	12	9	80	20	M8x25	49.52	69.16	1.16	0.81	0.81	1.56	6.30	
HGW 45CC								97	139.4	13																								
HGW 45HC	60	9.5	37.5	120	100	10	80	128.8	171.2	28.9	10	12.9	M12	15.1	22	15	8.5	20.5	45	38	20	17	14	105	22.5	M12x35	77.57	102.71	1.98	1.55	1.55	2.79	10.41	
HGW 55CC								117.7	166.7	17.35																								
HGW 55HC	70	13	43.5	140	116	12	95	155.8	204.8	36.4	11	12.9	M14	17.5	26.5	17	12	19	53	44	23	20	16	120	30	M14x45	114.44	148.33	3.69	2.64	2.64	4.52	15.08	
HGW 65CC								144.2	200.2	23.1																								
HGW 65HC	90	15	53.5	170	142	14	110	203.6	259.6	52.8	14	12.9	M16	25	37.5	23	15	15	63	53	26	22	18	150	35	M16x50	163.63	215.33	6.65	4.27	4.27	9.17	21.18	

Note : 1 kgf = 9.81 N

Figure B.1.6: Complete linear roller guide package [7].

B.2 Top-Drive-Specifications

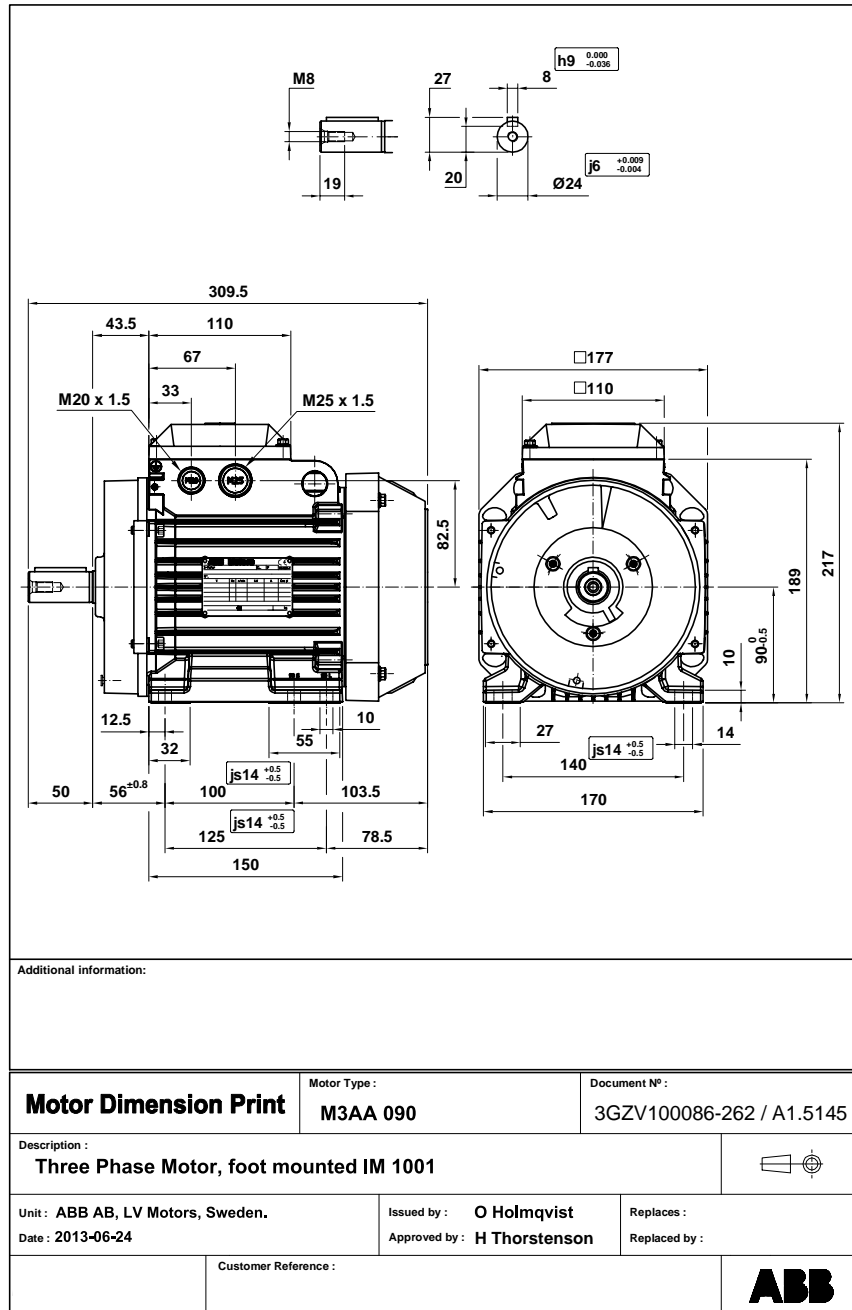


Figure B.2.1: Top drive motor (3GAA091520-ASJ).

B.3 BHA

design

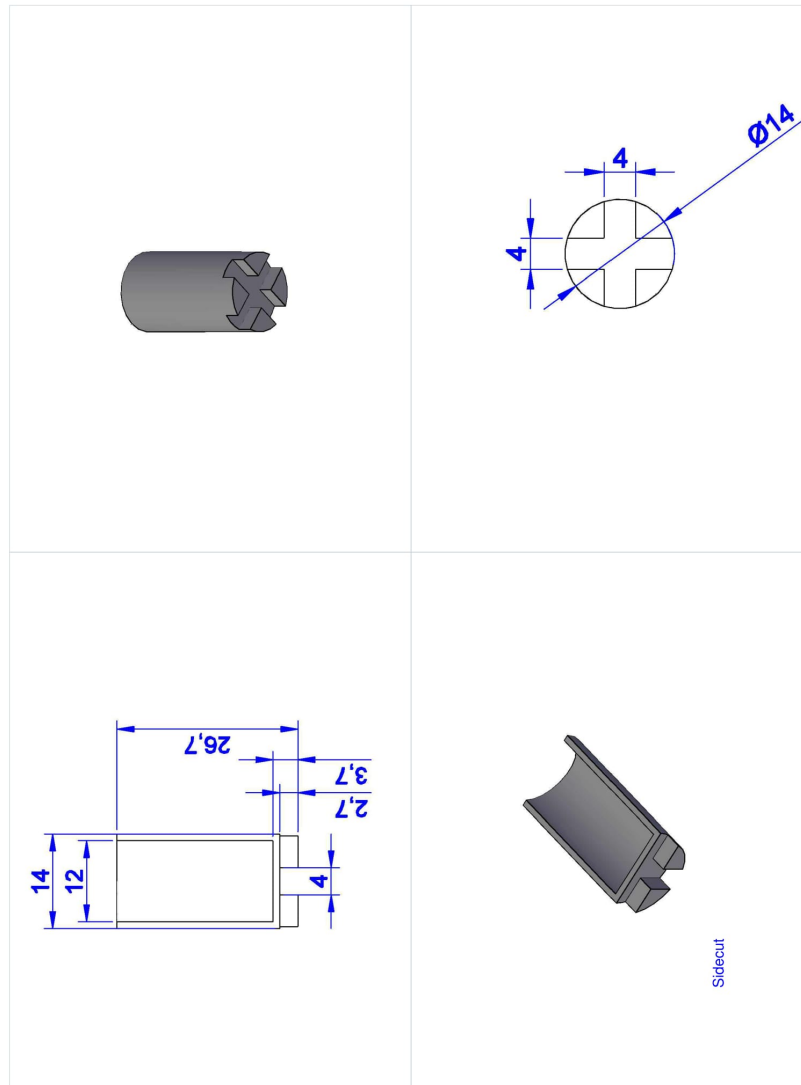


Figure B.3.1: Sensor cover inside BHA.

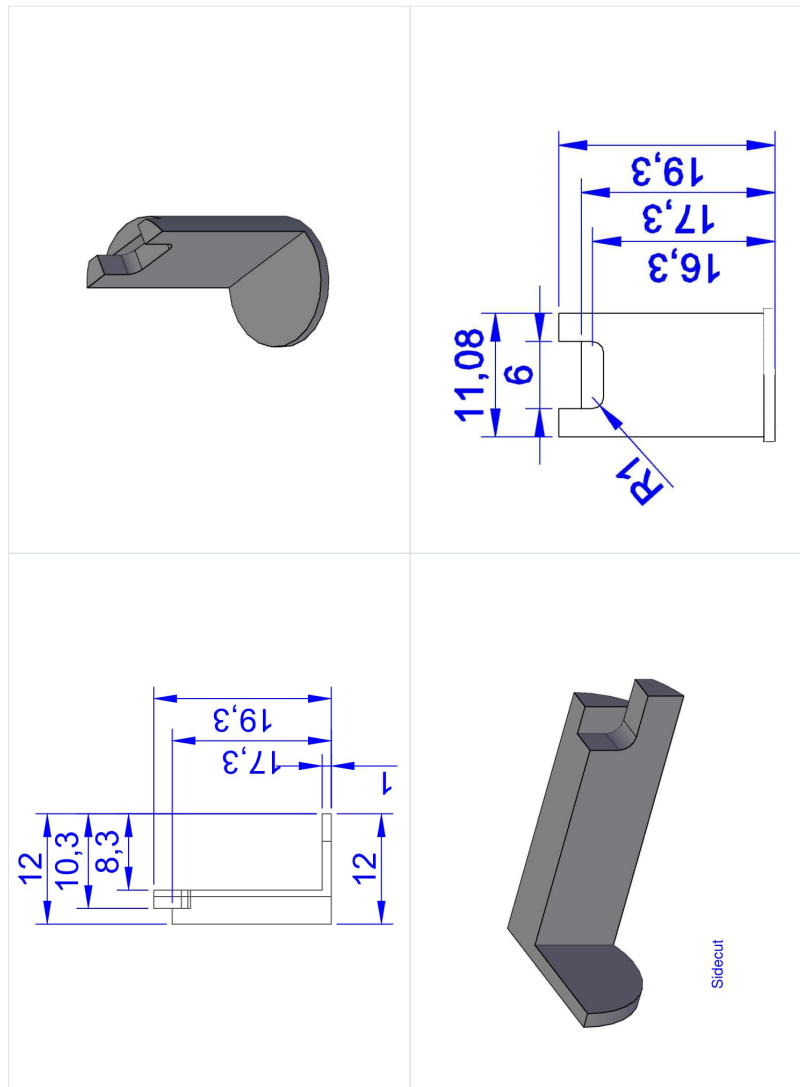


Figure B.3.2: Holder for the sensor inside BHA.

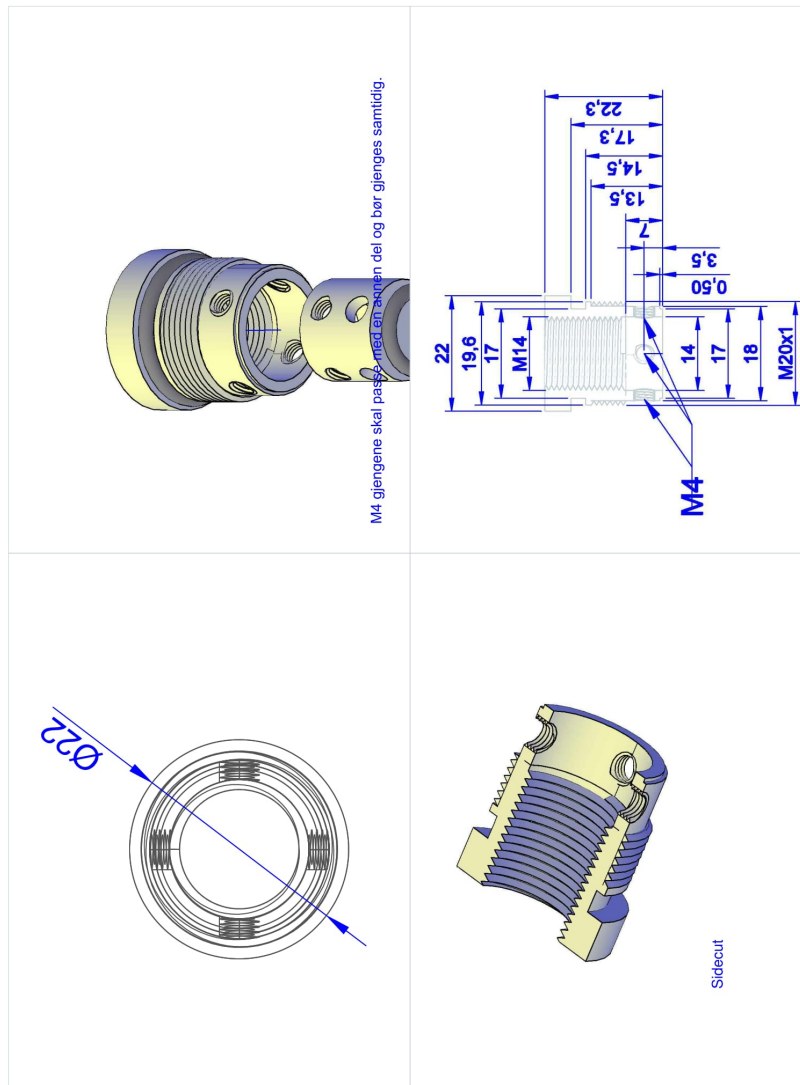


Figure B.3.3: Top of BHA.

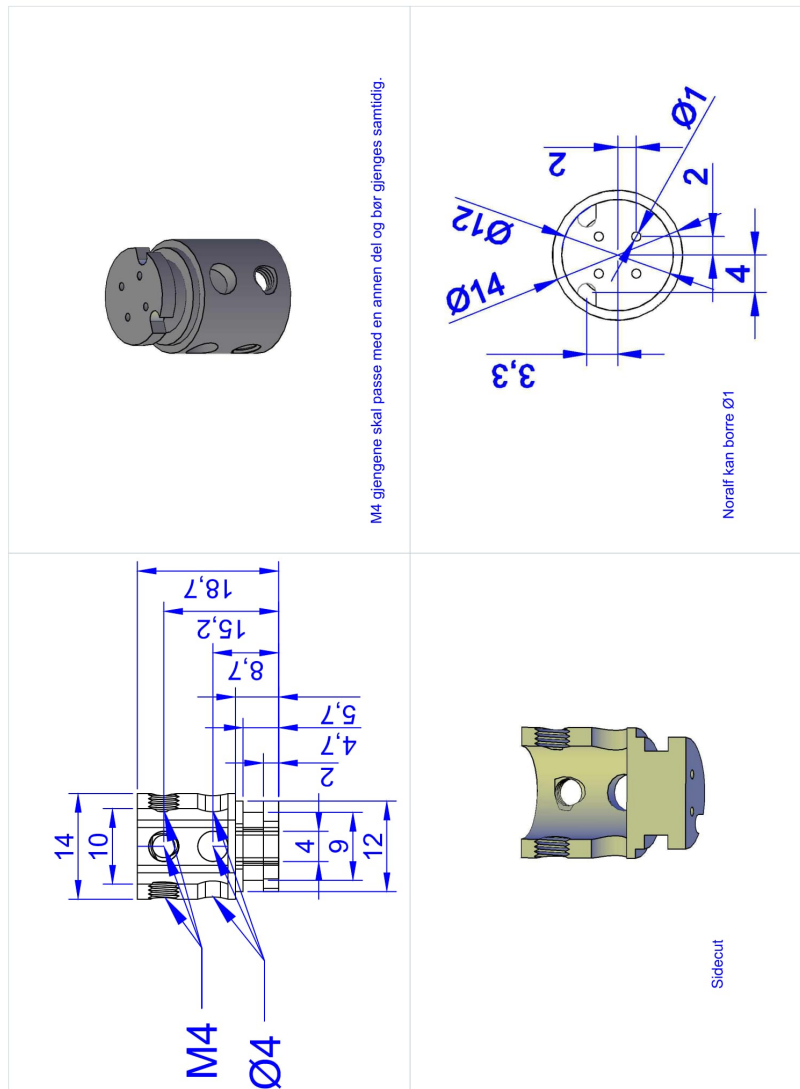


Figure B.3.4: Middle section inside BHA.

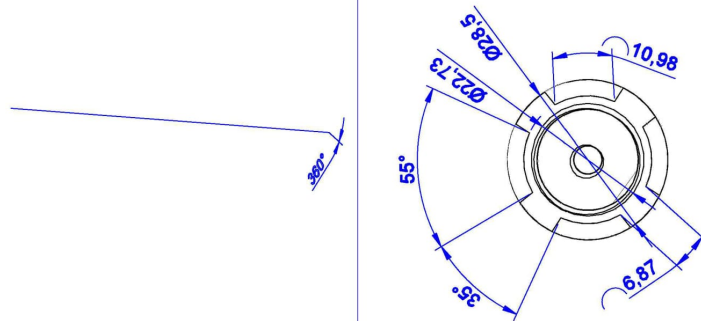
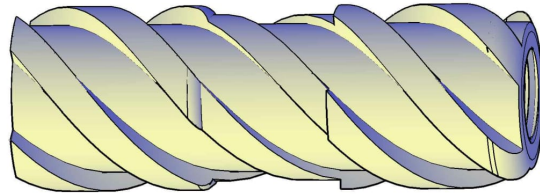


Figure B.3.5: BHA Body.

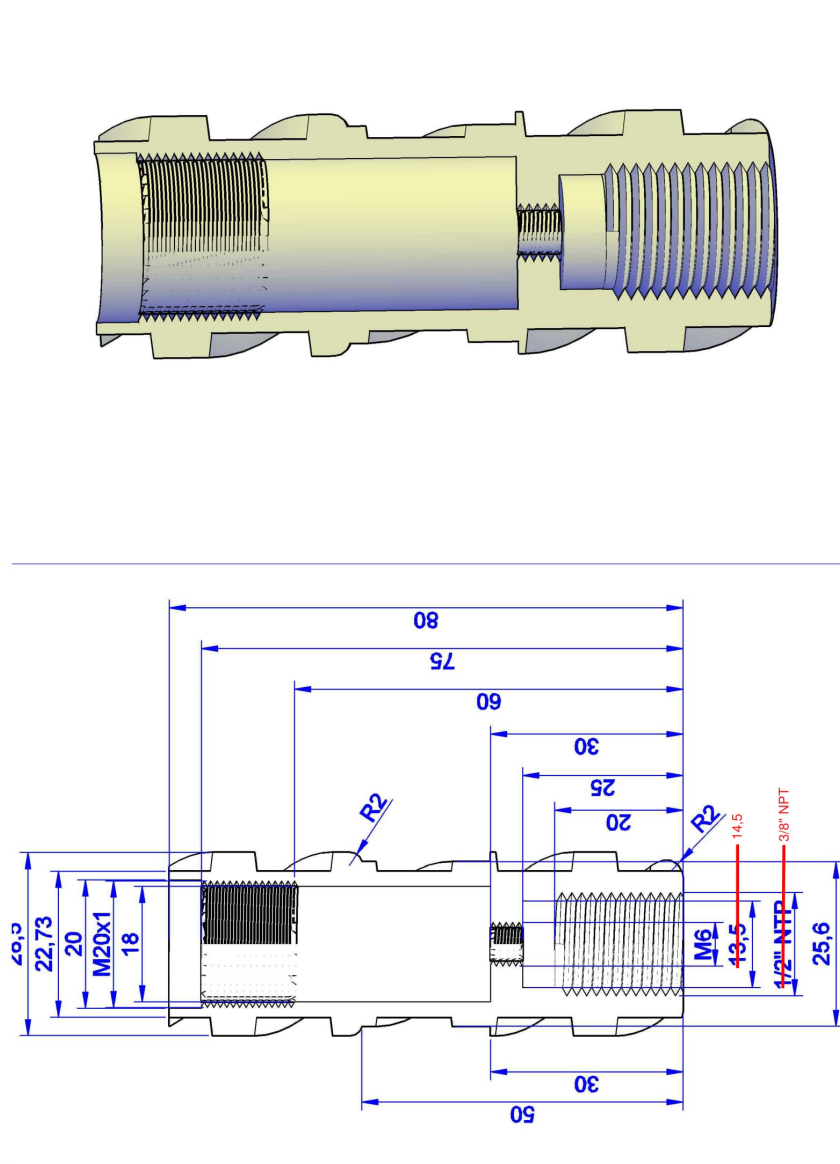


Figure B.3.6: Cross section of the BHA body.

B.4 Swivel

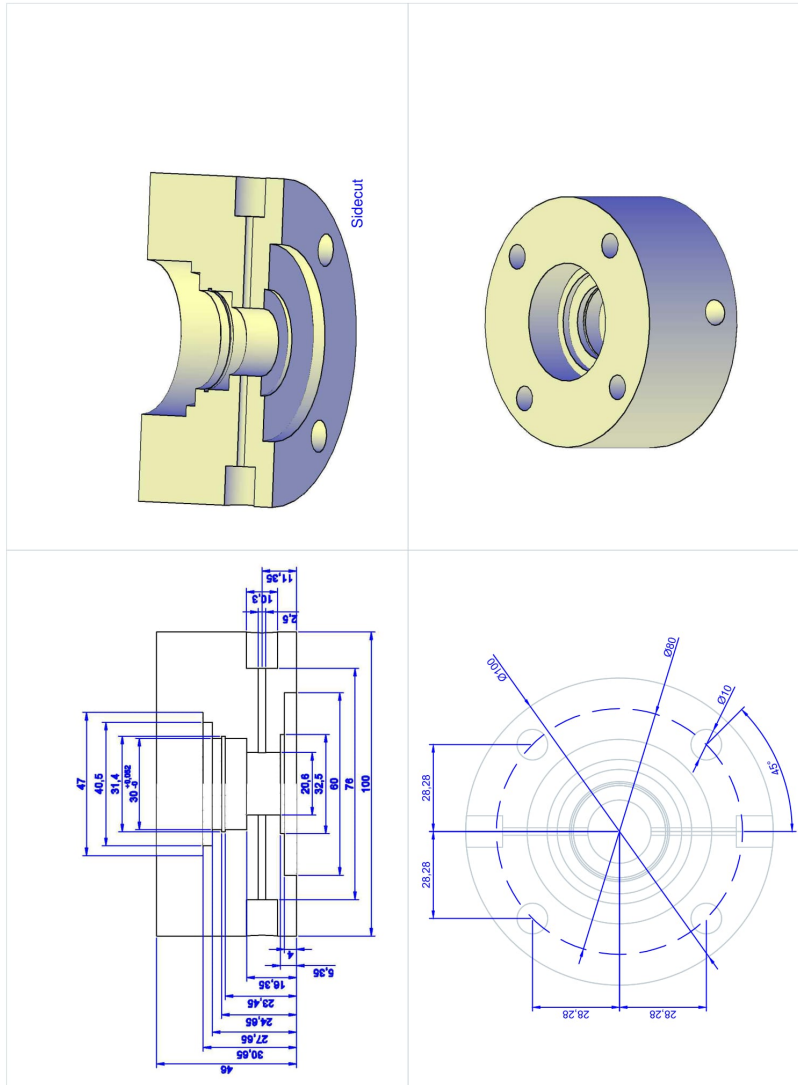


Figure B.4.1: Top- and bottom part of the swivel.

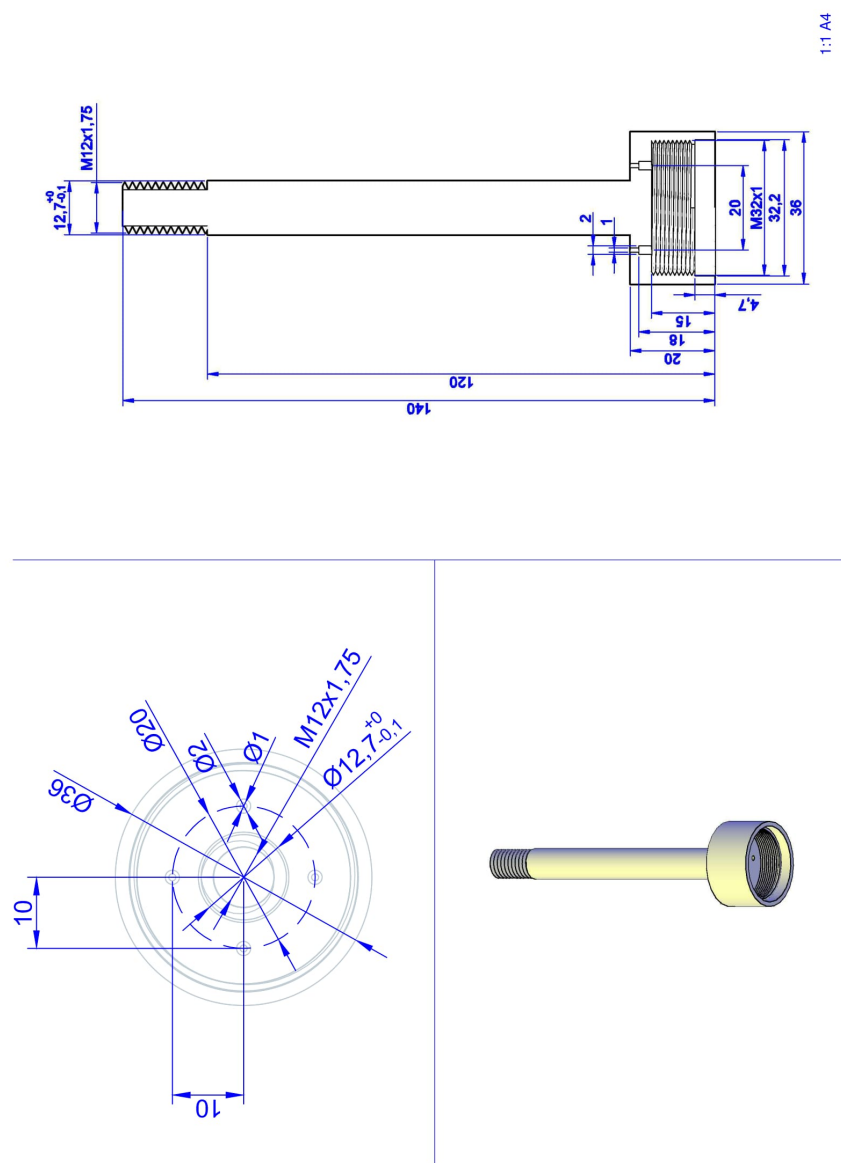


Figure B.4.2: Shaft for sensor wiring.

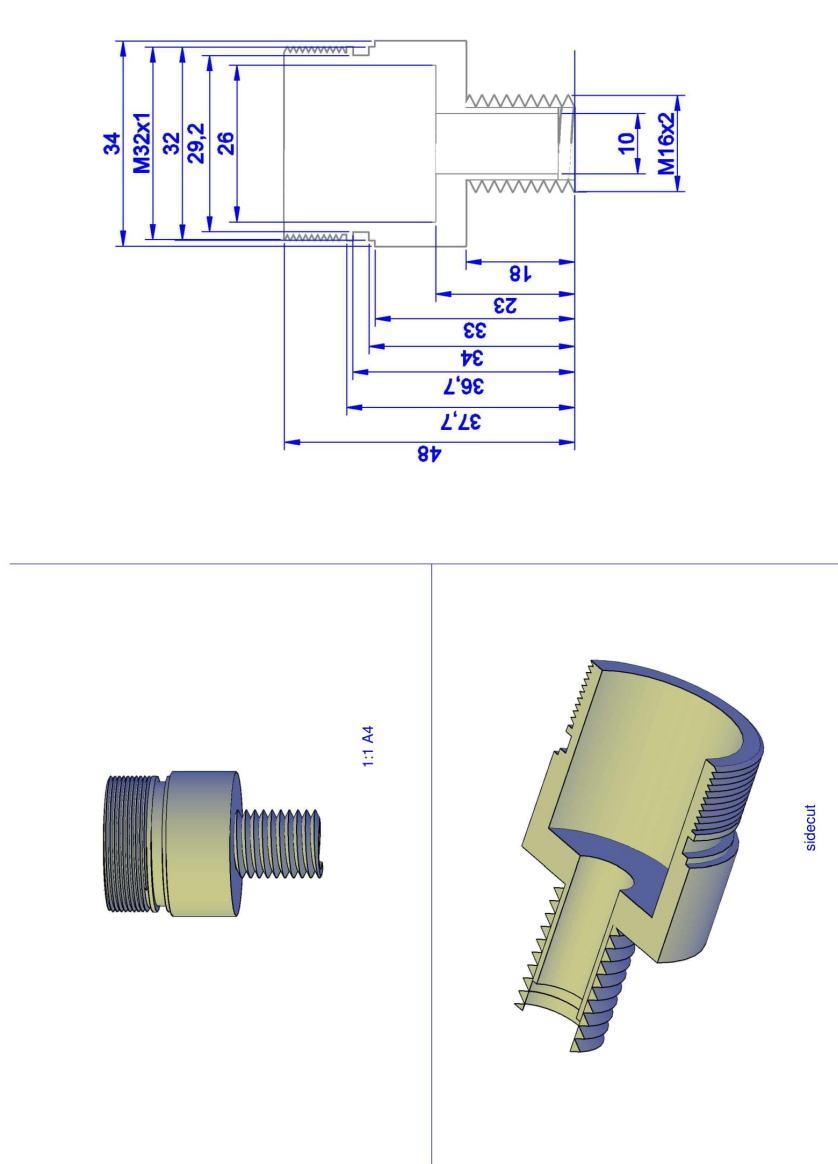


Figure B.4.3: Electrical housing for sensor.

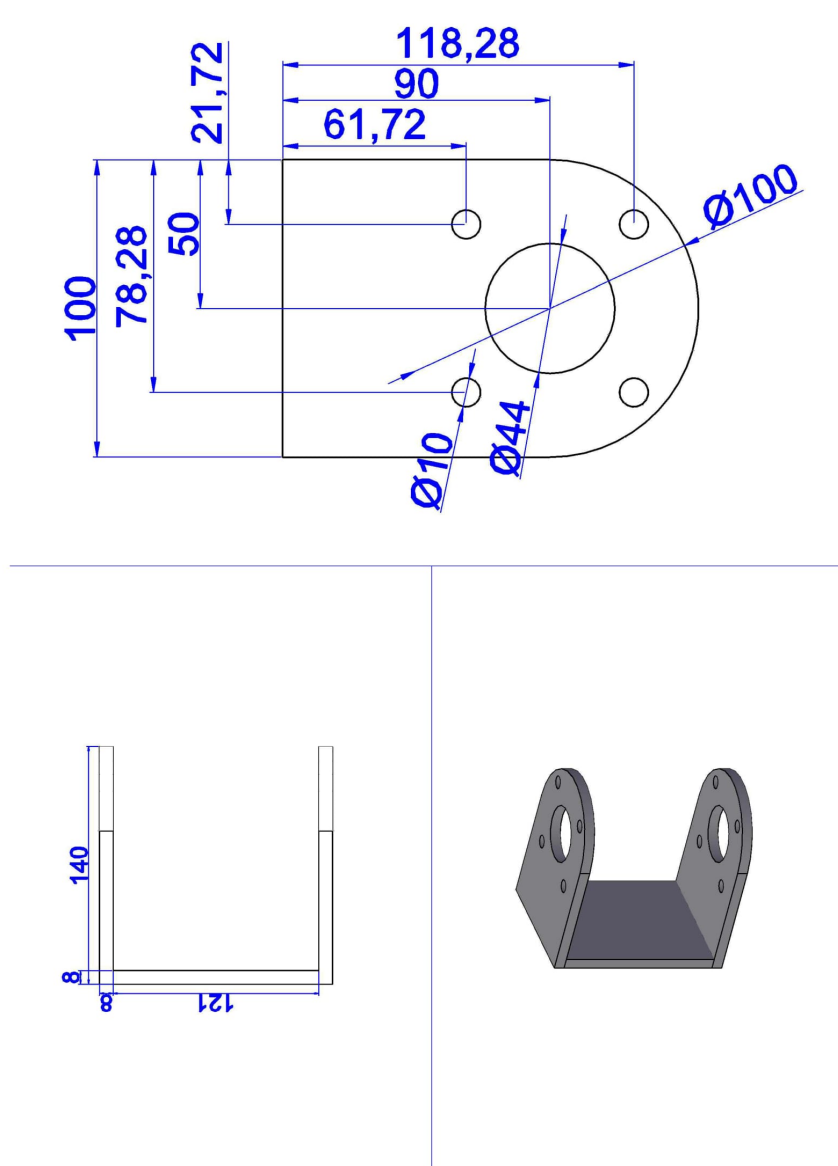


Figure B.4.4: Holder for the swivel.

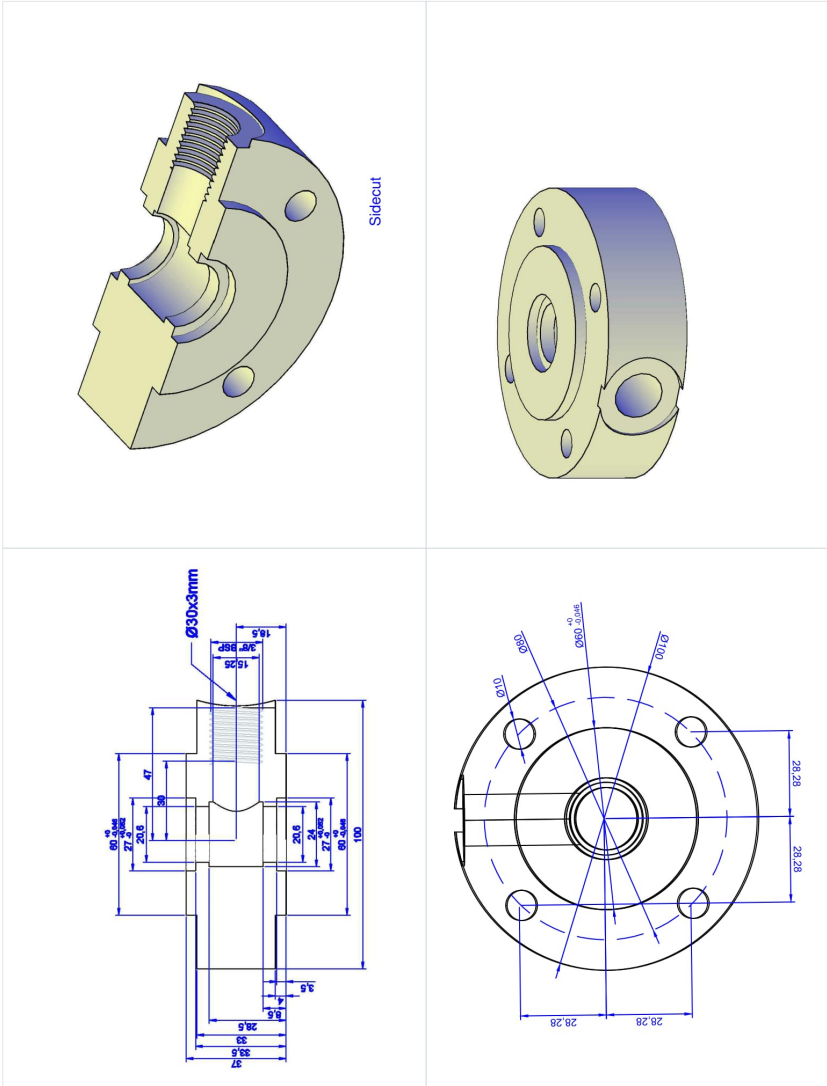


Figure B.4.5: Middle section of the swivel.

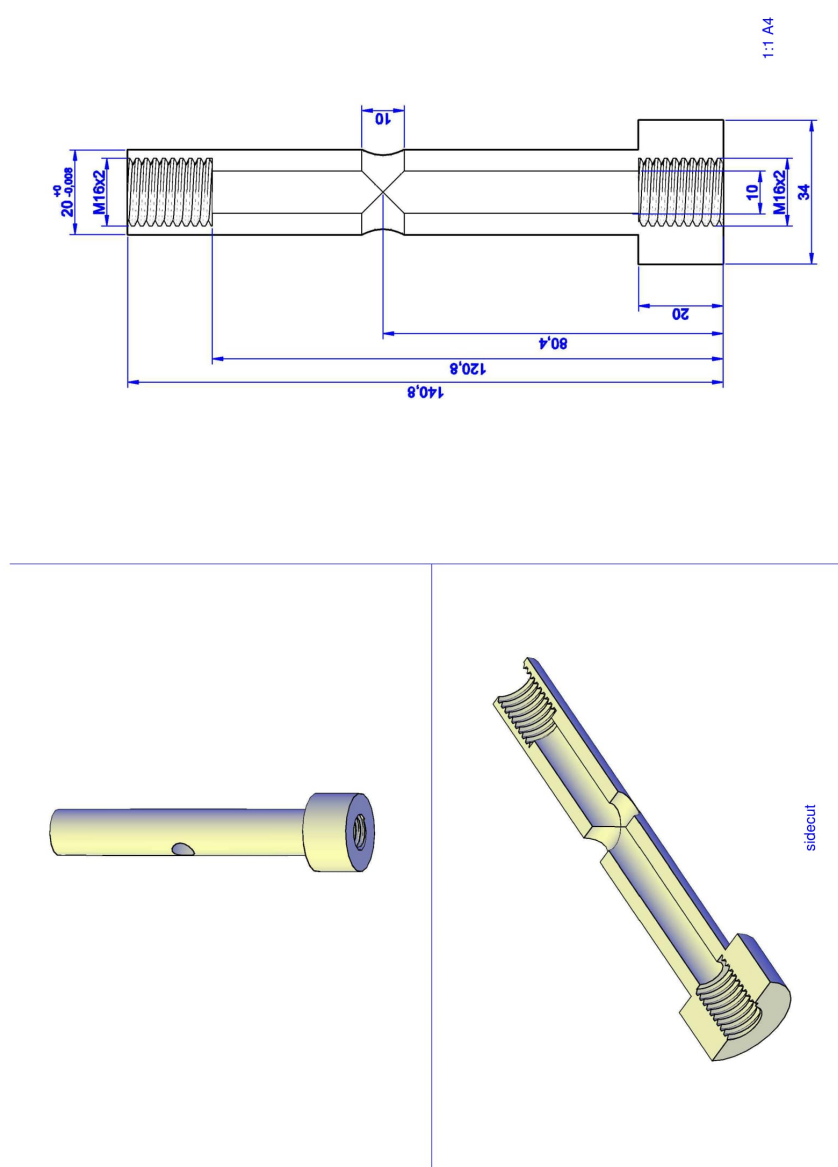


Figure B.4.6: Hollow shaft for water circulation.

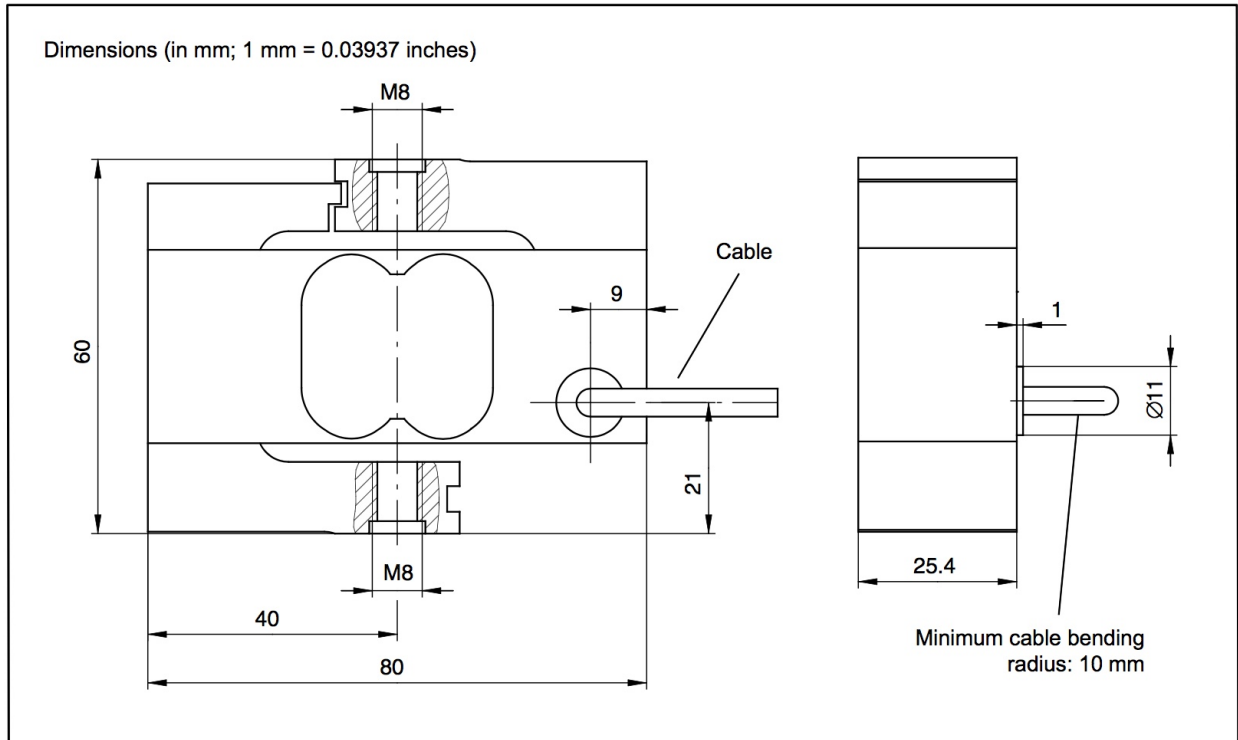
B.5 Load**Cell****Specifications**

Figure B.5.1: Load cell (HBM S2M 500 N, CLIP AE301) dimensions. [18].

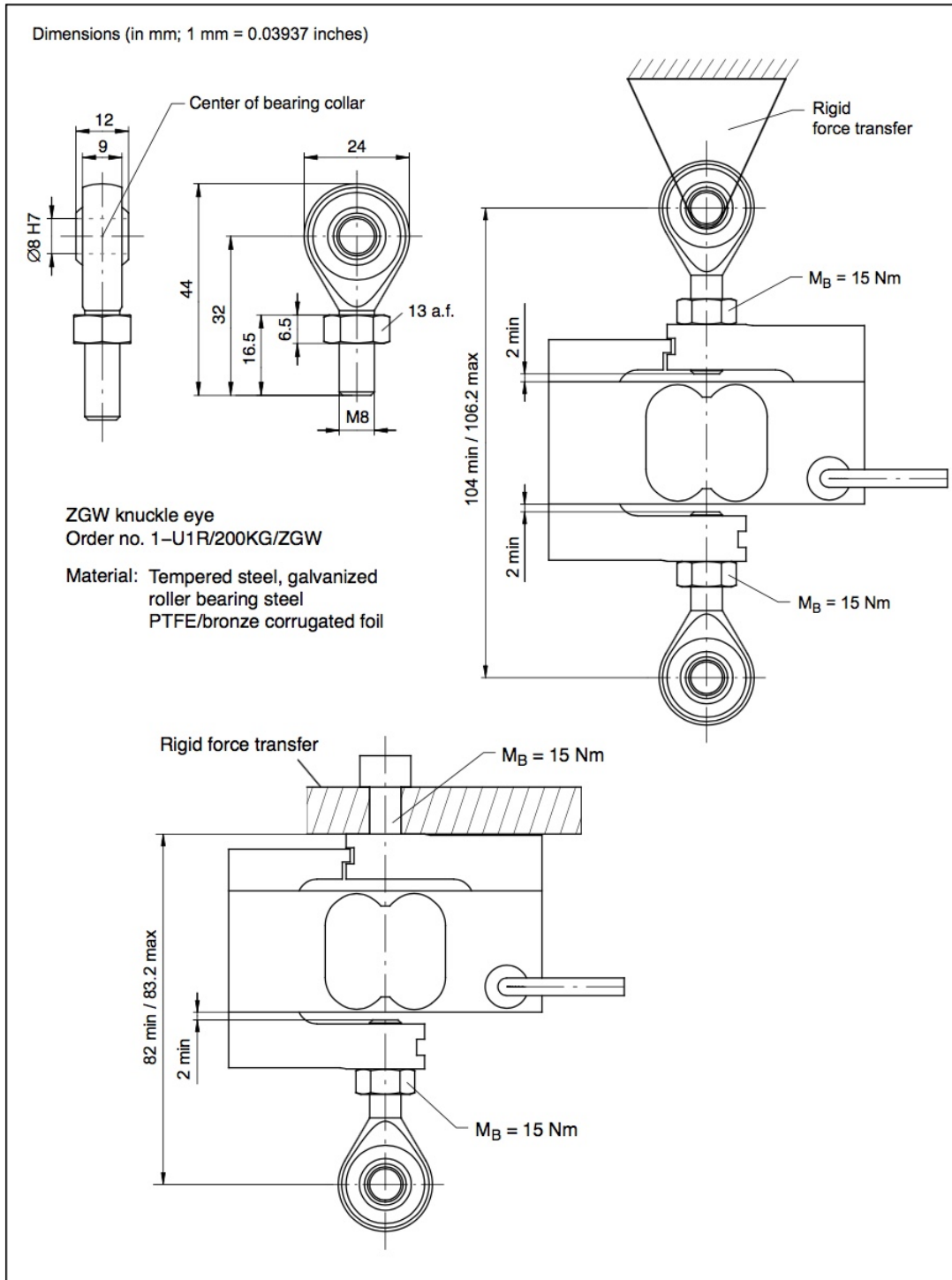


Figure B.5.2: Load cell (HBM S2M 500 N, CLIP AE301) dimensions. [18]

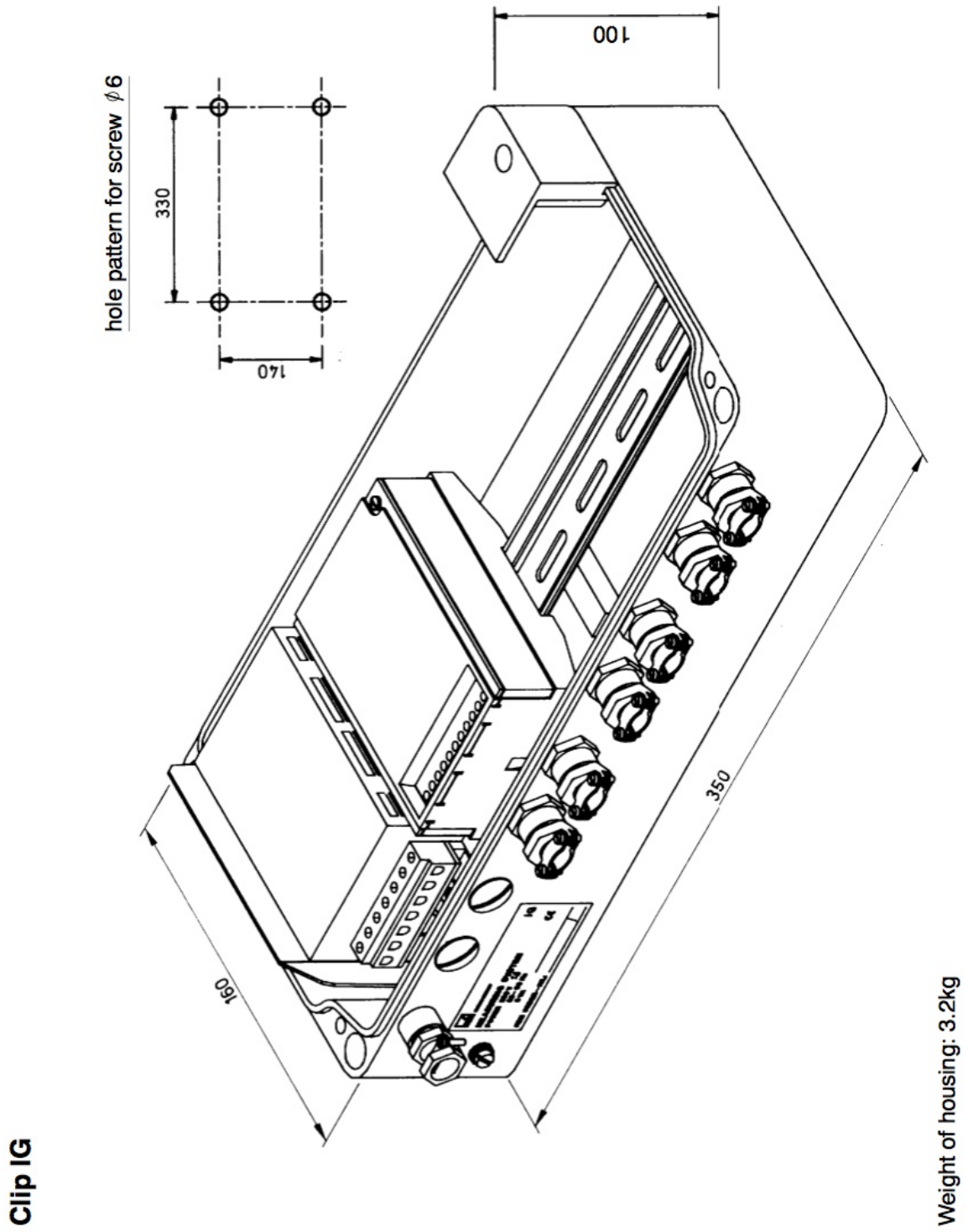


Figure B.5.3: Load cell (HBM S2M 500 N, CLIP AE301) dimensions [18].

B.6 Lyng Miniature Drill Bit Design

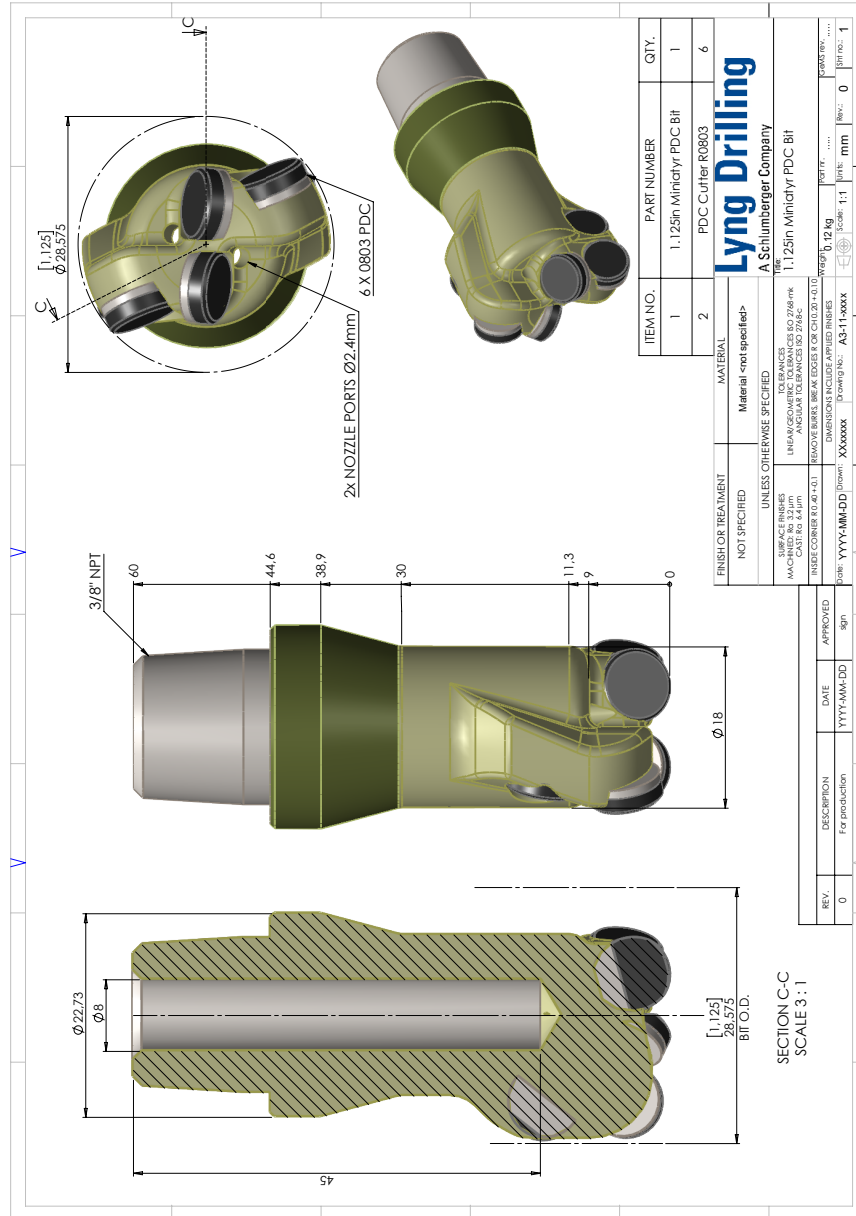


Figure B.6.1: Miniature drill bit from Lyng Drilling AS.

B.7 Rig

Design

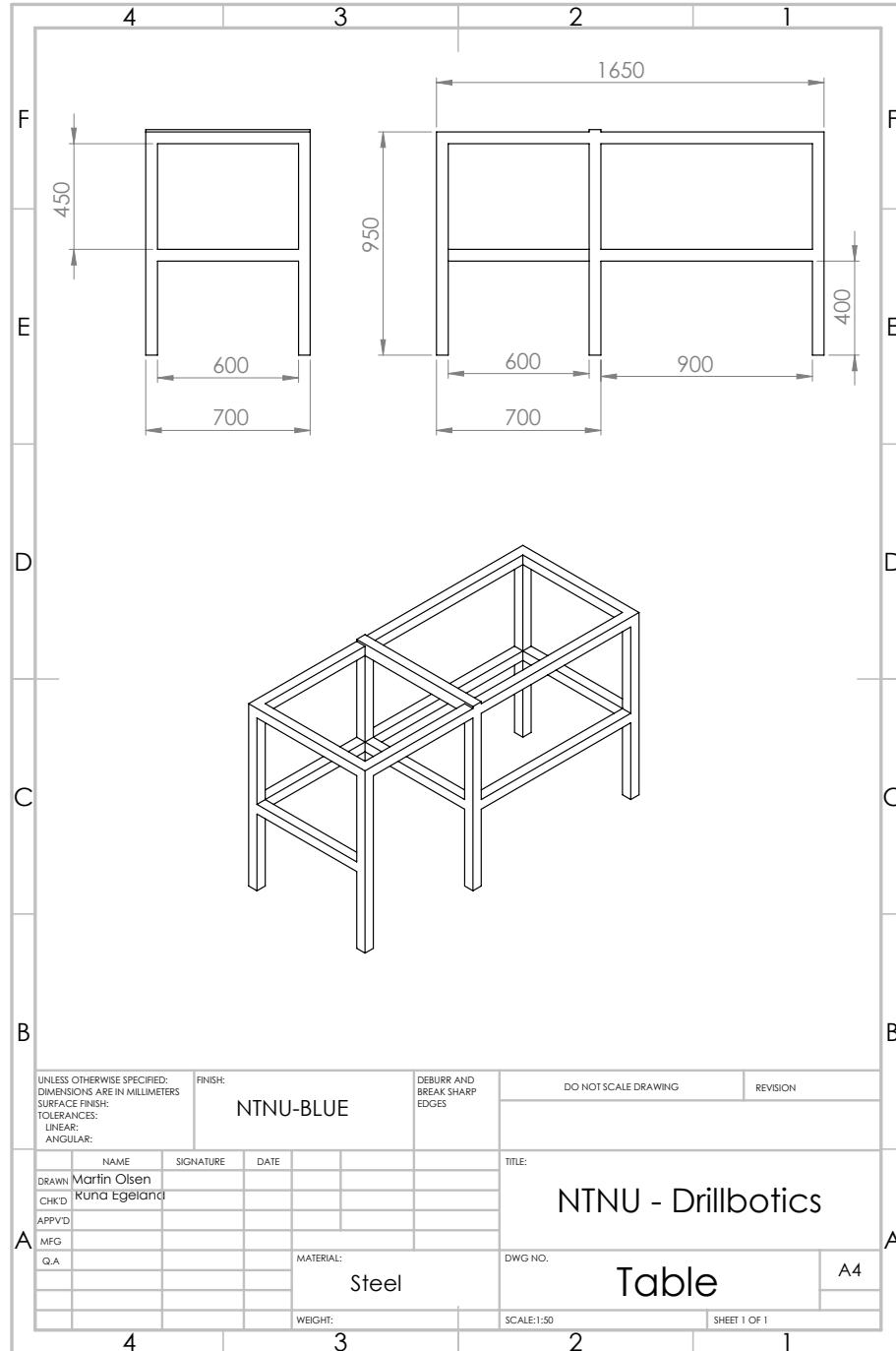


Figure B.7.1: Substructure of rig. All dimensions in mm.

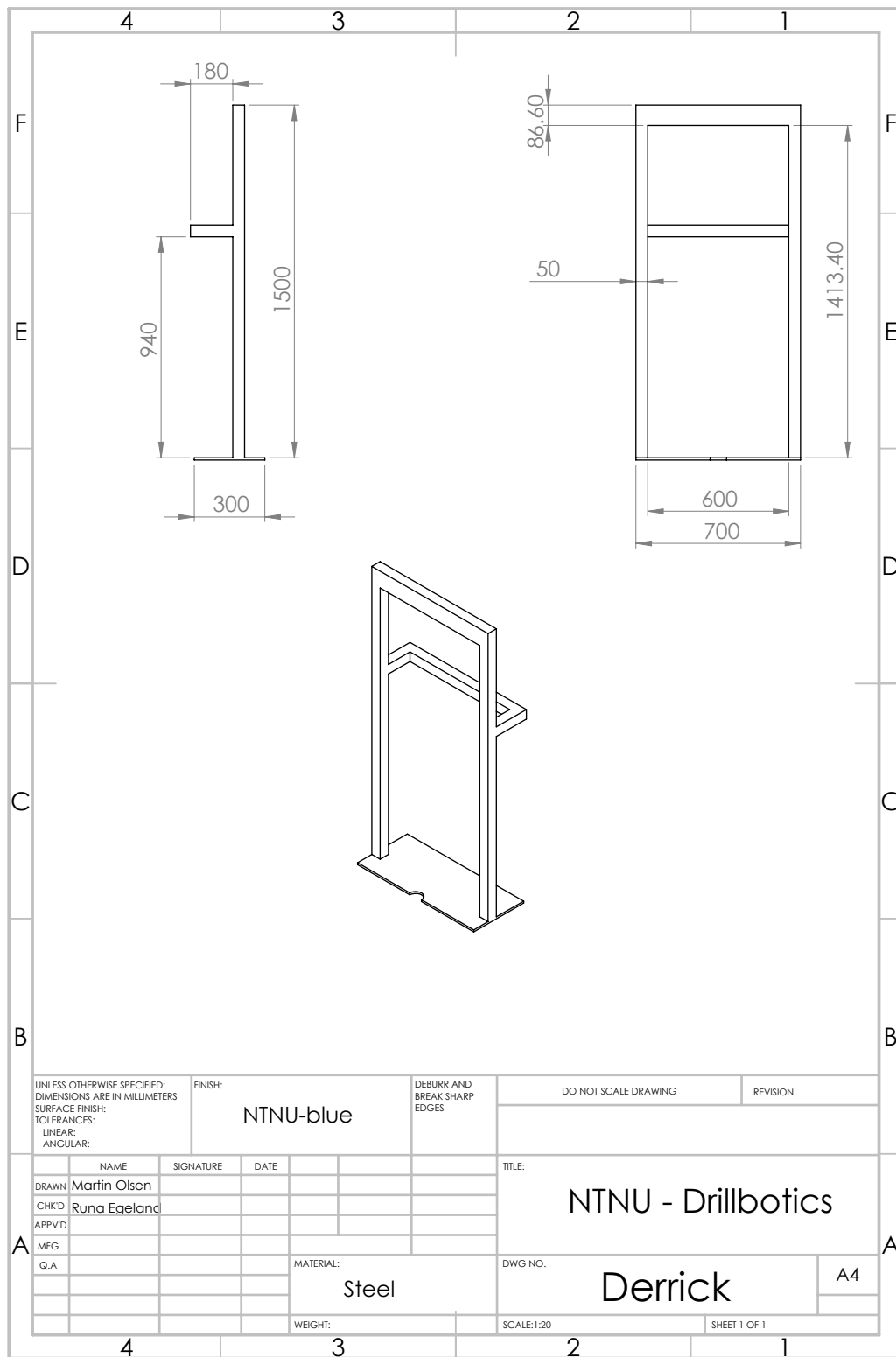


Figure B.7.2: Derrick. All dimensions in mm.

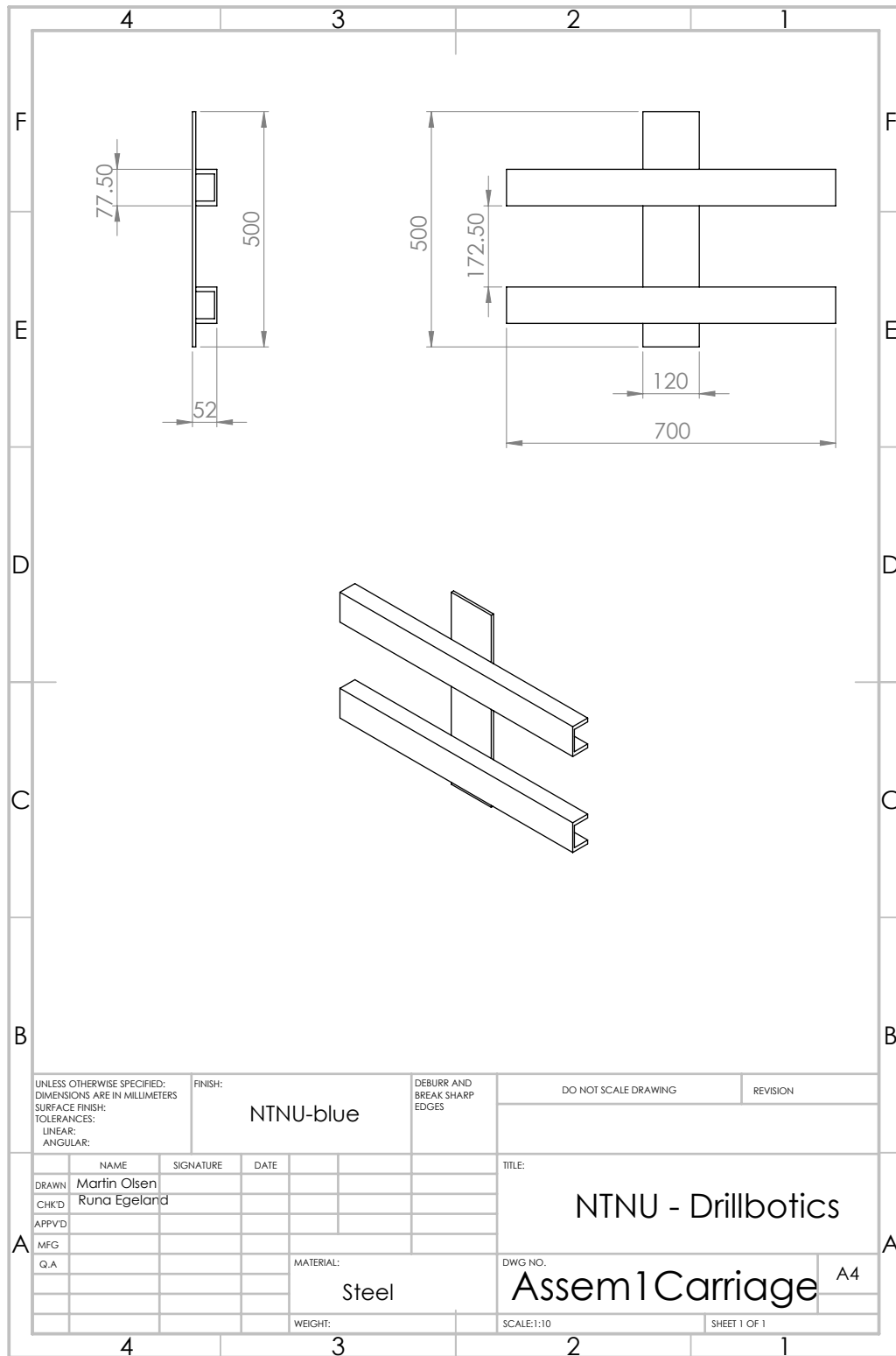


Figure B.7.3: Carriage. All dimensions in mm.

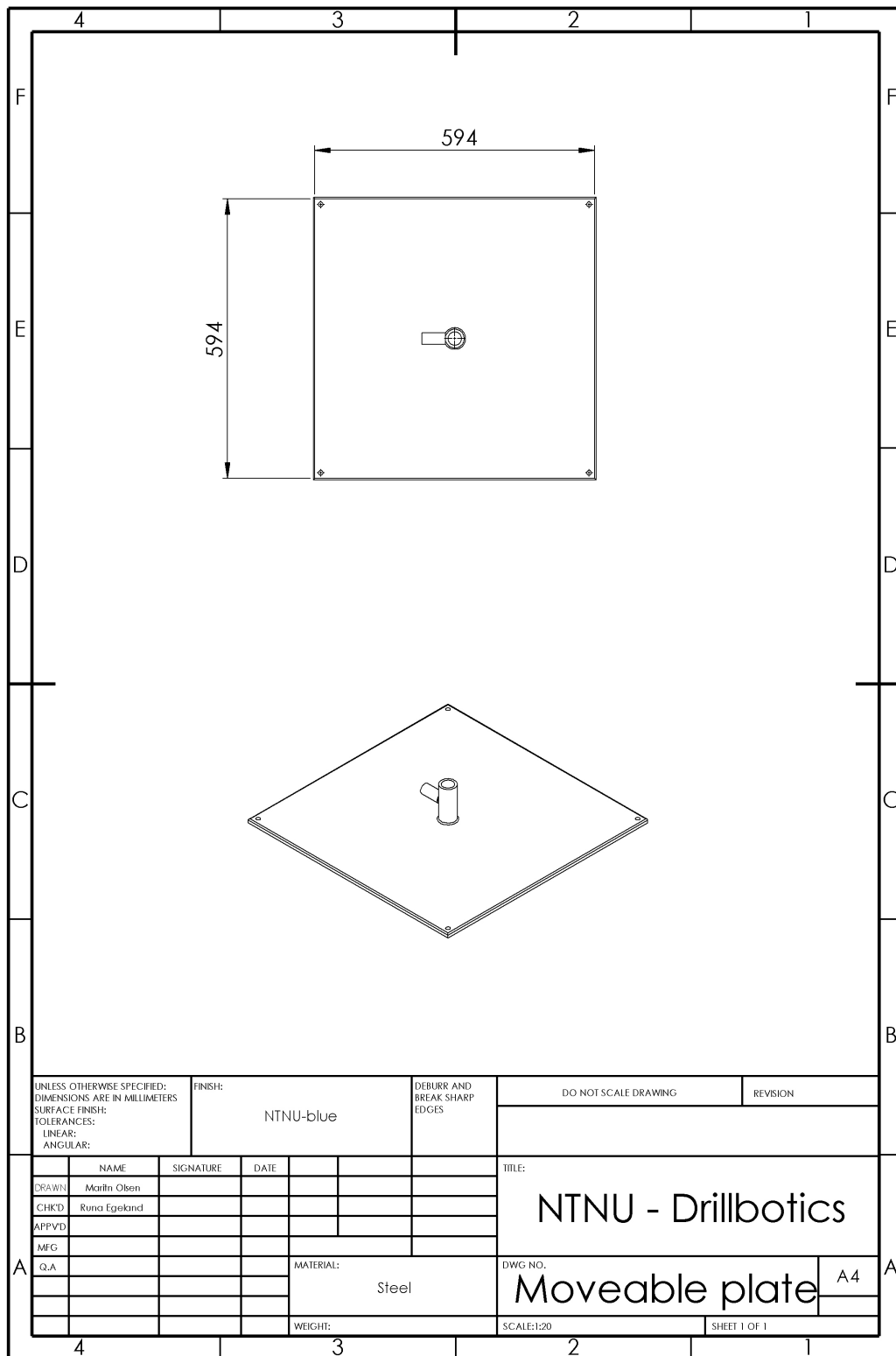


Figure B.7.4: Moveable plate with riser. All dimensions in mm.

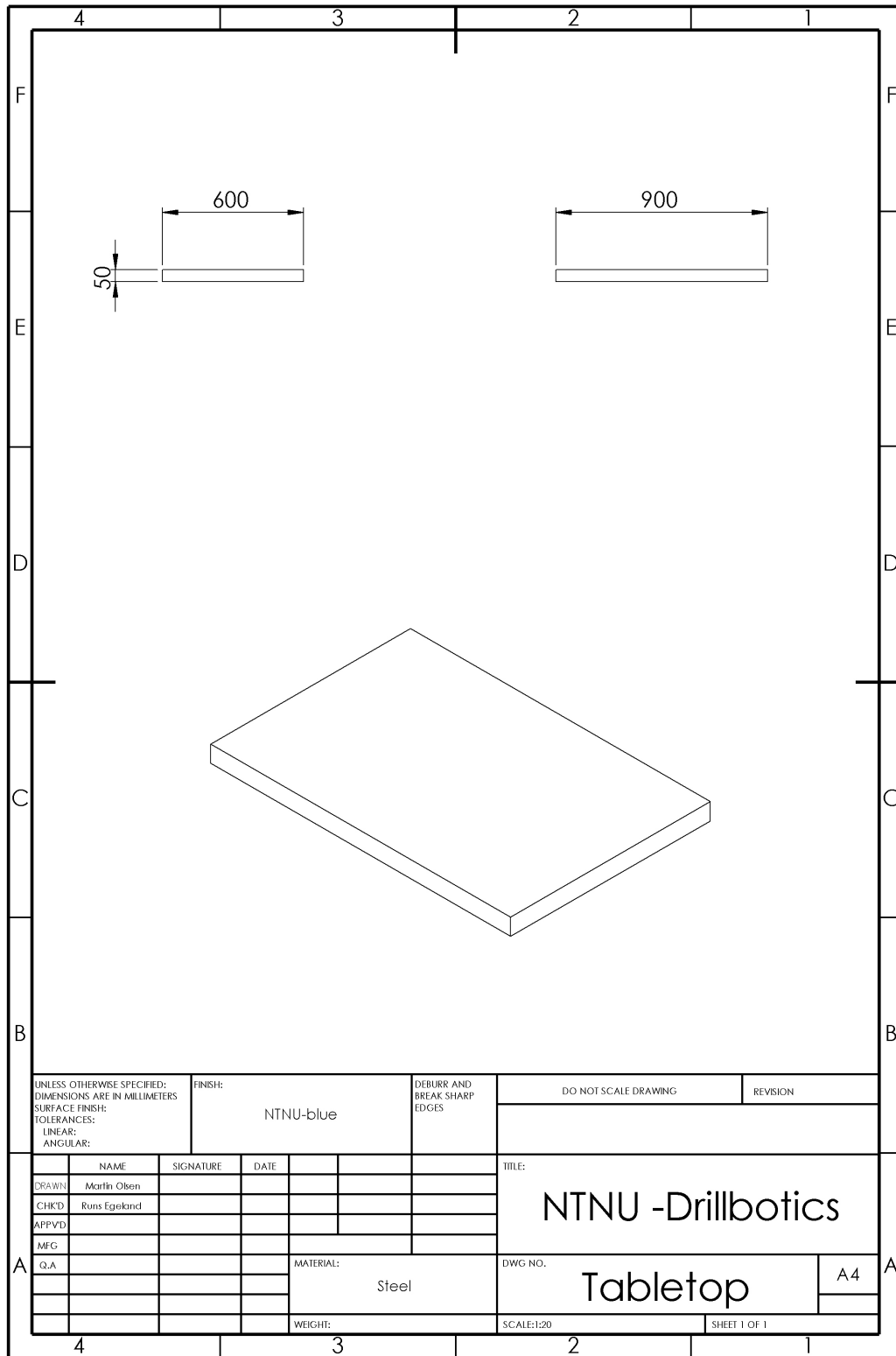


Figure B.7.5: Tabletop. All dimensions in mm.

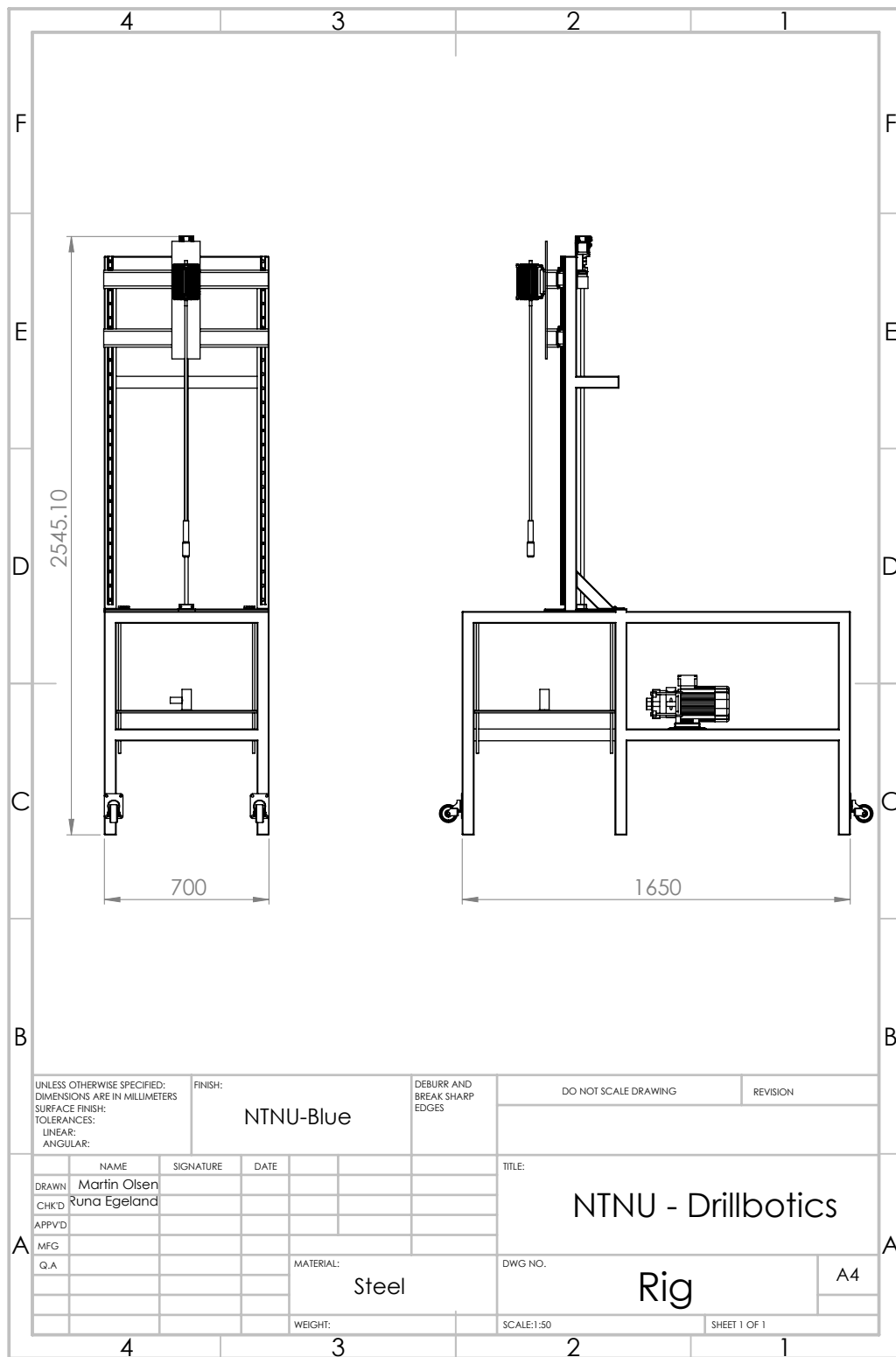


Figure B.7.6: Rig viewed from front and side. All dimensions in mm.

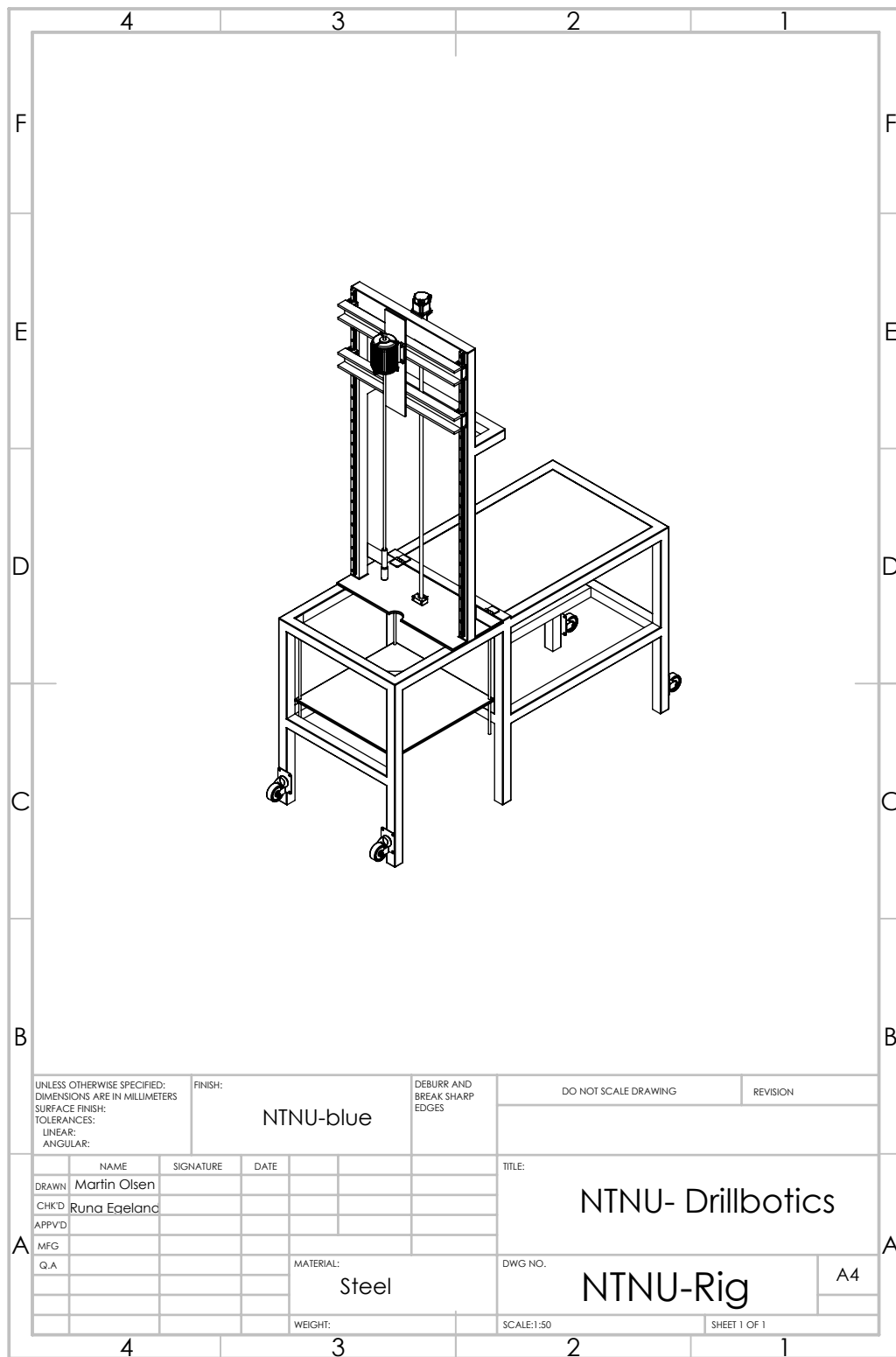


Figure B.7.7: Assembled rig.

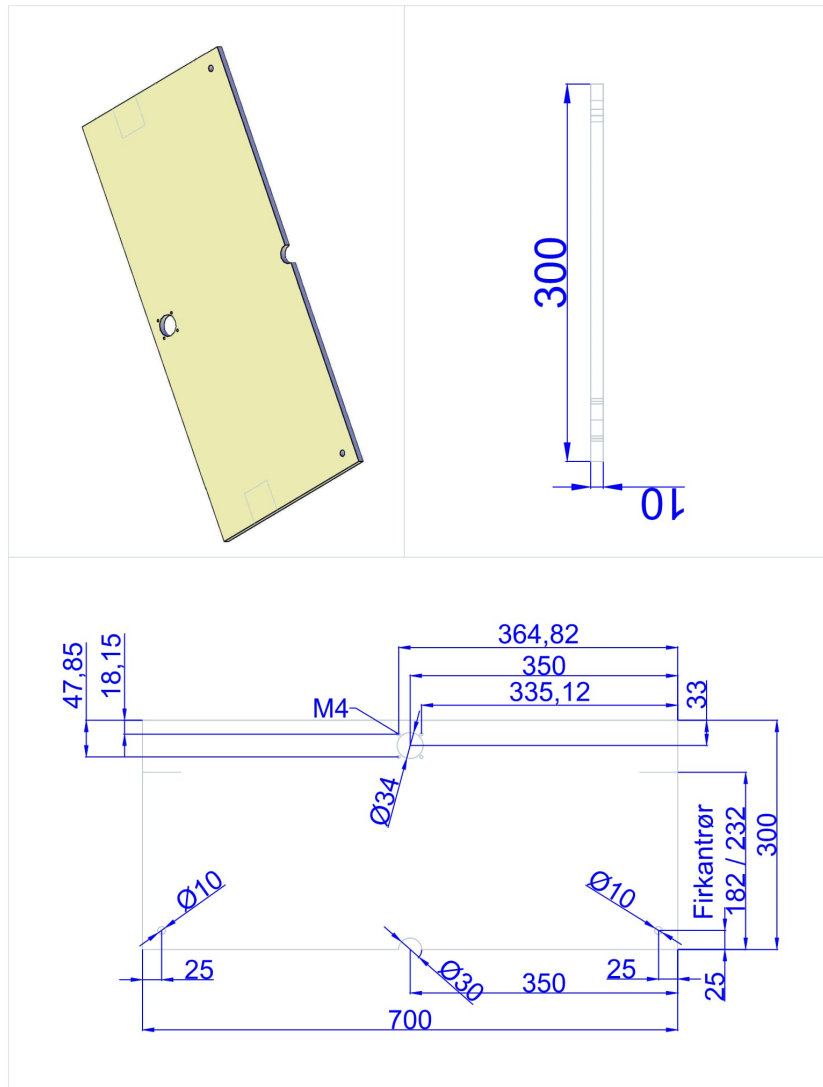


Figure B.7.8: Drilldeck.

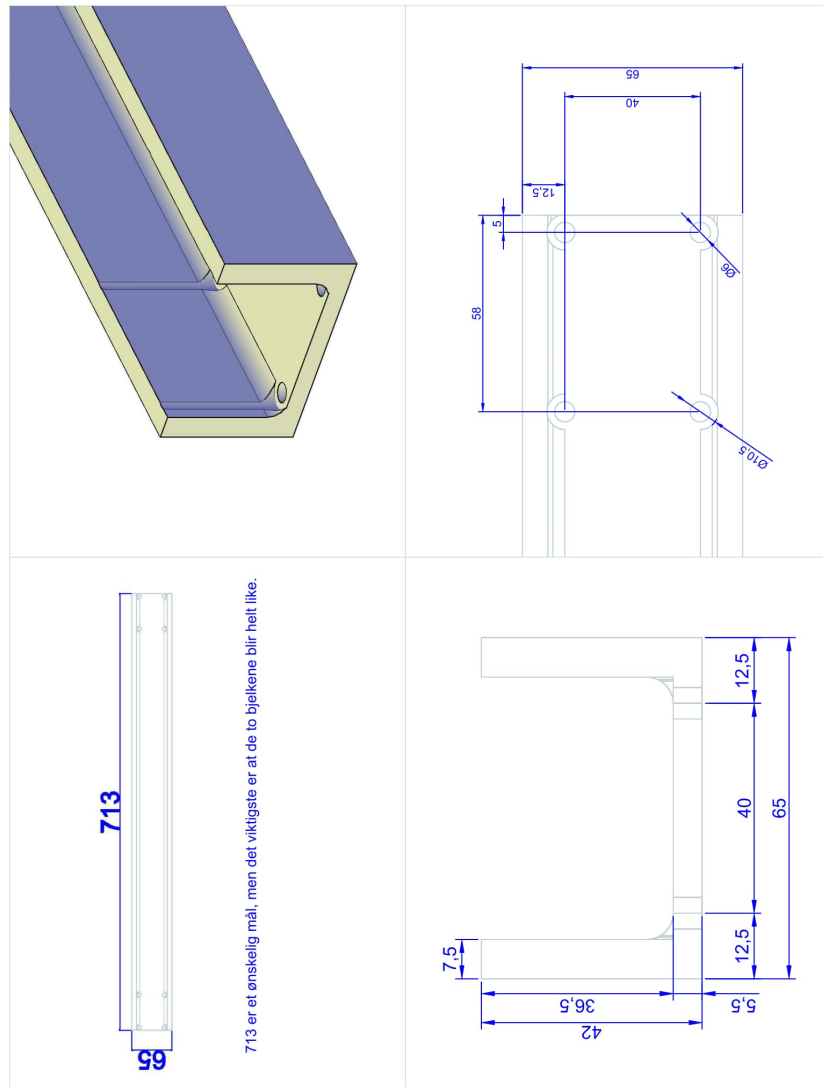


Figure B.7.9: Strut for carriage.

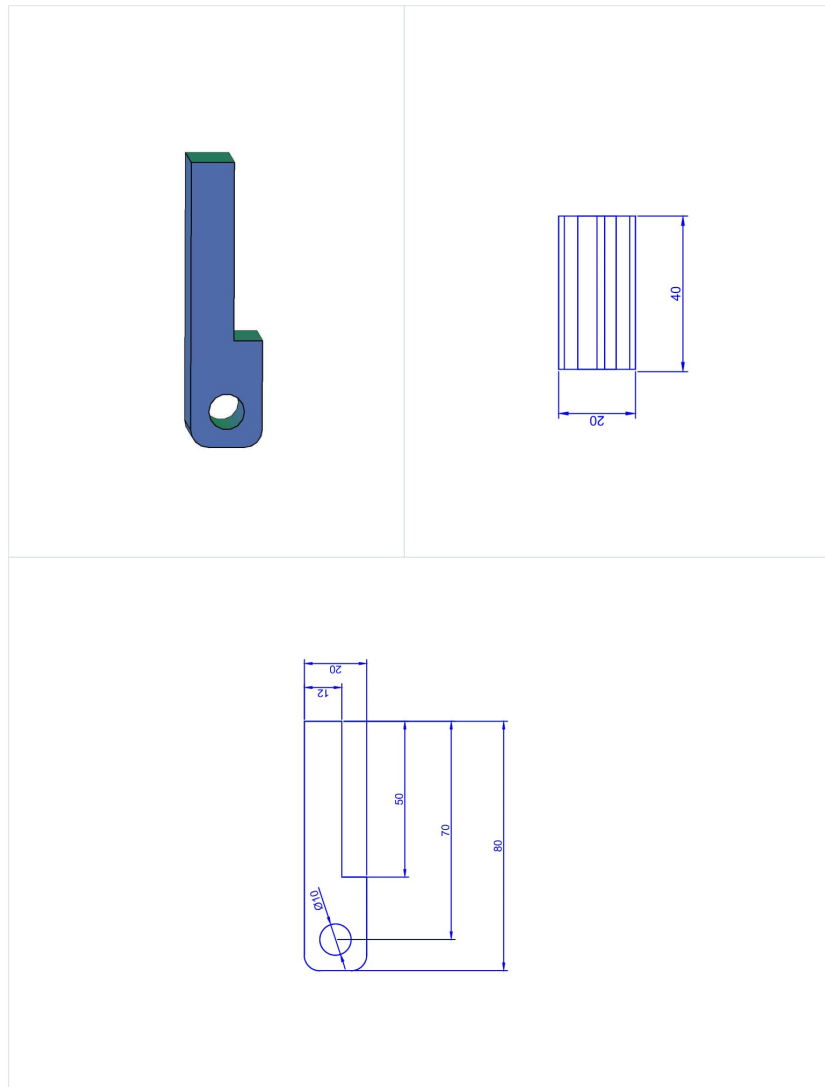


Figure B.7.10: Hinge part 1.

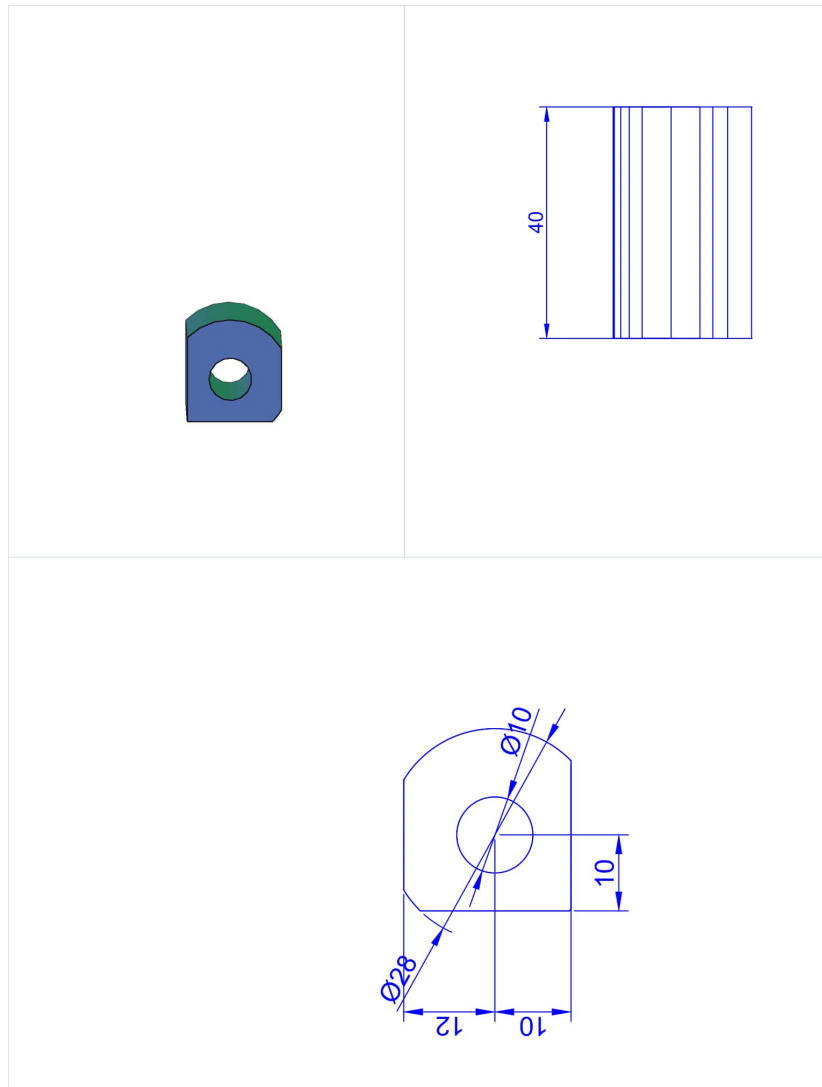


Figure B.7.11: Hinge part 2.

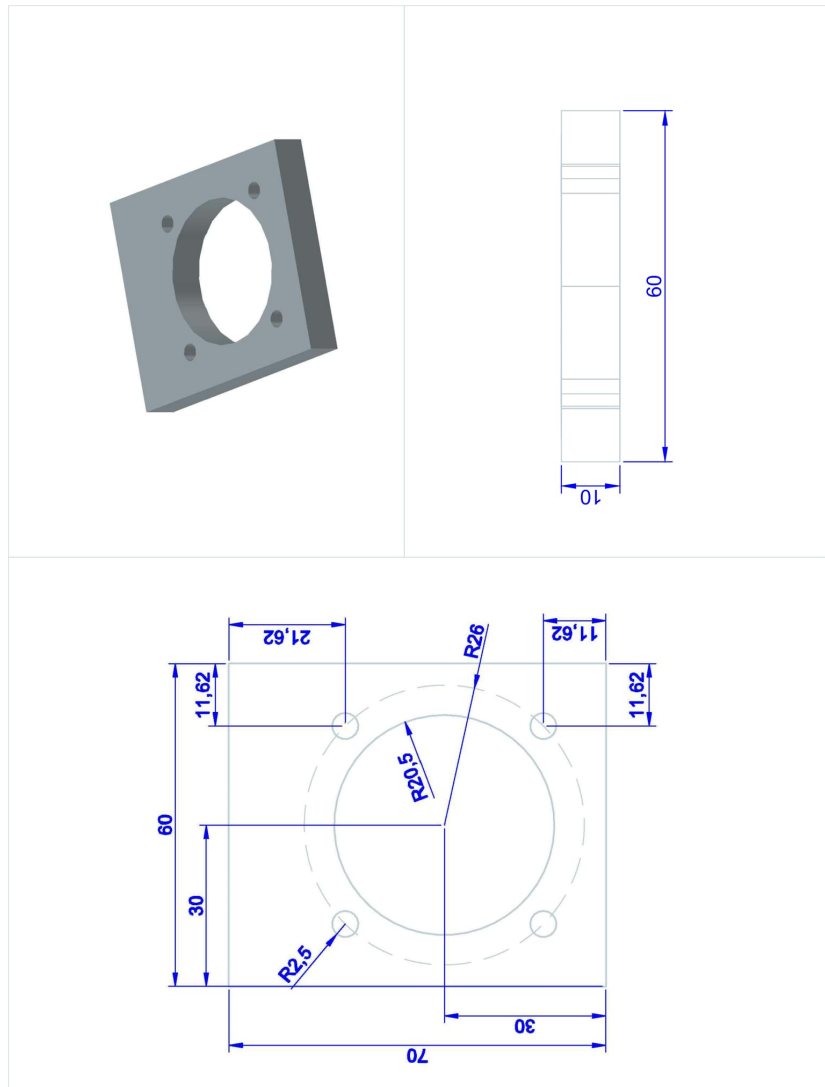


Figure B.7.12: Top mount for hoisting motor.

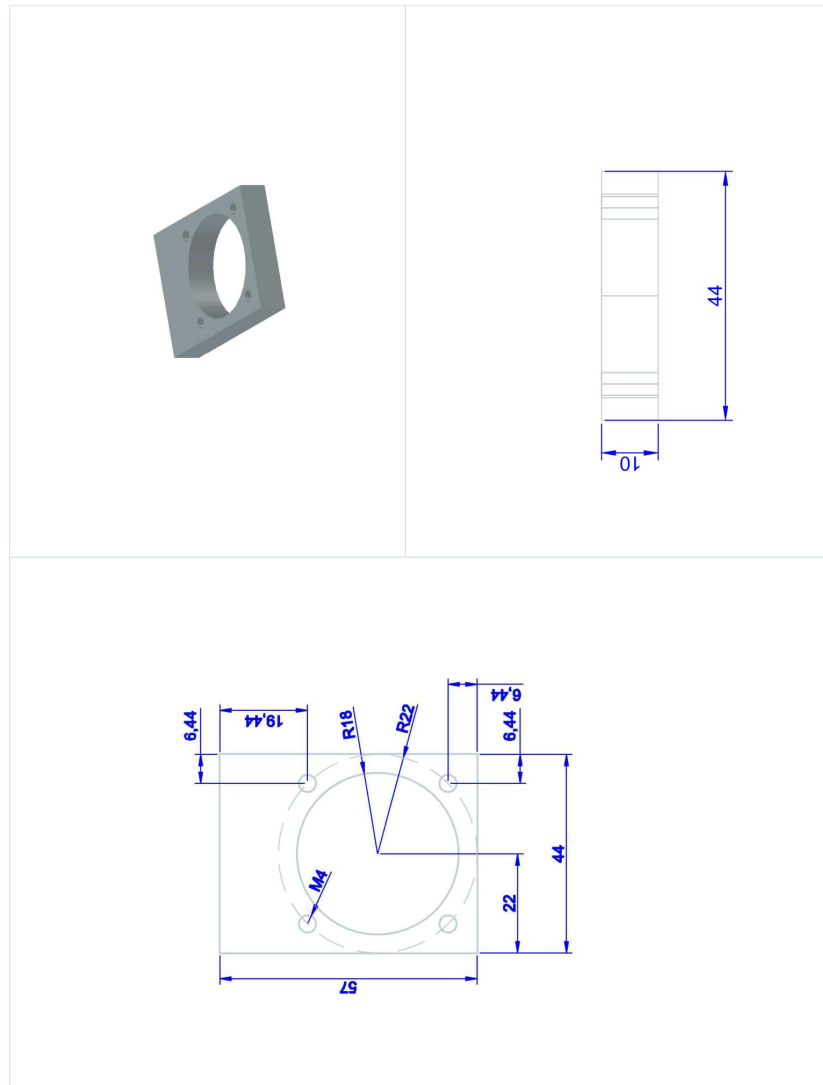


Figure B.7.13: Bottom mount for hoisting motor.

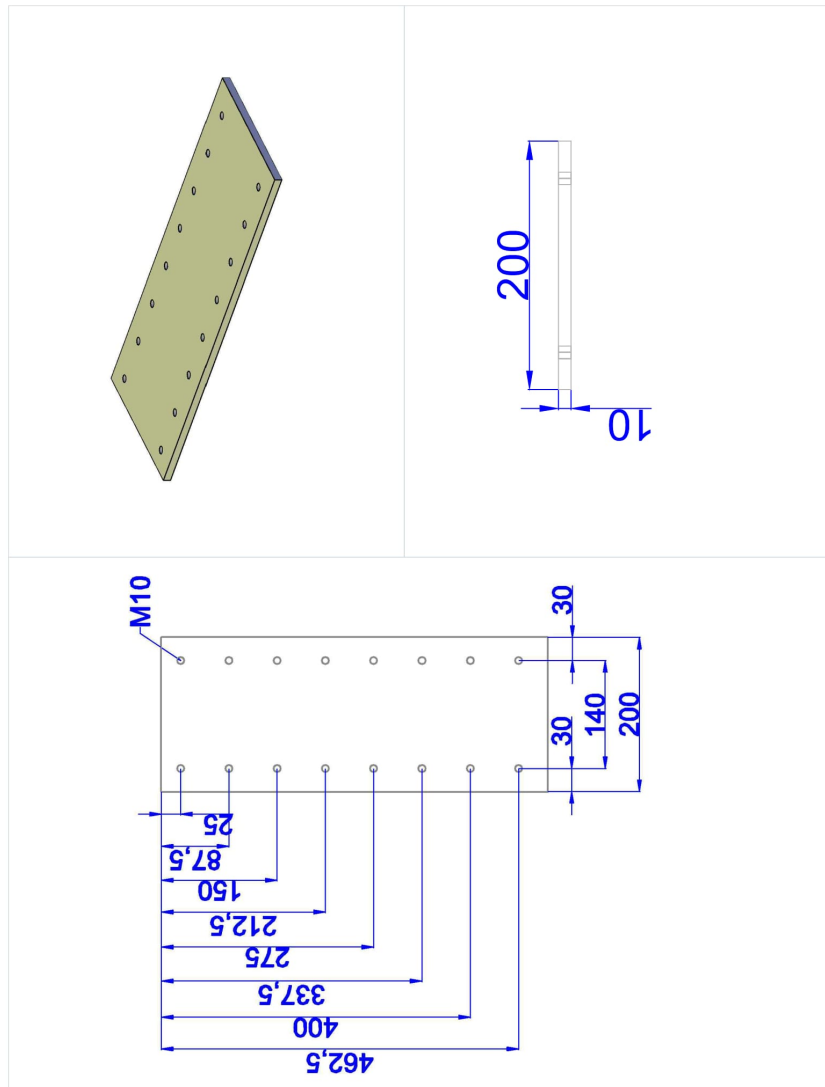


Figure B.7.14: Carriage mount for top drive motor.

Automation

C.1 Control System Architecture

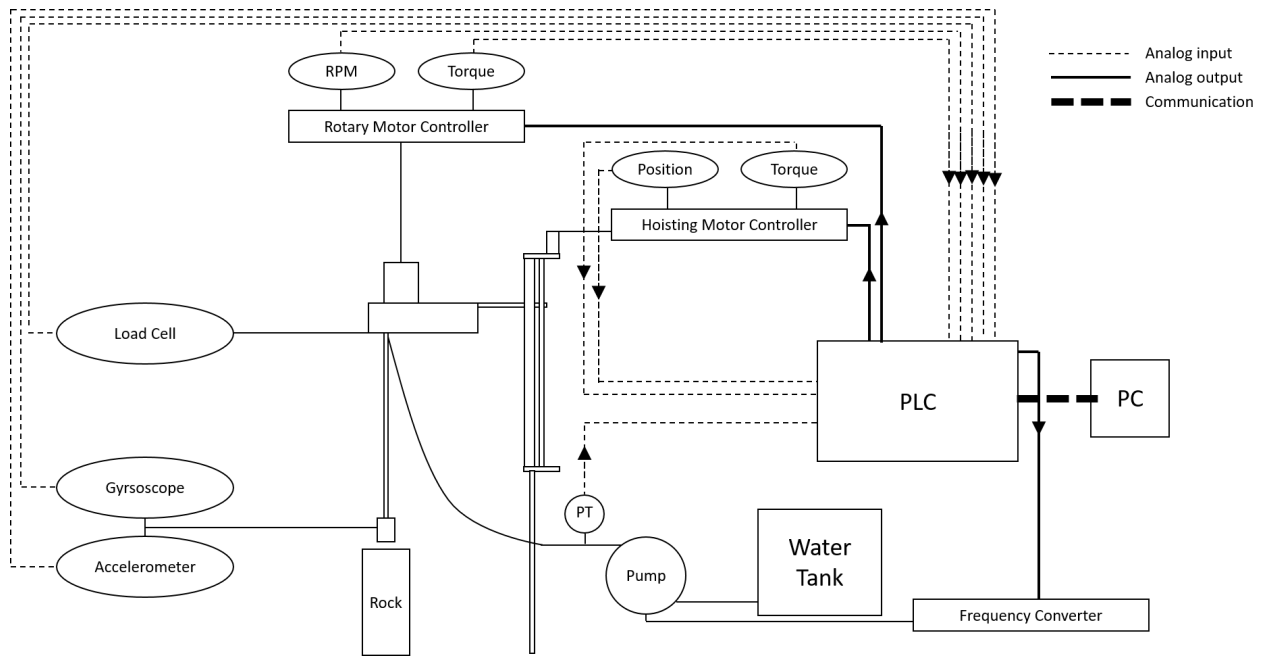


Figure C.1.1: Control system.

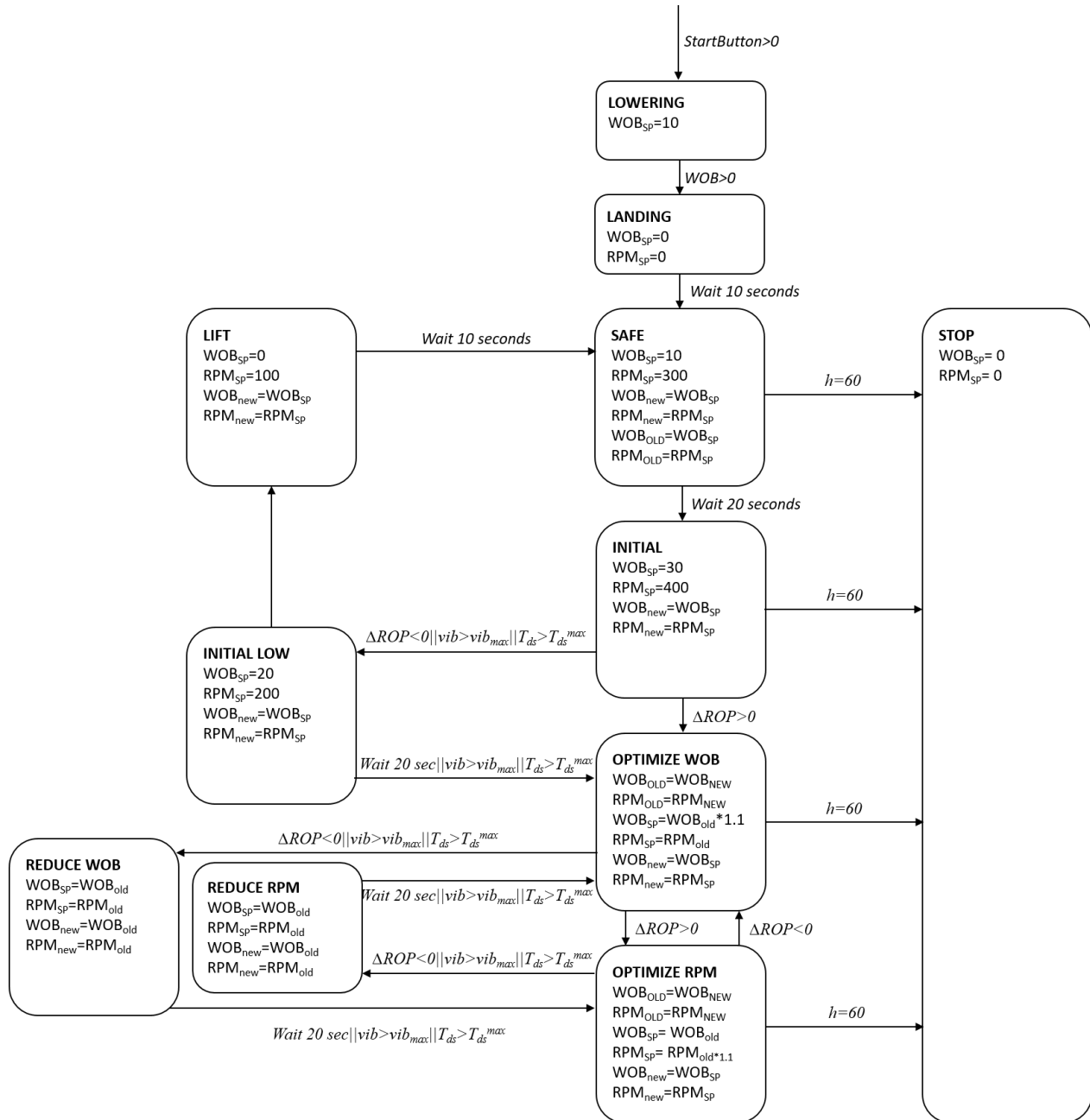


Figure C.1.2: Drilling algorithm.

Testing

D.1 Factory-Acceptance-Testing

FAT – Factory acceptance test

The main objective of a factory acceptance test (FAT) is to test the safety instrumented system, where the logic solver and associated software are being tested together. The test is used to verify the functionality of the system, where the goal is to make sure that the equipment is working as it should and that it delivers what is needed for the subsequent use for drilling with automatic control. It is a procedure that is normally executed during the final part of the design and engineering phase before the final installation at the plant.

The whole point is to check everything that you would need in the operation and to do that in tests that, if failed, would uniquely identify the problem. (some tests may involve several functionalities acting together and due to that, if the test is failed, it is not clear which functionality caused it).

During the FAT, it is checked as far as possible that:

1. When the system is powered on, the equipment does not give any errors.
2. Sensors: The sensor signals received, displayed and logged by Simulink are observed physically and checked that they are in accordance with the reality. Check that the signals are not too noisy, as it may be an indication of a connection problem or some external distortion.
 - a. Pressure transducer: Pump is powered on, check readings from pressure transducer.
 - b. Load cell: Hoisting motor is powered on, supplying weight on bit, check readings from load cell.
 - c. Gyroscope and accelerometer: Top drive motor is powered on, supplying rotation of the drill string, check readings from downhole sensor.
3. Actuators: A set-point for a motor (hoisting, top drive or pump) is set to a certain value (torque or RPM) in Simulink. Observe physically that there is a corresponding change in the motor and that their operation, according to the received sensor data in Simulink is according to the set-point.
4. Accuracy: Check that the torque/RPM control is accurate. Set different set-points and observe that the motor follows that set-point.
5. Safety system: Check that when the rig goes out of its safe operational range (e.g. max torque, max/min values for position, etc.) that the safety system stops the operation to prevent the operation.
6. Emergency stop: Check the functionality of the emergency stop button.
7. Operating range: Check that the hoisting system can move freely within its operating range (max/min position).

FAT – Factory Acceptance Test

Test number	Name	Description/Desired outcome	Outcome: OK/not OK, comments
START1	Power on	The equipment is powered on (in certain sequence – to be specified). Equipment is ready, no errors.	Ok/not OK
S1PT	Sensor: Pressure Transducer	Pump is powered on and fluid is circulating at a certain flow rate. Check that readings from pressure transducer are realistic based on pump speed.	
S1LC	Sensor: Load Cell	Hoisting motor is powered on, torque/RPM is increased and carriage is moving downwards applying weight on bit. Check that readings from load cell are realistic based on torque/RPM.	
S1GA	Sensor: Gyroscope and Accelerometer	Top drive motor is powered on, torque/RPM is increased and the drill string is rotating. Check that readings from gyroscope and accelerometer are realistic based on torque/RPM.	
HM1	Actuator: Hoisting motor	Hoisting motor drive is in torque control mode. Set the hoisting motor torque set-point in Simulink to NN and observe that physical movement of the carriage has started. Observe that the hoisting motor rotation measurements (RPM and Torque) are received in Simulink. Observe that the torque/RPM measurement corresponds to the set-point.	
HM2	Hoisting motor control accuracy	Conditions as in HM1, change the set-point for torque in steps (specify concrete steps). Observe that the motor follows these steps.	
HM3	Hoisting motor safety check	Conditions as in HM1. Lower safety limit to below set-point. Check that the safety system stops the operation to prevent the operation.	
HM4	Hoisting motor operating range	Start hoisting motor and set torque/RPM set-point to NN. Check that the carriage stops before the end of the rails (needs to start slowing down before it reaches the end)	
TD1	Actuator: Top drive motor	Drillstring motor drive is in torque control mode. Set the top drive motor torque set-point in Simulink to NN and observe that physical rotation has started. Observe that the drillstring rotation measurements (RPM and Torque) are received in Simulink. Observe that the torque/RPM measurement corresponds to the set-point.	

D.2 Rock Samples use for Testing

In an early stage of phase II, it was planned what kind of tests that should be performed by the drilling rig as soon as it was fully built. It was consider a series of tests in order to test both the drilling rig and the control system to the optimum. In the DrillboticsTM competition, there will be handed a box consisting layers of random rocks with different characteristics. This is mentioned in both the guidelines and reports from previous years. To be prepared for this, it was concluded the drill rig and the control system should be tested with a big variety of different types of rocks. Rock samples with different grain size, cementation and hardness, from chalk, in the soft end and marble in the other end, and a fair amount of variety in the middle were chosen. It was also collected or made rock samples to simulate different types of drilling dysfunctions, such stick-slip, axial vibrations, etc. When discussing with the supervisors, it was concluded that buying different types of rock samples was not the cheapest alternative. Some of the rock samples were hard to get hold of and expensive as well. A cheaper solution were consider, so the projects budget was not exceeded. Professor Allen George Krill from the institute of geoscience and petroleum at NTNU was contacted, and he gave a lot of pointers were it might be a good idea to start. After contacting professor Krill, mails were sent to the different places and phone calls were made. Most of the places were more than happy to help us with the project and invited the team over whenever it suited us. The first visit went to Nidaros Domkirke Restaureringsarbeider, not that far away from Nidaros Cathedral. At this place, they had many leftovers from failed projects, and they were more than happy to give it away. Rock samples such as marble, granite and different types of clay stones were collected from this place.



Figure D.2.1: Picture of the collected rock samples from Nidaros Domkirke Restaureringsarbeider. A mix of marble, granite and different types of clay stones.

From the meeting with the supervisors, it was concluded that sandstone was too expensive to buy and a cheaper solution were planned. The plan was to make homemade sandstone, buy mixing cement and sand. Sandtak Tiller was contacted and they helped with the supply of sand. Different types of sand and grain size was collected, so it could be made sandstone with different types of properties. Later on a form made of table top was build, this form consisted of 6 smaller forms in a dimension of 30cm x 30cm x 10cm. A mixture containing cement, sand and water was poured into the forms. Each one of the smaller forms had plastic bag attached to the bottom, so the mixture would not leak. A vibrator was used to vibrate the air out of the mixture, after this the mixture was ready to solidify. A mixture of cement, water and variety of gain size was also made. This was a simple imitation of conglomerate and was mainly made to simulate drilling dysfunctions, such as vibration in the drill string.



Figure D.2.2: Picture of a homemade "sandstone" in the making. The mixture of sand, water and cement is poured into the forms and is ready to solidify.



Figure D.2.3: Picture of the finished product. Some of the rock samples were sawed, so it could be easier to study the distribution of the sand and the cement within the rock samples.

Professor Krill pointed out black shale (sorte skifer) from a breakage in Laanke in north Stjordal. Black shale is a sedimentary rock who may have similar composition and properties as in sedimentary rocks in an oil reservoir. There were also collected a rock made of shale with finer gains at the top, quartz in the middle and shale with coarser gains at the bottom. This rock was a perfect test for the control system.



Figure D.2.4: Picture of black shale collected in Laanke in north Stjordal.



Figure D.2.5: Picture of the rock sample made of shale with finer grain in the upper part, quartz in the middle and shale with coarser gains at the lower part.


The institute leader of geoscience and petroleum, Egil Tjaaland was contacted and he mentioned they had some left over rock samples from previous lab experiments that could be used in the project. This was forward to Jorn Stenebraaten at SINTEF and he supplied different types of rock samples such as, marble, dolomite, chalk and different types of sandstones.




Figure D.2.6: Picture of the rock samples provided by SINTEF. Marble in the right, two different types of sandstones in the middle and and dolomite in the left.

Competition

E.1 Drillbotics™ Guidelines



Society of Petroleum Engineers
Drilling Systems Automation
Technical Section (DSATS)



Drillbotics™ Guidelines
International University Competition
2016 - 2017

1. Introduction

This year marks the third competition for the title of Drillbotics champion and a chance for sponsored travel to present a paper at the next SPE Annual Technical Conference and Exposition (ATCE) at an event organized by DSATS. The past two years involved undergraduates, masters and doctoral students from a variety of disciplines who built innovative drilling machines and downhole tools while developing a deeper understanding of automating the drilling process. Everyone involved claims to have had a lot of fun while learning things that are not in the textbooks. This year's contest promises to be more challenging and hopefully more fun.

How did the competition first come about? The origins began in 2008 when a number of SPE members established the Drilling Systems Automation Technical Section (DSATS) to help accelerate the uptake of automation in the drilling industry. DSATS' goal was to link the surface machines with downhole machines, tools and measurements in drilling systems automation (DSA), thereby improving drilling safety and efficiency. Later, at an SPE Forum in Paris, the idea of a student competition began to take shape. A DSATS sub-committee was formed to further develop the competition format and guidelines. Several universities were polled to find out the ability of academic institutions to create and manage multi-disciplinary teams. The Drillbotics committee began small in 2014-2015 to see if the format could succeed. With fine tuning, we continue along those lines as we start the 2017 process.

The DSATS technical section believes that this challenge benefits students in several ways. Petroleum, mechanical, electrical or control engineers, gain hands-on experience in each person's area of expertise that forms a solid foundation for post-graduate careers. They also develop experience working in multi-disciplinary teams, which is so important in today's technology driven industries. Winning teams must possess a variety of skills. The mechanical and electrical engineers need to build a stable, reliable and functional drilling rig. Control engineers need to architect a system for real-time control, including selection of sensors, data handling and fast-acting control algorithms. The petroleum engineers need an understanding drilling dysfunctions and mitigation techniques. Everyone must work collectively to establish system functional requirements understood by each team member, properly model the drilling issues, and then to create a complete package working seamlessly together.

The oil and gas industry today seeks lower costs through efficiency and innovation. Many of the student competitors may discover innovative tools and control processes that will assist drillers to speed the time to drill and complete a well. This includes more than faster ROP, such as problem avoidance for dysfunctions like excessive vibrations, stuck pipe, and wellbore stability issues. Student teams built new downhole tools using 3D printing techniques of designs that would be difficult, if not impossible to machine. They used creative hoisting and lowering systems. Teams modeled drilling performance in particular formations and adjusted the drilling parameters accordingly for changing downhole conditions. While they have a lot to learn yet about our business, we have a lot to learn about their fresh approach to today's problems.

Good Luck!
From the DSATS Drillbotics Committee

Fred Florence (Chairperson)
Miguel Armenta
Mark Hutchinson
Aaron Logan
Nii Nunoo
Neil Panchal
Veronica Simmonds
Suresh Venugopal

Contents

1.	Introduction.....	1
2.	<i>Objectives for the 2016 Competition</i>	4
3.	<i>Background</i>	4
4.	<i>Competition Guidelines</i>	5
4.1.	Problem statement for the 2016-2017 competition:	5
4.2.	Two Project Phases	5
4.3.	Phase I – Design Competition	6
4.4.	Phase II – Drilling Competition	7
4.5.	Rock Samples	7
4.6.	Bits	8
4.7.	Drillpipe.....	10
4.8.	Tool joints	11
4.9.	Bit sub/drill collar/stabilizers	11
4.10.	Automated Drilling.....	12
4.11.	Sensors.....	12
4.12.	Data collection and handling	12
4.13.	Data visualization	12
4.14.	Measure and analyze the performance.....	13
4.15.	The test well.....	13
4.16.	Not included in the 2016-2017 competition	14
4.17.	Presentation to judges at Phase II Testing.....	14
4.18.	Project report.....	14
4.19.	Final report and paper	15
5.	<i>Team Members</i>	16
6.	<i>Expenditures</i>	16
7.	<i>Other Considerations</i>	17
8.	<i>Project Timeline</i>	17
9.	<i>Evaluation Committee</i>	19
10.	<i>Prizes</i>	20
11.	<i>Terms and conditions</i>	21
12.	<i>Marketing</i>	21

2. Objectives for the 2016 Competition

- 2.1. During the school year beginning in the fall of 2016, a team of students will organize themselves to solve a drilling related problem outlined in item 4 below. The team should preferably be a multi-disciplinary team that will bring unique skills to the group to allow them to design and construct hardware and software to demonstrate that they understand the underlying physics, the drilling issues and the usual means to mitigate the issues. We cannot stress enough the need to involve students with different technical training and backgrounds. They will need to develop skills to understand drilling dysfunctions and mitigation strategies, but they must also have the mechanical engineering capabilities to design the rig/drilling package. In past years, some entrants have not adequately considered the control network and algorithms needed for autonomous drilling. They have often misunderstood the need for calibrated sensors and fast, accurate data handling. All of this and more is needed to build and operate a complete automated drilling system.
- 2.2. The students could produce novel ideas leading to new drilling models, improved drilling machines and sensors, and the ability to integrate the data, models and machines that will hopefully create new, more efficient ways to drill wells in the future. Any such innovation will belong to the students and their university in accordance with the university's written policies.
- 2.3. The students, working as a multi-disciplinary team, will gain hands-on experience that will be directly applicable to a career in the upstream drilling industry.

3. Background

- 3.1. What is DSATS?
 - 3.1.1. DSATS is a technical section of the Society of Petroleum Engineers (SPE) organized to promote the adoption of automation techniques using surface and downhole machines and instrumentation to improve the safety and efficiency of the drilling process. More information is available about DSATS at the DSATS homepage (<http://connect.spe.org/DSATS/Home/>).
 - 3.1.2. The Drillbotics website at www.Drillbotics.com includes official updates to the competition guidelines and schedule, as well as FAQs, photos, and previous entrants' submittals and reports. Questions and suggestions can be posted here, or teams can email the sub-committee at 2017@Drillbotics.com.
- 3.2. Why an international competition?
 - 3.2.1. DSATS, as part of the SPE, is a group of volunteers from many nations, connected by their belief that drilling automation will have a long-term, positive influence on the

drilling industry. This diversity helped to shape the direction of the organization. The group feels that the industry needs to attract young professionals from all cultures and disciplines to advance drilling practices in all areas of the world. The winners of the competition will receive a grant for economy class transportation and accommodations to attend the next SPE Annual Technical Conference and Exhibition and will present an SPE paper that will be added to the SPE archives of One Petro¹. Additional teams may have an opportunity to present their work at the DSATS automation symposium preceding the conference, and may receive a grant for economy class transportation and accommodations². DSATS believes recognition at one of the industry's leading technical conferences will help encourage student participation. Also, the practical experience with drilling automation systems increases the students' visibility to the companies that are leading automation activities.

4. *Competition Guidelines*

4.1. *Problem statement for the 2016-2017 competition:*

Design a rig and related equipment to autonomously drill a vertical well as quickly as possible while maintaining borehole quality and integrity of the drilling rig and drillstring.

4.2. *Two Project Phases*

Fall Semester 2016

The first phase of the project is to organize a team to design an automatic drilling machine to solve the project problem. It is not necessary to build any equipment in this phase, but it is okay to do so. Design considerations should include current industry practices and the team should evaluate the advantages and shortcomings of today's devices. The design effort may be assisted by university faculty, but the students are encouraged to introduce novel designs for consideration. The level of student, faculty and technical staff involvement shall be reported when submitting the design.

Spring Semester 2017

During the second phase, the finalist teams selected by DSATS to proceed to the construction and drilling operation will use the previous semester's design to build an automated drilling machine. As per industry practices, it is common during

¹ Publication is subject to the ATCE program committee's acceptance of the abstract/paper.

² Subject to approval of the DSATS Board of Directors and organizers of the symposium.

construction and initial operations to run into problems that require a re-design. The team may change the design as needed in order to solve the problem.

4.2.1. Teams may use all or part of a previous year's rig.

4.3. Phase I – Design Competition

Design an automated drilling machine in accordance with the rules below.

4.3.1. DSATS envisions a small (perhaps 2 meters high) drilling machine that can physically imitate the functionality of full-scale rig machinery. The machine will be the property of the university and can be used in future research and competitions. New and novel approaches that improve on existing industry designs are preferred. While innovative designs are welcome, they should have a practical application to drilling for oil and gas.

4.3.2. The drilling machine will use electrical power from the local grid not to exceed 25 horsepower. Lower power consumption resulting from energy efficient designs will receive additional consideration.

4.3.3. The design must provide an accurate and continuous measurement of Weight-On-Bit (WOB) and other drilling parameters, as well as a digital record across the period of the test.

4.3.4. The proposed design must be offered in Phase I of the project, but changes are allowed in Phase II, as long as they are reported to the Committee via students' monthly reports. A summary of all significant changes, including the reason modifications were necessary, must be included in the students' final report.

4.3.5. Design submittal by the students shall include:

- 4.3.5.1. Engineering drawings of the rig concept, mechanical and electrical and auxiliary systems, if any
- 4.3.5.2. Design notes and calculations
- 4.3.5.3. Control system architecture. (The response time of measurements, data aggregation and control algorithms should be estimated.)
- 4.3.5.4. Key features for any models and control software
- 4.3.5.5. Proposed data handling and display
- 4.3.5.6. Specification for sensors and instrumentation, including the methods planned for calibration before and after the Phase II testing.
- 4.3.5.7. Plan for instrumentation of sensors in the BHA, as well as a method to utilize these sensors for real-time control of the drilling process.
- 4.3.5.8. An explanation of the implementation of the output of the BHA sensors to improve the trajectory of the wellbore and other drilling concerns.

- 4.3.5.9. Cost estimate and funding plan
- 4.3.5.10. A design summary video used to outline the design submittal not to exceed five (5) minutes in length. Videos shall be the property of the university, but DSATS shall have the rights to use the videos on its websites and in its meetings.
- 4.3.5.11. All design, construction and operation of the project are subject to the terms and conditions of section 11.
- 4.3.5.12. A safety case shall be part of the Phase I design. Include a review of potential hazards during the planned construction and operation of the rig, and for the unloading and handling of any rock samples or other heavy items.
- 4.3.6. A committee of DSATS members (the Committee) will review the Phase I designs and select the top five (5) teams³ who will progress to Phase II of the competition.
- 4.3.7. DSATS shall also award a certificate of recognition and publication on its website for the most innovative design. The design video will also be shown at the DSATS automation symposium at the ATCE.
- 4.3.8. DSATS will not fund any equipment, tools, software or other material, including labor, for the construction of the rig.

4.4. Phase II – Drilling Competition

- 4.4.1. In the spring term of 2017, qualifying teams will build the rig and use it to drill rock samples provided by DSATS. Drilling a vertical well efficiently though the sample while controlling drilling dysfunctions is the primary technical objective of the competition. The use of downhole measurements to control the drilling process in real-time is mandatory.
- 4.4.2. Once drilling commences, the test will continue until the depth reaches the bottom or the rock sample or two (2) hours, whichever comes first.
- 4.4.3. Drilling performance will be observed and measured by DSATS members invited to attend and witness.
- 4.4.4. DSATS will survey the completed wellbore and compare their survey with that of the students' downhole measurements.
- 4.4.5. The final test will be scheduled late in the school year or soon after graduation. The test will occur at the participating university in accordance with the timeline per section 8 below.

4.5. Rock Samples

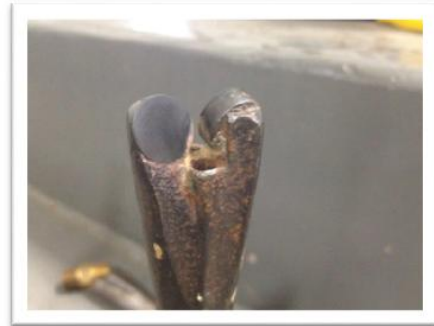
³ The number of finalists could be increased or decreased by the DSATS Board of Directors subject to available funding.

- 4.5.1.1. DSATS will prepare a set of nearly identical samples (appx. 12"W x 12"L x 24"H (30 x 30 x 60 cm) that will be packaged in a crate and shipped to each of the teams that qualified for the actual drilling test. The crates shall not be opened or tampered with, as the rock and formations shall remain unknown until after the test.
- 4.5.1.2. The rock sample will be a manufactured using cement, varying soil samples and perhaps some materials that are not typically encountered during regular drilling, but will imitate unusual downhole conditions experienced in some drilling programs. All simulated formations may not be parallel to each other (e.g. formation dip).
- 4.5.1.3. The university and/or students may acquire or produce rock samples as needed to verify the design and allow students to practice using their machine prior to the test. Drilling of the samples provided by DSATS prior to Phase II testing is not allowed and could lead to disqualification.

4.6. Bits

- 4.6.1. DSATS will send a drillstring and bit to the finalist teams for use in Phase II. It is expected that the BHA and pipe will cause some difficulty, both for causing drilling dysfunction and for sensor integration and data telemetry. The judges will look for creative concepts supported by sound reasoning showing an understanding of how the BHA, bit and drillstring function together, and how the downhole system measures, samples and truncates the drilling data.
- 4.6.2. Upon request, the bit shall be returned to the Committee following Phase II testing for reconditioning for use in future competitions.
- 4.6.3. One (1) bit, roller cone or PDC, will be provided by DSATS to be used during the Phase II tests. For 2016-2017 the bit will be:
 - 4.6.3.1. PDC micro-bit will be 1.125" in (28.6 mm) diameter, with brazed cutters and two nozzles.
 - 4.6.3.2. Cutter backrake is 20 degrees; Cutter diameter is 0.529 inches
 - 4.6.3.3. Nozzles are 2.35mm diameter, two each at approximately 180 degrees.
- 4.6.4. Students are encouraged to consider bit wear prior to the final test and its impact on drilling performance during the onsite testing.
- 4.6.5. Student teams may build or buy similar drill bits to test their design with the rock samples they sourced.

4.6.6. Students are also allowed to design and use their own bits for the Phase II on-dite test, within the dimensional limits of 4.6.2.1 above.



4.7. Drillpipe

4.7.1. The drill string provided by DSATS will be chosen to ensure drilling dysfunctions will be encountered. How these dysfunctions are mitigated is a key objective of the competition. Final details of the construction of this drill string will be furnished in late fall of 2016 to all entrants upon request. Preliminary specifications are listed below to assist with the mechanical and electrical design of the rig.

4.7.2. The drill pipe specifications for the 2016-2017 competition are subject to change, but should be:

4.7.2.1. Round Aluminum Tube 3/8 inch diameter x 36 inches long; 0.016 inch wall or equivalent

4.7.2.2. DSATS will provide the finalists four (4) joints of pipe. Any additional pipe needed can be purchased by the student teams or university if needed.

4.7.2.3. Tubing is usually available from various hobby shops such as K-S Hobby and Craft Metal Tubing and via Amazon and other suppliers.
<http://www.hobbylinc.com/htm/k+s/k+s9409.htm>

ROUND ALUMINUM TUBING		
OUTSIDE DIAMETER INCHES	WALL THICKNESS	ID
3/64 (.047)	.014	.019
1/16 (.0625)	.014	.035
5/64 (.078)	.014	.050
3/32 (.094)	.014	.066
	.016	.062
7/64 (.109)	.014	.081
1/8 (.125)	.014	.097
9/64 (.141)	.014	.113
5/32 (.156)	.014	.128
11/64 (.172)	.014	.144
3/16 (.187)	.014	.159
	.022	.143
	.035	.117
	.049	.089
13/64 (.203)	.014	.175
7/32 (.219)	.014	.191
	.022	.175
	.035	.149
15/64 (.235)	.014	.207
1/4 (.250)	.014	.222
	.016	.218
	.022	.206
	.035	.180
9/32 (.281)	.049	.152
	.014	.253
5/16 (.312)	.016	.249
	.014	.284
	.016	.280
	.035	.242
11/32 (.344)	.049	.214
	.016	.312
3/8 (.375)	.016	.343
	.035	.305
	.049	.277
13/32 (.406)	.016	.374
7/16 (.437)	.016	.405
	.035	.367
15/32 (.468)	.016	.436
1/2 (.500)	.016	.468
	.035	.430
17/32 (.531)	.016	.499
9/16 (.562)	.016	.530
5/8 (.625)	.016	.593

4.8. Tool joints

4.8.1. Students may design their own tool joints as long as the design concept is included in the Phase I proposal.

4.8.2. Alternately, students may use commercially available connectors/fittings attached to the drillpipe using threads, epoxy cement or other material, and/or may use retaining screws if desired, as long as the design concept is included in the Phase I proposal. (A fitting used successfully in 2016 is available from Lenz (<http://lenzinc.com/products/o-ring-seal-hydraulic-tube-fitting/hydraulic-straight-connectors>) uses a split-ring to allow a torque transfer across the fitting.

4.8.3. Students must state WHY they choose a tool joint design in the Phase I proposal.

4.9. Bit sub/drill collar/stabilizers

4.9.1. Upon request, DSATS will provide a bit sub 3/8" NPT box down by 1/4" NPT box up by 3" long. However, it is expected that each team will design and build their own bit sub.

4.9.2. Additional weight may be added to the bit sub provided by DSATS, or surface weight/force (above the rock sample) may be applied to provide weight on bit and drillpipe tension. However, the additional weight shall not directly impose lateral forces to stabilize the drillstring. This weight is meant to add to string tension/compression but shall not improve steering through interaction with the rock.

4.9.3. The student team will be evaluated on how the weight is designed and how it attaches to the drill string. Advise the committee of your choice and why and include this in the Phase I design.

4.9.4. Stabilizers are permitted, but excessive stabilization to stiffen the drillstring to avoid buckling or torsional failure is disallowed. The maximum combined length of stabilizers is 3.5" (8.9 cm). This year's shorter stabilizers should make steering more of a challenge than in previous years. The student team will be evaluated on how the stabilizers are designed and how they attach to the bit sub. Advise the committee of your choice and why and include this in the Phase I design.

4.9.5. Students may add sensors to the drillstring, but are not permitted to instrument the rock samples. The sensors cannot appreciably increase the stiffness of the drillstring or add significant weight (see [4.9.2](#)). They must have a smaller diameter than the stabilizers and bit by at least 10%. Please include design concepts in the Phase I design.

4.9.6. The addition of along-string sensors to measure vibrations, verticality and/or tortuosity or other parameters will receive extra consideration. They must have a smaller diameter than the stabilizers and bit by at least 10%.

4.10. Automated Drilling

4.10.1. Drilling automation should be considered a combination of data, control AND modeling so that the control algorithm can determine how to respond to differences between the expected and actual performance. Process state detection can often enhance automation performance. Refer to documents posted on the DSATS website for more information.

4.10.2. Once drilling of the sample commences, the machine should operate autonomously. Remote operation and/or intervention is not allowed.

4.11. Sensors

4.11.1. The team may elect to use existing oilfield sensors or may look to other industries for alternate sensors.

4.11.2. The team may develop its own sensors if so desired.

4.11.3. Sensor quality differs from data quality. Both are important considerations in this competition.

4.11.4. The final report shall address which sensors were selected and why. The sensor calibration process shall also be explained.

4.12. Data collection and handling

4.12.1. The team may elect to use standard data collection and recording techniques or may develop their own. Data handling techniques and why they were chosen should be described in the Phase I submittal.

4.12.2. The final report shall address which data systems were selected and why.

4.12.3. The observed response time of measurements, data aggregation and control algorithms should be compared to the Phase I estimate.

4.13. Data visualization

4.13.1. Novel ways of presenting the data and progress of drilling in real time while drilling will receive particular attention from the judges.

4.13.2. Visualization of the processes (automation, optimization, drilling state, etc. should be intuitive and easily understood by the judges, who will view this from the perspective of the driller operating a rig equipped with automated controls.

4.13.3. Data must be presented in a format that allows the judges to easily determine bit depth, elapsed drilling time, ROP, MSE, verticality/inclination, vibration, and any other

calculated or measured variable used to outline the drilling rigs performance to the judges. Lack of an appealing and usable Graphic User Interface (GUI) will be noted to the detriment of the team.

4.13.4. All depths shall use the industry-standard datum of rotary/kelly bushing interface (RKB), which should be the top of the rig's "drill floor."

4.14. **Measure and analyze the performance**

4.14.1. The drilling machine should react to changing "downhole" conditions to select the optimal drilling parameters for improved performance, as measured by the rate of penetration (ROP), mechanical specific energy (MSE), verticality, cost per foot or meter, and other standard drilling measures or key performance indicators. **Adding parameters such as MSE to the control algorithms will receive special attention from the judges.**

4.14.2. Design limits of the drilling machine shall be determined and shall be incorporated in the programming of the controls during the construction phase.

4.14.3. The final report (see Clause [4.19](#)) shall outline drilling performance and efficiency criteria and measured results.

4.15. **The test well:**

4.15.1. Will be drilled as a vertical well. Verticality and drift will be measured by the judges and compared with the students' measurements, so calibration issues should be carefully considered

4.15.2. Should be drilled with a maximum allowable Weight-On-Bit dependent on the rig and drillstring integrity.

4.15.3. Will not require a closed-loop fluid circulation system, but the bit and machinery should be cooled with air or fluid/water if needed. The design of the fluid system, if any, should be included in the Phase I design.

4.15.4. The rock sample may simulate the drilling of hydraulic hazards such as lost circulation, surge, swab and other effects, but no well control equipment for over-pressure considerations will be necessary. Note that the rock samples may leak at the junctions between the simulated formations, so a rig design that includes a containment system is strongly suggested.

4.15.5. Will not require casing or cement

4.15.6. Will not be drilled with a mud motor or turbine.

4.15.7. Will not require a rig move, walking or skidding, but the mobility of the rig will be considered in the design phase.

4.16. Not included in the 2016-2017 competition

4.16.1. The drilling will not include automating the making or breaking of connections. If this is necessary due to the rig and drillstring design, connections should be made manually, and the time involved with the connections will be added with respect to its effect on drilling performance (rate of penetration reduction).

4.17. Presentation to judges at Phase II Testing

4.17.1. The judges will arrive at the university to meet with the student teams and advisors immediately prior to the Phase II testing. The university should provide a suitable meeting room for discussion lasting about two hours.

4.17.2. The students will present a BRIEF summary of their final design, highlighting changes from their Phase I design, if any. Include an explanation of why any changes were necessary, as this indicates to the judges how much students learned during the design and construction process. Explain what measurement and control features have been deployed. Describe novel developments or just something learned that was worthwhile. Also include how actual expenses compared with the initial estimate. (Previous teams used a short PowerPoint presentation of about ten slides or so. Use any format you like.) Be sure to include all your team members as presenters, not just one spokesperson. At some time during your talk, let us know who the team members are and what background they have that pertains to the project.

4.17.3. Judges will ask questions to ascertain additional details about the design and construction process and to see if all team members have a reasonable understanding how all the various disciplines used for the rig design and construction fit together.

4.18. Project report

4.18.1. The student team shall submit to DSATS a short monthly project report that is no more than one page in length (additional pages will be ignored) due on or before the last day of each month that will include:

4.18.2. Phase I

-) Key project activities over the past month.
-) Rig design criteria, constraints, tradeoffs, and how critical decisions were determined
-) Cost updates
-) Significant new learning, if any

4.18.3. Phase II

- J Construction issues and resolution
- J Summary of recorded data and key events
- J Drilling parameters [such as WOB] and how they impact the test
- J Other items of interest
- J To teach students that their work involves economic trade-offs, the monthly report should include at a minimum a summary estimate of team member labor hours for each step in the project: design, construction, testing, reporting, and a cost summary for hardware and software related expenditures. Also include labor for non-students that affect the cost of the project. Labor rates are not considered, as to eliminate international currency effects. Labor is not considered in the cost limits of item 6.1, but should be discussed in the report and paper.

4.19. Final report and paper

- 4.19.1. The finalists shall prepare a project report that addresses the items in 4.19.6 below. We suggest you use the format of most SPE papers. For reference, please see <http://spe.org/authors/resources/>
- 4.19.2. The winning team shall update the report as needed to comply with SPE ATCE paper submittal guidelines to write a technical paper for publication by the SPE at its Annual Technical Conference and Exhibition. SPE typically requires that the manuscript is due in June. While the Drillbotics committee will make every effort to have the paper presented during the ATCE, the ATCE Program Committee has authority over which papers will be accepted by the conference. If the paper is not accepted by the conference, the Drillbotics committee will endeavor to have it presented at the DSATS Symposium and will use its contacts to have the paper published via other related SPE conferences.
- 4.19.3. The report, paper and all communications with DSATS shall be in the English language. The presentation will be made by at least one member of the student team.
- 4.19.4. The timing for submittal of the abstract and paper will be the published deadlines per the call for papers and conference guidelines as posted on the SPE's website (www.spe.org).
- 4.19.5. The abstract must generate sufficient interest with the SPE review committees to warrant publication, although DSATS will help promote acceptance where possible
- 4.19.6. The paper should address at a minimum

- 4.19.6.1. The technical and economic considerations for the rig design, including why certain features were chosen and why others were rejected.
- 4.19.6.2. The setup of the experimental test, the results and shortcomings.
- 4.19.6.3. Recommendations for improvements to the design and testing procedures.
- 4.19.6.4. Recommendations for improvements by DSATS of the competition guidelines, scheduling and provided material.
- 4.19.6.5. Areas of learning gained through the competition not covered in the university course material.
- 4.19.6.6. A brief bio or CV of the team members and their sponsoring faculty.

5. *Team Members*

- 5.1. DSATS envisions that the students would be at least senior undergraduate or Masters level, well versed in the disciplines needed for such a project. The maximum number of students per team is five (5) and the minimum shall be three (3). Any team that loses team members during the project can recruit a replacement.
- 5.2. At least one member of the team must be a Petroleum Engineering candidate with sufficient coursework completed to understand the physics relating to the drilling problems and the normal industry practices used to mitigate the problem.
- 5.3. Students with a background in mining, applied mathematics, mechanical and electrical engineering, as well as controls, mechatronics and automation or software development, are the most likely candidates, but students with any applicable background is encouraged.
- 5.4. A multi-disciplinary team simulates the working environment in the drilling industry today, as most products and services are produced with the cooperation of technical personnel from differing backgrounds and cultures.
- 5.5. A university may sponsor more than one team but must submit only one team/design for Phase II evaluation.

6. *Expenditures*

- 6.1. Teams selected to advance to the second phase must limit the cost of the rig and materials to US\$ 10,000 or its equivalent in other currencies. The students shall find a source of funding and report the source in the Phase I proposal. All funding and procurement should comply with university policy. These funds are intended to cover the majority of expenses for hardware, software and labor to construct and operate the team's equipment. DSATS shall not be liable for any expenditure other than DSATS provided material and specified travel expenses.

- 6.2. DSATS will assist when possible to obtain free PLCs or similar control devices from suppliers affiliated with the DSATS organization. Such “in-kind” donations shall not be included in the team’s project costs.
- 6.3. Students and universities may use other “in-kind” contributions which will not be included in the team’s project costs. Such contributions may include modeling software, laboratory equipment and supplies, and similar paraphernalia usually associated with university laboratory projects.
- 6.4. Any team spending more than US\$ 10,000, or its equivalent in other currencies, may be penalized for running over budget.
- 6.5. DSATS reserves the right to audit the team’s and university’s expenditures on this project.
- 6.6. Any devices built for the project will become the property of the university and can be used in future research and competitions. Any maintenance or operating costs incurred after the competition will not be paid by DSATS.

7. Other Considerations

- 7.1. The design concepts shall be developed by the student team under the supervision of the faculty. Faculty and lab assistants should review the designs to ensure student safety.
- 7.2. Construction of the equipment shall be supervised by the student team, but may use skilled labor such as welders and lab technicians. The use of outside assistance shall be discussed in the reports and the final paper. DSATS encourages the students to gain hands-on experience with the construction of the rig since this experience will be helpful to the career of individuals in the drilling industry.
- 7.3. University coursework and credit: Each university will decide whether or not this project qualifies as a credit(s) towards any degree program.

8. Project Timeline

Phase I - Design:	Fall 2016
Submit monthly reports	On or before the final day of each month
Submit final design to DSATS	31 Dec 2016, midnight UTC
Submit an abstract to DSATS*	31 Dec 2016, midnight UTC
Phase II – Construction and Testing	Spring 2017
DSATS to announce finalists	On or about 15 Jan 2017
Construction	Spring 2017
Monthly reports	On or before the final day of each month

Drilling Test	Specific on-site test dates at each university to be arranged not later than 31 March 2017. The testing will typically occur in late May or early June. All tests must be completed by 15 June.
Prepare and submit paper	Per SPE deadline*
Prepare and submit presentation	Per SPE deadline
Present paper at ATCE	Per SPE and DSATS schedule

*DSATS will submit an abstract to the SPE that will include excerpts from the student abstracts by the conference paper-submittal deadline, typically in mid-January, for consideration of a paper by the ATCE program committee.

9. *Evaluation Committee*

9.1. DSATS will select an evaluation committee from its membership

9.2. Criteria/Weighting (see chart):

Criteria	Parameter	Weighting
Phase I:		
a.Safety	Safety: construction and operation	10
b.Mobility of rig	Rig up, move, rig down	5
c.Design considerations and lessons learned		10
d.Mechanical design and functionality, versatility		25
e.Simulation/Model/Algorithm		25
f.Control scheme	Data, controls, response times	25
	Total	100%
Phase II:		
a.Creative Ability	Analysis, concepts, development	10
b.Engineering Skills	Problem/Goal, design criteria, feasibility	10
c.Construction Quality		10
d.Cost Control		10
e.Performance		20
Various parameters such as:	ROP, MSE, Landing Bit, Inclination, and other	
Are these used within the control algorithms		
	Optimal landing of bit	
f.Quality of wellbore		20
	Verticality, tortuosity, caliper, other	
g.Data	Data handling, data visualization, data comparison to judges' wellbore logs, and other	
	Total	100%
Intangibles	Additional score may be added or subtracted by the judges at their discretion	

10. Prizes

- 10.1. The winning team will be sponsored by DSATS to attend the next SPE Annual Technical Conference and Exhibition. Upon submittal to DSATS of a valid expense statement (typically a spreadsheet supported by written receipts) covered expenses will be reimbursed by the treasurer of DSATS for the following:
 - 10.1.1. Round trip economy airfare for the team and one university sponsor/supervisor to the gateway city of the next SPE ATCE conference. Entrants should use the SPE approved carrier where possible to minimize cost. Information of reduced fare flights is available on the ATCE website. Please note that reservations must be made before the SPE published deadline. Airfares that exceed the SPE rate must be pre-approved by the committee or the reimbursement will be limited to the SPE rate. The departure point will be a city near the university, the student's home, or current place of work, subject to review by the Committee. Alternately, a mileage reimbursement will be made in lieu of airfare should the entrants decide to drive rather than fly to the ATCE. The reimbursement is based on current allowable mileage rates authorized by the US Internal Revenue Service.
 - 10.1.2. One rental car/van at the gateway city for those teams that fly to the ATCE.
 - 10.1.3. Lodging related to one hotel room per team member will be reimbursed at a rate not to exceed the SPE rate. Note that the room reservations are limited, so entrants must book their rooms early. Room and taxes for the night before the DSATS symposium, the night of the symposium and for the nights of the conference are covered. Charges for the room on the last day of the conference need to be pre-approved by the Committee as most conference attendees depart on the last day of the conference unless there are unusual circumstances.
 - 10.1.4. A per diem will be pre-approved by the Committee each year, which will vary with the cost of living in the gateway city. The per diem is intended to cover average meals (breakfast, lunch and dinner) and incidentals.
 - 10.1.5. ATCE registration will be reimbursed. Students should register for the ATCE to obtain the student rate. Early registration is appreciated.
- 10.2. Individual award certificates will be presented to all participants, with special certificates given to all finalists.
- 10.3. DSATS may provide additional awards, at its sole discretion.
- 10.4. The evaluation and all decisions on any matter in the competition by the DSATS judges and DSATS board are final.

11. Terms and conditions

- 11.1. In no event will SPE, including its directors, officers, employees and agents, as well as DSATS members and officers, and sponsors of the competition, be liable for any damages whatsoever, including without limitation, direct, indirect, special, incidental, consequential, lost profits, or punitive, whether based on contract, tort or any other legal theory, even if SPE or DSATS has been advised of the possibility of such damages.
- 11.2. Participants and Universities agree to indemnify and hold harmless SPE, its directors, officers, employees and agents, as well as DSATS members and officers, and sponsors of the competition, from all liability, injuries, loss damages, costs or expenses (including attorneys' fees) which are sustained, incurred or required arising out of participation by any parties involved in the competition.
- 11.3. Participants and Universities agree and acknowledge that participation in the competition is an agreement to all of the rules, regulations, terms and conditions in this document, including revisions and FAQs posted to the DSATS and Drillbotics websites (see section [3.1](#)).
- 11.4. Winning teams and finalists must agree to the publication of their names, photographs and final paper on the DSATS web site.
- 11.5. All entries will be distributed to the Drillbotics Committee for the purpose of judging the competition. Design features will not be published until after all teams have been judged and a winner is announced. Previous years' submittals, reports, photos and similar documentation will be publically available to foster an open exchange of information that will hopefully lead to faster learning for all participants, both new and experienced.
- 11.6. DSATS and the SPE cannot provide funding to sanctioned individuals and organization per current US law.
- 11.7. Participants must comply with all local laws applicable to this contest.

12. Marketing

- 12.1. Upon request, DSATS will provide a link on its website to all participating universities.
- 12.2. If university policy allows, various industry journals may send a reporter to witness the tests and interview students to publicize the project.

- End -

FAQ Update

Revision 2

2 May 2017

This revision includes changes to the following sections:

- 4.6.1 It looks the bit could split at around 12 cm in the picture attached. Is it possible?

Yes, you can split the parts and separate the bit sub from the bit. Baker Hughes asks that you use the washer between the bit and your bit sub to prevent damage to the bit, since it will be reconditioned and used next year.

- 4.6.6 A company designed a drilling bit for us. Are we allowed to use this drill bit on the competition day?

Per 4.6.5 Student teams may build or buy similar drill bits to test their design with the rock samples they sourced, and

Per 4.6.6 Students are also allowed to design and use their own bits for the Phase II on-site test, within the dimensional limits of 4.6.2.1 above

Since your team did not design and build your own bit, you must use the Baker Hughes bit for the Phase II test. You may use the commercial bit for any testing you wish to do prior to the final on-site test when DSATS judges are present.

- 4.7 Can we substitute steel pipe instead of aluminum?

No. You may build your own tooljoints, but you will still be limited by the buckling of the Aluminum pipe.

- 4.8 Can we make fittings using an interference fit with the tubing?

Yes. Since several schools asked this question during Phase II, we are waiving the requirement of 4.8.1 that states they can make the tooljoints only if the design is proposed in Phase I.

10. Will the winning team present at the next SPE Annual Technical Conference and Exhibition?

No, due to recent changes with the SPE program committees, Drillbotics now has a permanent slot in one of the sessions at the SPE/IADC Drilling Conference. SPE has also granted us a booth to showcase the winning rig. Please substitute "SPE/IADC Drilling Conference" in place of "ATCE" in the Guidelines.

- 10 Can we submit a paper about our competition to other industry conferences?

We want to caution you about a SPE rule regarding previous publications. SPE will reject an abstract for work that has previously been published. As long as the papers are significantly different, this could be allowed, but you could be disqualified if the works are seen as duplicates. We all know members of the program committees for the other conferences and we can assist to avoid any conflicts as long as we communicate clearly, but the final decision rests with the conference program committee, not DSATS.

4.7.2.1 The specification for the pipe wall was incorrectly copied from a previous version of the guidelines. This year, the tubing will be 0.035 inch wall, not the 0.016 inch used in the first year's competition.

4.8.2 *I wonder if the committee is planning on using the same tube fittings this year. If so, could you please provide us with the correct model # from Lenz?*

This is what was ordered last year. Each pipe needs a male and a female. If your drillpipe is longer than one joint, you need a union (tubing x tubing).

Item	Part no.	Description	Reference
1	100-6-6 W/SLV	O-RING SEAL - MALE CONNECTOR W/STAINLESS STEEL SLEEVES	http://lenzinc.com/sites/default/files/1_0.pdf
2	250-6-6 W/SLV	O-RING SEAL FEMALE CONNECTOR STAINLESS STEEL SLEEVE	http://lenzinc.com/sites/default/files/2_0.pdf
3	300-6-6 W/SLV	O-RING SEAL UNION WITH STAINLESS STEEL SLEEVE	http://lenzinc.com/sites/default/files/2_0.pdf

This is the contact we had last year.

Holly Sherer

Lenz Inc

P: 937-277-9364 Ext 13

Fax: 937-277-6515

Holly@lenzinc.com



Innovative Hydraulic Solutions and Manufacturing *Since 1946*

The following were previously published ...

Revision 0 – Initial Release

23 October 2016

- *Are the "Drillbotics Guidelines" the only set of rules we should take into account, or are there other documents? We can't seem to find any.*

The guidelines and the updates per the FAQs are the only documents relevant to the competition rules. Per section 3.1.2 The Drillbotics website at www.Drillbotics.com includes official updates to the competition guidelines and schedule, as well as FAQs, photos, and previous entrants' submittals and reports. Questions and suggestions can be posted there, or teams can email the sub-committee at 2017@Drillbotics.com.

- *The lengths and diameters in the guidelines are nominally in imperial units, such as 3/8" tubing, 36" long, etc. Are teams allowed to substitute comparable equipment and devices readily available in metric units?*

Yes. Please note the changes in your monthly reports and in the Phase I design report.

- 4.3.1 *"While innovative designs are welcome, they should have a practical application to drilling for oil and gas." Regarding judging criteria, will solutions that may not be transferable to the industry have a negative effect on the overall score?*

It is okay, and even encouraged, for teams to come up with non-industry techniques, since you may become the ones who change industry practices. For example, WVU used a counter-balance system last year. Judges felt it would be difficult to replicate on a conventional rig, but perhaps others could find corollary designs that could someday be implemented, so it was allowed. Please avoid laser or plasma drilling, as this is too far afield for today's operations and those of the not-too-distant future.

- 4.3.2 *The guidelines indicate a 25 hp limit on power usage, which is much higher than last year's limit of 2.5 hp. Would you mind confirming the power limit for this year's competition?*

The committee does not want to arbitrarily limit horsepower this year, so a very high number was chosen that should exceed restrictions resulting from any drillpipe or BHA developed. The system components will be the limiting factors.

- 4.3.5.2 *What should be included in the design notes and calculations?*

The Phase I design report should include the team's assumptions used to calculate the mechanical and electrical load expected, as well as other design considerations. It should include theoretical mechanical analysis resulting from the drillstring constraints, anticipated torque and drag and other considerations normally encountered when designing a well and

choosing the rig, mud system, downhole tools and other associated equipment necessary to drill a well safely and efficiently. See previous design reports available on the website.

- 4.4.1 *Our team is currently working on implementing downhole measurements into our new design, as specified in section 4.4.1 of the guidelines. In our field experience, there are a wide range of downhole parameters that can be measured and used for different applications. The statement in the guidelines is very general and our team is wondering if there are specific measurements the competition wants the teams to be focusing on this year?*

The committee does not want to arbitrarily limit team choices. Consider the problem statement involves directional drilling with a drillstring susceptible to high vibrations. So include the sensor(s) of your choice. At least one must be used in the control algorithm in real-time or near real-time. Explain your selection in the Phase I report.

- 4.4.4 *Can you give any details about the survey method that the judges use to measure borehole verticality?*

One of the judges is building a survey tool to run into the wellbore after it is drilled. No details are currently available.

- 4.5.1.2 *"Atypical materials might be encountered in the test block." Can we be assured that these materials will be rock/cement (ie. there won't be a steel plate thrown in there)?*

There will not be a steel plate, but the formations will contain other materials that could simulate stick/slip and similar dysfunctions.

- 4.6.3 *The guidelines for 2017 gives us the liberty to design our own drill bit within the dimensional limits listed in 4.6.3. This section gives a specific dimension of the roller cone/PDC to be given by DSATS. We wanted to know the upper and lower limit on these specifications. Length of bit, material limitation are also not mentioned.*

The committee wishes to remove many restrictions, but not allow using the bit to be so long that it powers straight through the formation like the long bit subs/stabilizers used last year. The bit should be shorter than 2.5 inches (64 mm). Should a team wish to use a longer bit, please contact the committee to explain why this would be necessary.

- 4.9 *What are the rules regarding the construction of the BHA? I can't seem to find them explained explicitly.*

The guidelines allow teams to build their own BHAs with as much creativity as possible, within the constraints of this section.

- 4.9. *We did not notice a limit on the WOB for this year's competition. Does this mean we are free to use any WOB as long as we don't break the drill string and rig equipment?*

There is no arbitrary weight limit this year. Use as much as you want without damaging the equipment.

- 4.9 *We are trying to make the rig and the string as similar to the industry as possible, and want to build the bha as combination of the drill-bit and drill collars. Is it allowed to build the bit-sub/bha as drill collars from steel? How long can the drill collars be, if they are smaller than the bit by at least 10 %? What is the definition of a stabilizer? Would it be considered a stabilizer once it has a diameter within 10 % less than the bit?*

Steel is certainly acceptable. The BHA, except for stabilizers, must be narrower than the bit. We do not want a long BHA that is effectively one long stabilizer. The stabilizers used in 2016 packed the hole and allowed teams to just power their way through the formations. This year, we want it to be a little harder to control the resulting issues.

Yes, a section where the BHA is within 10% of the hole diameter will be considered a stabilizer.

- 4.9 *Are we allowed to add a riser in order to engage stabilizers that are higher up than the bottom-hole assembly? If not, are we allowed to construct a pilot hole? If so, what is the allowed length of the pilot hole?*

Last year, the long stabilizers and the riser made the directional drilling aspect of the competition rather trivial. Please limit the riser to 4 inches (100 mm).

A pilot hole should be pre-drilled using the same bit as you use in the on-site test, and it shall be no deeper than 1 inch (25 mm). Total depth of this pilot hole will be measured in the presence of the judges to calculate ROP and other metrics.

- 4.9.2 *"Additional weight shall not directly impose lateral forces to stabilize the drillstring. This weight is meant to add to string tension/compression but shall not improve steering through interaction with the rock." Does this mean that the BHA can't be as wide as the bit, or would that be ok?*

The BHA needs to be more than one stiff stabilizer pushing against the formation. The BHA within 10% of the hole diameter is considered a stabilizer and the total length of stabilization must be 3.5" (90 mm) or less.

- 4.9.4 *The guidelines indicate a 3.5" limit on the combined length of stabilizers. Is there a limit on the length of the bottom-hole assembly?*

The team must use at least one length of drillpipe (3/8" tubing) which is nominally 36" (914 mm).

- 6.1 *Will the team receive funds from Drillbotics, or would we have to provide the funds ourselves?*

DSATS shall not be liable for any expenditure other than DSATS provided material and specified travel expenses. Funding for the rig components, its construction and operation are the responsibility of the student team and their university. Donations from others is allowed, either as cash or in-kind contributions. Any donors wishing to be listed as a sponsor of the competition should contact the committee at 017@Drillbotics.com.

- 6.2 *Regarding the possibility of obtaining free PLC's, do you know in advance which manufacturers supply them if we wish to obtain a couple of them for our rig?*

Siemens indicated they would. Contact information will be available shortly.

- 9.2 *On page 19 it appears that the percentage breakdown of Criteria/Weighting for "Phase II, Data" is missing.*

The weighting for this element is 20%

- A U.S. Trademark application has been filed for the term "Drillbotics™" and the Drillbotics logo. Any teams wishing to use either of these for their reports or to publicize their activities within university publications or outside sources may request a no-cost license for this purpose. The use of the term Drillbotics with other logos is not permitted. This is required by trademark law to avoid confusion among users or consumers. This is not meant to impede student/university use, but to ensure these marks are not used for purposes beyond this completion and to allow the competition continued use of these marks.
- Additionally, we are interested in learning about the design and operation of the 2016 winning team, West Virginia University's rig; however, we had some trouble locating their SPE paper. Will their final report be made available? If so, what is the best way for us to access it?

The WVU abstract was not accepted by the ATCE program committee, so it is not in OnePetro. An abstract was submitted to another conference in the hopes of getting their paper published. There are other options that the committee is also pursuing. Their paper will be added to the website soon, as long as it does not jeopardize their chances at publication. Meanwhile, the WVU design report is on the website now.

E.2 NTNU Monthly Reports Phase II

Monthly Report January 2017 – NTNU

Activities this month:

- Spent time on contacting suppliers and ordering equipment
 - Aluflex – not possible anymore, now ordering from Aratron
 - ABB – sent mail to order PLC
 - Ordered steel
 - Top drive
 - Linear roller guide rail, wagon for carriage, ball screw system, hoisting motor (ARATRON)
- Created an overview of:
 - How the control system will work
 - Which sensors we are using and what data they provide us with
 - Drilling dysfunctions and responses
- Started creating matlab code for drilling dysfunctions
- Started writing about how we visualize the algorithm to work (drilling dysfunctions and responses, optimization, monitoring, display)

Problems and concerns:

- How to be able to detect drilling dysfunctions

Expected activities next month:

- Create a simulator to test our codes
- Finish ordering equipment

Monthly Report February 2017 – NTNU

Activities this month:

- Equipment has been ordered
 - Top Drive under discussion
- Made time plan for the remaining weeks
- Picked up different rocks for test drilling at Nidaros Restaurering
- Started reading on PID controlling
- Started writing on the report, where theory from the previous project has been added.
- Continued writing about how we visualize the algorithm to work (drilling dysfunctions and responses, optimization, monitoring, display)
- Continued working on the simulator
- Research regarding drilling vibrations and expected natural frequencies has been performed

Problems and concerns:

- Being able to receive all the equipment on time
- Top Drive:
 - Challenging to find a motor that can provide sufficient RPM
- Problems regarding simulating real-time response in Matlab

Expected activities next month:

- Finish ordering equipment
 - Top drive remains
- Obtain sandstone or cement something similar to sandstone
- Have a look at if percussive drilling is possibility if we reach any hard formations

Monthly Report March 2017 – NTNU

Activities this month:

Simulator:

In the meeting with the supervisors, it was agreed to make a simulator in Matlab Simulink. A research of different models that could be used in the simulator were done in the first week.

The simulator was divided into four main models that together simulate the whole drilling system, the circulation system, rock rheology, drill string and hoisting system.

The *circulation system* describes the friction loss in the entire system (hose, swivel, pipe, nozzle, BHA, bit nozzle and annulus). The pump is controlled using the error between the measured pump pressure and its set point.

The *hoisting system* is controlled using the error between the measured ROP and its set point. The ROP is estimated using Bourgoyne and Young's ROP model which requires the WOB (obtained using the torque of the hoisting motor, T_h) and the rotational speed of the top drive, ω_{ds} . It also requires several constants which vary with changing formations, bit quality, ... These constants have been chosen in order to simulate changes in the formation and thus test the control system.

For the *rotary system*, the error between the measured ω_{ds} (rotation speed of the drill pipe) and the set point is used to control the top drive motor. The model uses the torque applied on the drill string, T_{ds} , and the torque loss due to friction, T_{fric} (function of WOB, radius of bit and friction coefficient) to estimate ω_{ds} .

Three separate PID-controllers are used for the three different motors.

We have also been working on implementing logics in the model. This has been done in order to simulate drilling dysfunctions. The main issue has been that we have not modelled vibrations and also that most dysfunctions are based on empirical observations and are therefore not easy to simulate in Simulink. We have therefore focused on how changes in the rock hardness affects the drilling variables.

The main result has been that we have simulated a hard layer occurring approximately halfway in the simulation. The increase in RH causes a reduction in ROP which is then detected and causes an increase in the w_{ds} set point.

There is not currently a limitation to the rotational speed of the string. The most critical measurement is the torque of the hoisting motor which is limited by the buckling limit of the pipe. This means that in a normal operation, the set point of the hoisting motor cannot be increased because it is already at its limit.

Started writing about the simulator and the different models that have been used in the model.

Construction of the rig:

The steel pipes have been sawn and the table has been welded. The hoisting system is required before the rest of the rig can be built. The hoisting system is expected to arrive on Monday the 20th of March. Further construction will continue after that.

Worst case scenario, the top drive will not arrive before 4th April.

- HSE Risk Assessment has been done
- The team has completed the HSE course for the NTNU lab
- To do list (in the lab) for the next three weeks has been made
- A testing schedule has been made
- Bought
 - o cement, wooden boxes and sand for making lithology blocks
 - o Table tops
- Cemented rock samples
- Finished derrick design

Problems and concerns:

- How will the actual programming be done?
- Problems regarding the connection between PLC and PC

Expected activities next month:

Simulator:

- Work more with logics (dysfunctions)
- Try to find a model for vibrations?
- Add noise to the simulator

Construction:

- The hoisting system arrived Monday 20th of March and has been sent to machining. It is assumed to be done with the machining within a couple of days.
- Working with the rails and hinges

Monthly Report April 2017 – NTNU

Activities this month:

The first three weeks of April went away with the Main Excursion to Rio de Janeiro for the students, but the construction of the rig has continued in the work shop. The last week focus has been on finished the construction, obtain communication between motors, drives, PLC and computer, and writing in the final report and master thesis.

Construction of the rig:

- Steel structure of the rig is finished.
- Electrical cabinet is mounted to the rig.
- Top drive motor and drive is mounted to the rig and connected to the PLC.
- Hoisting motor and drive is mounted to the rig and connected to the PLC.
- Circulation pump is mounted to the rig.

Programming and Testing:

- Factory acceptance test (FAT) has been made.
- User interface, HMI, has been made in both MatLab and Simulink
- List of inputs and outputs to the motor controller system (analogue, digital) has been set up
- Focus on exporting and saving test data from Simulink

General:

- More rock samples has been gathered. Oppdals-shale that is very similar to normal sandstone is obtained from Sorte Skiferbrudd.
- Some types of sandstone and marble was obtained from the institute.
- Limits on current and power:
 - o Put in the limit when we configure the drive
 - o Put a braker in the cabinet
 - o Drive also monitors electrical parameters (don't work with it, but use it for safety, need a display on the drive to see the error)
 - o Make a list of the most likely errors
- Safety:
 - o High pressure and rotation are dangerous for the environment → Implement plexi glass in the design.
 - o Can we program that the load releases when you press the button? Can program it directly in the PLC (STOP → lift motor slightly → brake)
- Systems:
 - o Hoisting system:
 - **Speed set point** and **max torque** as inputs to the motor
 - **Digital input for direction** (as input)
 - **Brake signal** (stops current in the motor and brakes) ("big red" button connected to this) (as input)
 - *PLAN B: specify torque set point in Simulink*
 - **Check user manual: torque or speed control?** (MX20D → Oriental Motors) (send to Alexey)
 - o Rotary system:

- Need RPM and torque outputs
 - Need torque input
 - Check user manual: switch between torque control and speed control (send to Alexey)
 - Pump:
 - Speed input
 - Speed output
- We use torque control for the two motors and speed/RPM for the pump
 - Top drive can switch between torque and speed control
 - For the hoisting motor we need to choose torque or speed control (but can change set points and limits while drilling)
 - Can also make PID based on load cell measurements
 - Set point speed → max torque → don't need PID controller for this system
 - Test this on Tuesday! (missing one connector, but it's ordered)
 - Need digital direction to set clockwise or counter clockwise
 - Find translation from RPM to actual speed of carriage
 - Pump: pump speed (PID controller with feedback on pressure, don't need feedback loop for speed), only need speed measurement (feedback: feedback the control)

Problems and concerns:

- Problems regarding the connection between the drives and PLC (close to solution).
- Waiting on analogue input blocks for the PLC from ABB
- Waiting on high pressure swivel for drilling with circulation system
- Waiting on the BHA

Expected activities next month:

- Start drilling and testing phase with temporary BHA → continue with the actual BHA when finished.
- Complete the construction of the high-pressure swivel and BHA.
- Update the CAD-files for the final report and master thesis.
- Choose and design the optimization algorithm.

Monthly report May 2017

Activities this month:

In the beginning of the month, it was decided that the aim should be to finish assembling the rig and its different components by the end of the month.

In an attempt to create a dashboard for the control system, several different methods were reviewed and tested (Dashboard in Simulink, guide in Matlab, App Designer in Matlab etc.). Since our control system runs in Simulink, the simplest solution is to use the Dashboard Blocks that are already integrated in the module and it was therefore chosen as the best option. A proposal for the design of an HMI was developed based on the measurement and switches required to run the drilling operation.

Since safety is the number one priority, a big red emergency button was connected and installed on the rig. In case something unexpected should happen, especially during testing, one student always stands close to the emergency button and is ready to push it. The main intention is to prevent any injury or damage to personnel or the equipment.

Components of the rig:

- The drill deck bushing with radial and linear ball bearings was attached to the rig.
- The riser was built.
- Plexiglass was attached to the rig, preventing water from splashing on the electric equipment.

After the hoisting system and the top drive system were connected to the rig, the Factory Acceptance Tests were conducted. A scaling block in the PLC, as well as some conversions in Simulink, was used to get the right units for the different signals. Looking at the readings from the sensors, some noise and deviation from the actual values was observed. A filter was used to smooth the signals and a proper calibration was done.

Since the circulation system was not operational, dry (test without circulation system) identification tests were done. This gave a better understanding of the safety range of the drilling parameters. It is expected that this will change when the circulation system is implemented.

Stateflow was planned to be used in Simulink to implement a State Machine as control system. An effort was made to get a better understanding of Stateflow. Some simple models were made, and simple, autonomous drilling could be done without an optimization function. A modified control system with an optimization algorithm is almost finished and soon ready to be tested.

The BHA, which is planned to be used during the on-site testing day is built and the down hole sensors are ready to be added to the BHA. The only thing missing is the wires, connecting the sensors to the control system.

With some help from our supervisor, a sponsorship deal with Statoil was made. They agreed to sponsor the project with 10,000 NOK.

Team t-shirt has been designed and received.

A finalised cost estimate of the rig has been done.

Problem and concerns:

Many unexpected problems were encountered during this time, delaying the progress of the project. The hoisting system did not work as expected, where the vertical movement was uneven. This was because the output signal of the drive was set in 1 V increments, which gave low resolution and poor ability to control the hoisting system. A new round of search for a new hoisting motor with the needed specification was done. Due the long delivery time, it was hard to complete this task. Luckily, a hoisting motor with desired specification was used in a different project by the Department of Petroleum and Geoscience at NTNU which could be borrowed to us.

Poor estimation of the number of analogue inputs and outputs for the PLC was done. This made it difficult to receive all the desired measurements from the system. An extra analogue input and an extra analogue output was ordered, but received at a late stage due to long delivery time. More analogue inputs and outputs could have been useful, but could not be ordered due to the long delivery time and the limited amount of time left before the on-site testing day.

From the early phase of the project, the top drive did not work as it should do. The top drive stops, in what seems like random situations. It is difficult to see a trend in the situations when it stops. The problem behind that is not found, and the supplier of the top drive has been contacted.

There have been delays related to the swivel and the components isolating the

pressure. The circulation system can therefore not be set up before this is in place and is delayed compared to the initial plan.

Expected activities next month:

- Some further work in optimization of the control system.
- Connect the downhole sensors to the control system
- Conduct inclination- and vibration analysis
- Set up the circulation system
- Tests how increasing the pressure in the pipe increases the weight on bit.